IL-17A-dependent giant cells in human tuberculosis granulomas : mechanisms of formation, survival and functions

Mohamad Bachar Ismail

THESE

en vue d'obtenir le grade de

Docteur de l'Ecole Normale Supérieure de Lyon - Université de Lyon

Spécialité: Sciences de la Vie – Immunologie

Laboratoire CNRS UMR5239 « Dendritic cells & immune plasticity »

Ecole doctorale de Biologie Moléculaire Intégrative et Cellulaire

Présentée et soutenue publiquement le 24/09/2012 par

Mohamad Bachar ISMAIL

IL-17A-dependent giant cells in human tuberculosis granulomas: mechanisms of formation, survival and functions

Directrice de Thèse
Pr Christine DELPRAT

Jury

Dr Olivier NEYROLLES	**Rapporteur**
Dr Geneviève MILON	**Rapporteur**
Dr Nathalie WINTER	**Examinateur**
Dr Glaucia PARANHOS-BACCALA	**Examinateur**
Dr Pierre JURDIC	**Examinateur et président**
Pr Christine DELPRAT	**Directrice de thèse**

Acknowledgements

In the first place, I would like to express my gratitude and my sincere thanks to my research supervisor, Pr Christine Delprat. Thank you for everything you taught me. Thank you for your understanding, patience, expertise, extraordinary dynamism and your passion for immunology. Thank you also for your advices and useful remarks which guided my work. I am thankful that you used a part of your precious time to read this thesis and give your critical comments about it.

Very special thanks go out to my team members: Alexandre and Carine which help me from the beginning of my project, Nathalie and Giulia for their continuous assistance and Karène for her great advices and fruitful scientific discussions as well as for her assistance with her vast knowledge and skills in many areas. It was a pleasure to work with you and it is a pleasure to convey my gratitude to you in my humble acknowledgment. Thanks also for Emilien and Hélène who have recently joined the team.

I would like to thank professors Françoise Berger, Abdellatif Tazi, Maurizio Aricò and Jan-Inge Henter for providing us with biopsies from patients with Tuberculosis, pLCH and LCH. The technical assistance of Béatrice Bancel is also gratefully acknowledged.

I gratefully acknowledge Dr Nathalie Winter and her team members Emilie and Florence for CFU studies and Dr Daniel Hanau for electron microscopy.

Many thanks go in particular to the members of my thesis committee: Thanks for Dr Olivier Neyrolles and Dr Geneviève Milon who evaluated my work and provided beneficial, useful and constructive comments. Big thanks also to Dr Pierre Jurdic, Dr Nathalie Winter and Dr Glaucia Paranhos-Baccalà who in the midst of all their activity, they accepted to be members of the reading committee.

At the personal level, I wish to express my gratitude, my deep acknowledgment and my sincere thanks to my family. Thanks for my parents, Khaled and Samar, who have always encouraged me to continue my education and helped me to achieve this goal. Thank you for your inspiration, support and sacrifices. Thanks also to my brothers Baraa and Baligh and my sister Elee who supported me during this time.

Thank you my little angel Samar. You are a very special gift that illuminate my road, encourage me and give my life a great and fantastic meaning. With you it was impossible to work at home!!

Finally, I will be eternally grateful to my wife, Rawaa, for her patience and support. You sustained me in all my difficult moments and helped me anytime I needed it. Thank you for your understanding, endurance and encouragement. This work would not have been possible without your permanent assistance and enthusiasm. To you go my most grateful acknowledgments.

Sommaire

1 Part I: Immune response to Mycobacteria with focus on Tuberculosis 7
1.1 Main species and general characteristics of Mycobacteria 8
1.1.1 Main pathogenic and opportunistic Mycobacterium species 8
1.1.2 *M. tuberculosis* consists of six lineages with differential geographic distribution 9
1.1.3 General microbiologic properties of Mycobacteria 11
1.1.4 *M. tuberculosis* activates a specific latent genetic program during hypoxic conditions 11
1.1.5 Intracellular growth of dormant *M. tuberculosis* bacilli relies on lipid catabolism 12
1.1.6 Mycobacteria are characterized by an unusual cell wall structure 13
1.2 Tuberculosis disease 14
1.2.1 The natural history of tuberculosis 14
1.2.2 *M. tuberculosis* and HIV: dangerous liaison for a lethal combination 16
1.2.3 Tuberculosis histopathology 19
1.2.4 Tuberculosis symptoms and diagnosis 19
1.2.5 Tuberculosis treatment 21
1.2.6 Tuberculosis vaccination: current challenges and future strategies 22
1.3 Innate response can be not sufficient against *M. tuberculosis* 26
1.3.1 Host innate receptors involved in mycobacterial recognition. 26
1.3.2 Mycobacterium-receptor interactions determine infection outcomes 27
1.3.3 Mycobacteria resist phagocytosis-induced destruction 27
1.3.4 Innate cells involved in anti-mycobacterial responses 33
1.3.5 Processing of intracellular mycobacterial antigens 38
1.4 The anti-mycobacterial adaptive immunity relies on a granulomatous response 41
1.4.1 Structure and cellular composition of granulomas 41
1.4.2 Granuloma myeloid cells are long-lived and express destructive enzymes 42
1.4.3 Different phases of granuloma formation 46
1.4.4 Pivotal regulators of the granulomatous immune response in tuberculosis 50
1.5 Origins and key mediators of giant cell formation 59
1.5.1 Physiological and pathological giant cells 59
1.5.2 Osteoclast: the bone-resorbing giant cell 59
1.5.3 The myeloid giant cells formed in chronic inflammation 61
1.5.4 IL-17A characteristics and biological functions 62

2 Part II: RESULTS 71

2.1 Manuscript 1: BFL1, a new biomarker of long lifespan and chemoresistant human dendritic cells: application to Langerhans cell histiocytosis treatment 73

2.2 Manuscrit 2: IL-17A-dependent maintenance of human tuberculosis granuloma is mediated by BFL1, CCL20 and CCL2 107

2.3 Manuscript 3: (in preparation) Giant Myeloid Inflammatory Cell: a new anti-Mycobacterium effector of the human immune system 135

2.4 Manuscrit 4: (in preparation) IL-17A^{+}MMP-12^{+}CSTD^{+} DC accumulation leads to bronchoepithelium destruction: relevance in pulmonary LCH 159

3 Part III: DISCUSSION 173

3.1 Differential physiopathological roles of granulomas among species & diseases 173

3.1.1 Evolution of the granuloma role in vertebrates 173

3.1.2 Contributions and limitations of the murine models to understand granulomatogenesis 175

3.1.3 Emergence of the role of granulomas in the chronic control of cancer cells 176

3.2 IL-17A-induced genetic program promotes granulomatogenesis 178

3.2.1 Is IL-17A a constitutive molecular player in granulomatogenesis? 178

3.2.2 The role of IL-17A-induced CCL20 and CCL2 in granulomatogenesis 179

3.2.3 The role of IL-17A-induced CCL20 and CCL2 in cell-cell fusion 181

3.2.4 The role of IL-17A-induced BFL1 in myeloid cell maintenance 183

3.2.5 Multiple stimuli for NF-κB -dependent activation of BFL1 in granuloma, *in vivo* 184

3.3 The IL-17A-induced Giant Myeloid Inflammatory Cell (GMIC) 185

3.3.1 GMIC: a novel multinucleated cell type of the immune system characterized by MMP12 & CTSD co-expression 185

3.3.2 Comparison of GMICs with the giant cells of LCH and TB granulomas 187

3.3.3 Microbicidal role of GMIC against Mycobacteria, *in vitro* 189

3.3.4 The destructive role of GMIC against human broncho-epithelial cells 191

3.3.5 Regulation of IL-17A-mediated responses 193

4 Part IV: CONCLUSIONS & PERSPECTIVES 197

5 REFERENCES 201

ABBREVIATIONS

A

APC: Antigen-presenting cell

B

BCG: Bacille de Calmette et Guérin

BCL-2: B-cell lymphoma 2

C

CCL: Chemokine (C-C motif) ligand

CCR: Chemokine (C-C motif) receptor

CR: Complement receptor

CTS: Cathepsin

D

DC: Dendritic cell

DC-SIGN: DC-specific intracellular adhesion molecule grabbing non integrin

DC-STAMP: DC -specific transmembrane protein

E

EEA1: Early endosomal antigen

ER: Endoplasmic reticulum

ESAT-6: Early secreted antigenic target-6

F

FasL: Fas ligand

FBGC: Foreign body giant cell

G

GM-CSF: granulocyte macrophage colony-stimulating factor

GMIC: giant myeloid inflammatory cell

H

HIV: Human immunodeficiency virus

I

ICL: isocitrate lyase

IFN-γ: interferon-gamma

IL: interleukin

iNKT: Invariant natural killer T

iNOS: Inducible nitric oxide synthase

L

LAM: Lipoarabinomannan

LCH: Langerhans cell histiocytosis

LSP: large sequence polymorphism

LXA_4: lipoxin A_4

M

M.: Mycobacterium

ManLAM: Mannosylated lipoarabinomannan

M-CSF: Macrophage colony-stimulating factor

MDR-TB: Multidrug-resistant tuberculosis

MGC: Multinucleated giant cell

MHC: Major histocompatibility complex

MMP: Matrix metalloproteinase

MP: Macrophage

***Mtb*:** *Mycobacterium tuberculosis*

N

NADPH ox: nicotinamide adenine dinucleotide phosphate-oxidase

NEMO: NF-κB essential modulator

NF-κB: nuclear factor-kappa B

NK: Natural Killer

NLR: Nucleotide–binding oligomerization domain (NOD)-like receptor

NO: nitric oxide

NOD: Nucleotide–binding oligomerization domain

O

OC: osteoclast

P

PG: Peptidoglycans

PGE_2: prostaglandin E_2

PI3P: Phosphatidylinositol 3-phosphate

PIM: Phosphatidyl inositol mannosides

PMN: polymorphonuclear neutrophil

PRR: Pathogen receptor recognition

R

RANKL: Receptor activator of nuclear factor kappa-B ligand

RD1: Region of deletion 1

RNI: Reactive nitrogen intermediates

ROI: Reactive oxygen intermediates

T

TB: Tuberculosis

TCR: T cell receptor

TGF-β: Transforming growth factor beta

Th: T helper lymphocyte

TLR: Toll-like receptor

TNF-α: Tumor necrosis factor-alpha

TRAF: TNF receptor-associated factor

TRAIL: TNF-related apoptosis-inducing ligand

TST: Tuberculin skin test

V

V-ATPase: Vacuolar ATPase

W

WHO: World health organization

WT: wild-type

X

XDR-TB: Extensive drug resistant tuberculosis

1 Part I: Immune response to Mycobacteria with focus on Tuberculosis

Mycobacteria belong to the Mycobacterium genus, the single genus within the family of Mycobacteriaceae in the Corynebacterineae suborder of the Actinomycetales order. They fall into two main groups: slow and fast growers. Slow-growers include several pathogens (strict and opportunistic) while most of the fast growers are non-pathogenic Mycobacteria. Among strict pathogens, two species, *Mycobacterium tuberculosis* (*Mtb*) and *Mycobacterium leprae*, cause two of the world's oldest diseases: tuberculosis (TB) and leprosy, respectively.

TB is mainly a pulmonary disease characterized by the formation of small inflammatory nodules formed by a collection of immune cells in lungs. The formation of these structures requires cell recruitment and clustering and is driven by several cytokines and chemokines. TB granuloma consists of a myeloid cell core surrounded by T lymphocytes. A cellular hallmark of granulomas is the presence of multinucleated giant cells (MGCs) formed by the fusion of several myeloid cells. In humans, mechanisms of granuloma and MGC formation and their functions are largely unclear.

Recent data showed that the cytokine IL-17A is involved in the formation of TB granulomas in mice. Moreover, our group discovered that this cytokine induces the fusion of human myeloid dendritic cells (DCs) into MGCs *in vitro*. Based on these data, we suggested a potential role of IL-17A in the formation of human giant cell-associated granulomas.

During this thesis, we investigated the molecular mechanisms which regulate the survival, clustering and MGC formation in the IL-17A-dependent pathway. We also searched if similar mechanisms are involved in the formation and maintenance of granulomas in TB as well as in another giant cell-associated granulomatous disease called pulmonary Langerhans cell histiocytosis (pLCH). Then, we investigated the phenotype, the immune functions and the anti-mycobacterial abilities of the IL-17A-induced MGCs that we called GMICs (giant myeloid inflammatory cells).

To introduce this work in its scientific context, we first present Mycobacteria and their characteristics with a focus on TB disease. Then, we describe the innate immune response and its main effectors against Mycobacteria and show how pathogenic strains can evade this response. Afterwards, we present the adaptive granulomatous response to Mycobacteria and we document essential host factors required for granuloma formation and maintenance. Finally, we describe the different types of myeloid giant cells with a focus on the IL-17A-dependent pathway as well as the characteristics and biological functions of IL-17A.

1.1 Main species and general characteristics of Mycobacteria

1.1.1 Main pathogenic and opportunistic Mycobacterium species

Mycobacterium is a highly diverse genus [1] in which we distinguish the following species:

-The *Mtb* complex: this complex is formed by species closely related to *Mtb* at the genetic level, but with distinct host tropisms. *Mtb* is the main etiologic agent of most cases of TB in humans who are reservoir of this pathogen. In addition to *Mtb*, *Mtb* complex contains *M. bovis*, *M. africanum*, *M. microti*, *M. canettii*, *M. caprae* and *M. pinnipedi* [2] [3]. *M. Bovis* causes TB in cattle and humans which serve as reservoirs. An attenuated strain of *M. Bovis* is called Bacille de Calmette et Guérin (BCG) and is used as a TB vaccine. *M. africanum* specifically infects humans and is a significant cause of TB in the western countries of Africa. *M. canettii* is a rare strain of the *Mtb* complex and was isolated from TB patients mostly in the horn of Africa. *M. microti* specifically causes disease in small rodents; *M. caprae* infects goats, while *M. pinnipedii* primarily affects seals.

***-M. leprae**:* a slow growing intracellular pathogen and the etiologic agent of leprosy, a chronic but curable human disease affecting the skin, peripheral nerves, eyes and mucosa of the upper respiratory tract. Leprosy is a granulomatous inflammation driven by mycobacterial antigens that activate a destructive immune response [4]. Even though its prevalence has decreased dramatically, 228 474 new cases of leprosy were detected worldwide in 2010, thus indicating active *M. leprae* transmission. Human beings are the principal reservoir of infection. However, the exact mechanism of transmission is not fully clear although the aerosol spread of nasal secretions is considered as the predominant transmission mode [4].

-M. ulcerans: behind *Mtb* and *M. leprae*, *M. ulcerans* is the third most common mycobacterial pathogen of humans. *M. ulcerans* is a slow-growing pathogen and the causative organism of Buruli ulcer disease characterized by devastating necrotic lesions called ulcers and resulting in extensive destruction of the skin and soft tissues [5] [6]. Infection by *M. ulcerans* seems to occur in or near stagnant water and slow flowing rivers in humid tropical regions [5] [6]. The mode of transmission in humans is unknown, but it was suggested that aquatic insects and salt marsh mosquitoes may be involved in transmission [5] [6].

-*M. avium* complex: This complex consists of a heterogeneous group of Mycobacteria including, among others, *M. avium* and *M. intracellulare*. *M avium* is further divided into various subspecies including *M. avium avium* and *M. avium paratuberculosis*. All these species are slowly-growing environmental Mycobacteria [7] considered as opportunistic microorganisms that mostly induce diseases in immuno-compromised patients. In humans, *M. avium* infection is widely associated with disseminated infections immuno-compromised human beings. *M. intracellulare* is more common among immuno-competent individuals. *M avium paratuberculosis* is a well-known causative agent of paratuberculosis (Johne's disease), a chronic granulomatous enteric disease of ruminants. In addition an etiologic link between this Mycobacterium and Crohn's disease in humans was proposed but remains controversial and to be proven.

-M. marinum: an environmental/atypical Mycobacterium which was first discovered in salt water fish. *M. marinum* was lately identified as an opportunistic pathogen in humans in whom infection may cause localized nodular skin lesions called "swimming pool granuloma" or "fish tank granuloma".

1.1.2 *M. tuberculosis* consists of six lineages with differential geographic distribution

Traditionally, it was thought that the *Mtb* complex is a highly homogeneous clonal population which displays limited genetic variability [8] [9]. However, recent advances in mycobacterial comparative genomics revealed that substantial genetic variation exists at the whole-genome level of this complex, suggesting that it is more heterogeneous than appreciated initially [10]. Using large sequence polymorphisms (LSPs) genetic markers, Gagneux and colleagues found that *Mtb* consists of six main strain lineages, designated Lineage 1 through Lineage 6, two of which were initially designated *M. africanum* **(Fig.1, Top)** [10]. They can be further divided into "ancient" and "modern" lineages based on the presence or absence of a genomic deletion known as TbD1 [11]. Importantly, the six identified *Mtb* strain lineages show biogeographic specificities as they are associated with particular geographic regions and human populations **(Fig.1, bottom)** [10].

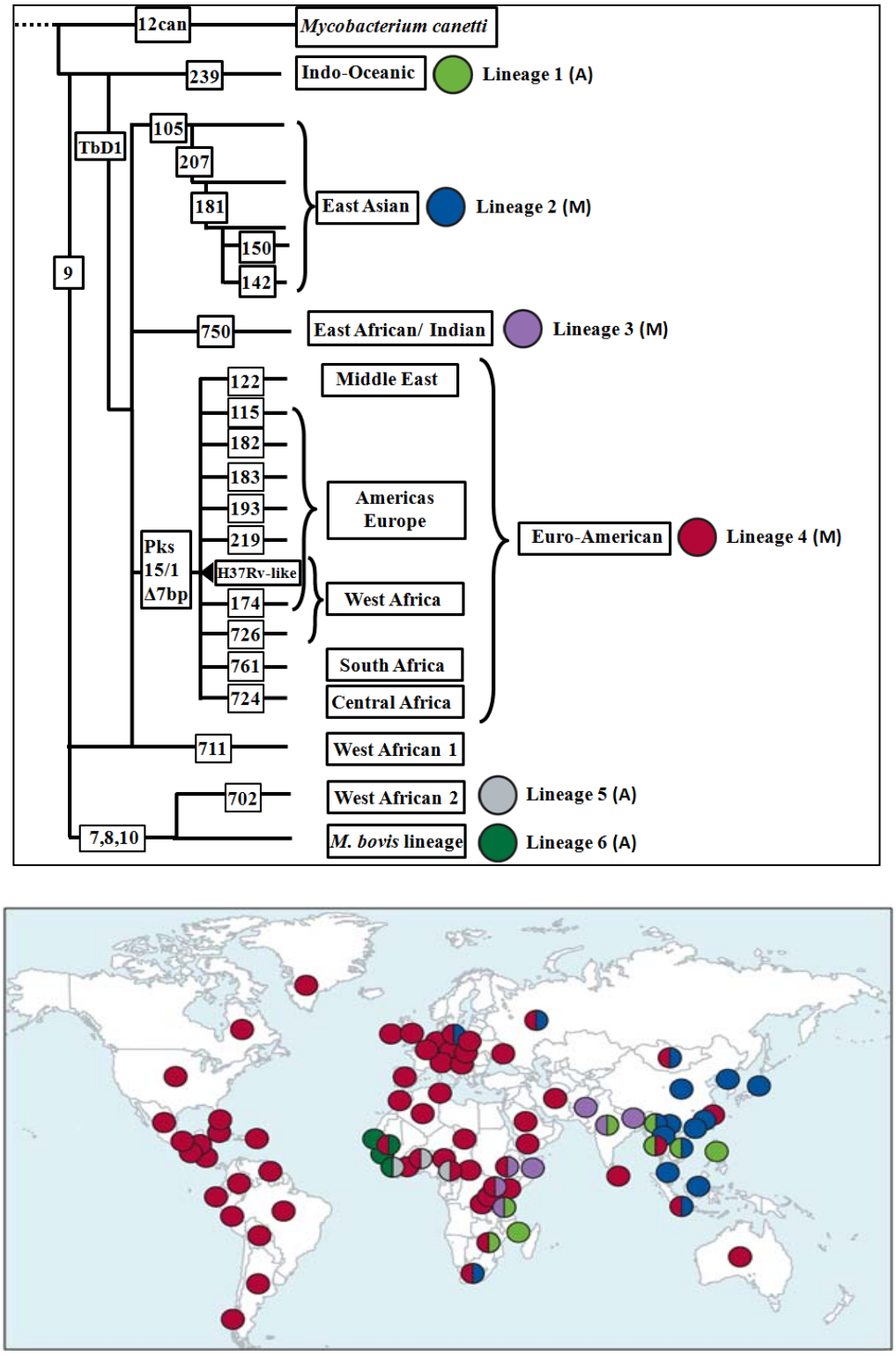

Figure 1: Global phylogenetic classification and phylogeographic distribution of *Mtb*. Adapted from ref [10].

Top: The global population structure of *Mtb* consists of six main strain lineages (1 to 6). Each lineage is symbolized by a colored circle. Numbers in rectangles refer to LSP markers. Pks: polyketide synthase gene. (A): Ancient lineage. (M) Modern lineage.

Bottom: Global phylogeography of *Mtb*. Colored circles indicate the dominant lineage in country.

1.1.3 General microbiologic properties of Mycobacteria

Mycobacteria are thin and long bacilli that measure about 1 to 10 µm. A distinctive characteristic of Mycobacterium species is the property of acid-fastness as they resist decolorization with a mixture of acid and alcohol due to their specific cell wall composition. However, they are routinely stained with the Ziehl-Neelsen colorization, a basic carbofuchsin staining method. Mycobacterium slow-growers need prolonged incubation periods. For example, *Mtb* divides every 15–20 hours, which is a particularly slow generation time compared to other bacteria. Mycobacterial growth requires selective solid or liquid culture media including the commonly used Middlebrook media. Cultures of slow-growing Mycobacteria including *Mtb* require four to eight weeks of incubation to grow on solid media while liquid media allow more rapid mycobacterial growth. I*n vitro*-grown *Mtb* colonies appear as small, friable, rough and white to light-yellow colored colonies **(Fig. 2)** [12].

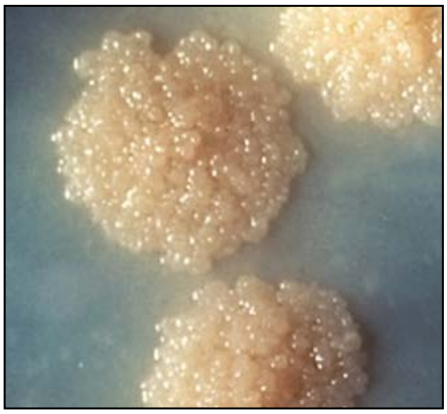

Figure 2: *Mtb* Colonies on a solid culture medium. Centers for Disease Control and Prevention (CDC).

1.1.4 *M. tuberculosis* activates a specific latent genetic program during hypoxic conditions

In response to environmental stresses such as nutrient deprivation and hypoxia inside host cells, *Mtb* bacilli precede to a dormant state defined as a stable but reversible non-replicating state [13]. In this dormancy phase, bacilli persist with a reduced metabolic activity that facilitates their survival under hypoxic conditions [14]. However, dormant bacilli keep their ability to resume growth when conditions become favorable [15]. *Mtb* ability to terminate replication and shut down its own central metabolism renders these bacilli extremely resistant to both host defense and drugs [14].

Voskuil *et al.* revealed that hypoxic microenvironment activates a specific genetic program leading to latent *Mtb* survival [16]. They showed that inhibition of respiration by NO

(nitric oxide) production and O_2 limitation, constrains *Mtb* replication rates. This non replicating state is driven by a 48-gene regulon under the control of a transcription factor named DosR [16]. DosR adapts the organism for survival during prolonged periods of *in vitro* dormancy. It is also required for maintaining energy levels and redox balance for *Mtb* survival during anaerobic dormancy and ensures rapid *Mtb* recovery and optimal transition from an anaerobic or nitric oxide-induced nonrespiring state to aerobic growth [17].

1.1.5 Intracellular growth of dormant *M. tuberculosis* bacilli relies on lipid catabolism

Several lines of evidence indicate that, in hypoxic conditions, Mycobacteria switch to lipid catabolism to ensure their survival. Genomic studies and transcriptomic analysis of entirely sequenced *Mtb* genome show that this bacillus displays a wide range of diverse lipophilic molecules involved in lipogenesis and lipolysis [18]. For example, there are 250 distinct enzymes related to fatty acid metabolism in *Mtb* compared with only 50 in *Escherichia coli* [18]. Among them, several enzymes could catalyze the first step in fatty acid degradation providing thus different metabolites and fuel for the bacteria [18]. Functional studies of some of these enzymes have revealed that they play an important role in the persistence of *Mtb* in their hosts. For example, isocitrate lyase (ICL), an enzyme induced by oxygen limitation and essential for the metabolism of fatty acids, has been reported as required for persistence and virulence of *Mtb* [19]. ICL is a key component of the glyoxylate shunt, by which microorganisms bypass the tricarboxylic acid cycle to incorporate carbon from acetate and fatty acids into carbohydrates. ICL regulates *Mtb* long-term survival in the murine lung while its deletion attenuates *Mtb* virulence as ICL-deficient mutant survived in resting but not in activated macrophages (MPs) contrary to the Wild-type (WT) strain [19].

Mtb persists in a non-replicating state inside adipocytes and accumulates lipid droplets inside these cells [20]. This suggests that the adipose tissue might constitute one important cellular reservoir in which *Mtb* could persist in a dormancy-like state. Consistent with these findings are data showing that *Mtb* metabolize host-derived cholesterol and that disruption of the *mce4* gene, encoding a cholesterol transporter, results in the failure of *Mtb* to maintain chronic infection in mice [21]. A recent report showed also that *Mtb* residing within the phagosomes of hypoxic human MPs utilizes, accumulates and stores host triacylglycerol in the form of intracellular lipid droplets [22]. In these conditions, *Mtb* replication is severely inhibited and bacilli acquire a dormancy-like phenotype [22]. In mice, BCG infection induces time- and dose-dependent lipid body formation in infected MPs [23]. More recently, a study

revealed that *Mtb*, namely through its oxygenated mycolic acids, triggered the differentiation of human MPs into lipid laden foamy cells in which Mycobacteria switched to dormant non-replicative bacilli and accumulate host cell lipids [24].

Taken together, these data suggest that, during dormancy, *Mtb* intracellular growth relies on the lipid catabolism as the main carbon source. This ensures not only survival in hypoxic conditions, but also its adaptation to carbohydrate starvation.

1.1.6 Mycobacteria are characterized by an unusual cell wall structure

Mycobacteria have a specific cell wall structure which distinguishes species of the Mycobacterium genus from other prokaryotes [25]. this unusual cell wall structure is responsible of the acid fastness property of Mycobacteria and is related to mycobacterial resistance to drying, alkali, many chemical disinfectants and therapeutic agents [26]. It consists of three major parts: the plasma membrane, the cell wall core and the capsule-like outermost layer **(Fig. 3)** [25]. The cell wall core is close to the plasma membrane and consists of a mycolyl-arabinogalactane-peptidoglycan (mAGP) complex. This core unit is an insoluble complex formed by peptidoglycans (PG) covalently attached to arabinogalactans (AG) which in turn covalently bound mycolic acids [25] [27]. These latter, for which the Mycobacteria are named, constitute ~ 60% of the bacillus total weight. They are very long chain ($C_{60\text{-}90}$) α-branched, β -hydroxy fatty acids and are considered as the most distinctive feature of the mycobacterial cell wall.

The capsule-like outermost layer of the cell wall is composed of a variety of free lipids, lipoglycans, and proteins including porins (pore-forming proteins) [25]. Lipoglycans, including lipoarabinomannan (LAM) and phosphatidylinositol mannosides (PIMs), are prevalent components of the mycobacterial cell wall. In contrast to the insoluble cell wall core, free lipids, proteins, LAM and PIMs are solubilized and form signaling, immunologically active effector molecules which play important biological functions in the pathogenesis of *Mtb* [25] [27].

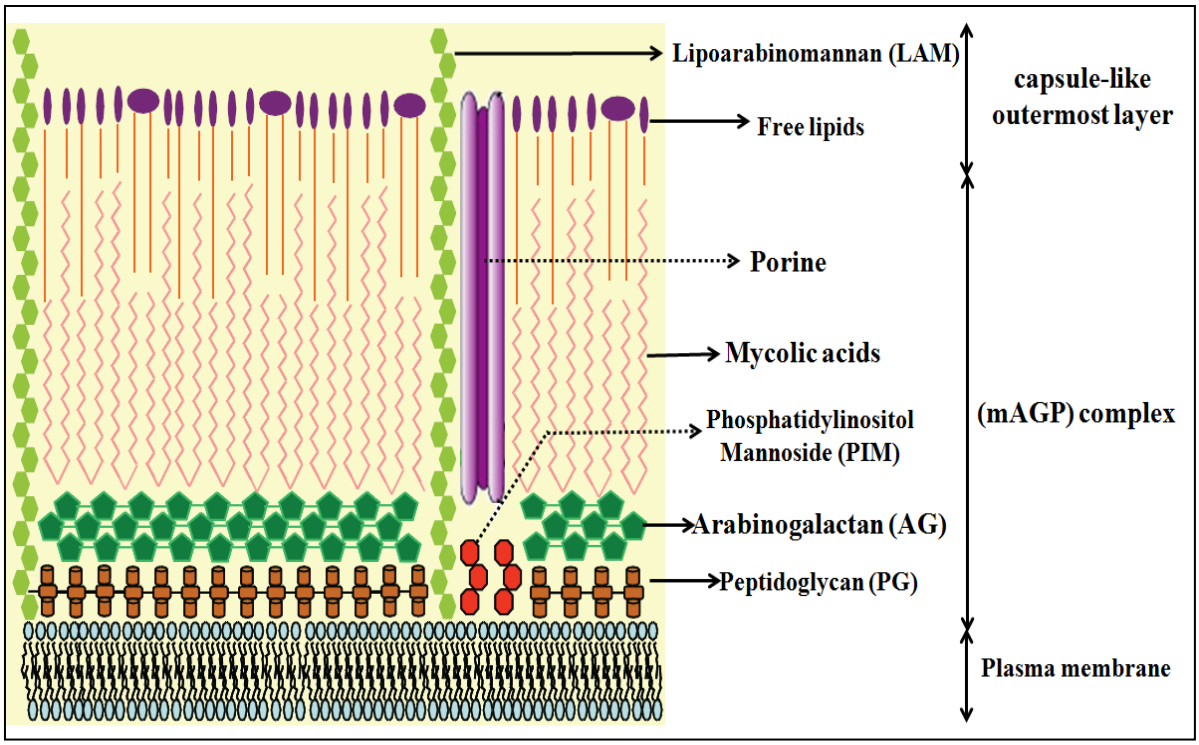

Figure 3: Schematic representation of the unique wax-rich cell wall of Mycobacteria. Adapted from ref [28].
Close to the plasma membrane is the (mAGP) complex. It forms the core unit of the mycobacterial cell wall and consists of PG connected to AG which are covalently linked to mycolic acids. The upper segment is the capsule-like outermost layer which includes a variety of free lipids. The mycobacterial cell wall contains many signaling and effector molecules including LAM and PIM which support mycobacterial survival and virulence. Porins cross the cell wall to allow molecule diffusion into Mycobacteria.

1.2 Tuberculosis disease

1.2.1 The natural history of tuberculosis

In 1882, the German scientist Robert Koch identified *Mtb* as the etiologic agent of human TB disease. In 1998, the complete genome sequence of the well characterized H37Rv strain of *Mtb* was determined. It comprises 4,411,529 base pairs, contains approximately 4047 predicted genes, and has a very high guanine + cytosine (G+C) content [18]. Although *Mtb* was identified more than 130 years ago, it remains currently one of the most pernicious of human pathogens, and TB disease is more prevalent in the world today than at any other time in human history. In 2010, the world health organization (WHO) reported an annual burden of ~ 8.8 million cases of disease resulting in ~1.4 million deaths which mostly occurs in poor world countries [29].

Mtb infection occurs by an efficient person-to-person transmission mode and the main infection route is the respiratory tract **(Fig. 4)**. Bacilli are transmitted via airborne droplets

expelled into the atmosphere by patients with active pulmonary TB most commonly during coughing or sneezing. These droplets can be later inhaled by healthy individuals in who they proceed distally to the lung where *Mtb* can induce the infection. However, exposure to *Mtb* bacilli results in a wide spectrum of outcomes. It is estimated that only 30% of exposed individuals get infected [30]. This suggests that innate immune responses in exposed but not infected persons may rapidly clear the inhaled bacilli, although this has not been formally proven. Among infected individuals, a minority (around 10% - most commonly infants or children of young age) progress to primary active TB disease with clinical symptoms within 1-2 years following infection. In contrast, the majority (90%) of infected individuals remains asymptomatic and free of tissue damage. However, they carry viable but dormant bacilli which can persist for decades, thereby developing latent TB infection [14] [30] [31]. Individuals with latent TB don't transmit *Mtb* bacilli to other persons but are the largest reservoir for potential subsequent transmission [30]. They show an equilibrium state in which they develop an effective acquired immune response that controls but not entirely eradicate *Mtb* bacilli. Unfortunately, they have a subsequent 10% risk of reactivation and development of post-primary (secondary) TB throughout their life time [30] [31].

TB is a multifactorial disorder: in addition to pathogen, several environmental and host risk factors are associated with *Mtb* reactivation and disease development. The most potent risk factor is HIV but other factors including anti-TNF therapy, host genetic factors, malnutrition, smoking, alcohol and bad life conditions are also involved in this process [31] [32]. TB is mainly a pulmonary disease: in 85% of immuno-competent infected individuals disease preferentially occur in lungs [33]. However, *Mtb* can also spread to any part of the body and TB can develop in different organs resulting in extrapulmonary TB [34]. extrapulmonary TB develop most commonly in lymph nodes (tuberculous Lymphadenitis), pleura, bones and joints (with a form affecting the spine, called Pott's disease) and central nervous system (the most common presentation is tuberculous meningitis affecting meninges) [34]. Other sites include pericardium (tuberculous pericarditis), the gastrointestinal and genitourinary tracts [34].

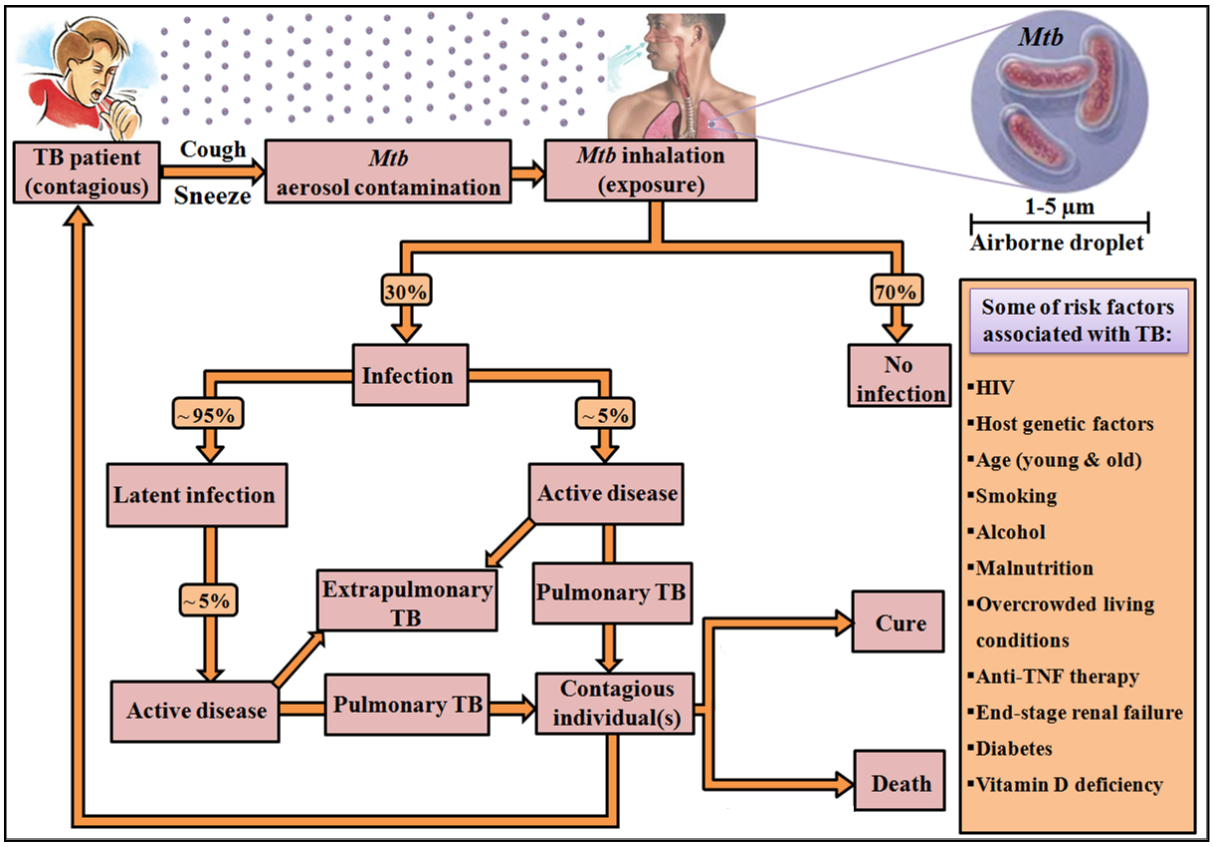

Figure 4: Natural history and outcome spectrum of TB.

TB is a contagious disease caused by *Mtb* infection. Bacilli are acquired by the inhalation of airborne droplets containing *Mtb*. Infection occurs in ~30% of exposed individuals. Only ~10% of infected individuals develop active disease: ~5% at primoinfection and ~5% following reactivation after latent infection. TB disease mainly affects lungs, but can also develop in other organs (extrapulmonary TB). If treated, the majority of patients with drug-susceptible-TB are cured while a high mortality occurs in untreated patients. Several risk factors increase the risk of TB development (orange box). Smokers, alcoholics and individuals having weak immune systems, genetic impairment, unfavorable living conditions or compromised by some diseases, malnutrition, or medical intervention show a higher risk of *Mtb* reactivation and TB development.

1.2.2 *M. tuberculosis* and HIV: dangerous liaison for a lethal combination

HIV-infected persons are more likely to develop active TB, and clinical studies suggest that HIV leads to an increased risk of developing TB shortly after HIV infection. Moreover, while healthy persons are mostly resistant to *M. avium* complex infections, patients with AIDS (acquired immunodeficiency syndrome) are susceptible to *M. avium* complex and develop disseminated disease upon infection with these opportunistic species. Progression to active TB can in turn increase HIV replication and accelerate the progression to AIDS [35]. Additionally, while TB is restricted to the lungs in most cases, *Mtb*/HIV co-infected persons

easily develop systemic and more quickly lethal TB [36]. Indeed, HIV^+ TB, opposed to HIV^- TB patients, include a higher proportion of cases with extra-pulmonary or disseminated disease involving multiple organs. Referring to WHO, people immuno-compromised by HIV and infected with *Mtb* are up to 20-37 times more likely to develop active TB in their life-time than people who are HIV^-. Recent WHO report revealed that in the 8.8 million new persons infected with *Mtb* in 2010, 12.5% were co-infected by HIV [29]. In addition, of the 1.4 million people who died of TB in 2010, 25% were co-infected by HIV [29]. Both diseases are associated to poverty and unfavorable low-social life conditions and their highest prevalence are found in the same regions of the world **(Fig. 5)**.

HIV infects $CD4^+$ cells which are not only T cells, but also alveolar MPs, the primary target of *Mtb* [37] [38]. HIV and *Mtb* can therefore share the same host cell. Several studies showed that these two pathogens potentiate one another to increase and exacerbates its risk. Several hypotheses were proposed to explain how this occurs and a recent paper summarizes these hypotheses in four main points: (i) HIV replication is increased at sites of *Mtb* infection, leading to increased pathology, (ii) HIV induces primary or reactivated TB through killing of $CD4^+$ T cells (mandatory for TB control), (iii) HIV manipulation of MP function prevents *Mtb* killing, and (iv) HIV induces functional changes in *Mtb*-specific T cells that decrease their ability to contain *Mtb* [39].

Overall, *Mtb*-induced TB and HIV-induced AIDS form together a lethal combination in which each speeding the other's progress.

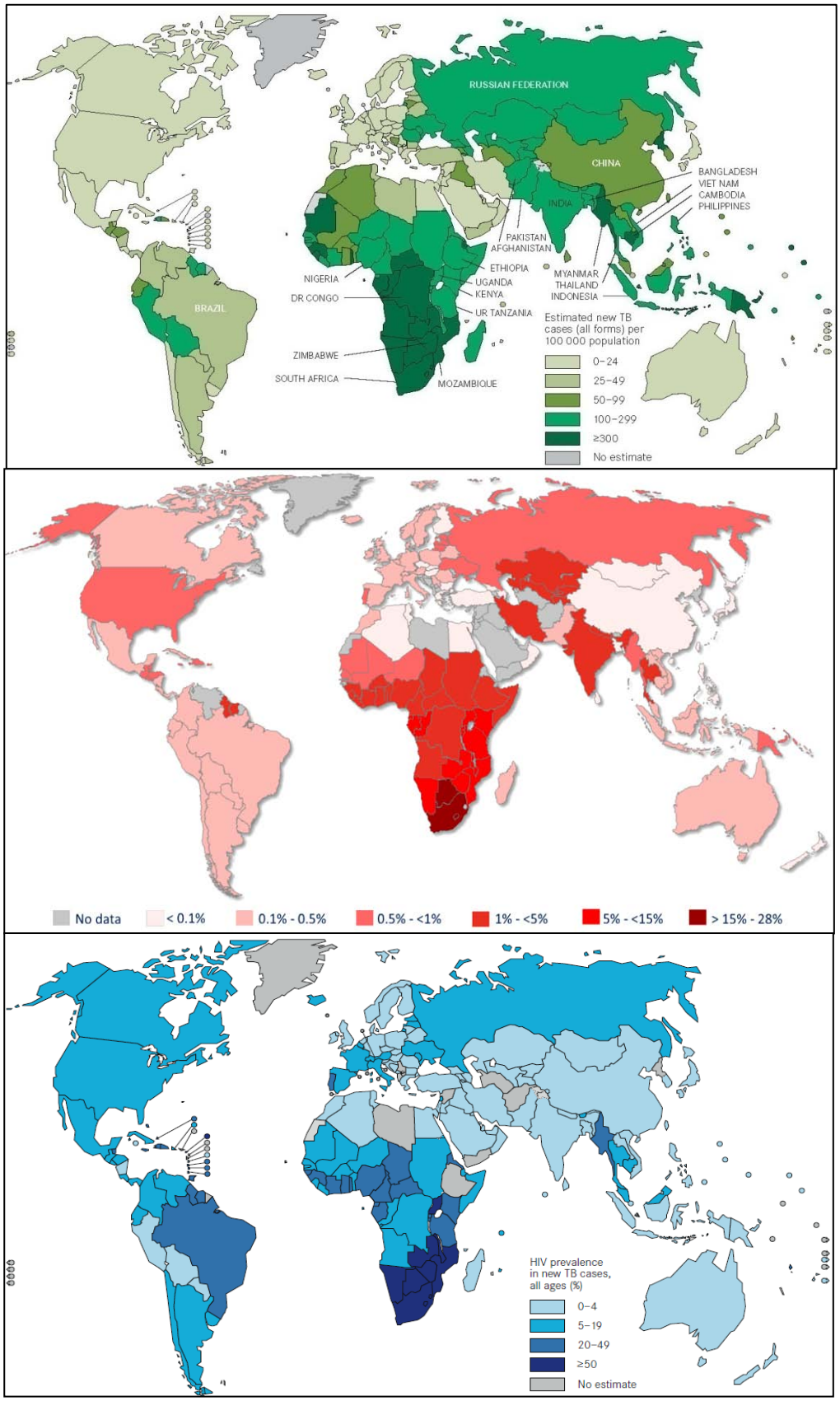

Figure 5 : Estimations of: TB incidence rates in 2010 **(top)**, HIV prevalence rate in individuals aged 15-49 in 2009 **(middle)** and HIV prevalence in new TB cases in 2010 **(bottom)**. Note that both diseases are highly prevalent in the same countries of the World.

Sources: Top and bottom: WHO report, global tuberculosis control, 2011. Middle: UNAIDS, report on the global AIDS epidemic, 2010.

1.2.3 Tuberculosis histopathology

Typically, *Mtb* infection induces a specific type of inflammation characterized by the formation of granulomas, small focal inflammatory nodules formed by a collection of immune cells. In humans, TB granulomas are highly organized with specific architectural structures forming an interface between bacteria, host immune response and host tissues **(See 1.4.1)**.

Many of TB granulomas persist as solid structures showing an equilibrium state which is generally successful in containing, although not eliminating, *Mtb* bacilli. However, granuloma can proceed either to localized sterilization of the infection and mineralization of the lesion or to localized central necrosis [40]. Necrosis induces the extracellular release of *Mtb* bacilli and results in characteristic necrotic centers called caseum, essentially formed by host cell debris. Granulomas with caseating material are known as caseous granulomas and their development characterize the progression toward disease [41]. Caseating material greatly supports the extracellular growth and replication of *Mtb*. It has a yellow-white color with an initial solid cheesy texture. In advanced stages, it liquefies and cavitates the lung causing ruptures into the lung airway and release of infectious *Mtb* bacilli. In patients with active TB, all granuloma forms (solid, necrotic and caseous) can coexist.

1.2.4 Tuberculosis symptoms and diagnosis

(Fig. 6, left)

TB patients may show several symptoms which are often vague and non specific including persistent cough (pulmonary TB), anorexia, weight loss, chest pain, hemoptysis, and night sweats. In extra-pulmonary TB, symptoms can vary according to the affected organ(s). However, symptoms might be absent in some TB patients especially in the early stages of disease [32].

Most common tests used for TB diagnosis include cultures, sputum smear microscopy, nucleic acid amplification tests, radiology, the tuberculin skin test (TST) and IFN-γ release assays (IGRAs) [42]. In contrast to other methods which detect active TB cases, TST and IGRAs are used for the immuno-diagnosis of latent TB by identifying the existence of an adaptive immune response to mycobacterial antigens [42].

TB can be difficult to diagnose, especially in children, HIV-infected individuals and patients developing extrapulmonary forms [32]. Moreover, different diagnostic tests cited above provide information only on the state of the disease in a precise single time point (active or latent TB). Therefore, a major obstacle to TB control is the lack of reliable

biomarkers for different stages of infection [43]. Such biomarkers are needed to help to diagnose TB, to provide correlates of risk of TB and correlates of protection against active disease, and to determine the response to therapy [44]. Moreover, TB biomarkers may also accelerate screening and early selection of potential TB drug and vaccine candidates [43].

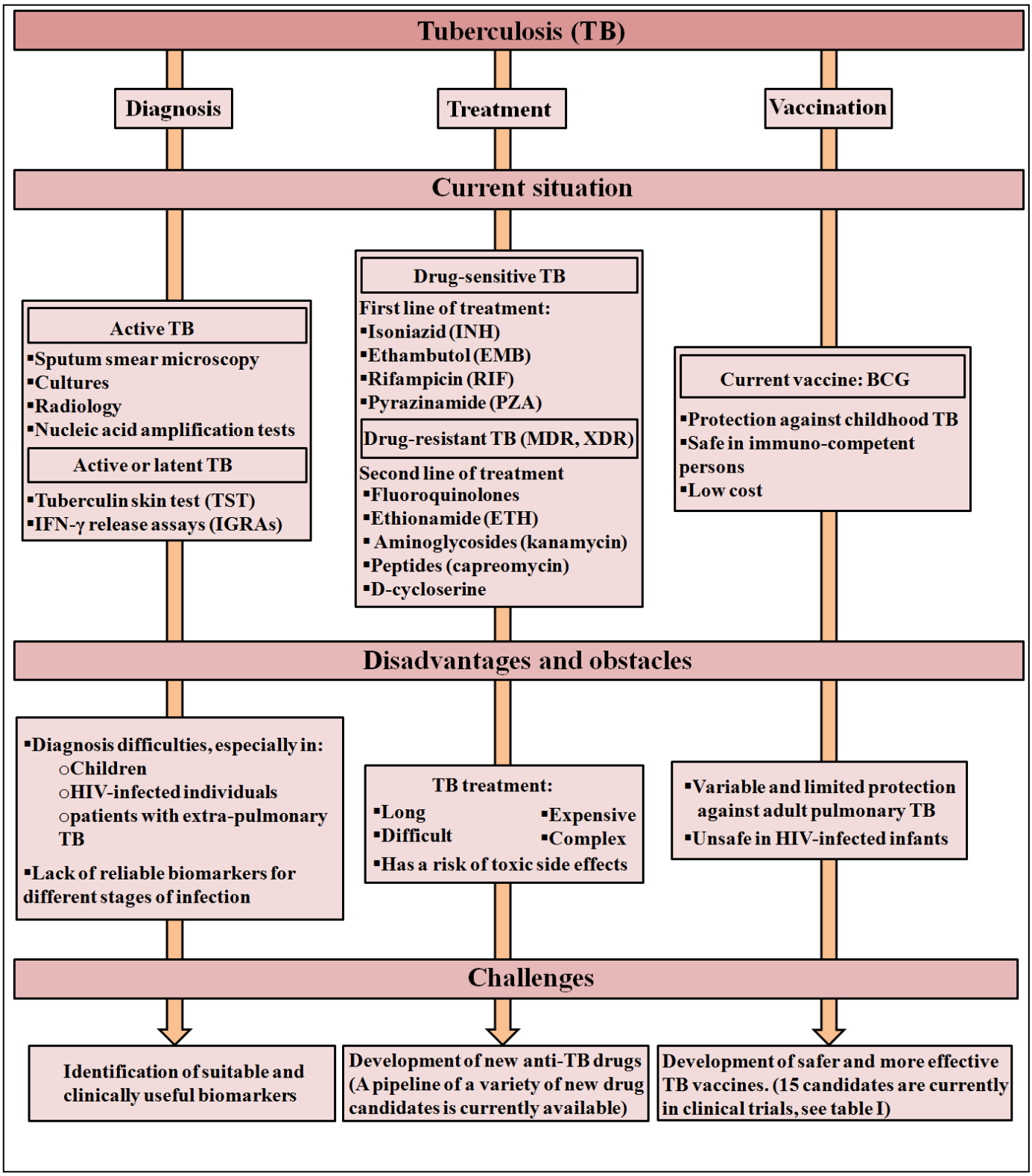

Figure 6: Current situation, obstacles and challenges in TB diagnosis, treatment and vaccination

1.2.5 Tuberculosis treatment

(Fig. 6, middle)

TB is considered as a treatable disease provided that a full course of anti-tubercular drugs is regularly taken. However, treatments of TB are very long, difficult, expensive, complex and have a risk of toxic side effects. Essential anti-TB drugs, discovered in 50's and 60's, are isoniazid (INH), ethambutol (EMB), rifampicin (RIF), and pyrazinamide (PZA). Isoniazid and ethambutol interfere with the biosynthesis of the mycobacterial cell wall by targeting mycolic acids and arabinogalactan, respectively. Rifampicin is an inhibitor of transcription which blocks the synthesis of *Mtb* messenger RNA by inhibiting bacterial RNA polymerase. Pyrazinamide is a prodrug converted by bacterial pyrazinamidase into its active form: the pyrazinoic acid. Recently, Shi et al. found that pyrazinoic acid binds to the ribosomal protein S1 (RpsA) in the ribonucleoprotein complex realizing trans-translation, a key process that ensures high fidelity protein translation. Following error detection, this complex releases ribosomes (scarce in dormant bacteria), while tagging abnormal bacterial proteins for their downstream degradation. Inhibition of trans-translation control by pyrazinoic acid may thus explain the ability of this drug to eradicate persisting Mtb bacilli [45]. These cited four standard anti-TB drugs form the first-line treatment of TB. In drug-sensitive TB patients, treatment involves a combination regimen with an initial phase with all four drugs for the first two months followed by a continuation phase of four months of isoniazid and rifampicin [46] [47] [48]. Such combination is efficacious and up to 95% of people with drug-sensitive TB can be cured in six months with this four-drug regimen [48]. However, several problems may occur including interactions between different TB drugs and interference with the efficacy of HIV-1 antiretrovirals in *Mtb*/HIV-1 co-infected individuals [46]. Moreover, Zhang *et al.* showed that the standard four-drug therapy results in drug resistance in immune-deficient mice [49]. This may present serious implications for the treatment of immuno-compromised individuals such as those with AIDS [46].

Misuse of anti-TB drugs and/or lack of adherence to the treatment regimen allow the emergence of drug resistant *Mtb* strains such as MDR-TB (multidrug-resistant TB) and lately XDR-TB (extensive drug resistant TB). Drug resistant TB treatment requires second-line drugs and is longer, more expensive and more complex than the standard first line with higher toxic side effects. Both MDR-TB and XDR-TB patients can be cured with this second line of treatment, but the likelihood of success of XDR-TB is much smaller than in patients with MDR-TB. Unfortunately, recent last years witnessed the development of strains that are resistant to all anti-TB drugs (totally drug-resistant TB) as reported in Italy, Iran South Africa

and more recently in India [50]. Currently, a pipeline for new anti-TB drugs is advancing with several candidates under clinical investigation [29]. Development and validation of new anti-TB drugs may result in shorter and more effective treatments not only in drug-susceptible but also drug-resistant TB patients. For example, a very recent clinical trial reports positive results for one of these new drugs, delamanid, in people with MDR-TB [51]. Delamanid, also termed OPC-67683 is an inhibitor of mycolic acid synthesis.

1.2.6 Tuberculosis vaccination: current challenges and future strategies

1.2.6.1 Bacille de Calmette et Guérin : success and limitations

(Fig. 6, right)

Currently, BCG is the only available vaccine against TB. This vaccine is a live attenuated strain of *M. bovis* which has lost its virulence, but not antigenicity, by continual passaging in artificial media for years. It was first administered to humans in 1921 in France. Dissemination of the BCG vaccine over many years and geographic regions has led to the derivation of multiple sub-strains.

The attenuation of BCG compared to *Mtb* or *M. bovis* may be explained by genetic deletions. Behr *et al.* showed that 11 regions (encompassing 91 open reading frames) of *Mtb* H37Rv were absent from one or more *M. bovis* strains and that in addition to these deletions, BCG isolates uniformly lack one region and are polymorphic for four other deletions [52]. An important differentially expressed region identified by comparative genomic analyses is a 9.5-kb DNA region called region of deletion 1 (RD1). RD1 is present in virulent *Mtb* and *M. bovis* strains but is deleted in all attenuated BCG vaccine strains suggesting that its deletion was an original attenuating mutation which arose in the derivation of BCG [52] [53]. Deletion of RD1 region from *Mtb* results in attenuation similar to BCG [54]. RD1 encodes components of the mycobacterial ESX-1 specialized protein secretion system. This latter, is responsible for the secretion of two proteins ESAT-6 (early secreted antigenic target-6) and CFP-10 (culture filtrate protein-10) which are important immuno-dominant *Mtb* antigens which elicit potent immune responses.

BCG vaccination consists of a single intradermal dose delivered soon after birth. Important characteristics of BCG are its protective effect, low cost and high safety. BCG confers consistent protection against severe forms of childhood TB including TB meningitis and disseminated TB. Unfortunately, BCG is not able to prevent the establishment of persistent latent TB, and fails to afford protection against the predominant adolescent and adult pulmonary form of TB which accounts for the major burden of global TB mortality and

morbidity worldwide. Different trials showed that BCG has a protective efficacy of between 0 and 80% against pulmonary TB [55]. BCG vaccine may also present additional complications. For example, HIV-infected infants have a higher risk of disseminated BCG disease compared to their uninfected counterparts [56], and HIV infection in infants severely impairs the BCG-induced immune response [57]. BCG may be therefore unsafe and provide little, if any, vaccine-induced benefit in HIV-infected infants. Consequently, BCG vaccination in HIV-infected infants is no longer recommended by WHO.

1.2.6.2 New candidates and strategies for tuberculosis vaccination

Regarding BCG limitations and its safety issues in infants with HIV infection, more effective and safer TB vaccines are urgently needed. 15 candidates are currently evaluating in clinical trials **(Table I)**. Most of them aim to over-express immunodominant *Mtb* antigens in (i) attenuated Mycobacteria (e.g. recombinant BCG), (ii) live, non-replicating viral vectors or (iii) protein/adjuvant formulations [58] [59] [60]. Some of these vaccines (e.g. rBCGΔureC:Hly) aim to induce a broad immune response which includes not only $CD4^+$ but also $CD8^+$ T cell activation. This occurs by the expression of a protein which facilitates the passage of mycobacterial antigens to the cell cytosol, thereby inducing cross-priming (class I antigen presentation). Other vaccines (e.g. Hybrid 56-IC31) express antigens of the dormancy phase of *Mtb* and may thus protect against reactivation of this pathogen. Other TB vaccination strategies rely on the use of detoxified and fragmented *Mtb* bacilli or atypical Mycobacteria (e.g. *M. vaccae*) which provide cross-reactive antigens (shared with *Mtb*) [58].

Additional vaccine candidates in preclinical trials are based on live attenuated *Mtb* strains lacking virulence genes. Examples include MTBVAC01 and *Mtb*ΔRD1ΔpanCD. MTBVAC01 vaccine is based on attenuation of *Mtb* by inactivation of phoP (a virulent transcription factor) and fadD26 (required for the biosynthesis of phthiocerol dimycocerosates) genes [61]. *Mtb*ΔRD1ΔpanCD strain lacks RD1 region and has two mutated genes, panC and panD, required for the synthesis of pantothenate, essential for *Mtb* virulence [62]. Finally a recent report highlights a new vaccine candidate termed IKEPLUS based on the fast grower *M. smegmatis* strain in which the *esx-3* locus encoding for a secretion system was replaced with that of *Mtb* [63].

Vaccine	Status	Description
Recombinant live vaccines		
rBCG30	Phase I (completed)	rBCG expressing the 30 kDa *Mtb* Antigen 85B
rBCGΔureC:Hly (VPM1002)	Phase II	rBCG expressing the lysterial protein listeriolysin (to perforate the phagosomal membrane) and carries a urease deletion (to ensure an acidic pH required for listeriolysin activity in phagosomes)
Aeras-422	Phase I	rBCG expressing perfringolysin and Ag85A, 85B and Rv3407
Subunit and live vector-based vaccines		
Fusion proteins		
M72	Phase II	Recombinant fusion of *Mtb* antigens Rv1196 and Rv0125 and adjuvant AS01 or AS02
Hybrid1-IC31	Phase II	Recombinant fusion of Ag85B-ESAT-6 in IC31 adjuvant
Hybrid 1-CAF01	Phase I	Recombinant fusion of Ag85B-ESAT-6 in CAF01 adjuvant
HyVac4/Aeras-404-IC31	Phase I	Recombinant fusion of Ag85B-TB10.4 in IC31 adjuvant
Hybrid 56-IC31	Phase I	Fusion of Ag85B, ESAT-6, and the dormancy antigen Rv2660 in IC31 adjuvant
Viral vectors-based vaccines		
MVA85A	Phase IIb	Modified vaccinia Ankara vector expressing *Mtb* Ag85A
AERAS 402	Phase IIb	Replication-deficient adenovirus 35 vector expressing *Mtb* antigens 85A, 85B and TB10.4
AdAg85A	Phase I	Replication-deficient adenovirus 5 vector expressing *Mtb* Ag85A
Inactivated whole-cell mycobacterial vaccines		
M. vaccae	Phase III (completed)	Heat-Inactivated *M. vaccae*
(*M. indicuspranii*)	Phase III	Whole cell saprophytic Mycobacterium
M. smegmatis	Phase I (completed)	Whole cell extract
RUTI	Phase II	Detoxified and fragmented *Mtb* in liposomes

Table I: New TB vaccine candidates in clinical trials currently. Adapted from: Tuberculosis vaccine candidates-2011 (Stop TB Partnership Working Group on New TB Vaccines) http://www.tbvi.eu/fileadmin/user_upload/Documenten/News/TB_Vaccine_Pipeline_2011.pdf

Future vaccination strategies must follow two different approaches: pre-exposure and post-exposure vaccination [58] [64] **(Fig.7)**. The former aims at prevent disease in uninfected-individuals while the second intend to inhibit disease reactivation in latent infected-individuals. Moreover, some emerged vaccines (e.g. detoxified and fragmented *Mtb* bacilli or atypical Mycobacteria) may be used as therapeutic vaccines for application after disease development [59] [64] . Pre-exposure vaccines will most likely prevent TB disease, without achieving sterile eradication of *Mtb* bacilli [59] [64]. They contain either recombinant live mycobacterial vaccines such as genetically modified BCG which aim to replace the current BCG or subunit and live vector-based vaccines consisting of recombinant *Mtb* derived-antigens. Importantly, Pre-exposure TB vaccine development is currently focused on the consecutive use of these two types in a so-called "heterologous prime-boost strategy" which combine both formulations. In this strategy, newborns are "primed" with BCG or recombinant/genetically modified BCG and then "boosted" with subunit vaccines delivered in a different way, hence "heterologous" [65].

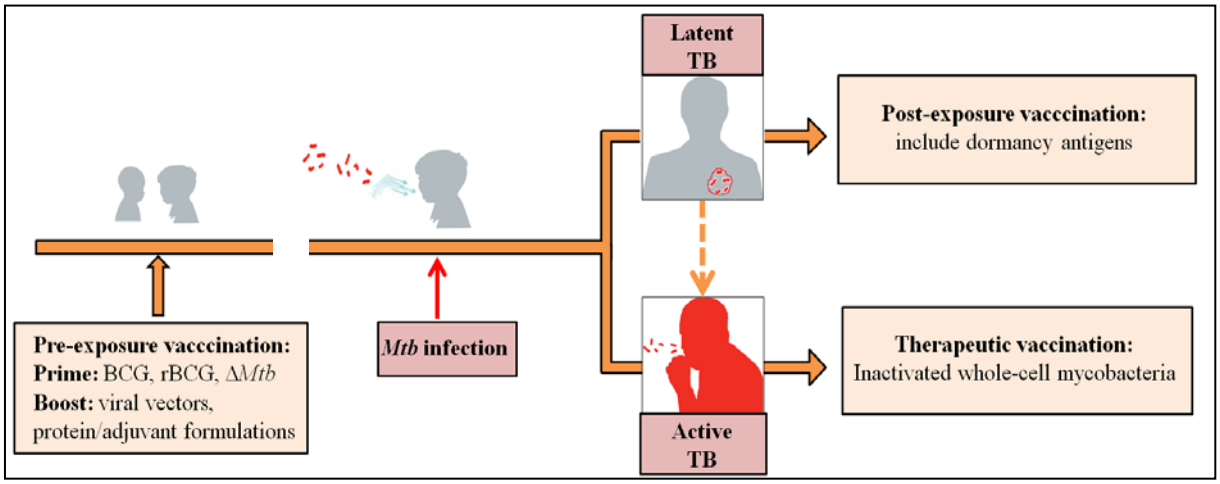

Figure 7: A global view of future TB vaccination strategies. Adapted from ref [60].
Soon after birth, BCG or BCG replacement vaccine (e.g. rBCG) will be given then boosted by viral vectors or protein/adjuvant formulations. Upon infection, latent infected-individuals must be vaccinated with post-exposure vaccines in which it might be an advantage to include dormancy antigens. In persons who develop active TB, inactivated whole-cell mycobacterial vaccines can be used as immuno-therapeutics along with anti-TB drugs.

1.3 Innate response can be not sufficient against *M. tuberculosis*

After inhalation, infectious Mycobacteria are recognized by several host innate receptors known as pattern recognition receptors (PRRs). PRRs are expressed in phagocytes including MPs, DCs and polymorphonuclear neutrophils (PMNs), but also in non immune cells (e.g. lung epithelial cells) which can be also infected. Here we focused on mycobacterial interaction with phagocyte PRRs.

1.3.1 Host innate receptors involved in mycobacterial recognition.

Specific receptors involved in Mycobacterium recognition include TLRs (Toll-like receptors), C-type lectin receptors, NLRs (nucleotide–binding oligomerization domain (NOD)-like receptors), CRs (complement receptors), SRs (scavenger receptors) and other receptors such as FcγR (Fc receptor γ chain) and CD14 [66] [67] [68] [69]. This diversity of PRRs involved in mycobacterial infections may be explained by the complexity of the mycobacterial cell wall.

This panel of PRRs interacts with both opsonized and non opsonized Mycobacteria and some of these interactions regulate bacterial internalization into phagocytes. For example, Bacilli opsonized with complement molecules is internalized via the complement receptor 3 (CR3) [70] while IgG-opsonized Mycobacteria may be internalized through the FcγR (Fc receptor γ chain) [71]. Other receptors such as the mannose receptor (MR) mediate direct uptake of non opsonized Mycobacteria after a direct interaction with their cognate mycobacterial ligands expressed essentially in the cell wall. Receptors of the TLR family are considered as signaling receptors rather than phagocytic receptors and are essentially involved in the modulation of the immune response through the induction of signaling cascades. Several TLR receptors including TLR2, TLR4 and TLR9 were involved in the recognition of mycobacterial ligands. However, whether TLRs are host protective in mycobacterial infection *in vivo* remains unresolved [72].

Mtb infects MPs and DCs by using different receptors of these cells. While CR3 and MR are the main *Mtb* receptors on MPs, this pathogen infects DCs essentially via ligation of the C-type lectin receptor DC-SIGN (dendritic cell-specific intercellular adhesion molecule-3 grabbing nonintegrin) [73]. DC-SIGN was found expressed in freshly isolated human lung DCs. Importantly, mycobacterial antigens were detected within DC-SIGN-expressing cells, possibly DCs, within the lymph nodes of TB patients, suggesting that *Mtb* effectively interacts with DC-SIGN *in vivo* during TB [73]. Additional studies showed that DC-SIGN is

also induced in alveolar MPs of TB patients and constitutes an important receptor for the bacillus in these cells [74]. DC-SIGN interact with mannose-containing motifs of several mycobacterial ligands including ManLAM and α-glucan [75] [73]. Internalized Mycobacteria and their derived-components can also interact with endosomal receptors such as TLR9 and cytosolic receptors such as the NLR family member NOD2. TLR9 may recognize CpG motifs from mycobacterial DNA [76] while NOD2 senses muramyl dipeptide, a component of bacterial peptidoglycan [77].

1.3.2 Mycobacterium-receptor interactions determine infection outcomes

The signaling pathways activated by innate receptors direct host responses and cytokine secretion, thereby dictating the outcome of infection. Although recognition of *Mtb* may be beneficial for the host in that it activates innate immune responses, it may also allow mycobacterial persistence and development within host phagocytes. Indeed, while receptors such as TLRs may elicit pro-inflammatory signals, others such as the mannose receptor repress inflammatory signals and may thus contribute to bacterial persistence [67]. Early studies suggested that DC-SIGN might enable *Mtb* to escape the immune system [78]. However, recent *in vivo* findings in the murine model suggest that this receptor mediates protection against *Mtb*, possibly through the secretion of pro-inflammatory cytokines including tumor necrosis factor (TNF) [79].

1.3.3 Mycobacteria resist phagocytosis-induced destruction

Phagocytosis of a pathogen results normally in its destruction and clearance. However, *Mtb* has developed several strategies to escape phagocytosis-mediated destruction.

1.3.3.1 Phagosome maturation

Phagocytosis is the cellular engulfment of large particles (≥ 0.5 µm in diameter) into a phagosome, generated from the cell plasma membrane [80]. The phagosome undergoes then sequential fusion and fission events with components of the endocytic pathway. This process, known as phagosome maturation, leads to the modification of the composition of the phagosomal membrane and contents [80]. During maturation, phagosome progress in three essential stages: early phagosome, late phagosome and the phagolysosome **(Fig. 8)**.

Nascent phagosome interacts firstly with early endosome to form an early phagosome expressing Rab5, a member of the Rab GTPases (guanosine triphosphate phosphohydrolase). Rab5 recruits additional effectors such as VPS34 and EEA1 (early endosomal antigen). VPS34 is a kinase which catalyzes the generation of phosphatidylinositol 3-phosphate (PI3P)

on endosomal membranes [81]. PI3P promotes proper membrane trafficking events within the endosomal system and ablation of VPS34 kinase activity dramatically impairs phagosome maturation [81]. Phagocytosis is accompanied by the increase in cytosolic Ca^{2+} required to the activation of VPS34 and subsequent PI3P production [82]. This occurs through the Ca^{2+}-binding protein calmodulin which associates with various effector proteins including CaMKII ($Ca^{2+/}$calmodulin kinase II). EEA1, which promotes the fusion of cellular organells [83] is recruited to endosomal membranes by both Rab5 and PI3P [84].

Early phagosome progresses to a more mature stage leading to the formation of late phagosome. These organelles interact with late endosomes and are characterized by the acquisition of distinct markers including lysosomal-associated membrane proteins (LAMPs) 1 and 2, the small GTPase Rab7 and the Rab7-interacting lysosomal protein (RILP), which replace the early phagosomal markers such as Rab5 [80].

The terminal step of phagosome maturation is the biogenesis of the phagolysosome, formed as a result of the fusion of late phagosome with lysosomes. phagolysosomes showed a highly acidic and oxidative milieu and contain destructive lysosomal enzymes necessary for target degradation [80].

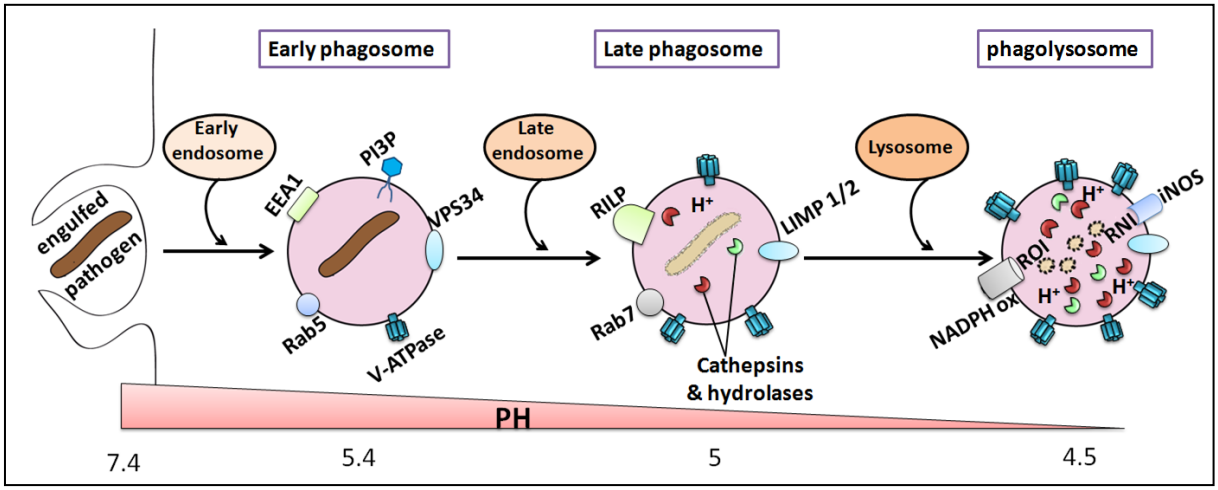

Figure 8: Essential steps of phagosome maturation and phagolysosome formation.
Each step is characterized by specific membrane markers. Accumulation of V-ATPases gradually acidifies phagosomal organelles. Within phagolysosomes, low pH, cathepsins, hydrolases, ROI and RNI induce collectively pathogen degradation and destruction.

1.3.3.2 Acidification and microbicidal properties of phagolysosomes

phagosome maturation is associated with a gradual acidification of these organelles due to delivery of H^+ protons into the phagosomal lumen via the multi subunit protein-pump complex vacuolar ATPase (V-ATPase) **(Fig. 8)**. The acidic milieu promotes phagosomal

destructive properties by restricting microbial growth and activating proteolytic enzymes such as cathepsins. Moreover, mature phagosomes produce reactive oxygen and nitrogen intermediates (ROI and RNI) which play important roles in phatogen destruction [80]. ROI are produced by the NADPH oxidase (nicotinamide adenine dinucleotide phosphate oxidase) enzyme. NADPH oxidase is composed of a membrane-bound catalytic core comprised of $gp91^{phox}$/NOX2 and $p22^{phox}$, and four cytosolic proteins ($p40^{phox}$, $p47^{phox}$, $p67^{phox}$ and Rac2) [85]. In unstimulated cells this complex is unassembled. However, once phagocytes are activated, cytosolic proteins translocate and associate with the catalytic core resulting in a fully functional enzyme which catalyzes the formation of superoxide anions (O_2^-). Then O_2^- dismutates H_2O into hydrogen peroxide (H_2O_2), a reactive component that generates toxic hydroxyl radicals (ROI). RNI production requires iNOS (inducible nitric oxide synthase) which generate nitric oxide (NO), a toxic product *per se*, which can also react with ROI to form additional toxic RNI. ROI and RNI act in synergy to damage vital microbial molecules and impair bacterial growth [86].

Overall, phagosomes undergo maturation and acidification to convert into potent microbicidal organelles central to pathogen clearance and host protective responses.

1.3.3.3 M. tuberculosis blocks phagosome maturation and acidification

Mtb exploits phagocytosis through a variety of effector molecules which alter phagosome maturation and ensure bacterial persistence **(Fig. 9)** and **(Table II)** [87]. *Mtb*-carrying phagosome expresses the early Rab5 but not the late Rab7 phagosomal marker suggesting that it is arrested at the early stage of maturation [88]. The recruitment of Rab5 effectors, EEA1 and VPS34 to the mycobacterial phagosomes is also greatly impaired [89]. Consequently, VPS34-dependent PI3P generation and accumulation are reduced. A recent report showed that the mycobacterial nucleoside diphosphate kinase (Ndk) inhibits phagosome maturation through the inactivation of both Rab5 and Rab7 and the inhibition of the recruitment of their respective effectors EEA1 and RILP [90].

Mycobacterial LAM inhibits the activity of VPS34 which generates PI3P most likely by preventing the increase in Ca^{2+} fluxes and by interfering with the Ca^{2+}/calmodulin/CaMKII pathway within the infected cells [82]. Another mycobacterial product called SapM (secreted acid phosphatase of *Mtb*) dephosphorylates and removes PI3P from the phagosome, thus inhibiting fusion with late endosomes/lysosomes [91]. By preventing PI3P accumulation on the phagosomal membrane, LAM and SapM also alter the PI3P-dependent recruitment of EEA1 which is strengthened by its binding to PI3P [89] [84].

Mtb possesses the protein tyrosine phosphatase (PtpA) which interferes with host trafficking processes by dephosphorylating VPS33B (vacuolar protein sorting 33B), a regulator of membrane fusion [92]. PtpA is also involved in the blockage of phagosome acidification by binding to subunit H of V-ATPases, thus excluding these proton pumps from the phagosome during infection [93].

Mycobacterial lipoamide dehydrogenase C (LpdC) interacts with a host actin-binding protein called coronin-1 /TACO [94]. In normal conditions, coronin-1 associates transiently with normal phagosomes. Strikingly, it remains retained by Mycobacterial phagosomes, and this prevents phagosome maturation and cargo delivery to lysosomes [95]. It was proposed that Coronin-1 retention on phagosomes activates the Ca^{2+}-dependent phosphatase calcineurin, which blocks phagosome-lysosome fusion [96]. Retention of coronin-1 by mycobacterium containing phagosome was identified in murine MPs. However, a report showed that this is not the case in human MPs and authors suggest that other proteins or lipids are responsible for the block in phagosome maturation in these cells [97].

Mtb also uses a secreted serine/threonine protein kinase G (PknG) to mediate phagosome maturation inhibition. In MPs, PknG is secreted within phagosomes, accesses the cytosol and inhibit phagosome-lysosome fusion [98]. The mechanism of cytosolic translocation of PknG and its precise action on host trafficking machinery are unclear. However, it was proposed that PknG may act through the phosphorylation of an unknown host protein thereby preventing its activity in carrying out phagosome-lysosome fusion [96].

In addition to studies that identify individual bacterial components which block phagosome maturation and acidification, other studies used various genome-wide approaches to identify mycobacterial virulence factors involved in this blockade process. Such studies mainly rely on genetic screens that facilitate the isolation of mutants defective in arresting the maturation of their phagosomes [99] [100] [101]. For example, a recent study which combines such screening technologies with automated confocal microscopy analyzed an 11,180-member mutant library and identifies ten mutants that had lost their ability to resist phagosome acidification [101]. Importantly, molecular characterization of these mutants revealed that they carry genetic disruption in genes involved in cell envelope biogenesis, ESX-1 secretion system, molybdopterin biosynthesis and production of acyltrehalose-containing glycolipids. Such approaches which investigate microbial virulence genes involved in phagosome maturation arrest are useful for the study of intracellular parasitism by different pathogenic microorganisms, to identify new targets for vaccines as well as to discover new anti-microbial drug.

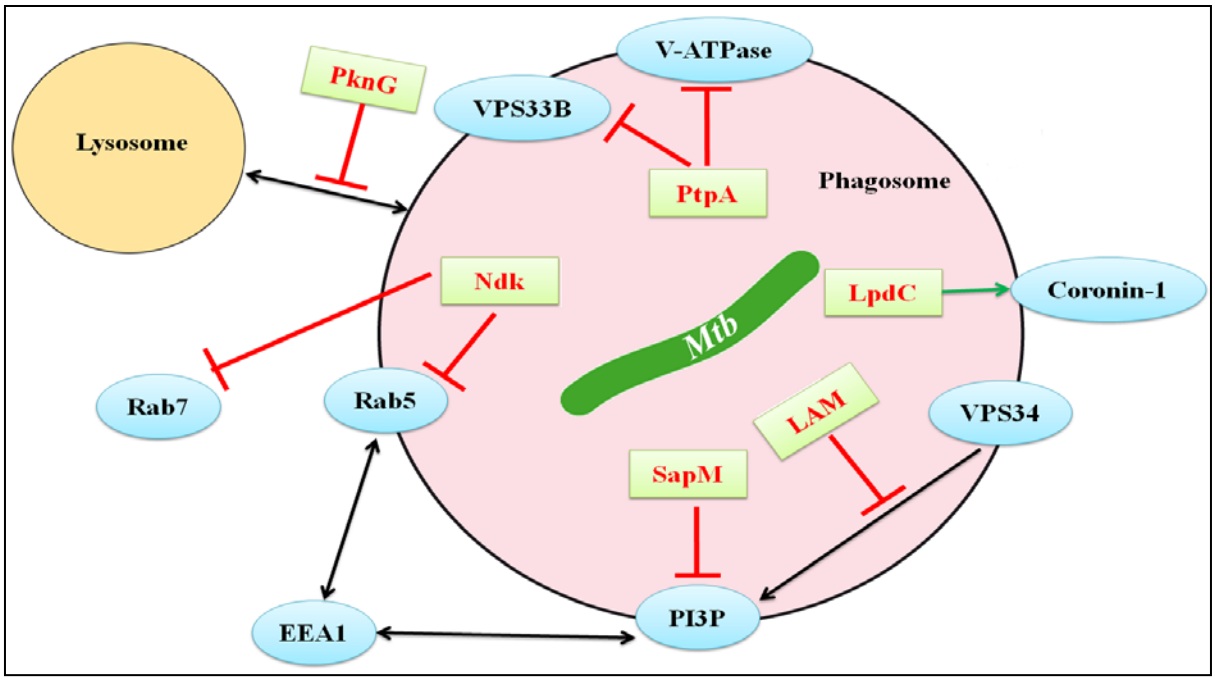

Figure 9: Effector mycobacterial molecules (green) **involved in the arrest of phagosome maturation and acidification with indication of their host targets** (blue).

effector	Mechanism	Ref
Ndk	Inactivates Rab5 and Rab7, thereby inhibiting their respective effectors recruitment	[90]
LAM	Interferes with the Ca^{2+}/calmodulin/CaMKII pathway, suppressing VPS34 activation	[82]
SapM	Hydrolyzes PI3P, inhibiting phagosome-late endosome fusion	[91]
PtpA	Dephosphorylates VPS33B, arresting phagolysosome fusion	[92]
	Blocks V-ATPase trafficking and phagosome acidification	[93]
LpdC	Retains coronin-1 on the phagosomal membrane, arresting phagosome maturation possibly via calcineurin activation	[94] [96]
PknG	Possibly phosphorylates a host molecule, preventing its activity in mediating phagosome-lysosome fusion	[96, 98]

Table II: Effector mechanisms suggested to be used by pathogenic Mycobacteria to block phagosome maturation and acidification

1.3.3.4 *Mtb counteracts the toxic microbicidal effects of ROI and RNI*

Activation of infected phagocytes by inflammatory signals such as IFN-γ enables them to overcome the inhibition of phagosome maturation and promote RNI and ROI production. However, *Mtb* has evolved several strategies to detoxify and scavenge ROI and RNI **(Fig. 10)** [102].

Mycobacterial LAM is a potent scavenger of toxic oxygen free radicals [103]. *Mtb* produces also the catalase peroxidase KatG, which can deactivate ROI by decomposing hydrogen peroxide (H_2O_2) into water and oxygen [104]. *Mtb* lacking katG displayed no catalase activity and was hyper susceptible to H_2O_2 in culture [104]. A variety of mechanisms contribute also to *Mtb* resistance to toxic effects of RNI and nitrosative stress. *Mtb* truncated hemoglobin, HbN, is a nitric oxide scavenger which, due to its nitric oxide dioxygenase activity, very efficiently converts NO into harmless nitrate [105]. *Mtb* encodes also a proteasome which promotes its defense against RNI possibly by functioning in the elimination or refolding of proteins damaged by RNI [106] [96]. More recently, it was shown that mycobacterial coenzyme F_{420} reduced and converted NO_2 back to NO and might thus protect *Mtb* from nitrosative damage as this pathogen is more sensitive to NO_2 than NO under aerobic conditions [107].

Finally, it is important to note that *Mtb* may block the initial event which promotes phagocyte activation and phagosome maturation such as IFN-γ stimulation. Indeed, *in vitro*, *Mtb* uses two distinct components, the 19-kDa lipoprotein and the cell wall PG, to inhibit the IFN-γ signaling pathway in human and murine MPs at a transcriptional level [108].

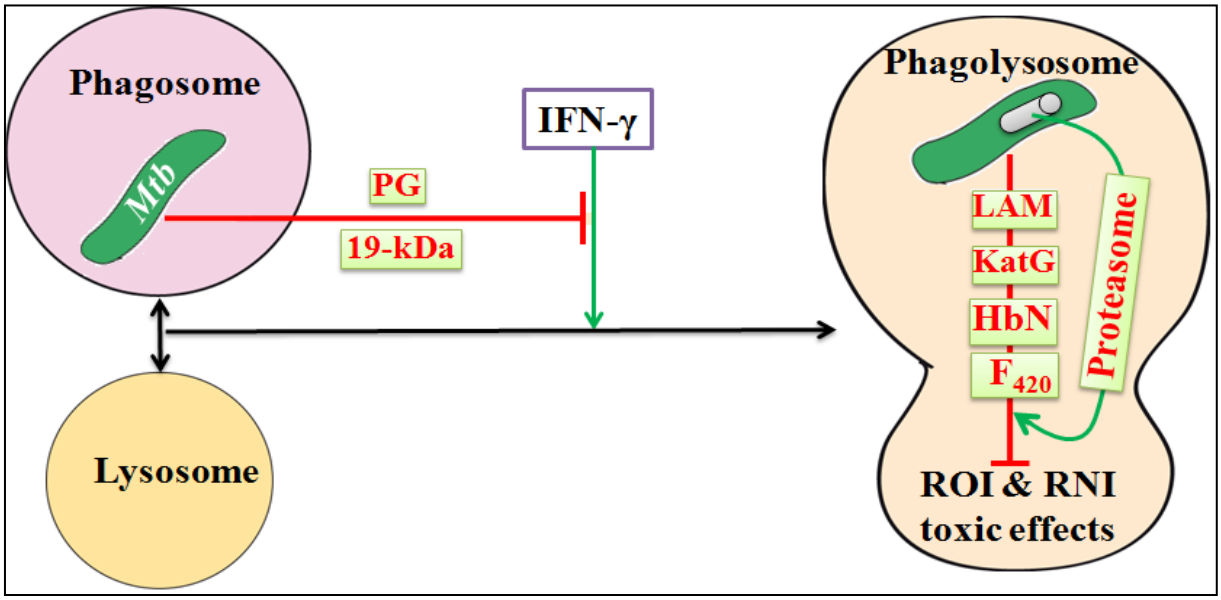

Figure 10: Mycobacterial molecules involved in the blockage of IFN-γ signaling and the counteraction of ROI and RNI toxic effects.

1.3.4 Innate cells involved in anti-mycobacterial responses (Fig. 11)

1.3.4.1 Differential growth of M .tuberculosis in resident phagocytes

In the alveolar lung space, *Mtb* bacilli are rapidly surrounded by resident airway myeloid phagocytes such as alveolar MPs and DCs. Alveolar MPs have been considered as the first immune cells to encounter and engulf the bacilli, and the vast majority of TB literature has focused on the interactions of *Mtb* with this cell type. However, DCs are present as a dense network in the airway mucosa and several *in vitro* and *in vivo* studies showed that they internalize and respond to Mycobacteria. *In vitro*, uptake of *Mtb* and BCG activate human monocyte-derived DCs [109] [110]. *In vivo*, using green fluorescent protein (GFP)-labeled BCG, it was shown that bacilli not only infect alveolar MPs but also DCs in the murine lungs [111]. Myeloid DCs are one of the major cell populations infected with *Mtb* in mouse lungs and lymph nodes [112]. Importantly, in addition to lung resident DCs, murine monocyte-derived DCs are recruited to the lung interstitium from the bloodstream and take up live GFP-labeled BCG bacilli within 48 h of intranasal infection [113].

In their resting state, infected MPs form the primary host cell for *Mtb* replication. In such cells, *Mtb* blocks phagosome maturation and acidification to evade killing. Moreover, *Mtb*-containing phagosomes in MPs showed permanent fusion events with host cell endosomes, thereby ensuring continuous access of the pathogen to extracellular nutrients [114]. In contrast, studies with both murine and human DCs showed that these cells are not permissive for intracellular mycobacterial growth, even though bacilli are not killed [115] [116]. Tailleux *et al.* showed that, as observed in MPs, *Mtb*-containing vacuoles are not acidic and don't fuse with lysosomes in human DCs [116]. However, these vacuoles have no access to DC recycling endosomes and biosynthetic pathways in contrast to that observed within MPs. Authors suggest that this process impairs access of intracellular Mycobacteria to host molecules including possible essential nutrients such as iron and cholesterol, resulting in constrained intracellular survival of *Mtb* in DCs [116]. More recently, transcriptomic approaches which study simultaneous gene expression of both the host and the pathogen showed that *Mtb* induces differential responses in human MPs and DCs, and respond differently to phagocytosis by these two cell types [117]. These studies suggest that, in comparison to MPs, DCs restrict access of intracellular Mycobacteria to important nutrients. On the pathogen side, many mycobacterial genes overexpressed in DCs are known to be induced during dormancy *in vivo*, during nutrient starvation and in limiting O_2 conditions.

Therefore, *Mtb* perceives the DC phagosome as a well constraining environment in which it develops a clear mycobacterial stress response signature and probably a dormancy genetic program. In contrast, *Mtb* gene expression inside MPs reflects a profile of replicating bacteria.

1.3.4.2 Resident phagocytes initiate inflammation and recruit neutrophils and innate lymphocytes

Innate interaction and internalization of *Mtb* by resident MPs and DCs, results in the secretion of several pro-inflammatory cytokines and chemokines [118] **(Fig. 11)**. Among others, the wide range of pro-inflammatory mediators induced after *Mtb*-interaction with MPs and DCs include TNF-α, IL-12, IL-15, IL-18 and IL-23 cytokines as well as CXCL8/IL-8, CCL2, CCL3 and CCL5 chemokines [118] [119] [120]. Consequently, focal infected phagocytes attract and activate additional innate inflammatory cells. TNF-α orchestrates early induction of chemokines which recruit additional leukocytes to control mycobacterial infection as shown in the murine model [121]. CXC chemokines such as CXCL8 sustain the intense recruitment of PMNs to the site of infection. At this early stage, IL-12, IL-15 and IL-18 stimulate IFN-γ-production by γδ T, NK (natural killer) and NKT (natural killer T) cells while IL-23 stimulate IL-17A secretion by γδ T cells [122]. However, *Mtb* may also induce the production of anti-inflammatory mediators which impair the host response but also limit tissue destruction [118]. For example several studies showed that the anti-inflammatory cytokine IL-10 was produced by murine and human MPs after phagocytosis of Mtb [123] [124]. IL-10 can promote *Mtb* survival by blocking phagosome-lysosome fusion in infected phagocytes, down-regulating IL-12 secretion and antagonizing MP activation [125] [126].

1.3.4.3 Cooperation between resident and recruited phagocytes

Although both clinical and experimental studies have shown that acute pulmonary TB is accompanied by an influx of PMNs, the exact role of these cells in host defense against *Mtb* remains conflicting and poorly understood [127]. Recruited PMNs internalize Mycobacteria, and were recently shown to be the predominant cell type infected with *Mtb* in the airways of TB patients [128]. While some studies using antibody-mediated depletion of murine PMNs advocate a role for these cells in TB control, others do not [72]. Moreover, whether PMNs play a role in *Mtb* killing remains controversial. Indeed, while some reports suggest that these cells kill or restrict the growth of *Mtb* in both mouse and humans, other studies showed that they form a permissive site for active replication of the bacilli (reviewed in [127]). However, PMNs recruited to the infection sites produce TNF-α and additional chemokines, amplifying thus the initial innate response [119].

DCs infected with Mycobacteria undergo maturation and travel to lymph nodes where they activate host naïve lymphocytes, thus linking innate and adaptive immune responses. *In vivo*, mice with deficient DC migration from the lungs to the lung draining lymph nodes fail to induce naïve T cell activation [129]. However, *Mtb* may also use DCs as a vehicle to spread inside the host, as migration of *Mtb*-containing DCs to lymph nodes may contribute to its extra-pulmonary dissemination. Importantly, in a study using a murine model of intradermal infection with BCG expressing enhanced GFP, the group of N. Winter showed that PMNs carried BCG from the skin into the draining lymph nodes [130]. BCG-infected PMNs activated DCs via physical interactions and this cooperation promoted human and mouse T cell responses *in vitro* [131]. More recently, a study showed that murine PMNs are mandatory for efficient DC migration from the lung to mediastinal lymph nodes *in vivo* [132]. The authors suggest that PMNs deliver *Mtb* to DCs and this process promote DC migration and T cell responses.

Previous *in vitro* studies showed that human MPs and PMNs infected with *Mtb* undergo apoptosis [133] [134] [135]. In this context, it has been observed that apoptotic vesicles containing mycobacterial antigens can be engulfed by bystander DCs facilitating thus their presentation through MHC-I and CD1 molecules, a process referred to as cross-presentation [133] [136]. Phagocytosis of Mtb-induced apoptotic PMNs by other phagocyte can also promote inflammatory responses. For example, it up-regulates the production of TNF-α by human MPs [134] [135] and induced functional maturation and activation of human DCs [137].

1.3.4.4 The role of innate lymphocytes

Innate NK, γδ T and NKT are involved in the activation of *Mtb*-infected phagocytes, essentially through IFN-γ secretion, thereby promoting their bactericidal functions (e.g. ROI and RNI production).

Human NK cells can be activated and produce IFN-γ by direct binding of their NKp44 receptor to the mycobacterial cell wall, although the ligand remains undetermined [138]. In *Mtb*-infected mice, NK cells increased in the lungs over the first 21 days and produce IFN-γ [139]. In the same way, the pleural fluid of patients with TB pleurisy is enriched for NK cells which form the predominant source of IFN-γ [140].

In healthy humans, the majority of γδ T cells express Vγ9Vδ2 TCRs. They recognize phosphorylated antigens (phosphoantigens), and mycobacterial phosphoantigens were identified as potent stimulators of Vγ9Vδ2 T cell functions [141]. *In vitro*, human γδ T cells

are an important source of IFN-γ production in the presence of *Mtb*-infected monocytes [142] and γδ T cells from BCG-infected mice proliferate and produce IFN-γ upon stimulation with *Mtb* [143]. More recently, it was shown that murine γδ T cells are an important source of the pro-inflammatory cytokine IL-17A following mycobacterial infections in both mice and humans [122] [144] [145]. *In vitro*, murine γδ T cells produce IL-17A facing to DCs provided that they were infected with *Mtb* and produced IL-23 [122]. IL-17A induces the release of CXC chemokines especially from epithelial cells, thereby promoting PMN recruitment [120].

NKT cells recognize glycolipid antigens presented by CD1d molecule. They are divided into two subsets: diverse NKT with diverse TCR rearrangement, and invariant NKT (iNKT) showing a highly conserved TCR rearrangement. Mycobacterial PIM is recognized in a CD1d-restricted fashion by murine and human NKT cells resulting in IFN-γ release [146]. *In vitro*, *Mtb*-infected murine MPs activate iNKT cells, which in turn produce IFN-γ that stimulate NO production by infected-MPs, thus suppressing *Mtb* growth [147].

In vitro studies showed that innate lymphocytes play also a direct role in the destruction of *Mtb*-infected cells. *In vitro*, human NK cells were able to directly lyse *Mtb*-infected monocytes and alveolar MPs. This depends on the NK receptors NKG2D and NKp46, which respectively bind to stress-induced ligand protein and vimentin expressed by infected mononuclear phagocytes [148]. However, the mechanism by which NK cells lyse *Mtb*-infected cells is unclear, and it was proposed that it is independent from both cytotoxic granule release (perforin/granzyme/granulysin system) and Fas/Fas ligand-dependent mechanisms [149]. Human Vγ9Vδ2 T cells kill *Mtb*-infected MPs and intracellular bacilli through perforin and granulysin, *in vitro* [150] [151]. These cells were also able to kill extracellular *Mtb*, in a perforin-independent, but granulysin-dependent mechanism [151]. In the same way, *in vitro*, human activated NKT cells exerted lytic activity and restricted the growth of intracellular *Mtb* within phagocytic cells in a mechanism which potentially depends on granulysin secretion [152].

Despite *in vitro* evidences of a role of innate lymphocytes against *Mtb*, *in vivo* studies suggest that innate lymphocytes may not be required for optimum anti-mycobacterial responses. Indeed, mouse models in which NK cells are defective or are depleted *in vivo* showed that NK cells are not essential for immunity to TB [139]. In the same way, although mice lacking γδ T cells were more susceptible to *Mtb* in high dose intravenous infection models [153], they showed similar survival and bacterial containment to that of WT animals in low dose aerosol infection models [154]. Previous studies suggest also that mice deficient in NKT cells or CD1d molecule required for NKT cell antigen presentation were not

significantly different in their susceptibility to infection than control mice. However more recent studies showed that adoptively transferred iNKT cells mediate protection against *Mtb* infection in mice, suggesting an *in vivo* contribution of these cells to host defense [147]. The cytotoxic activity of innate lymphocytes may be also impaired *in vivo*. For example, the lytic function of NK cells isolated from TB patients was reduced and may be modulated by monocyte-secreted regulatory cytokines such as IL-10 [155]. Moreover, although *in vitro* studies showed that perforin is required for *Mtb* killing by some innate lymphocytes, *in vivo* studies reported that the course of *Mtb* infection in perforin deficient mice is the same as reported in WT animals [156] [157]

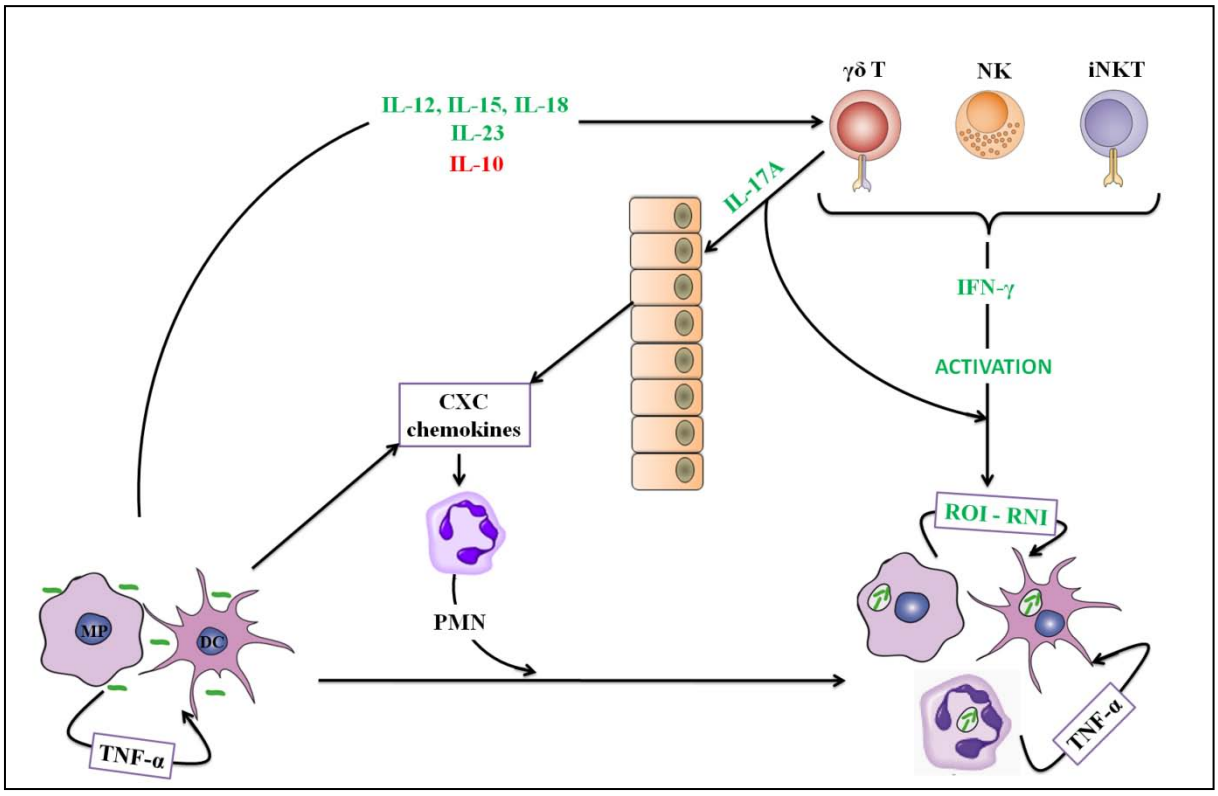

Figure 11: Innate host effectors and responses against *Mtb*.

In response to *Mtb*, alveolar MPs and resident DCs are rapidly activated and release several pro-inflammatory cytokines and chemokines leading to the recruitment and activation of both PMN and innate lymphocytes (γδ T, NK and iNKT cells). *Mtb*-infected phagocytes produce also the anti-inflammatory cytokine IL-10 which can circumvent the protective host response. PMN amplify the anti-mycobacterial response by the release of several inflammatory mediators including TNF-α. γδ T cells produce IL-17A which activates epithelial cells to release CXC chemokines, thus increasing PMN recruitment. Innate lymphocytes are an important early source of IFN-γ which synergizes with TNF-α to promote the bactericidal functions of phagocytes through the induction of ROI and RNI.

1.3.5 Processing of intracellular mycobacterial antigens

Phagocytes are antigen-presenting cells (APCs) which can present *Mtb*-derived antigenic peptides to adaptive T lymphocytes. The pivotal role in this process is played by DCs which travel to lymph nodes where they encounter and stimulate naïve T cells. APCs present *Mtb* peptides by several pathways involving major histocompatibility complex class II (MHC-II), MHC-I and CD1 molecules. This leads to the activation of different T cell populations.

1.3.5.1 Classical MHC-II direct presentation is biased by Mtb

MHC-II molecules are synthesized and assembled in the endoplasmic reticulum (ER) then transported to endosomes and phagosomes. During phagosome maturation, proteins from captured pathogens are degraded into peptides able to associate with MHC-II molecules. The resulting peptide-MHC-II complexes are then transported to the cell surface for presentation to αβ $CD4^+$ T cells.

Following phagocytosis, residence of *Mtb* within the phagosomal compartment can ensure that mycobacterial antigens have access to the MHC-II antigen-processing/presentation machinery [158]. However, *Mtb* may block the presentation of its peptide antigens by MHC-II molecules using different mechanisms including reduced transcription and surface expression of these molecules [159]. *Mtb* interferes also with phagosome maturation and functions, essential for MHC-II-dependent presentation [159]. Nevertheless, arrest of phagosomal maturation by *Mtb* is incomplete and some phagosomes mature to form phagolysosomes, especially in activated phagocytes (e.g. IFN-γ-stimulated cells) [158]. The presentation of *Mtb* antigens by MHC-II molecules is reflected by the activation of αβ $CD4^+$ T cell which play important protective roles against *Mtb* **(see 1.4.3.3).**

1.3.5.2 Presentation of M. tuberculosis antigens by MHC-I and CD1a molecules

MHC-I and CD1 molecules share structural similarities in that they are formed of a heavy α chain non-covalently associated with a light β_2-microglobulin (β_2m) chain. Both chains are synthesized and assembled in the ER.

MHC I-restricted T cells are $CD8^+$ lymphocytes while the CD1-restricted T cells express either CD4, CD8, both or none of these co-receptors. MHC-I molecules bind peptides that come from cytosolic antigens degraded through the proteolytic activity of the cell proteasome and transported into the ER by transporter proteins called TAP (transporter associated with antigen processing). In contrast, CD1 molecules bind self or foreign lipids for presentation to T cells. As described before, the mycobacterial cell wall contains abundant

and diverse lipids. A variety of these molecules can be processed and presented by both group I (CD1a, CD1b and CD1c) and group II (CD1d) CD1 molecules **(Table III)**. CD1 molecules may bind mycobacterial lipid-derived antigens in different endosomal and phagosomal compartments because they have contact with the phagosomal continuum at different stages of its maturation [158] [160].

Mycobacterial antigen	CD1 isoform
Mycolic acids	CD1b
Glucose monomycolate (GMM)	CD1b
Sulpholipid (diacylated sulphoglycolipid)	CD1b
Phosphatidylinositol mannosides (PIMs)	CD1b, CD1d
Mannosylated lipoarabinomannan (ManLAM)	CD1b
Mannosyl-β1-phosphomycoketides (MPM)	CD1c
Didehydroxymycobactin (DDM)	CD1a

Table III: Mycobacterial lipid antigens recognized and presented by CD1 molecules. From ref [161].

$CD8^+$ T cells specific for mycobacterial antigens are detected in TB patients, indicating active MHC-I-dependent presentation of *Mtb* peptides [162]. However, as MHC-I molecules present only cytosolic-derived peptides, it was unclear how *Mtb*, believed to be restricted to phagosomes, could stimulate these cells. Currently, several findings may explain how this occurs. Among them, the process of cross-presentation is strongly believed to be relevant to *Mtb* infection [163]. Cross-presentation allows the presentation of antigens from phagosome-enclosed pathogens (e.g. Mycobacteria) on MHC class I molecules and stimulate $CD8^+$ T-cell immunity. This may occur through a direct passage of mycobacterial antigens from the phagosome to the cytosol. Indeed, it was suggested that Mycobacteria permeabilize the phagosomal membrane allowing bacterial proteins < 70 kDa in molecular size to cross the phagosomal membrane [164] [165]. This process may involve mycobacterial secretion systems and their proteins such as ESX-1 and ESAT-6 in *Mtb* [166] or other ESX complexes and ESAT-6 homologues in other Mycobacteria [163]. Another possibility relies on a role of apoptotic bodies generated by *Mtb*-infected MPs or PMNs and captured by bystander DCs to facilitate the cross-presentation of *Mtb* antigens [133] [136]. Within DCs, *Mtb* antigens loaded in apoptotic bodies may be released into the cytosol through several mechanisms. One

possibility is the fusion between the apoptotic body and ER membrane resulting in the transport of *Mtb* antigens by TAP into the cytosol. Peptide antigens may thus gain access to the proteasome and are then processed and presented by the MHC-I machinery. Apoptotic bodies from BCG-infected murine MPs injected in mice cross-prime CD8 T cells *in vivo*, and this process requires homing of DCs to draining lymph nodes [167]. Remarkably, vaccination with these apoptotic bodies generated immunity that protected mice against challenge with virulent *Mtb*.

As host cell apoptosis promotes cross-presentation and protective anti-mycobacterial responses, virulent *Mtb* might inhibits apoptosis and triggers necrosis in a process which depends on prostaglandin E2 (PGE_2) inhibition. Prostaglandin induce plasma membrane repair and prevent mitochondrial damage; together these events protect infected macrophages against necrosis and instead promote apoptosis. Recent findings showed that virulent *Mtb* strongly induces the production of lipoxin A_4 (LXA_4), which prevents PGE_2 biosynthesis [168]. Without the protective actions of PGE_2, the infected MP is more likely to undergo necrosis which allows for the bacteria to escape into the extracellular space and infect surrounding MPs. Necrosis-induced death prevents the cross-presentation of *Mtb* antigens by DCs and alters the initiation of T cell immunity [169]. However, viable Mycobacteria released after necrosis can be also phagocytosed by DCs. In these experiments, cross-presentation through apoptotic bodies was not possible since necrosis of infected cells replaced apoptosis. Source of Mycobacterium antigen for cross-presentation can only come from phagosomes. Therefore, absence of cross-priming may signify that *Mtb* antigens cannot cross the phagosomal membrane to be cross-presented, apoptosis of infected cells is required for efficient cross-presentation.

Importantly, in addition to mycobacterial proteins, apoptotic bodies contain glycolipid antigens of these bacilli. In general, group I CD1 molecules are only highly expressed on DCs. Therefore, transfer of mycobacterial lipid antigens from infected MPs to DCs through apoptotic bodies may represent a key mechanism in promoting cross presentation of CD1-dependent antigens. This process is involved in the presentation of *Mtb* -derived lipids by CD1b [133]. However, *Mtb* infection can cause a reduced CD1 transcription and cell surface expression, thus interfering with this pathway [159].

1.4 The anti-mycobacterial adaptive immunity relies on a granulomatous response

Innate immunity to *Mtb* represents the initial stage of the host response which may be successful in the people who are not latently infected. However, it is not sufficient to fully control *Mtb* in infected individuals and a next stage of host response is therefore required. This second stage is characterized by the emergence of cell-mediated adaptive immunity and the formation of specific histological structures called granulomas. Classically, these structures are considered as protective structures which imprison Mycobacteria and prevent further dissemination of the disease in the short term.

1.4.1 Structure and cellular composition of granulomas

Granulomas are small nodules classically described as compact collections of mature mononuclear phagocytes which may or may not be accompanied by accessory features such as infiltration of other inflammatory leukocytes or necrosis [170]. In addition to TB, granulomas are described in several inflammatory disorders. Part of them is formed following other infections such as schistosomiasis granulomas, others appears after foreign body reaction, and finally some granulomas of unknown etiologies such as crohn's disease, sarcoidosis and Langerhans cell histiocytosis (LCH) destroy the host tissues through an immunopathological process. In TB granulomas, myeloid cells exhibit several phenotypes including DCs [171], epithelioid MPs, foamy MPs, and MGCs [170] [171] **(Fig. 12)**. Epithelioid showed a morphology which differs from MPs and DCs and resembles to epithelial cells. Foamy MPs contain high amounts of lipid and may constitute a nutrient-rich reservoir used by *Mtb* for long-term persistence [40]. MGCs result from the fusion of multiple mononuclear phagocytes and form the cellular hallmark of a variety of granulomatous structures. Myeloid/epithelioid cells of TB granuloma are surrounded by T lymphocytes.

An important physical characteristic of the caseous granulomatous lesions in which *Mtb* resids is hyoxia, as demonstrated in human samples of tuberculous lung tissues as well as in several animal models including guinea pigs, rabbits, and nonhuman primates [172] [173]. This implies that *in vitro* studies should mimic this physical feature.

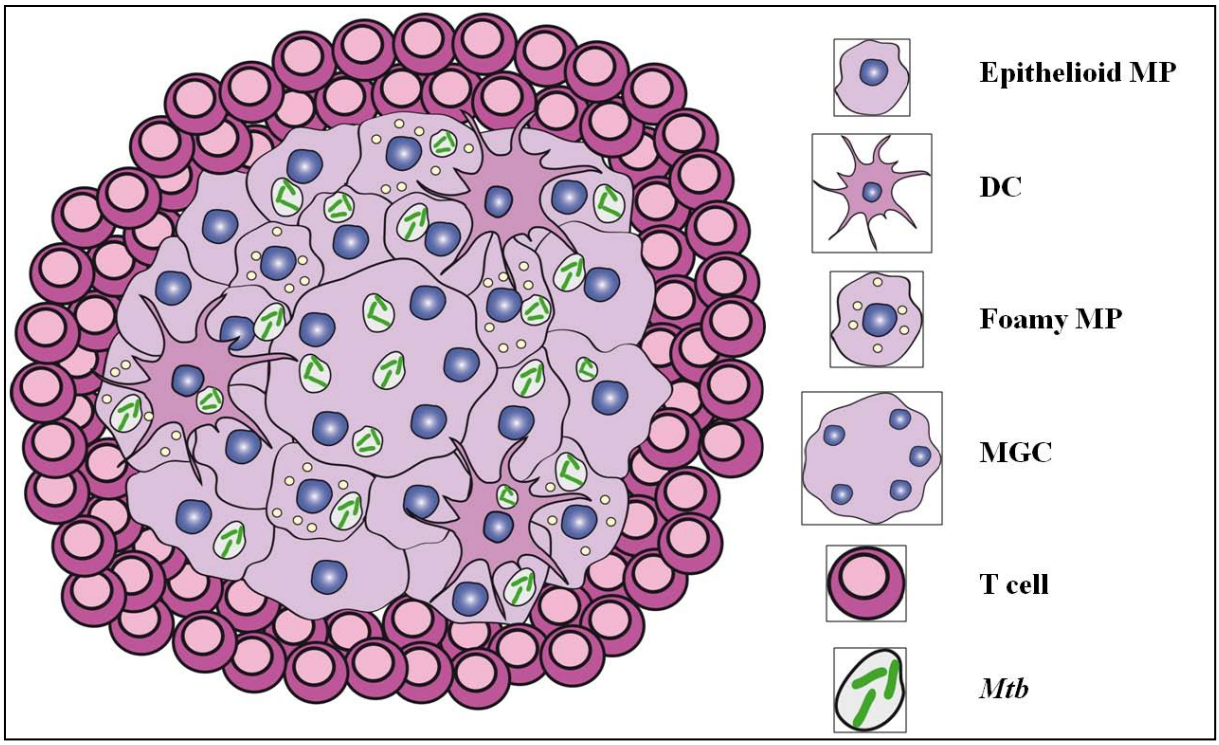

Figure 12: Schematic representation of TB granuloma.

TB granuloma is the archetype of granulomatous structures with a well-organized texture. Building blocks of this structure are essentially mononuclear phagocytes which can be present under different forms including epithelioid MPs (large mature cells), foamy MPs (lipid laden cells) and MGCs (fused cells with several nuclei). DCs are also present within these structures. Mononuclear phagocytes form the myeloid/epithelioid core of the granuloma which is surrounded by T lymphocytes.

1.4.2 Granuloma myeloid cells are long-lived and express destructive enzymes

In a mouse model of infection with BCG, Egen *et al.* reported that myeloid MPs which capture and internalize BCG persist at least several weeks after infection [174]. Indeed, myeloid cells in the infection site at three weeks post infection represent the same population that was present prior to infection [174]. This showed that MP persistence did not result from cell proliferation, but rather from long-term survival. These findings are in line with histological observations which reflected the absence of mitosis and division of myeloid cells in human TB granulomas. Moreover, in their study, Egen *et al.* showed that persistent myeloid cells nucleate the formation of granulomas through the attraction of uninfected MPs and blood monocytes [174]. Therefore, myeloid cells of the granuloma can survive for long periods and are supplemented by additional myeloid cells recruited to these sites. Together, these two features ensure granuloma maintenance. Although myeloid cell recruitment to granulomas is largely studied, myeloid cell survival within these structures is less understood. Increased myeloid cell survival may be explained by two mechanisms: the effect of

exogenous activators of cell survival (i.e. hematopoietic growth factors) and the blockade of apoptosis. Here we focus on the inhibition of apoptosis of myeloid cells after *Mtb* infection, *in vitro*, and within mycobacterial granulomas.

1.4.2.1 Extrinsic and intrinsic pathways of apoptosis

Apoptosis is a natural process of programmed cell death. It can be initiated by two main pathways: the death receptor or 'extrinsic' and the mitochondria-mediated or 'intrinsic' pathways **(Fig. 13)**. Apoptosis involves the activation of a group of cysteine-proteases called caspases which are constitutively expressed in their inactive form but become proteolytically active upon apoptosis induction.

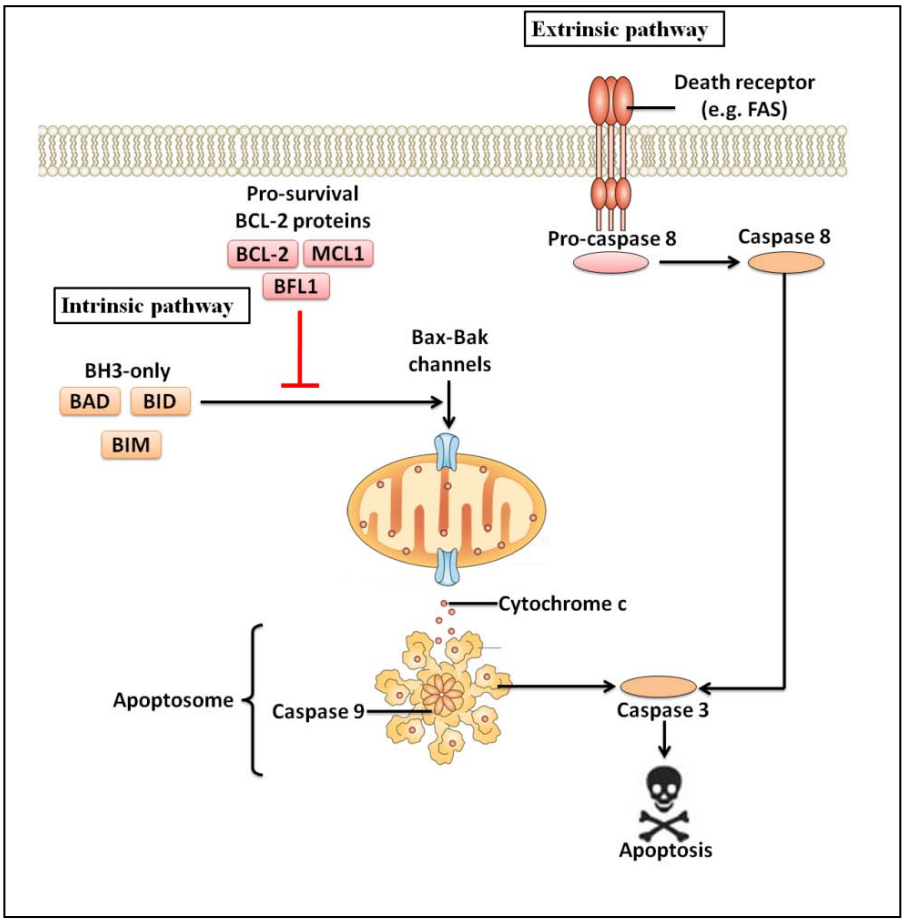

Figure 13: Schematic illustration of the extrinsic and intrinsic pathways of apoptosis.

In the extrinsic pathway, the binding of extracellular death ligands to their receptors results in the activation of caspase 8 which subsequently activate the effector caspase 3. In the intrinsic pathway, BAX-BAK channels mediate the mitochondrial release of Cytochrome c. Anti-survival BH3 only proteins of the BCL-2 family enhance this effect while pro-survival BCL-2 proteins inhibit it. Cytochrome c promotes apoptosome assembly and caspase 9 activation leading to the activation of caspase 3. Caspase 3 activation by both extrinsic and intrinsic pathways culminates in apoptosis.

The extrinsic pathway of apoptosis is activated by transmembrane death receptors belonging to the TNF receptor superfamily such as Fas receptor (Fas/CD95), TNF receptor 1 (TNFR1) and TNF-related apoptosis-inducing ligand (TRAIL) receptors (TRAIL-R1) and (TRAIL-R2). Interaction of these receptors with their cognate ligands (FasL, TNF-α and TRAIL, respectively) results in the recruitment and activation of procaspase-8. This leads to the activation of additional effector or executioner caspases such as caspase-3 which cleave numerous cellular proteins resulting in cell death. Apoptosis mediated by death receptors can be prevented by the recruitment of the degenerated caspase homologue c-FLIP (cellular FLICE-inhibitory protein) which modulate activation of procaspase-8 [175]. In some instances, this pathway can be also blocked by TNFR associated factors (TRAFs). These proteins are intracellular adaptors which can initiate signaling pathways that promote cell survival [176].

Mitochondria-mediated or intrinsic pathway of cell death is triggered by several stimuli including DNA damage, inhibition of DNA repair and cellular stress. It involves proteins of the BCL-2 (B-cell lymphoma 2) family which regulate cytochrome c release from mitochondria into cytoplasm leading to caspase-9 activation. This leads to the activation of other caspases including caspase-3, culminating in apoptosis. BCL-2 proteins form a family of cell death regulators which can be either pro-apoptotic such as BAX, BAK, BAD, BID and BIM or anti-apoptotic such as BCL-2, BCL-XL, BCL-w, MCL1 and BFL1(also termed A1) [177]. BCL-2family members share sequence homology in their BCL-2 homology (BH) domains. Some as Bad, Bid and Bim possess only the BH3 motif and are known as BH3-only proteins. The pro-apoptotic proteins BAX and BAK have an essential role in mediating cytochrome c release from mitochondria as they can oligomerize to form pores in the outer mitochondrial membrane. The BH3-only proteins can activate BAX and BAK, thereby triggering the release of cytochrome c. In contrast, anti-apoptotic BCL-2 proteins such as MCL1 and BFL1counteract the activation of BAX and BAK and maintain cell survival.

1.4.2.2 Mycobacterial infection inhibits apoptosis of myeloid cells

Although some studies have suggested that under some conditions Mycobacteria may induce apoptosis of infected cells, several others showed that these intracellular bacilli stimulate and support strong anti-apoptotic mechanisms.

Mycobacteria are able to interfere with the extrinsic apoptosis pathway. For example, infection of human MPs with virulent *Mtb* enhanced the release of soluble TNF-α receptor class 2 (TNFR2), leading to the inactivation of TNF-α [178]. This results in less stimulation

of the TNFR1, thereby reducing apoptosis signaling. In addition, *Mtb*-infected human MPs showed reduced susceptibility to FasL-induced apoptosis, potentially through bacilli-mediated down-regulation of Fas expression on these cells [179]. Down-regulation of Fas mRNA expression was also reported in *Mtb*-infected murine macrophagic cells of the J774 cell line [180]. In THP-1 cells, lipoglycans of the *Mtb* cell wall stimulated the activation of NF-κB via TLR-2 leading to the up-regulation of cFLIP and resulting in inhibition of FasL-mediated apoptosis [181]. *In situ*, Ordway *et al.* showed that during the chronic stage of *Mtb* infection, myeloid cells of the granuloma express high levels of several anti-apoptotic proteins of the TRAF family (TRAF-1, TRAF-2 and TRAF-3) [182]. This was associated with resistance to apoptosis, and authors conclude that anti-apoptotic mechanisms are more predominant than apoptosis within the granuloma environment.

Mycobacteria interfere also with the intrinsic apoptosis pathway. *In vitro* studies showed that BCG infection prevents apoptosis of resting human monocytes and murine MPs and demonstrated that this was associated with the up-regulation of BFL1 mRNA levels [183] [184]. BCG-mediated inhibition of apoptosis was abrogated in murine MPs derived from BFL1-deficient mice, indicating a requirement of this anti-apoptotic protein for the survival of infected-cells [184]. J774 murine MP cell line infected with virulent *Mtb* was found to express BCL-2 mRNA which leads to anti-apoptotic activity [180]. *Mtb* infection of the human promonocytic cell line THP-1 or human monocyte-derived MPs induces the expression of MCL1, and knocking down MCL1 expression using anti-sense oligonucleotides increases apoptosis of infected cells [185]. Similarly, it was suggested that *M. leprae* restricts apoptosis in THP-1 cells by up-regulating MCL1 and down-regulating BAD and BAK mRNA expression [186]. In lung tissues of *Mtb*-infected mice, Mogga *et al.* reported an increased expression of BCL-2 and reduced expression of BAX in MPs containing *Mtb* [187].

Overall, Mycobacteria able to inhibit induction of host cell apoptosis via multiple mechanisms which interfere with both intrinsic and extrinsic pathways of this process.

1.4.2.3 Mycobacterium-infected myeloid cells express proteolytic enzymes

Mtb-infected myeloid cells express a variety of proteases, especially of matrix metalloproteinases (MMP) and cathepsin (CTS) families.

MMPs are zinc-dependent proteases which consist of two conserved domains, a prodomain and a catalytic domain. They are essentially involved in the degradation of the extracellular matrix components. MMPs are not stored in cells, except PMNs, and their expression is tightly regulated at the transcription level [188]. Several studies reported that

Mtb drives the expression of some MMPs in infected-myeloid cells. *In vitro*, *Mtb*-dependent expression of MMP9 is described in murine and human myeloid cells [189] [190] [191]. In the same way, *Mtb* infection of human MPs induces gene expression and secretion of MMP1 and MMP7 *in vitro* [192]. *In situ*, immunohistochemical staining revealed that MMP9, MMP1 and MMP7 were highly expressed by the myeloid cells in the center of granulomas in *Mtb*-infected patients [193] [192].

CTSs are a large family of lysosomal serine, cysteine or aspartic proteases. They function in intra-lysosomal protein degradation and participate in tissue remodeling responses by degrading extracellular matrix proteins. *Mtb*-infection up-regulates the expression of several CTS proteases in myeloid cells *in vitro* and within TB granulomas. For example, the expression of lysosomal CTSB and D was up-regulated in THP-1 cells upon *Mtb* infection [194]. CTSB, D and H were increased in lung granulomas of *Mtb*-infected mice and their expression was associated with MP within these structures [195]. CTSG expression was also detected in MPs of hypoxic lung granulomas in mice as well as in caseous human granulomas of patients with active pulmonary TB [196]. Similarly, CTSK was highly expressed in myeloid mono-and multinucleated giant cells within human TB granuloma [197].

Therefore, *Mtb*-infection up-regulates the expression of several proteolytic enzymes of the MMP and CTS families, and TB granuloma myeloid cells express these proteases *in situ*. Such proteases participate in the formation of granulomatous structures [198].

1.4.3 Different phases of granuloma formation

Granuloma formation is a dynamic process based on a series of different steps which can be schematically divided into four stages: initiation, maturation/maintenance, effector, and resolution or calcification [199].

1.4.3.1 Initiation

In this initial step, mononuclear phagocytes are the first cells which attempt to contain the danger (resistant pathogen, foreign body or unknown stimulus). This allows the basic formation of the granulomatous structure and depends on the sequential production of chemokines and expression of adhesion molecules for the spatial organization of granuloma. Initiation of granuloma formation by mononuclear phagocytes (e.g MPs) can occur without the need of specific antigen recognition as in foreign body granulomatous reactions. The contribution of other cells such as T lymphocytes at this stage seems less required and some previous reports demonstrated the initiation of granuloma formation in a T-cell independent manner [200] [201]. However, it was proposed that non-granuloma T cells specific for other

antigens and present in the organism may infiltrate and participate but still play an auxiliary role in this phase [199].

1.4.3.2 Maturation/maintenance

This stage of granuloma formation is characterized by an intense cell accumulation and organization. After initiating the granulomatous response, mononuclear phagocytes continue to play important roles in granuloma maturation through the induction of cell-mobilizing molecules. However, the dominant role in this phase is played by $CD4^+$ T lymphocytes [199]. For example, mice with deleted genes for CD4 or MHC-II molecules (necessary to $CD4^+$ T cell activation) are markedly susceptible to Mycobacteria and show disorganized granulomatous lesions [202] [203] [204]. Similarly, failure of granuloma formation after infection with *Schistosoma mansoni*, was observed in mice lacking $CD4^+$ T cells after depletion or due to deficiency in MHC-II molecules [205] [206]. In humans, evidence of the role of $CD4^+$ T cells in granuloma maturation comes from HIV patients having a marked quantitative drop in this cell type and showing high susceptibility to pathogens that induce a granulomatous response including Mycobacteria (*Mtb*, *M. avium*) [207] and Fungi (*Histoplasma capsulatum*, *Pneumocystis carinii*). In HIV/*Mtb* co-infected patients, it has been suggested that HIV-induced depletion of $CD4^+$ T cells within granulomas leads to a direct disruption of the containment of *Mtb* infection [39].

Overall, $CD4^+$ T cells appear to play a central role in this maturation/maintenance phase of granuloma formation, and are mandatory in organizing the cell infiltrate into a well-structured granuloma.

1.4.3.3 Effector

Events occurring during the effector phase are highly variable depending on the type of granuloma and its inciting event. This phase involves an intense communication and interaction between different granuloma components especially mononuclear phagocytes and lymphocytes. Here again, $CD4^+$ T cells play important roles through the secretion of key inflammatory cytokines. However, the nature of the cytokine response depends on the granuloma type [208]. For example, TB granuloma is considered as a Th1-type granuloma, as Th1 related cytokines such as IL-12, IFN-γ, and TNF-α are essential players against *Mtb*. In contrast, helminth-induced granulomas such as schistosomiasis granulomas are Th2-type granulomas in which Th2 related cytokines (IL-4, IL-5 and IL-13) predominate and play pivotal roles. Cytokines produced in the granuloma micro-environment regulate cellular interactions and functions. In TB granuloma, IL-12 primarily produced by phagocytes is

essential for the induction and the maintenance of $CD4^+$ Th1 cells [209] which in turn produce IFN-γ. IFN-γ synergizes with TNF-α to promote phagocyte bactericidal functions, especially through RNI and ROI production. RNI are mandatory for *Mtb* control in mice. Animals unable to generate RNI show rapid mycobacterial growth with high burdens in affected organs associated with necrotic granulomas and rapid death [210]. However, mice unable to express ROI are slightly susceptible to *Mtb* infection and show only a transient loss of resistance to pulmonary TB **(Table IV)** [211]. In contrast, in humans, it is unclear if RNI play a protective role against Mycobacteria, while a critical protective role of ROI is well established. This is reflected by the phenotype of individuals deficient in NADPH oxidase who develop chronic granulomatous disease (CGD) and are highly susceptible to TB [212]. Moreover, in these patients, disseminated BCG-osis, local disease (BCG-itis) and disease caused by *M. avium pneumonitis* have been reported.

In addition to $CD4^+$ T cells, other T cell subsets are also involved in the effector phase during TB. αβ $CD8^+$ MHC-I-restricted T cells are required for the optimal host resistance to *Mtb*. They can produce IFN-γ but also play cytolytic roles to kill infected MPs and Mycobacteria [158] [162]. Mice lacking the T-cell accessory molecule CD8 were unable to control a chronic pulmonary infection with *Mtb* **(Table IV)** [213] [214] . CD1-restricted T cells may also contribute in effector granuloma mechanisms by producing IFN-γ and expressing cytolytic activity [158]. Importantly, mice deficient for β_2m (shared by MHC-I and CD1 molecules) thus lacking both $CD8^+$ and CD1-restricted T cell activities were more susceptible than CD8-deficient mice to *Mtb* [215], suggesting an important role of CD1-restricted T cells. However, several reports showed that CD1d-deficient mice were not significantly different in their susceptibility to *Mtb* infection than control mice [213] [216]. Therefore, further investigation is required to clarify the important role of β_2m in mycobacterial infections. β_2m may participate to a new unknown pathway of antigen presentation, important for the processing of mycobacterial antigens, and involving other molecules than MHC-I and CD1.

KO strain	Survival (days)	effects	Ref
CD4	150	Increased bacterial growth, poor mononuclear cell recruitment, increased PMN, the normal granulomatous response did not occur.	[204]
CD8	>150	Increased bacterial growth, increased PMN, Normal granuloma development initially apart from increased lymphocytes	[214]
β_2m	~85	High susceptibility, extensive pathology, diffused histiocytic infiltration and lower numbers of lymphocytes	[213]
CD1	Normal	No increased susceptibility, normal granuloma formation	[213] [217]
iNOS	33–45	No RNI, high susceptibility, rapid bacterial growth, necrotic granulomatous pneumonitis	[210]
NADPH oxidase	Normal	No ROI, normal control of infection, normal granuloma formation with some showing increased PMN numbers.	[211]

Table IV: Effects on the anti-mycobacterial host response in mice lacking different T cell subsets, β_2m, iNOS (RNI) or NADPH oxidase (ROI).

1.4.3.4 Resolution or calcification

As the essential function of granulomas is the containment and clearance of the inciting agent, these structures may resolve if this aim is achieved. An example of this process is the response to BCG vaccine. Indeed, cutaneous inflammatory papules and granulomas are common within the first few weeks after vaccination. This then develops into an ulcer healing within three months of onset to leave a small flat scar.

Previous studies suggested that γδ T lymphocytes may down-modulate the granulomatous inflammation. In mice with *Mtb*-induced granulomas, it was proposed that γδ T cells may limit the access of inflammatory cells that do not contribute to protection but may cause tissue damage [154]. Similarly, a previous report suggested that γδ T cells down-regulate αβ T cell responses during *Listeria monocytogenes*-induced granulomatous inflammation [218].

Instead of resolution which doesn't alter the tissue in which they are embedded, granulomas may progress toward fibrosis. This process involves the accumulation of fibroblasts and extracellular matrix around and within the granulomas resulting in formation

of fibrotic visible scares which may undergo subsequent calcification. This can cause progressive organ damage and is a significant part of the pathology associated with granulomatous diseases. Cytokines such as IL-4, IL-13 and TGF-β regulate fibrosis, activate fibroblasts and promote collagen formation and deposition [219] [220] [221].

1.4.4 Pivotal regulators of the granulomatous immune response in tuberculosis

Formation of mycobacterial granuloma is a complex process involving several cellular and molecular effectors which interact to coordinate cell recruitment, stabilize granuloma architecture and control the danger.

1.4.4.1 GM-CSF is mandatory for granulomatous control of Mycobacteria in mouse

GM-CSF (granulocyte macrophage colony-stimulating factor), a monomeric protein, is a hematopoietic growth factor produced by different cell types including T cells, MPs, endothelial cells and fibroblasts in response to cytokine or inflammatory stimuli. Its receptor, expressed essentially on myeloid cells, is a heterodimeric complex composed of α and β subunits. GM-CSF stimulates survival, proliferation, differentiation, and functional activation of myeloid cells, including monocytes, MPs, PMNs and DCs.

Facing to Mycobacteria, GM-CSF facilitate containment of these pathogens in granulomas and preserves alveolar structure [222] [223]. *Mtb*-infected mice lacking GM-CSF showed lower numbers of monocytes, MPs, and DCs in their lungs compared to infected WT mice [222]. Concomitantly, they had impaired ability of controlling aerosol *Mtb* infection as reflected by their high bacterial load and their rapid death [222]. Compared to WT mice, those lacking GM-CSF also showed defective and markedly attenuated granuloma formation facing to Mycobacteria [222] [223] **(Table V)**. This was associated with the development of extensive lesions with severe necrosis, edema and alveolar epithelial destruction in the *Mtb*-infected lungs [222] [223]. More recently, a study showed that delivery of GM-CSF to the lungs, expressed by recombinant BCG vaccine, resulted in increased pulmonary DC numbers and IL-12 secretion and accelerated $CD4^+$ T cell priming and recruitment, leading to an increased protection against *Mtb* infection [224].

In humans, GM-CSF mRNA levels were significantly more abundant in TB granulomas than in control biopsies, and expression of this cytokine was detected in both epithelioid cells and lymphocytes surrounding and infiltrating the lesions [225]. *In vitro*, GM-CSF contributes to the up-regulation of the T cell-stimulating activity of Mycobacterium-infected human MPs by promoting Th1 cell-mediated immunity [226] [227]. Recent studies showed that GM-CSF is essential for the successful control of *Mtb* replication in human MPs *in vitro* [228]. The

dramatic susceptibility to *Mtb* in GM-CSF-deficient mice is similar to that observed in mice lacking IFN-γ **(see 1.4.4.2)**. Nevertheless, while deficiency in IFN-γ signaling is associated with human susceptibility to Mycobacteria, there are no clinical case reports on GM-CSF/ GM-CSF receptor deficiency. Consequently, the exact role of GM-CSF in the anti-mycobacterial response in humans *in vivo* is not clearly defined

1.4.4.2 IL-12/IFN-γ axis is critical in mouse and human anti-mycobacterial responses

IL-12 is a pro-inflammatory heterodimeric cytokine which share structural similarities with another cytokine called IL-23 **(Fig. 14)**. Due to this, and before the characterization of IL-23, some functions of this latter were attributed to IL-12. Both cytokines share a common p40 subunit that is linked either to a p35 subunit to form IL-12 or to a p19 subunit to form IL-23 [229]. Receptors of these two cytokines also shared a common IL-12Rβ1chain paired to IL-12Rβ2 to form IL-12 receptor or to IL-23R chain to form the receptor of IL-23 [229]. IL-12Rβ2 chain is expressed on naive T cells whereas IL-23R is expressed on activated memory T cells [230].

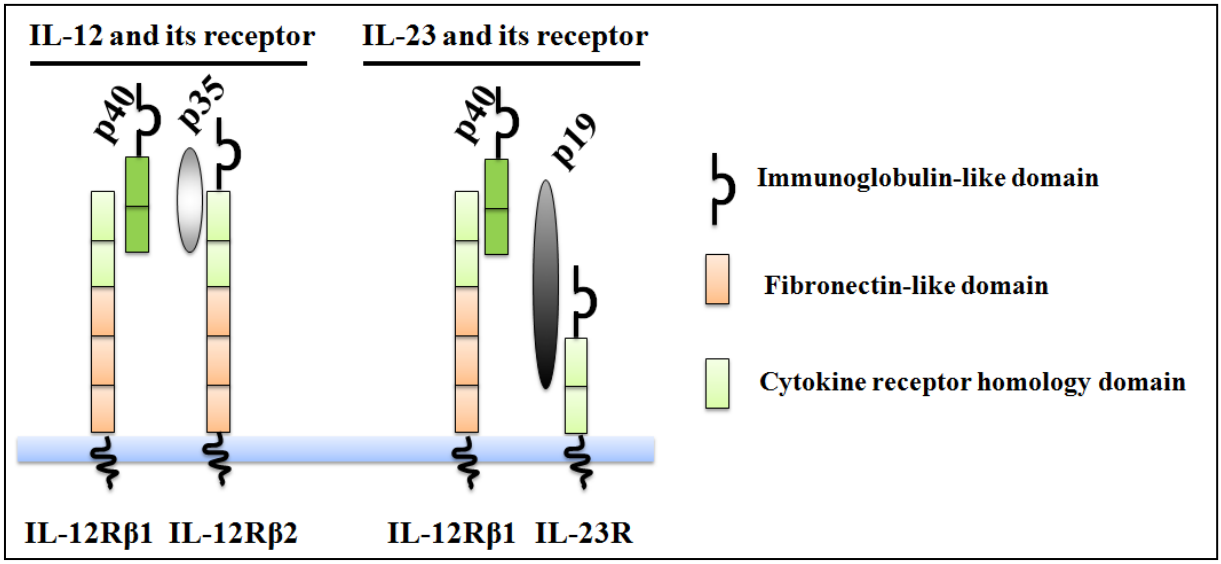

Figure 14: Schematic illustration of the molecular structure of IL-12, IL-23 and their receptors. Adapted from ref [229]

Phagocytic cells and APCs, including monocytes, MPs and DCs are the primary producers of IL-12. This cytokine induces IFN-γ production by NK and NKT cells in the early phases of the immune response, and induces the differentiation of naive $CD4^{+}$T cells into IFN-γ-producing Th1 cells [229]. IFN-γ is a dimeric prototypic cytokine which signals through a

ubiquitously expressed heterodimeric receptor (IFN-γR) formed by two chains: IFN-γR1 and IFN-γR2. IFN-γ retro-activates IL-12 secretion by APCs.

Deficiencies in IL-12 or IFN-γ signaling leads to a similar phenotype after mycobacterial infections in both mouse and human: they are highly susceptible to mycobacterial infections. Mice lacking IL-12p40 or having a disrupted IFN-γ gene were unable to contain *Mtb* infection. They showed higher bacterial burden, reduced survival and defective granuloma formation compared to WT mice [231, 232] [233] **(Table V)**. The maintenance of a protective Th1 host response as well as granuloma formation and bacterial control in *Mtb*-infected mice require a continuous and persistent IL-12 production [234]. In humans, gene mutations in IL-12p40, IL-12Rβ1, IFN-γR1 or IFN-γR2 are associated with increased susceptibility to mycobacterial infections [235] **(Fig. 15)**. Disseminated BCG and *M. avium* infections were reported in individuals with such mutations. More recently, IL-12Rβ1 chain deficiency was also shown associated with *Mtb* infection and TB development in both children and adults [236] [237]. Human studies revealed also that other elements of the IL-12/IFN-γ axis are required for anti-mycobacterial responses. Indeed, IL-12 production by APCs is regulated by two signaling pathways: the first involves IFN-γ, STAT1 (signal transducer and activator of transcription 1) and IRF8 (Interferon regulatory factor 8) while the second is dependent of CD40, NEMO (NF-κB essential modulator) and NF-κB (nuclear factor-kappa B). Human mutations in genes encoding STAT-1, NEMO and more recently IRF8 were found associated with disseminated BCG and *M. avium* infections [238].

Altogether, data presented above emphasize the critical role of the IL-12/IFN-γ axis in the control of mycobacterial infections. Importantly, a very recent study identified ISG15 as a novel player in the IFN-γ-dependent immunity to Mycobacteria [239]. ISG15 is an intracellular IFN-α/β-inducible protein that conjugates to proteins in an ubiquitin-like fashion. Humans with inherited deficiency in ISG15 had reduced IFN-γ production and showed enhanced susceptibility to mycobacterial disease. In the same way, mice lacking ISG15 encoding gene succumbed earlier than WT counterparts upon *Mtb* infection. Authors found that the lack of mycobacterium-induced ISG15 secretion by leukocytes, mainly granulocytes, reduced the lymphocytic IFN-γ production, especially by NK cells [239]. Consequently, they proposed that the ISG15/IFN-γ axis, operating between granulocytes and NK, may be an "innate" complement to the more "adaptive" IL-12/IFN-γ axis, operating between mononuclear phagocytes and T cells.

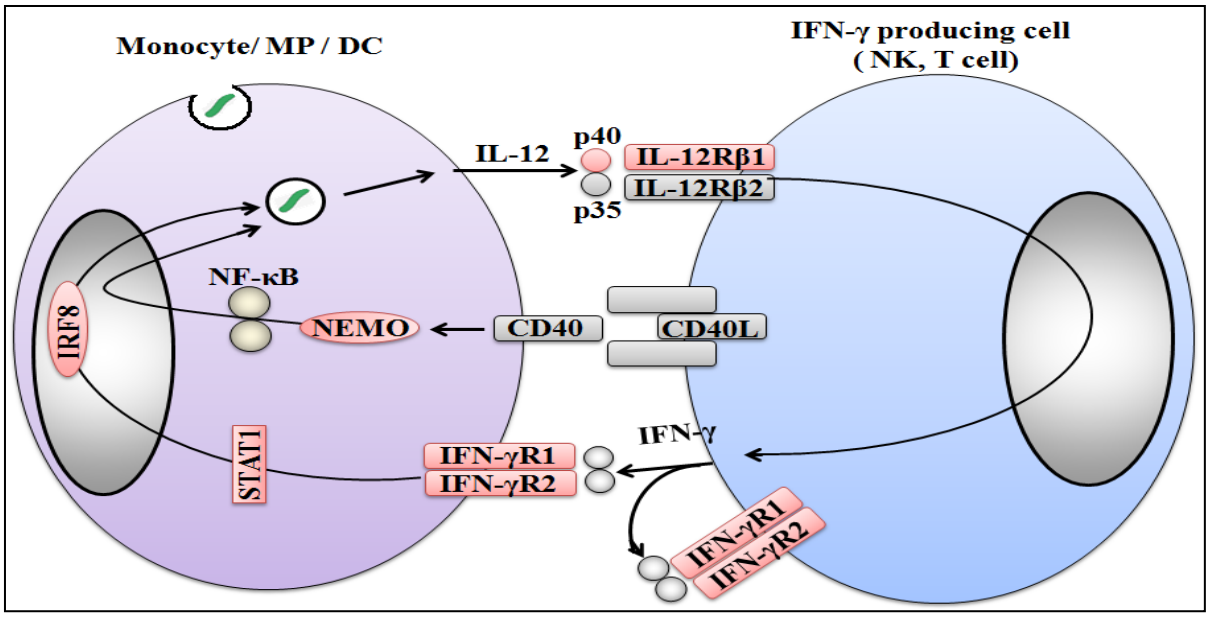

Figure 15: Mutations in seven molecules (pink) **of the IL-12/IFN-γ axis are associated with human genetic predisposition to mycobacterial infections.** Adapted from ref [238].

1.4.4.3 Recent implication of the IL-23/1L-17A axis in mycobacterial infections

At the beginning of this thesis, there was accumulating evidence for a role of the pro-inflammatory cytokine, IL-17A, in mycobacterial infections in animal models.

IL-17A is mostly, but not exclusively, produced by $CD4^+$ Th17 cells whose expansion and maintenance depends of the cytokine IL-23 produced by MPs and DCs **(See 1.5.4.3)**. Previous studies documented the production of IL-23 by *Mtb*-infected murine DCs, and showed that Th17 cells are present and expanded in the lungs during infection [122] [240]. In the aerosol model of *Mtb* infection, the absence of IL-23 resulted in a profound reduction in the frequency and number of Th17 cells and in local IL-17A mRNA production in the lung. This revealed that IL-23 is essential for the expression of Th17 cells and IL-17A response during *Mtb* infection in mice.

Additional studies showed that IL-17A production occurs rapidly upon mycobacterial infection. IL-17A mRNA was detected in the lungs of BCG-infected animals as early as one day after infection [144]. Importantly, these studies reported that IL-17A was mainly produced by γδ T cells rather than $CD4^+$ T lymphocytes in both *Mtb*- and BCG-infected animals[122] [144]. IL-23 is also mandatory for IL-17A production by γδ T cells. Indeed, supernatants from *Mtb*-infected DCs that contain IL-23 could induce IL-17A secretion by γδ T cells purified from naïve or *Mtb*-infected mice [122].

Compared to the IL-12/IFN-γ axis, the IL-23/IL-17A pathway is less important in the control of mycobacterial infections than the IL-12/IFN-γ axis [240]. Indeed, mice lacking IL-

23 or deficient for IL-17A signaling (IL-17AR-deficient mice) were not more susceptible than WT control mice to *Mtb* [240] [241]. However, in the absence of functional IL-12, IL-23 provide some protective immunity by promoting the generation of IFN-γ producing $CD4^+$ T cells, thus compensating IL-12 effects. These results obtained in mice with low dose aerosol *Mtb* infection suggest that IL-17A is not essential to anti-mycobacterial responses. However, subsequent studies in mice infected intratracheally with a high dose of BCG showed that IL-17A produced by γδ T cells is directly involved in the regulation of mycobacterial granuloma formation **(Table V)** [144]. BCG-infected mice lacking IL-17A showed impaired granuloma formation as reflected by the reduced number and size of granulomas in their lungs compared to WT control animals. Granulomas in IL-17A-deficient mice were also less densely packed with mononuclear cells. A role of the IL-23 and IL-17A was also demonstrated in vaccination-induced protection against *Mtb* in mice. In this model, vaccination induces a population of antigen-specific IL-17A producing memory T cells which populate the lungs [242]. IL-17A produced by this population of induced several chemokines which promote the recruitment of memory Th1 cells, thus enhancing protective responses [242]. Taken together, data obtained from murine models revealed that in the presence of functional IL-12/IFN-γ axis, IL-23/IL-17A axis is not crucial for primary protection against mycobacterial infections, but play important roles in vaccine-induced immunity and granuloma formation.

In humans, the role of the IL-23/IL-17A pathway in mycobacterial infections is less clear. In response to *Mtb*, human DCs preferentially produce IL-23 [243]. Mycobacteria specific human Th17 cells have been described, in peripheral blood of persons exposed to or diseased by Mycobacteria [244]. Additional report showed that peripheral blood human γδ T cells are an important source of IL-17A, and the subset of IL-17A-producing γδ T cells increased in TB patients [145]. However, if IL-17A is essential to human anti-mycobacterial responses remains largely unclear.

1.4.4.4 Antagonistic roles of TNF-α and IL-10 in mycobacterial responses

TNF-α versus IL-10 play opposite roles during mycobacterial infections: TNF-α improves granuloma formation and maturation while IL-10 antagonizes these effects.

TNF-α is a multifunctional cytokine which mediates its pleiotropic actions through two distinct cell surface receptors: TNFR1 and TNFR2. During Mycobacterial infections, TNF-α is produced by phagocytes and synergizes with IFN-γ for the maximal activation of their bactericidal mechanisms (NO production) as well as for granuloma formation [245] [246]. TNF-α regulate both formation and maintenance of granulomas by inducing several

chemokines including CCL3, CCL4, CCL5, CXCL9 and CXCL10 thus attracting T and myeloid cells [121] [247]. In BCG-infected mice, TNF-α neutralization increases bacterial numbers and dramatically impairs with the development of granulomas both in number and size [248]. During *Mtb* infection, reduced survival time associated with higher bacterial burden and granuloma necrosis were observed in mice lacking TNF-α or TNFR1 but not in control animals [249]. In humans, the use of Infliximab, a monoclonal antibody against TNF-α utilized for the treatment of rheumatoid arthritis and Crohn's disease, reactivates latent TB in infected patients causing progression to active TB disease. Same effects were also reported in a mouse model of latent TB [250]. These data highlight the key role of TNF-α in promoting granuloma maturation and maintenance of their integrity **(Table V)**.

IL-10 is a homodimeric cytokine generally considered as an anti-inflammatory cytokine with a broad spectrum of immunosuppressive and anti-inflammatory effects. Many cell types can produce IL-10, including phagocytes, T, B, and NK cells. The IL-10 receptor is composed of two subunits, IL-10R1 and IL-10R2. Both chains of the IL-10 Receptor are expressed on many hematopoietic cells, including lymphocytes, monocytes and PMNs. During *Mtb* infection, IL-10 is produced early by myeloid phagocytes and later by $CD4^+$ T lymphocytes [125]. Transgenic mice constitutively expressing IL-10 showed large numbers of Mycobacteria and were less capable of clearing BCG infection [251]. Similarly, mice overexpressing IL-10 were more susceptible to *Mtb* and showed evidence of TB reactivation with a highly significant increase in bacterial numbers during the chronic phase of the infection [252]. Concomitantly, such mice showed decreased mRNA production for TNF-α and IL-12p40 [252]. In contrast, IL-10 deficient mice infected with *Mtb* showed enhanced control of the infection with reduced bacterial pulmonary load, accelerated Th1 responses in lungs and decreased dissemination to the spleen [253]. IL-10 negatively influences granuloma formation during mycobacterial infection. In the absence of this cytokine, BCG-infected mice had an enhanced granulomatous response characterized by an increased number of granulomas showing higher cellularity and increased size as compared to WT mice [254] **(Table V)**. In humans, patients with active TB have reduced IFN-γ levels compared to healthy individuals, and this effect may depend on IL-10 [255]. Indeed, studies on PBMCs (peripheral blood mononuclear cells) obtained from such patients have shown that neutralization of endogenous IL-10 increased IFN-γ release by enhancing monocyte IL-12 production [255].Therefore, IL-10 counteracts the inflammatory protective anti-mycobacterial response and limits granuloma formation. However, by dampening the Th1 inflammatory response, IL-10 may also limit fatal host-mediated immunopathology as reported recently [256].

Mouse	Myco strain	Bacterial growth	Mouse survival (days)	IFN-γ production	Granuloma formation	Ref
WT	*Mtb* BCG	Controlled	yes	+++	Normal	
GM-CSF-KO	*Mtb*	++	No (35)	+	Highly impaired	[222]
IL-12p40-KO	*Mtb*	+++	No (40-45)	+/-	Defective	[231]
IFN-γ-KO	*Mtb*	+++	No (15-32)	Absent	Defective	[232] [233] [257]
TNF-α-KO	*Mtb*	++	No (28-35)	+++	Impaired	[258]
IL-17A-KO	BCG	Controlled	yes	++	Impaired	[144] [259]
	Mtb	++	ND	ND	Impaired	[259]*
IL-10-KO	BCG	Decreased	yes	Slightly increased	Increased	[254]
	Mtb	Decreased	yes	Increased	ND	[253]

Table V: Survival and immune responses upon mycobacterial (*Mtb*, BCG) infection of mice with transgenic gene inactivation of selected cytokines. ND: not determined.
*: recent paper published during the thesis, discussed later in the discussion part.

1.4.4.5 Cellular recruitment to granuloma depends on chemokines

Chemokines are a class of small proteins that play essential roles in immune responses. Specifically, they mediate constitutive and inflammatory recruitment of leukocytes such as lymphocytes and phagocytic cells from the blood into tissues by directing their trafficking and organizing their migration [260]. Chemokines exert their biological effects through seven-transmembrane domain/G protein-coupled receptors. Released chemokines form concentration gradients, thereby recruiting cells expressing their cognate receptors. The human chemokine system is complex, with approximately 50 chemokines and 20 receptors identified currently [260]. Chemokines and their receptors are classified into four structurally related families designated CC, CXC, C, or CX3C. This classification is defined on the basis of the position of the cysteine residues at their amino terminus (C represents the cysteine amino acid; X/X3, one or three non-cysteine amino acids) [260]. Chemokine ligands are named with an ‘L’ and the receptors with an ‘R’.

During the host response to mycobacterial infections, the establishment of chemokine gradients is crucial for the recruitment of different type of inflammatory cells and their aggregation to form granulomas [261]. In response to Mycobacteria or their derived antigens, host cells produce a wide range of both CC (CCL2, CCL3, CCL4, CCL5, CCL19, CCL20, CCL21, and CCL22) and CXC (CXCL1, CXCL2, CXCL7, CXCL8, CXCL9 and CXCL10) chemokines *in vitro* [262] [263]. Compared to healthy controls, elevated levels of CCL2, CCL3, CCL5, CCL20, CXCL8 and CXCL10 have also been reported in the serum and/or bronchoalveolar lavage fluid of TB patients [261] [264]. However, chemokine/chemokine receptor system shows an elevated degree of redundancy with the possibility that a chemokine binds different chemokine receptors, and one receptor may be the target of several chemokines [260]. This forms an important difficulty to dissect the exact role of each of these factors in host anti-mycobacterial response and granuloma formation. In this way, mice deficient for one chemokine or chemokine receptor were generally no more susceptible to Mycobacterial infections than control mice. Indeed, deficient mice showed a transiently impaired response at early stage but were finally able to control infection and form granuloma as well as WT mice at more advanced times **(Table VI)**. For example, BCG infection of mice deficient in CCR6, the unique receptor of CCL20 involved in immature DC and memory T cell recruitment, showed impaired clearance of Mycobacteria at early stage. Nevertheless, CCR6 was not required for the establishment of T cell-mediated adaptive immunity and CCR6-deficient mice eliminated Mycobacteria [265]. Similarly, mice deficient for CCL2 or CCL5 chemokines showed an early reduced recruitment of immune cells to the lungs after *Mtb* infection. However, later, they were able to establish normal responses and granuloma formation, most likely as a result of compensation by other chemokines [266] [267]. In the case of CCL5-deficient mice, it was shown that the CCL5-related ligand CCL4, but not CCL3, partially compensates for the lack of CCL5 during early *Mtb* infection. Therefore, the chemokine/chemokine receptor network is working with a high redundancy and the lack of one element is compensated by others to ensure optimal host responses. Notably, it was shown that after high dose intravenous *Mtb* infection, CCR2-deficiency markedly impairs MP recruitment to sites of inflammation, inducing the mouse death early after infection with 100-fold more Mycobacteria in their lungs compared to WT mice [268]. However, subsequent studies showed that this effect was dose dependent: after low-dose *Mtb* infection, mice lacking CCR2 did not have increased bacterial loads in the lungs compared to WT mice and successfully formed granulomas [269].

Chemokine or receptor	strain	Effects compared to WT control animals	Ref
CCR1	*Mtb*	No effect on bacterial growth or granuloma formation	[261]
CCR2	*Mtb*	high dose: mice succumb rapidly, defects in early MP and later DC and T cell accumulation in lungs	[268]
		Low dose: normal immunity and granuloma formation	[269]
CCR4	BCG	Impaired early bacterial clearance, normal bacilli elimination later, reduced late stage inflammation, abrogated recall granuloma formation (in response to myco antigen-coated beads)	[270]
CCR5	*Mtb*	Control of bacterial growth, normal granuloma formation	[271]
CCR6	BCG	Early bacterial clearance defect – Normal T cell-mediated adaptive immunity and bacilli elimination later.	[265]
CCR7	*Mtb*	Impaired DC migration from lungs to lymph nodes, higher bacterial burden and compromised resistance to high dose infection, generation of adaptive immunity and almost similar survival as WT animals following low dose infection.	[272]
CXCR2	*M. avium*	No difference in bacterial growth , normal PMN recruitment	[273]
CXCR3	*Mtb*	Early and transient defect in granuloma formation, normal granulomas development later	[274]
CX3CR1	*Mtb*	Normal bacterial load and granuloma formation	[275]
CCL2	*Mtb*	Minor and transient increase in bacterial load, fewer mononuclear cells in granulomas by day 70 post infection	[266]
CCL5	*Mtb*	Early and transient increase in bacterial burden and delayed T cell migration, control of bacterial growth and normal granuloma formation at more advanced times	[267]

Table VI: Anti-mycobacterial responses and granuloma formation in chemokine- or chemokine receptor-deficient mice.

1.5 Origins and key mediators of giant cell formation

1.5.1 Physiological and pathological giant cells

Giant cells are observed in both physiological and pathological conditions. Physiological giant cells include syncytial trophoblast in placenta, syncytial myofibers in skeletal muscles, the bone marrow megakaryocytes responsible for the production of blood platelets and OCs, the bone-resorbing cells critical for bone homeostasis. Pathological MGCs are described in chronic inflammatory granulomatous conditions including already cited diseases: TB, schistosomiasis, foreign body reaction sarcoidosis, crohn's disease and LCH. Giant cells originate from both non hematopoietic (syncytial trophoblast and syncytial myofibers) and hematopoietic (megakaryocytes, OCs, pathological MGCs) precursor cells. Except of megakaryocytes formed by a process called endomitosis (repeated incomplete mitosis without cell division), giant cells generally results from cell-cell fusion. In inflammatory granulomatous conditions, MGCs arise from the fusion of myeloid cells at the granulomatous site [276] [277]. In this part we will focus on giant cells which originate from cell-cell fusion of hematopoietic myeloid cells: OCs and pathological MGCs.

Among the different myeloid giant cells, OCs were the most studied. In contrast, precise phenotype, mechanisms of cell fusion and functions of pathological MGCs are less known.

1.5.2 Osteoclast: the bone-resorbing giant cell

OC formation, also termed osteoclastogenesis, is important for the homeostasis of the bone tissue. Indeed, the maintenance of bone remodeling is tightly controlled by a fine balance between bone formation by osteoblasts and bone resorption by OCs. OCs are large giant cells which contain 15 to 20 nuclei. Three different origins of OC formation were identified so far: bone-marrow progenitors [278], monocytes [279] and immature DCs [280]. Differentiation of OC precursors into mature OCs involves an extrinsic pathway which requires two cytokines: M-CSF (macrophage colony stimulating factor) and RANKL (receptor activator for nuclear factor κB ligand) [281-284] **(Table VII)**. M-CSF is a growth factor required for the survival, proliferation and differentiation of precursors of the monocyte/macrophage lineage. RANKL (also designated TRANCE, OPGL or ODF) is a homotrimeric member of the TNF receptor ligand family. The critical role these two cytokines in osteoclastogenesis was confirmed in deficient mice which lack osteoclasts and have a profound defect in bone resorption resulting in osteopetrosis, characterized by high bone density [284-286].

Chemotactic stimuli are also required for OC formation. In this context, it was shown that CCL2 is mandatory for the fusion of both human and murine myeloid cells into giant OCs [287-290]. Neutralization of CCL2 significantly reduced human osteoclastogenesis *in vitro* [289], and OC formation was notably inhibited in cells derived from CCL2-deficient mice [290].

The mechanisms that allow myeloid cells to fuse into OCs remain poorly understood, although some molecular mediators were identified. One of these mediators is a membrane protein called DC-STAMP (DC -specific transmembrane protein). Yagi *et al.* found that DC-STAMP was highly expressed in OCs but not in MPs, and showed that cell fusion into OC was completely abrogated in DC-STAMP-deficient mice [291]. The ligand for DC-STAMP involved in cell-cell fusion is not known. Additional molecule belonging to the immunoglobulin superfamily such as MFR/SIRPα (macrophage fusion receptor) was strongly expressed in MPs at the onset of fusion and is involved in myeloid cell fusion leading to multinucleation [292]. MFR regulates this process by virtue of interacting with its ligand CD47 which also belongs to the immunoglobulin superfamily [293].

OCs are responsible for the degradation of the bone matrix. During activation towards bone resorption, OC cytoskeleton undergoes extensive reorganization. These cells are characterized by the presence of podosomes composed of a central actin-bundle core surrounded by surrounded by a ring of by a ring of vinculin and talin and stabilized by microtubules [294]. Mature OCs plated on glass organize their podosomes into a precisely defined circle at the cell periphery (large belt-like structure). Podosome belt is thought to evolve into the sealing zone in actively resorbing OCs [295]. The sealing zone delineates an isolated extracellular compartment known as resorption lacuna between bone surface and the plasma membrane of OC [296]. Within the resorption lacuna, the bone matrix is degraded by an intense acidification and secretion of proteolytic enzymes including CTSK, TRAP (tartrate resistant acid phosphatase) and MMP9 [297].

A growing body of evidences has indicated that the skeletal and immune systems are closely related through cellular and molecular interactions, and the term osteoimmunology is currently used to describe the interface between bone biology and immunology [298] [299]. Immune function played by bone cells such as OCs represents an example of the cross-talk between bone and the immune system. Indeed, as OCs are differentiated from the same precursor of MPs and DCs, it is reasonably possible that OC themselves have immune

functions. In this context, a recent study showed that mature bone-resorbing OCs activated with lipopolysaccharide (LPS) or IFN-γ up-regulated their of expression both MHC-I and MHC-II molecules as well as the cofactors CD80, CD86 and CD40, necessary for antigen presentation [300]. Importantly, the study argued that OCs are also capable of presenting antigens to stimulate both $CD4^+$ and $CD8^+$ T cells. These results revealed that OCs can act as functional APCs *in vitro*.

Several cytokines are positively or negatively involved in the regulation of OC formation **(Table VII)** [298]. For example, cytokines such as IL-17A and TNF-α activate osteoclastogenesis through RANKL induction on mesenchymal cells (IL-17A and TNF-α) and synergy with RANKL effects (TNF-α). In contrast, others such as IFN-γ and GM-CSF inhibit RANKL signaling and negatively regulate OC formation.

Cytokine	Effect on OC formation	Mechanism
M-CSF	Activation	Survival and RANK induction
RANKL	Activation	OC differentiation induction
TNF-α	Activation	RANKL induction on mesenchymal cells; synergy with RANKL
IL-17A	Activation	RANKL induction on osteoblastes
IFN-γ	Inhibition	RANKL signaling inhibition
GM-CSF	Inhibition	RANKL signaling inhibition

Table VII: effect of some cytokines on osteoclastogenesis. Adapted from ref [298].

1.5.3 The myeloid giant cells formed in chronic inflammation

While OC formation occurs in a well defined localization, granuloma-associated MGCs can be found in a wide range of tissues. They were firstly identified in TB granuloma by Langhans in 1868 and lately described in several granulomatous diseases of known or unknown etiologies. Stimuli which induce MGC formation are largely unclear. MGCs were historically classified into two major types: (i) Langhans' giant cells showing a relatively small number of nuclei distributed in a peripheral circular fashion and (ii) foreign body giant cells (FBGCs) with much larger numbers of nuclei scattered in an irregular central manner [301]. Similarly to OCs whose extrinsic cytokine stimuli regulate their formation, several cytokine including IL-4 and IL-13 as well as IFN-γ and GM-CSF were proposed to be

involved in MGC formation [302] [303]. However the *in vivo* relevance of these factors was only confirmed for IL-4 involved in the formation of FBGCs. Indeed, injection of IL-4 neutralizing antibodies reduced the FBGC density while its exogenous administration increased it in mice with implanted-biomaterials [304].

Some mycobacterial components also promote MGC formation. Recent research using an *in vitro* human model of granuloma induced by mycobacterial antigen-coated beads showed that some of the major lipoglycans from *Mtb* cell wall are responsible for the aggregation and fusion of MPs in MGC [305]. In particular, mycobacterial PIMs, lipomannan, and trehalose 6,6'-dimycolate (TDM) promote MGC formation in a TLR-2-dependent pathway, whereas phosphatidylinositol and ManLAM do not [305]. However, if this promotion of MGC formation occurs through the production of extrinsic factors is unclear.

In 2008, our group identified a novel extrinsic pathway of myeloid cell fusion. The group demonstrated that *in vitro*, IL-17A induces the fusion of human monocyte-derived DCs resulting in MGC formation [306]. IL-17A-treated monocytes were unable to undergo cell fusion. However, when treated with a combination of both GM-CSF and IL-17A, monocytes become able to fuse in MGCs. IFN-γ potentiates this IL-17A-dependent pathway and significantly increases MGC size and nuclear content. These data identified IL-17A as a novel fusion mediator. In the next part we describe the properties and functions of this cytokine.

1.5.4 IL-17A characteristics and biological functions

1.5.4.1 Molecular characteristics of IL-17A

IL-17A was firstly described in 1993 after the characterization of its encoding gene in a rodent T cell library by subtractive hybridization [307]. This cytokine has ~58% of homology to an open reading frame encoded within *Herpesvirus saimiri* and was first called CTLA-8 (cytotoxic T lymphocyte antigen 8 (CTLA-8)). The human IL-17A was later characterized in T lymphocytes [308]. Subsequent genomic sequencing studies and database searches led to the characterization of several IL-17A homologue cytokines, forming thus the IL-17 cytokine family. In addition to IL-17A, this family includes IL-17B, IL-17C, IL-17D, IL-17E (also designated IL-25), and IL-17F [309].

IL-17A is the prototype and the best characterized member of the IL-17 cytokine family. In humans its encoding gene is located on chromosome 6p12 and is composed of three exons and two introns extending on 4252 bp of the human genome. The amino acid sequence of human IL-17A shares ~ 55% of homology with IL-17F which is also encoded by a gene closely located to the IL-17A gene in the same chromosomal region. Both IL-17A and IL-17F

can be secreted as homodimers, but they can also form a heterodimeric cytokine called IL-17A/F [310]. The human IL-17A chain is composed of 155 amino acids. A disulfide bond links two chains in the glycosylated homodimer [309].

1.5.4.2 IL-17A Receptor and signal transduction

Members of the IL-17 family signal through IL-17 receptors (IL-17R) that also form a family of five subunit members (IL-17RA to IL-17RE) [311]. IL-17A and IL-17F homodimers as well as IL-17A/F heterodimer signal through the same heteromeric complex receptor composed by IL-17RA and IL-17RC subunits. Both IL-17RA and IL-17RC are type I transmembrane proteins. IL-17RA is ubiquitously expressed, with particularly high levels in immune cells while IL-17RC is preferentially expressed in non-immune cells [311]. Therefore, it is not clear how myeloid cells which are IL-17RA^{+}/IL-17RC^{-} bind IL-17A. Like other members of the IL-17R family, IL-17RA and IL-17RC have cytoplasmic motifs with homology to a TIR domain (TLR/IL-1 receptor like signaling domain), termed ‘‘SEFIR’’ (for similar expression of fibroblast-growth-factor genes, and IL-17Rs) [312].

IL-17A binding to its receptor induces the recruitment of the adaptor molecule Act1 which also contains the conserved SEFIR domain, thus interacting with IL-17R through homotypical interaction via their respective SEFIR domains [313]. Interaction between Act1 and IL-17R is followed by the recruitment of another adaptor molecule, TRAF6 then the kinase TAK1 (transforming growth factor β-activated kinase 1). The formation of the Act1/ TRAF6/TAK1 complex activates the transcription factors NF-κB, C/EBP (CCAAT/Enhancer binding proteins) and AP-1 [309].

In 2011, two different studies characterized an original TRAF6-independent axis of IL-17R signaling. This pathway involves the inducible kinase IKKi (inducible inhibitor of NF-κB (IκB) kinase) which is recruited to the IL-17R-Act1 complex and mediates Act1 phosphorylation [314] [315].

1.5.4.3 Discovery and characterization of CCR6+ Th17 lymphocytes

Activation and differentiation of naive CD4^{+} T cells is directed by APCs and leads to the development and expansion of different Th cell subsets depending of the “local cytokine environment” **(Fig. 16)**. Previously, two distinct effector Th subsets, termed Th1 and Th2, were identified by Mosmann & Coffman based on their different patterns of cytokine production [316] [317]. More recently, researchers characterized a distinct Th subset called Th17 because they form an essential source of IL-17A production [318] [319] [320].

However, more recent studies showed that IL-17A cytokine is also secreted by other cell types than Th17 [321].

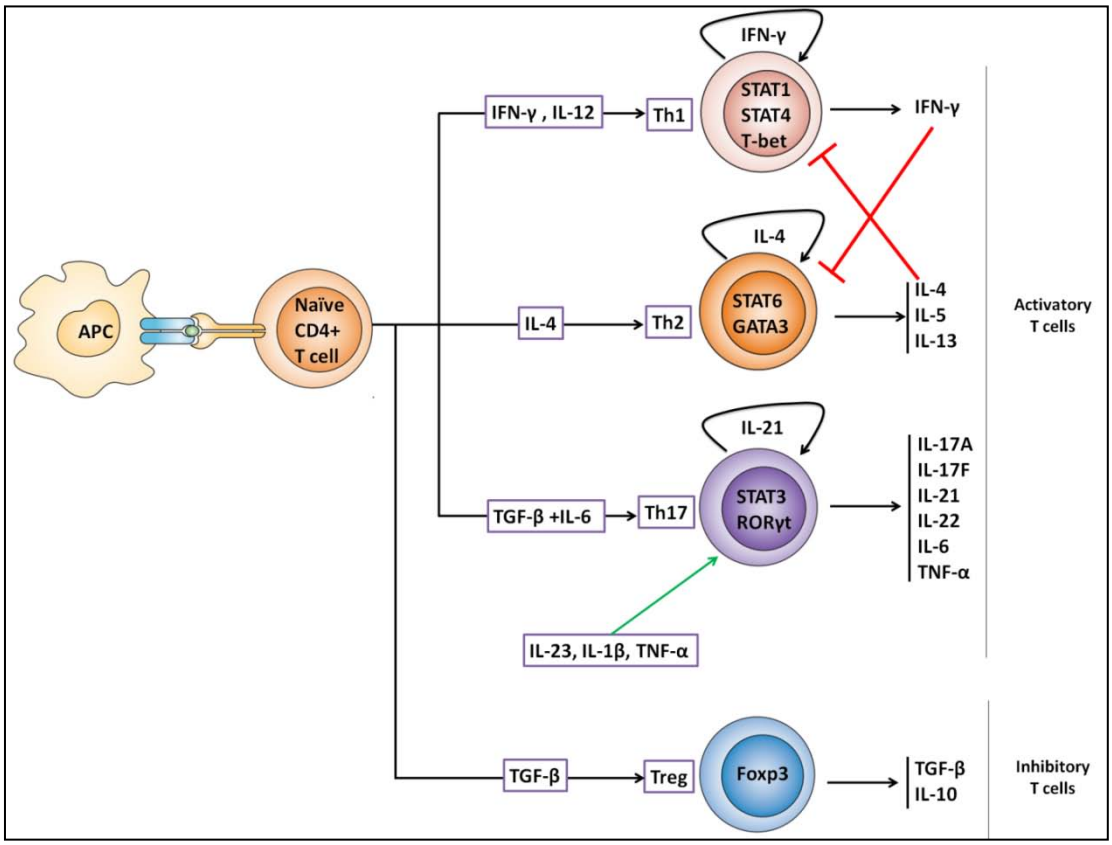

Figure 16: Schematic representation of the differentiation pathways of naive CD4 T cells with their molecular requirements in mice.

Although IL-17A was characterized in the 90's, Th17 were only identified in 2005. In addition to IL-17A, they produce a variety of cytokines including IL-17F, IL-21, IL-22, TNF-α and IL-6 in mice and IL-26 in humans. In mouse, several studies showed that Th17 cells originate mainly in the presence of TGF-β and IL-6 [322]. However, more recent reports challenged the requirement of these cytokines in Th17 polarization [323] [324]. In humans, the exact combination of cytokines that stimulate Th17 cell differentiation is a matter of debate, although several studies underline an important role of TGF-β, IL-1β and IL-6 cytokines in this process [325]. Several cytokines, such as IL-23, IL-21, IL-1β and TNF-α amplify Th17 cell differentiation and responses. IL-23 is necessary for expansion, maintenance and stabilization of the Th17 phenotype and may also serve as a survival factor for Th17 cells [326]. *In vivo*, both human and mouse Th17 cells characteristically express the chemokine receptor CCR6 [327] [328]. CCR6 forms an important functional marker for Th17 cells and contributes to their preferential migration to inflammation sites **(See 1.5.4.4)**. Since discovery, Th17 cells have received considerable attention regarding their dual role in

protective and pathological host immune responses. Indeed, IL-17A produced by these cells plays a crucial protective role in host immunity against a wide range of pathogens but is also major effector actor which drive chronic inflammation and autoimmune disorders [309] [329] [330] [331].

1.5.4.4 Immunological functions of IL-17A

IL-17A plays pleiotropic biological activities essentially by inducing or up-regulating the expression of several genes. IL-17A target genes include cytokines, chemokines, adhesion molecules, enzymes, matrix metalloproteinases and anti-microbial molecules [332] [333]. Through such induced-molecules, IL-17A regulates several host responses.

Early studies showed that, *in vitro,* IL-17A induces the production of G-CSF and CXCL8 by human stromal cells such as fibroblasts, epithelial and endothelial cells, [334]. IL-17A also up-regulates the expression of CXCL1, CXCL2 and CXCL5 chemokines in several stromal cell types including epithelial cells [333]. G-CSF sustains PMN production and survival and CXC chemokines are essential for their recruitment. Both *in vitro* and *in vivo* studies showed that IL-17A promotes granulopoiesis and PMN recruitment through these molecules [334] [335] [336]. For example, over-expression of IL-17A in mice induced a marked expansion of PMN progenitors in bone marrow and spleen and increase mature PMNs in peripheral blood, and this effect was markedly attenuated by neutralization of G-CSF [335]. Similarly, *in vivo* administration of IL-17A induced a selective recruitment of PMN which was blocked by anti-CXC chemokine antibodies [337] [338].

Through the induction of other CXC chemokines such as CXCL9, CXCL10 and CXCL11, IL-17A participates also in the recruitment of Th1 cells as cited previously upon BCG vaccination [242]. IL-17A also induces the expression of CCL20 in fibroblasts, epithelial cells and synoviocytes [333]. This cytokines mediate recruitment of immature DCs and $CCR6^+$ T cells. IL-17A response creates a positive loop that further attractsIL-17A-producing $CCR6^+$ cells through CCL20 induction [339]. Moreover, activated human tissue-infiltrating Th17 themselves express CCL20, thus creating a particular inflammatory environment favoring their own recruitment and sequestration [340].

IL-17A is also involved in host defense mechanisms to infectious pathogens. Rapid IL-17A production has been documented during the early stages of bacterial infection suggesting a role of this cytokine in host anti-bacterial immune responses [341] [342]. This was demonstrated by showing that IL-17A neutralization or abrogation of its signaling increases the susceptibility to several pathogens. Indeed, neutralization of IL-17A in mice infected with

Escherichia coli [341] or *Pseudomonas aeruginosa* [342] led to impaired bacterial clearance. In the same way, mice lacking IL-17RA showed enhanced susceptibility to infection with extracellular bacteria (*Klebsiella pneumonia*) [343], fungi (*Candida albicans*) [344] and parasites (*Toxoplasma gondii*) [345]. Impaired host immunity in mice lacking IL-17A responses was essentially due to impaired production of CXC chemokines, resulting in a defective recruitment of PMNs. The role of IL-17A against intracellular bacteria is less pivotal but this cytokine may contribute in the induction and maintenance of protective Th1 responses against some of such pathogens [346] [347].

In vitro, IL-17A potentiated the killing ability of human PMN and mouse MP facing to *Streptococcus pneumoniae and Bordetella pertussis* respectively [348] [349]. IL-17A also induces epithelial cells and keratinocytes to produce anti-bacterial peptides such as β-defensins, mucins, calgranulins and lipocalines required for host responses against infectious microorganisms [333]. Importantly, β-defensins can also play important chemotactic roles as shown for human β-defensins 1 and 2 which bind to CCR6, inducing chemotaxis in immature DCs and memory T lymphocytes [350]. In humans, numerous genetic diseases resulting in infectious phenotypes and linked to abnormalities in IL-17A responses have been recently identified **(Table VIII)**. Patients with these genetic defects in the Th17 axis suffer from recurrent infections with *Candida albicans* and *Staphylococcus aureus*.

Therefore, IL-17A is involved in protective responses against a variety of pathogens being required for some of them and helpful for others such as Mycobacteria [144]

Disease	Infectious manifestations	Mechanism	Affected gene	Ref
hyper-IgE syndrome (HIES)	mucocutaneous candidiasis staphylococcal abscesses	impairment in Th17 cells	*STAT3*	[351]
Dectin-1 deficiency	mucocutaneous candidiasis	impairment in Th17 cells	*Dectin-1*	[352]
CARD9 deficiency	mucocutaneous candidiasis	impairment in Th17 cells	*CARD9*	[353]
autoimmune polyendocrinopathy-candidiasis-ectodermal dystrophy (APECED)	mucocutaneous candidiasis	auto-antibodies against IL-17A, IL-17F, and/or IL-22	*AIRE*	[354]
IL-17RA deficiency	mucocutaneous candidiasis staphylococcal infections	defects in IL-17A & IL-17F signaling	*IL-17RA*	[355]
IL-17F deficiency	mucocutaneous candidiasis staphylococcal infections	defects in IL-17A/F & IL-17F signaling	*IL-17F*	[355]

Table VIII: Human genetic diseases characterized by recurrent fungal (*C. albicans*) and bacterial (*S. aureus*) infections involving IL-17A responses

Dectin-1 is involved in the development of Th17 responses; CARD9 is an adaptor molecule for dectin-1; Mutations in AIRE gene cause defects in thymic self-tolerance induction.

1.5.4.5 Immunopathological role of IL-17A

IL-17A is linked to the pathogenesis of a variety of inflammatory and autoimmune diseases. IL-17A concentrations are elevated in multiple human autoimmune disorders including multiple sclerosis, rheumatoid arthritis, psoriasis and inflammatory bowel disease [356]. Studies conducted in animal models revealed that IL-17A participates in the pathogenesis of these disorders. For example, IL-17A-deficient mice exhibited a delayed onset and diminished disease severity in EAE, while passive transfer of IL-17A-producing cells induced severe EAE in recipient mice [319]. Similarly, mice lacking IL-17A are resistant to collagen-induced arthritis (the animal model of rheumatoid arthritis) whereas local adenoviral IL-17A injection in mice accelerated the disease onset [357] [358]. In humans, polymorphisms in the IL-23R gene, necessary to maintain IL-17A responses, are associated with inflammatory bowel disease [359] and psoriasis [360]. IL-17A promotes inflammation by a variety of

mechanisms and acts in synergy with other pro-inflammatory mediators and cytokines. For example, in arthritis, it was proposed that IL-17A stimulates inflammatory mediators such as IL-1, IL-6, TNF-α and CXCL8 in a variety of local cells, thus promoting inflammation [361]. IL-17A may also enhance the development of this disease by inducing MMPs and RANKL which can respectively degrade cartilage matrix and stimulate osteoclastogenesis and bone erosion [361].

1.5.4.5.1 The role of IL-17A in langerhans cell histiocytosis

In 2008, our group demonstrated that IL-17A is also involved in langerhans cell histiocytosis (LCH), a rare inflammatory granulomatous disease of unknown etiology.

LCH belongs to the histiocytic disorders characterized by abnormal infiltration of certain organs by immune cells derived from monocyte/macrophage or dendritic cell lineage. In affected tissues, LCH is characterized by an abnormal accumulation of DCs in non-well organized and poorly defined granulomas containing MGCs [362]. Pathological DCs present in LCH lesions show several characteristics of the epidermal langerhans cells (LCs) distinguished by the presence of intracellular Birbeck granules, the organelles that are formed upon ligand binding to surface Langerin/CD207 [362]. In addition, these pathological cells express CD1a which, in humans, is a marker of LC but also of monocyte-derived DCs. LCs have many of the features of DCs, including morphology and capacity to stimulate allogeneic T-cell proliferation in vitro after activation. They develop from embryonic $CX3CR1^{+}CD45^{+}$ myeloid precursor cells that populate the epidermis before birth. However, unlike DCs, epidermal LCs are selfrenewing *in situ* as they are able to repopulate locally independently of circulating precursors [363]. It has been shown that LCs are present in CSF1/M-CSF-deficient mice but absent from CSF1 receptor-deficient mice suggesting the existence of another ligand for this receptor. Importantly, a recent work by Colonna *et al.* identified IL-34 as an alternative ligand of CSF1 receptor that can partially compensate for the absence of CSF1 [364]. Through the use of IL-34-deficient reporter mice, authors found that keratinocytes were the main sources of IL-34 and showed that such mice selectively lacked LCs, thus identifing this cytokine as a growth factor that direct the differentiation of LC progenitors in the skin epidermis. An epidermal LC, stimulated by either an inflammatory agonists or an oncogenic process might be capable of leaving the epidermis and migrating to skin-distant tissues to fund an extra-skin LCH lesion. Indeed, in normal conditions, maturation signal induces the egress of LCs from the epidermis to the skin-draining lymph node in a manner that is dictated by patterns of chemokine receptor expression. However, additional possible origins of

pathological cells in LCH were also proposed including dermal Langerin$^+$ DCs, lymphoid tissue-resident Langerin$^+$ DCs and mononuclear phagocyte precursors [362].

LCH disease occurs predominantly in children and may be classified as active or inactive. Clinical manifestations are heterogeneous and can vary from a single self-resolving lesion to a severe life-threatening systemic form. Multiple organs may be affected including skin, bone, lymph nodes, endocrine glands and central nervous system. LCH cumulates symptoms that are found separately in various IL-17A–related diseases, such as aggressive chronic granuloma formation, bone resorption and soft tissue lesions with occasional neurodegeneration. Our group showed that serum samples of LCH patients revealed a significantly higher IL-17A content in patients with active LCH, than in patients with inactive LCH and controls. Working on biopsies of LCH patients, the group demonstrated that IL-17A is strikingly produced by DC and MGCs inside LCH granuloma [306]. Based on these *in situ* findings and *in vitro* observations that IL-17A induces DC fusion in MGCs, it was suggested that, in LCH granulomas, IL-17A produced by DCs induce their fusion in MGCs. However, there is a controversy around IL-17A production in LCH as a recent paper reveals the absence of this cytokine in LCH biopsies [365]. Nevertheless, several technical problems were not screened by the reviewers in this alternative report including the negativity of positive controls (tonsils), or the use of IL-17A antibodies in inadequate applications such as western blot instead of ELISA. Therefore we maintain that IL-17A is produced in LCH. It was decided in 2008 to investigate IL-17A expression in another form of LCH: pLCH which occurs in adults [366]. pLCH mainly affects lungs of smokers, with an incidence peak at 20–40 years of age. In pLCH, DC granulomas destroy distal bronchioles then cavitate the lungs and form thick- and thin-walled cysts, which enlarge airway lumina resulting in respiratory function invalidation. Although childhood and pulmonary adult LCH display similar histopathological signs with granuloma of DCs and DC-derived MGCs, involvement of IL-17A in adult pLCH is not yet documented.

In conclusion, TB and LCH (childhood or pulmonary) are granulomatous diseases that share similar clinical and histological features such as the destructive ability, the possible dissemination to all organs and the chronic course. However, they differ in some histological details inside the granulomatous structures as well as in their etiology which is infectious for TB and unknown for LCH. Consequently, the treatments are also different: antibiotics in the case of TB and chemotherapy associated to immune suppressors in the case of LCH. For each disease, the pathways regulating recruitment, phenotype, survival and functions of the mono

and multinucleated myeloid cells are a challenge to limit associated immunopathology. Elucidating the molecular mechanisms that shape the myeloid cell fate and functions may preside not only to better understand the myeloid cell-mycobacterium interaction, but also to progress on the pathophysiological mechanisms associated to granuloma formation. Such scientific breakthroughs may lead to the discovery of new therapies to improve the treatment of the granulomatous diseases.

2 Part II: RESULTS

Our work during this thesis led to four manuscripts, two submitted and two in preparation:

I- BFL1, a new biomarker of long lifespan and chemoresistant human dendritic cells: application to Langerhans cell histiocytosis treatment. (Submitted)

II- IL-17A-dependent maintenance of human tuberculosis granuloma is mediated by BFL1, CCL20 and CCL2. (Submitted)

III- Giant Myeloid Inflammatory Cell: a new anti-Mycobacterium effector of the immune system. (In preparation)

IV- IL-17A+MMP-12+CSTD+ DC accumulation leads to bronchoepithelium destruction: relevance in pulmonary LCH. (In preparation)

2.1 Manuscript 1: BFL1, a new biomarker of long lifespan and chemoresistant human dendritic cells: application to Langerhans cell histiocytosis treatment

by Selma OLSSON ÅKEFELDT[1-6*], Carine MAISSE[2-6*], Alexandre BELOT[2-6,8], Marlène MAZZORANA [3-6,9], Giulia SALVATORE[2-6,10-11], **Mohamad Bachar ISMAIL**[2-6], Nathalie BISSAY[2-6], Béatrice BANCEL[7], Françoise BERGER[2-7], Pierre JURDIC [3-6,9], Maurizio ARICÒ [11], Chantal RABOURDIN-COMBE [4-6,12]†, Jan-Inge HENTER[1] and Christine DELPRAT[2-6,13]

**Contributed equally as first authors. †Deceased*

Affiliations

[1] Childhood Cancer Research Unit, Department of Women's and Children's Health, Karolinska Institutet, Karolinska University Hospital Solna, S-171 76 Stockholm, Sweden;

[2] CNRS, UMR5239, Laboratoire de Biologie Moléculaire de la Cellule, Lyon, F-69007, France ;

[3] Ecole Normale Supérieure de Lyon, Lyon, F-69007, France ;

[4] Université de Lyon, Lyon, F-69003, France ;

[5] Université de Lyon 1, Villeurbanne, F-69622, France ;

[6] UMS3444, Lyon, F-69007, France ;

[7] Hospices Civils de Lyon, Department of Pathology, Centre Hospitalier Lyon Sud, Pierre Bénite, F-69310, France ;

[8] Hospices Civils de Lyon, Hôpital Femme Mère Enfant, Bron, F-69500, France ;

[9] CNRS, UMR5242, Institut de Génomique Fonctionnelle de Lyon, Lyon, F-69007, France

[10] Université de Florence, Florence, I-50134, Italy ;

[11] Department Pediatric Hematology Oncology, Azienda Ospedaliero-Universitaria Meyer Children Hospital , Florence, I-50139, Italy;

[12] INSERM, U851, 21 Avenue Tony Garnier, Lyon, F-69007, France ;

[13] Institut Universitaire de France, 103 bd St Michel, Paris, F-75005, France

Contact information for correspondence

Christine DELPRAT

CNRS 5239-FACULTE DE MEDECINE LYON SUD

165 Chemin du Grand Revoyet : BP12

69921 OULLINS CEDEX
Phone : +33 426 235 980
Fax : +33 426 235 900
e-mail : cdelprat@free.fr

Acknowledgments

We would like to thank UMS3444 for the L3 security laboratory and the PLATIM imaging platform, D. Gavhed and E. Sieni for help with patient data and samples.

Statement of equal author's contribution

SOA and CM contributed equally to this manuscript.

Funding

This work was supported by grants from (F) CNRS, INSERM, Université de Lyon, Institut Universitaire de France, Fondation Innovations en Infectiologie, Fondation de France 2008002100, Agence Nationale de la Recherche 08-MIEN-001-02; (USA) Histiocytosis Association of America 2008; (I) Ministero Sanità, Progetto di Ricerca Finalizzata 2008: "Getting deeper in histiocytosis", Regione Toscana, Progetto di Ricerca Malattie Rare 2008, Associazione Italiana Ricerca Istiocitosi (AIRI); (S) the Swedish Children's Cancer Foundation, the Swedish Research Council, Märta och Gunnar V Philipson's Foundation, the Cancer and Allergy Foundation of Sweden, Karolinska Institutet (KID project) and the Stockholm County Council (ALF project).

Abbreviations used in this paper:

2CdA, cladribine; AraC, cytarabine; CIS, cisplatin; DOX, doxorubicine; DC, dendritic cell; LCH, Langerhans Cell Histiocytosis; MFI, mean fluorescence intensity; MGC, multinucleated giant cells; VBL, vinblastine; VCR, vincristine.

ABSTRACT (244 / 250 words)

Background

Langerhans cell histiocytosis (LCH) ranges from a self-resolving to a fatal disease following tissue damage by granulomas, enriched in dendritic cells (DC) and derived giant cells. We investigated Bcl-2 family member expressions, lifespan and chemoresistance of DC in LCH.

Design and Methods

DC were derived from peripheral blood monocytes of 13 LCH patients and compared to healthy donors. Bcl-2 family members were studied by transcriptome, flow cytometry and immunohistology. Flow cytometry quantification of viable versus apoptotic cells was performed following DiOC6 and propidium iodide stainings. We also investigated the sensitivity of BFL1-expressing DC to 17 chemotherapy agents in vitro.

Results

Healthy DC express one pro-survival Bcl-2 member named MCL1 and display a short 2-day lifespan. IL-17A induces NF-kappaB translocation, transcription of the Bcl2 family pro-survival member *BCL2A1*/BFL1 and increase of the DC lifespan beyond 14 days. Monocyte-derived DC of LCH patients constitutively express both MCL1 and BFL1 and exhibit a long lifespan. BFL1 is also expressed in LCH lesions, thus providing a new molecular link between monocyte-derived and lesional LCH DC. BFL1-expressing DC are broadly chemoresistant but apoptosis was induced by vinblastine following the decrease of MCL1 expression or by exposure to anti-IL-17A following BFL1 inhibition. Vinblastine and anti-IL-17A synergize to induce LCH DC death.

Conclusions

Expression of BFL1 induced by IL-17A enhances DC survival. Exposure to a low dose of vinblastine, combined with anti-IL-17A, *in vitro*, inhibits MCL1 and BFL1 expressions, and induces apoptosis in LCH DC. These results suggest a novel therapeutic approach for patients with LCH.

INTRODUCTION

Since more than twenty years, immunologists have studied the biology of immature human dendritic cells (DC) generated from monocytes in the presence of GM-CSF and IL-4, *in vitro*. The *in vivo* relevance of monocyte-derived DC was recently established in the mouse.[1] Monocytes and DC share phagocyte functions, the ability to differentiate into macrophages when cultured with M-CSF and to fuse into multinucleated giant cells (MGC) which are authentic osteoclasts when cultured with M-CSF and RANKL.[2] Two functional properties discriminate DC from monocytes. First, DC initiate adaptive immune responses versus tolerance, as demonstrated in mouse models of DC short-term ablation, *in vivo.*[3] Second, DC but not monocytes undergo cell fusion in the presence of IL-17A, a mechanism highly potentiated by IFN- γ.[4] MGC survive long term, thus demonstrating that survival pathways are activated along the DC fusion process, *in vitro*. Proteins of the Bcl-2 family regulate survival and sensitivity to apoptosis by governing mitochondrial outer membrane permeabilization.[5] They are divided into pro-apoptotic and pro-survival proteins. Each cell type expresses a specific subset of these proteins. *MCL1* was first discovered as an early induction gene during the differentiation of a human myeloblastic leukemia cell line[6] and is a pro-survival member as well as *BCL2A1*/BFL1, discovered in 1995 in B cell lymphoma.[7,8] Inhibition of pro-survival Bcl-2 proteins in cancer cells counteracts chemoresistance and cures cancer in a high percentage of mice.[9]

In the rare disease called Langerhans Cell Histiocytosis (LCH), IFN-γ -expressing DC,[10] form pathogenic granulomas following their accumulation and survival without proliferation (index <2%).[11] We have previously reported a new IL-17A-dependent pathway of DC fusion in LCH[4]. We detected IL-17A (by Elisa, flow cytometry and immunohistochemistry, and six different commercial antibodies) in serums from LCH patients, intracellularly in their monocyte-derived DC and in most of the lesional DC and MGC, *in situ*.[4] Recently, Allen e*t al*[12] did not detect IL-17A mRNA in sorted DC from the LCH lesions, thus raising a controversy on the presence of IL-17A or IL-17A-like molecules which was recently discussed by Hogarty[13]. Thus, further studies on IL-17A and IL17A-like molecules appear warranted in oder to define the possible indication to their clinical application in prospective trials.

Killing the lesional DC in LCH may be achieved in most patients by chemotherapy regimens containing the combination of prednisone and vinblastine (VBL) or, in salvage settings, cladribine (2CdA) and cytarabine (AraC).[14-16] Yet, 20% of patients with disseminated disease affecting vital organs remain at risk of death. Most of them are included

in the one third of patients who fail to respond promptly to chemotherapy. LCH-induced morbidity is characterized by liver and pulmonary fibrosis, multiple hormone deficiencies, bone deformities and progressive neurodegeneration.[17,18] Thus, novel therapeutic approaches are warranted with the aims of improving survival in patients at higher risk of early death and also reducing the number of disease reactivations and late sequelae in the remaining patients. In order to identify novel therapeutic pathways for LCH, we investigated the role of Bcl-2 family gene expressions and associated chemoresistance in monocyte-derived DC from patients and healthy donors, *in vitro*.[13]

DESIGN AND METHODS

Patients

We obtained blood samples from 23 healthy adult volunteers (Etablissement Français du Sang, Lyon, France) and from 13 patients with LCH, from Sweden (n = 8) and Italy (n = 5) (**Table 1**). We carried out immunohistological studies on LCH bone lesions from Sweden (n = 2). The local ethics committees (Karolinska Institutet, Stockholm; AOU Meyer, Florence; Research Committee for the Hospices Civils de Lyon) approved this study and we obtained informed consents.

Reagents

We purchased recombinant human GM-CSF, IFN-γ, IL-4 and IL-17A from PeproTech. Flow cytometry: CD14, CD1a, HLA-DR, CD40 and isotype controls were purchased from Becton Dickinson, anti-BFL1 (3401 anti- A1) from BioVision; anti-MCL1 (Y37) from Abcam. Biological assays: neutralizing anti-IL-17A (eBio64CAP17) from eBioscience. Toxic compounds: dexamethasone, 6-mercaptopurine and fludarabine were purchased from Sigma Aldrich and the remaining drugs were kindly provided by the Karolinska University Hospital pharmacy. The magnitude of the microenvironment concentration around cells, *in vivo*, following clinical dose administration, was calculated by approximating that the drug could be distributed in half of the body aqueous volume (30L) with the formula: [(injected concentration) x injected volume] / 30. The results are in the range of those indicated by pharmacokinetics studies. The following list includes class, target: name (abbreviation), *in vitro* range (optimal dose to kill IL-17A and IFN-γ -stimulated DC when efficient) in µM, and clinical dose in µM, respectively. Glucocorticoids, immune system: hydrocortisone (HC), 0.01-100, 10; methylprednisolone (MP), 0.01-100, 50; prednisolone (P), 0.01-100, 5; betamethasone (BM), 0.01-100, 1; dexamethasone (DEX), 0.01-100, 0.5. 11-aminoacid cyclic peptide, calcineurin and immune system: cyclosporine (CSA), 0.008-80, 0.5. Macrolide, calcineurin and immune system: tacrolimus (FK-506), 0.0001-1, 0.02. Purine analogues, DNA synthesis: cladribine (2CdA), 0.00035-3.5 (3), 0.02; 6-mercaptopurine (6-MP), 0.05-500, 5; fludarabine (FLU), 0.01-10, 5. Pyrimidin analogue, DNA synthesis: cytarabine (AraC), 0.8-800 (40), 14-140. Folate acid antagonist, DNA synthesis: methotrexate (MTX), 5-5000, 1.5-75. Organomettalic complex and purine linker, DNA synthesis: cisplatin (CIS), 0.17-170 (100), 20. Alkaloid, topoisomerase II: etoposide (ETO), 0.1-100, 12. Anthracycline antibiotic and intercalating agent, topoisomerase II:

doxorubicin (DOX), 0.001-10 (1), 0.2. Alkaloids, microtubule functions: vinblastine (VBL), 0.06-60 (0.6), 1.5; vincristine (VCR), 0.0001-1 (1), 0.2.

Monocyte purification, dendritic cell differentiation

$CD14^+$ monocytes were purified (>95% $CD14^+$) from the peripheral blood by ficoll and percoll gradients, followed by negative magnetic depletion of cells expressing CD3 or CD56 or CD19. HLA-DR^{+low} $CD1a^+$ $CD83^-$ immature monocyte-derived DC (>98%) were generated, *in vitro*, after 6 days of culture with 50 ng/ml GM-CSF and 500 U/ml IL-4[2].

Cultures

Cells were seeded in RPMI (Life Technologies) supplemented with 10% FCS, 10mM Hepes, 2 mM L-glutamine, 40 µg/mL gentamicin (Life Technologies) in the presence of IL-17A (2 ng/mL) and IFN-γ (2 ng/mL), at 4,800 cells/mm2 replenished every week. We added neutralizing antibodies at 15 µg/ml.

Affymetrix genechip study

RNA were purified from DC, either untreated, or cultured for 12 days with the above mentioned cytokines: after cell lysis, extraction in Trizol (Invitrogen) and purification on MEGAclear column (Ambion) to reach an RNA integrity number > 9 with Agilent bioanalyser, "ProfileXpert" (www.profilexpert.fr) performed the chip study (see supplementary methods).

Flow cytometry

Immunostaining of cells were performed in 1% BSA and 3% human serum-PBS, then quantified on a LSRII (Becton Dickinson) and analyzed using CellQuest Pro software. We used 2 µg/ml of primary or secondary (PE-F(ab')2 goat to mouse IgG, 115-086-062, Jackson Immunoresearch) antibodies. For intracytoplasmic staining, we blocked the Golgi apparatus with BD GolgiStopTM, fixed and permeabilized the cells with the Cytofix/Cytoperm reagents according to procedures from the manufacturer (Becton Dickinson).

Flow cytometry quantification of viable versus dead cells

$DiOC_6(3)$ (3,39-diexyloxacarbocyanine)-propidium iodide (PI) double staining was performed to detect apoptotic cells by flow cytometry until day 7 of culture. Cells were incubated 15 min at 37°C with 40nM $DiOC_6$ (Molecular Probes) in culture medium to evaluate mitochondrial transmembrane potential ($\Delta\Psi m$). Viable cells have stable $\Delta\Psi m$ whereas $\Delta\Psi m$ decreases with cell commitment to apoptosis. PI (0.5 µg/ml) was added before FACS analysis of the cells and incorporates into DNA of dead cells whose membrane is permeabilized. Living cells remain $DiOC_6^+PI^-$ whereas apoptotic cells are $DiOC_6^-PI^+$. Cells

were numbered by a time-monitored flow cytometry analysis during 2 min at high speed (1 µl/s). After day 7, cells strongly attached to the plastic and undergo cell fusion in the presence of IL-17A, therefore flow cytometry were replaced by TRAP/Hoechst staining as described below.

Tartrate resistant acidic phosphatase (TRAP) and Hoechst staining

We assessed TRAP activity using the Leukocyte acid phosphatase kit (Sigma-Aldrich). We stained DNA of the nuclei with 10 µg/ml of Hoechst 33342 (Sigma) for 30 min at 37°C and fixed with 1% formaldehyde. Following this staining, we counted the total number of active nuclei inside mononucleated and multinucleated cells to calculate the percentage of nuclei still active which reflects the percentage of viable DC. Counts were reported for 1 million of DC put in culture at day 0.

Immunocytofluorescence labeling

Cells were fixed, then labeled with anti-p65 / RelA (C-20, Santa Cruz Biotechnology, California, USA). We observed them using a Leica TCS-SP5 laser scanning confocal microscope (Leica, Wetzlar, Germany). Fixed bone biopsies were deparaffinized, rehydrated, labeled with mouse anti CD1a, (Acris Antibodies, DM363, 1:20 dilution) and rabbit anti-BFL1 (Biovision,A1/3401-100, 4µg/mL) and then analyzed by confocal microscopy using a Carl Zeiss MicroImaging Inc. LSM 510 confocal microscope. Image acquisition was performed using MetaMorph 7.0 Software (Molecular Devices).

Statistical analysis

Polynomial statistical analysis and Mann-Whitney U test from GraphPad Prism 5 software was applied to detect differences between subgroups; the cutoff level of $p < 0.05$ was significant.

RESULTS

IL-17A induced NF-κB translocation and *BCL2A1* / BFL1 in human dendritic cells from healthy donors

We cultured monocyte-derived DC from healthy donors with or without IL-17A and IFN-γ, *in vitro*. mRNA studies performed at day 12 indicated a major impact of IL-17A on *BCL2A1* expression, a pro-survival member of the Bcl2 family genes **(Figure 1A)**. *MCL1*, another pro-survival member, was also highly expressed but already present in untreated DC from healthy donors. Addition of IFN-γ did not strongly affect Bcl2 family gene expression. RelA is a known regulator of *BCL2A1* gene expression.[19] We investigated NF-κB nuclear translocation in DC by immunofluorescence detection of the nuclear factor NF-κB p65 / RelA subunit **(Figure 1B)**. In untreated immature DC, RelA was located in the cytoplasm, as demonstrated by fluorescent cytoplasm and black nuclei analyzed by confocal microscopy. One hour after IL-17A-stimulation, fluorescence stained nuclei in about 90% of the DC. Moreover, the NF-κB inhibitor Bay-11-7085 blocked IL-17A-dependent *BCL2A1* mRNA induction in healthy DC (*data not shown*). Translocation indicates that IL-17A induces NF-κB activation leading to *BCL2A1* induction. Quantitative RT-PCR confirmed induction of *BCL2A1* mRNA by IL-17A as soon as day 2 (*data not shown*) and intracellular flow cytometry demonstrated the detection of the related protein, called BFL1, in three healthy donors **(Figure 1C)**. Dose responses of IL-17A (eight points from 2 to 0.016 ng/ml) were performed to quantify MCL1 and BFL1 expressions in DC. All cells expressed MCL1 whose intensity remained stable and independent of the dose of IL-17A introduced in DC culture. By contrast, BFL1 percentages increased, according to the dose of IL-17A provided, with a plateau at 1-2 ng/mL, depending on the donors.

In conclusion, healthy untreated human DC constitutively express MCL1, but IL-17A stimulation induces NF-κB p65 / RelA subunit translocation and a strong and stable expression of an additional pro-survival member of the Bcl2 family gene called *BCL2A1*/BFL1.

BCL2A1 / BFL1 expression induced by IL-17A enhances dendritic cell lifespan

Healthy untreated DC, which only express MCL1, survived for 48h (**Figure 2A**), indicating that MCL1 alone is associated to a short lifespan. Exposure to IL-17A increased DC survival and converted short into long lifespan as demonstrated by the survival of about 50% of DC after two weeks. Dose responses of IL-17A (eight points from 2 to 0.016 ng/ml) were performed on DC from three healthy donors and showed that IL-17A sustained DC

survival in a dose-dependent manner, optimally at 1-2 ng/mL, depending on the donors **(Figure 2B).** Introduction of sh/siRNA by lipofection or nucleofection affected survival and phenotype of stimulated DC in the control experiment so that we could not directly investigate the consequences of *BCL2A1* mRNA blockade *(data not shown).* Therefore, we used a statistical approach to study the putative link introduced by IL-17A treatment on the three parameters that we quantified: MCL1 intensity, BFL1 induction and DC survival **(Figures 1C and 2B)**. For three independent healthy donors and cultures, we separately plotted eight couples of two data (BFL1, survival), (MCL1, survival) and (MCL1, BFL1), corresponding to each of the eight doses of IL-17A put in culture **(Figure 2C).** The statistical analysis showed that regardless of whether the donor was a moderate (donor C) or a good (donors A and B) responder to IL-17A **(Figure 2B)**, the ability of DC to survive was linked to BFL1 expression by a two parameter polynomial statistical analysis with a good correlation factor **(Figure 2C).** Although MCL1 intensity was not modified by IL-17A treatment, we noticed that healthy donors with higher MCL1 intensity (donor A and B), survived better when BFL1 was induced by IL-17A.

In conclusion, MCL1 is sufficient for short-term DC survival whereas additional strong and stable expression of BFL1, induced by IL-17A, establishes a long-term lifespan of DC.

BCL2A1 / BFL1 is expressed in monocyte-derived dendritic cell and delineates pathogenic myeloid cells in biopsies from patients affected by Langerhans cell histiocytosis

We performed mRNA studies at day six of DC differentiation from peripheral blood monocytes. Contrary to healthy donors, monocyte-derived DC from LCH patients **(Table 1)** showed a high constitutive expression of the *BCL2A1* gene **(Figure 3A)**. We studied survival, BFL1 and MCL1 expressions of monocyte-derived DC from 11 patients with LCH by flow cytometry. As documented by lines that did not cross on the figure **(Figure 3B),** the better the DC survived, the more they expressed BFL1. We previously documented that IL-17A is expressed by DC and MGC inside LCH lesions.[4] We hypothesized that some pathogenic DC from LCH lesions may come from accumulation of $CD1a^+$ $BFL1^+$ monocyte-derived DC that survive long-term under the influence of IL-17A. We looked for intralesional BFL1 expression with double staining (CD1a, BFL1) on LCH tissue sections from two patients (P7, P8) **(Figure 3 C-D)**. In both cases, green color stained $CD1a^+$ DC and red color stained $BFL1^+$ cells. Zoom showed that CD1a and BFL1 were co-expressed in DC, at the membrane

and in the cytoplasm, respectively **(Figure 3C)**. Strikingly, the BFL1 staining delineated LCH lesions better than CD1a **(Figure 3D)** and was expressed not only by $CD1a^+$ DC but also by MGC (asterisk) and $CD1a^-$ myeloid cells inside the granuloma.

This is the first demonstration that monocyte-derived DC from LCH patients as well as aggressive DC accumulated in LCH lesions, actually strongly express BFL1, an unusual pro-survival Bcl2 family member for the myeloid cells.

BFL1-expressing dendritic cells develop chemoresistance

BFL1 is known to confer chemoresistance in B cell leukemia.[20] Therefore, we next investigated the ability of drugs to affect $BFL1^+$ DC and MGC survival. IFN-γ was added to increase MGC formation, as previously documented[4]. We evaluated the resistance of IL-17A and IFN-γ-treated DC from healthy donors to chemotherapy agents targeting glucocorticoid receptors, calcineurin, DNA synthesis, topoisomerase II or microtubules **(Figure 4A).** At optimal culture conditions, we observed no cytotoxic effect of four glucocorticoids, fludarabine or etoposide, and unexpected pro-survival effects of dexamethasone, both calcineurin inhibitors, 6-mercaptopurine and methotrexate. Cyclosporine A has been clinically evaluated in LCH and was ineffective.[21] On the contrary, 2CdA, AraC, cisplatin (CIS), doxorubicin (DOX), VBL and vincristine (VCR) killed cytokine-stimulated DC. VBL and DOX were effective already at four hours, VCR and CIS at 24 hours, and AraC and 2CdA at 72 hours **(Figure 4B)**. Dose response studies showed that CIS, DOX and 2CdA killed only at high doses, exceeding the therapeutic doses **(Figures 4 C-D, H)** while, interestingly, VBL, VCR and AraC killed at low doses **(Figures 4 E-G)**. We observed that 24h of pre-incubation with the cytokines facilitated DC killing by CIS while, conversely, it protected DC from death induced by low doses of VBL or AraC. Altogether, these data demonstrate that IL-17A and IFN-γ-stimulated DC are chemoresistant to 11 of the 17 chemotherapy agents tested but highly sensitive to VBL and AraC, at concentrations used in clinical settings.

Anti-IL-17A neutralizing antibodies increase chemosensitivity of dendritic cells from patients with Langerhans cell histiocytosis

High but not low doses of VBL strongly decreased MCL1 expression and survival **(Figure 5A)** of IL-17A and IFN-γ-treated healthy DC. As expected, we also documented that VBL disorganized microtubules (*data not shown*). VBL did not affect BFL1 expression. Therefore BFL1 alone is unable to maintain healthy DC alive. We studied survival, MCL1

and BFL1 expressions of monocyte-derived DC from 11 patients with LCH. In the attempt to mimic current LCH therapies, we also added VBL. High doses of VBL decreased MCL1 expression and killed the DC **(Figure 5B),** while BFL1 expression was not affected. DC from one patient (P5) were resistant to high doses of VBL. Working with sub-lethal doses of toxic compounds, we added anti-IL-17A neutralizing antibodies, *in vitro*. As measured by flow cytometry, we observed that addition of anti-IL-17A alone impaired LCH DC survival and strongly decreased BFL1 expression **(Figure 5C).** Combination of VBL to anti-IL-17A neutralizing antibodies offered the best conditions to kill LCH DC, *in vitro*. We found similar results with the combination of AraC and 2CdA, the salvage therapy used in LCH. Interestingly, addition of anti-IL-17A biotherapy overcame the VBL resistance of patient P5. In **Figure 5D,** we calculated the specific anti-IL-17A-dependent cytotoxicity for each of the 11 patients. Anti-IL-17A licensed DC killing with sub-optimal doses of chemotoxic compounds and adding VBL was statistically more efficient than AraC and 2CdA.

As a conclusion, the combination of moderate chemotherapy with inhibition of IL-17A activity so far appears to be the best solution to kill DC from LCH patients, *in vitro*.

DISCUSSION

We demonstrated that while MCL1 sustains a 2-day-short DC lifespan, additional BFL1 expression induced by IL-17A increases DC lifespan beyond 14 days. Monocyte-derived DC from patients with LCH, as well as DC and MGC in LCH lesions, abnormally constitutively express BFL1. This extended survival of DC and MGC is also associated with resistance to most chemotherapy agents. They are nevertheless sensitive *in vitro* to VBL and AraC, two drugs revealed by clinical studies to be effective in LCH. The blockade of IL-17A activity results in a dramatic increase of VBL efficacy to kill LCH DC, *in vitro*. These findings help in the understanding of LCH and may provide the rationale for novel therapeutic approaches, targeting IL-17A, to be considered for future clinical trials.

Nuclear translocation of NF-κB provides the basis for up-regulation of BFL1 by dendritic cells in response to IL-17A

When IL-17A interacts with its receptor chain IL-17RA, Act1 and TRAF6 are recruited and further activate NF-κB (reviewed in[22]). In mastocytes, NFAT1 is alternatively used downstream IL-17RA.[23] We studied translocation of RelA because NFAT1 mRNA was undetectable in the transcriptomes of IL-17A-stimulated DC, and among the five NF-κB proteins known in mammals, only RelA was expressed. Furthermore, a RelA responsive element is located in the promoter of *BCL2A1* gene and positively regulates BFL1 expression.[19] We demonstrate that NF-κB is activated downstream IL-17A-stimulation in DC and activates *BCL2A1* transcription, as assessed by the shut off operated by NF-κB inhibitor. Thus, nuclear translocation of NF-κB provides the basis for up-regulation of BFL1 by IL-17A in DC.

Towards a monocytic origin for dendritic cells in Langerhans cell histiocytosis

In 2008, we proposed that LCH is a DC-related disease rather than an LC-related disease. We designed a model for LCH pathogenesis where monocyte-derived DC drive LCH, then leading to an uncontrolled accumulation process of long-term surviving aggressive DC, resistant to apoptosis[4]. This may explain why LCH lesions include various myeloid cells: mostly DC of the $CD1a^+$ families as Langerhans cell and monocyte-derived DC, but also macrophages. Monocytes may provide a continuous large source of DC precursors thus suggesting how sometimes large granulomatous LCH lesions are built in a very short time by their recruitment.

Following analysis of phenotype (IL-17A, mixed macrophage–DC markers, MMP-9 and MMP-12) and DC fusion, we have also proposed that IL-17A combined to IFN-γ is a potential driver of LCH-associated pathology.

To advance on the biology of LCH DC, we decided to study expression of the Bcl2 family molecules, in parallel with survival and chemoresistance of LCH DC. Interestingly, BFL1, a pro-survival member, was induced by recombinant IL-17A in healthy DC and constitutively produced by LCH DC. The molecule that stimulates BFL1 expression in LCH DC was blocked by the neutralizing anti-IL-17A antibody from e-biosciences (eBio64CAP17). This molecule may come from canonical but possibly transient or unstable human IL-17A mRNA; alternatively, it is transcribed from a different (genetically mutated or infection-derived) sequence encoding an IL-17A-receptor binding domain. BFL1 provides a new molecular link between monocyte-derived and lesional DC in LCH. This observation is consistent with the involvement of monocytes as lesional DC precursors.

Reconciliation of malignancy and reactive immune response as the etiology of Langerhans cell histiocytosis

Although BFL1 expression and survival are correlated as a function of IL-17A concentration in healthy DC, other signals may increase DC lifespan, *in vivo*. In addition, expansion of the DC number may be related to other processes than the increase of the DC lifespan in some LCH patients. A high prevalence of a single *BRAF* missense mutation has been identified in LCH lesions of half of the patients studied[25]. The authors suggested an inhibition of the RAF pathway as a treatment option. This finding awaits validation but is interesting because the BRAF pathway is used downstream of receptors of cytokines such as M-CSF or GM-CSF, expressed at the DC surface.[26,27] The association of IL-17A signaling and the MAP pathway activation closely resembles a co-treatment of DC by IL-17A and GM-CSF, which is a powerful cytokine combination to greatly expand DC, as recently demonstrated in mouse, *in vivo.*[28]

Refining therapy of Langerhans cell histiocytosis by a combination of vinblastine chemotherapy and anti-IL-17A biotherapy

By targeting LCH DC survival with chemotherapy agents, we could not achieve a complete DC apoptosis: at least 6% of the DC survived. This finding might be related to the high frequency of reactivation of LCH in patients with multisystem disease despite that they had a good response to the current standard chemotherapy regimens.[29] Although anti-IL-17A

biotherapy alone was less efficient than chemotherapy agents, the combination of chemotherapy and anti-IL-17A biotherapy synergized in achieving DC killing, *in vitro*. Our work provides clues to approach the mechanisms of VBL-induced DC death in LCH. VBL was first known as an agent targeting the microtubule network, increasing the ratio between free tubulin fragments and the centrosome anchored, polymerized tubulin forming microtubules.[30] Interestingly, recent results documented other activity of two microtubule-targeted agents: VCR and Taxol.[31] In response to these toxic compounds, kinases phosphorylate MCL1, thus licensing the recruitment of an ubiquitine-ligase complex that degrades MCL1 and induces cell death. We actually found that VBL, whose formula is close to VCR, also decreases amount of MCL1 when DC are killed.

Most LCH reactivations occur in patients soon after completion of 6-12 months of standard VBL therapy, possibly suggesting that a minority of pathogenic DC may escape VBL-mediated killing, as in cancer cell lines[32]. The combination of AraC and 2CdA is effective as a rescue therapy for patients with LCH refractory to steroids and VBL. However, this therapy is associated with a life-threatening toxicity in children. BFL1 expression was not impaired by these toxic compounds. Adding anti-IL-17A biotherapy to VBL let us target both MCL1 and BFL1 leading to the most powerful $BFL1^{+}$ DC death, *in vitro*. Our interpretation is that (i) MCL1 is required for short-term DC survival but unable to sustain DC survival longer than 48h ; (ii) BFL1 is required for long-term DC survival, in parallel with MCL1. This would explain why it is possible to recover LCH DC death by inhibiting BFL1 expression with anti-IL-17A antibodies and why it is so efficient to combine toxic compounds degrading MCL1 with anti-IL-17A antibodies preventing BFL1 induction. The role of other molecules in induction of BFL1 in LCH should also be investigated further.[13]

In conclusion, data obtained with LCH DC and human *in vitro* models of primary DC cultures offer interesting hints to devise novel therapeutic strategies for LCH patients. Our work supports the view that accumulated DC, which are the effectors for tissue damage in LCH and express BFL1 could be targeted by the combination of lower VBL chemotherapy and neutralization of IL-17A binding domain with anti-IL-17A biotherapy, now in preclinical development, internationally, for use in inflammatory diseases. Alternatively, development of BFL1 inhibitors may provide a future treatment opportunity.

Authorship contributions

CD, JIH, CRC and MA conceived and wrote the initial study proposal and contributed substantially to conception and design of the research study. SOA, CM, AB, MM, GS, MBI,

NB, BB and CD made substantial contributions to acquisition of data. CD, SOA, CM and AB performed data analysis and drafted the manuscript. FB, MA, and JIH managed clinical issues. CD, JIH, MA, PJ and CRC participated in interpretation of the results and editing of the manuscript. All authors approved the final version of the manuscript.

Disclosure of conflicts of interest

The authors have declared that no competing interests exist.

Running head

BFL1, a biomarker for long-lived dendritic cells

References:

1. Cheong C, Matos I, Choi JH, et al. Microbial stimulation fully differentiates monocytes to DC-SIGN/CD209+ dendritic cells for immune T Cell areas. Cell. 2010;143(1): 416–429.
2. Rivollier A, Mazzorana M, Tebib J, et al. Immature dendritic cell transdifferentiation into osteoclasts: a novel pathway sustained by the rheumatoid arthritis microenvironment. Blood. 2004;104(13):4029-4037.
3. Bar-On L, Jung S. Defining dendritic cells by conditional and constitutive cell ablation. Immunol Rev. 2010;234(1):76-89.
4. Coury F, Annels N, Rivollier A, et al. Langerhans cell histiocytosis reveals a new IL-17A-dependent pathway of dendritic cell fusion. Nat Med. 2008;14(1):81-87.
5. Frenzel A, Grespi F, Chmelewskij W, Villunger A. Bcl2 family proteins in carcinogenesis and the treatment of cancer. Apoptosis. 2009;14(4):584-596.
6. Kozopas KM, Yang T, Buchan HL, Zhou P, Craig RW. MCL1, a gene expressed in programmed myeloid cell differentiation, has sequence similarity to BCL2. Proc Natl Acad Sci U S A. 1993;90(8):3516-3520.
7. Feuerhake F, Kutok JL, Monti S, et al. NFkappaB activity, function, and target-gene signatures in primary mediastinal large B-cell lymphoma and diffuse large B-cell lymphoma subtypes. Blood. 2005;106(4):1392-1399.
8. Monti S, Savage KJ, Kutok JL, et al. Molecular profiling of diffuse large B-cell lymphoma identifies robust subtypes including one characterized by host inflammatory response. Blood. 2005;105(5):1851-1861.
9. Oltersdorf T, Elmore SW, Shoemaker AR, et al. An inhibitor of Bcl-2 family proteins induces regression of solid tumours. Nature. 2005;435(7042):677-681.
10. Egeler RM, Favara BE, van Meurs M, Laman JD, Claassen E. Differential In situ cytokine profiles of Langerhans-like cells and T cells in Langerhans cell histiocytosis: abundant expression of cytokines relevant to disease and treatment. Blood. 1999;94(12):4195-4201.

11. Senechal B, Elain G, Jeziorski E, et al. Expansion of regulatory T cells in patients with Langerhans cell histiocytosis. PLoS Med. 2007;4(8):e253.
12. Peters TL, McClain KL, Allen CE. Neither IL-17A mRNA Nor IL-17A Protein Are Detectable in Langerhans Cell Histiocytosis Lesions. Mol Ther. 2011;19(8):1433-1439.
13. Hogarty MD. IL-17A in LCH: Systemic Biomarker, Local Factor, or None of the Above? Mol Ther. 2011;19(8):1405-1406.
14. Bernard F, Thomas C, Bertrand Y, et al. Multi-centre pilot study of 2-chlorodeoxyadenosine and cytosine arabinoside combined chemotherapy in refractory Langerhans cell histiocytosis with haematological dysfunction. Eur J Cancer. 2005;41(17):2682-2689.
15. Gadner H, Grois N, Arico M, et al. A randomized trial of treatment for multisystem Langerhans' cell histiocytosis. J Pediatr. 2001;138(5):728-734.
16. Gadner H, Grois N, Potschger U, et al. Improved outcome in multisystem Langerhans cell histiocytosis is associated with therapy intensification. Blood. 2008;111(5):2556-2562.
17. Bernstrand C, Sandstedt B, Ahstrom L, Henter JI. Long-term follow-up of Langerhans cell histiocytosis: 39 years' experience at a single centre. Acta Paediatr. 2005;94(8):1073-1084.
18. Laurencikas E, Gavhed D, Stalemark H, et al. Incidence and pattern of radiological central nervous system Langerhans cell histiocytosis in children: A population based study. Pediatr Blood Cancer. 2011;56(2):250-257.
19. D'Souza BN, Edelstein LC, Pegman PM, et al. Nuclear factor kappa B-dependent activation of the antiapoptotic bfl-1 gene by the Epstein-Barr virus latent membrane protein 1 and activated CD40 receptor. J Virol. 2004;78(4):1800-1816.
20. Morales AA, Olsson A, Celsing F, Osterborg A, Jondal M, Osorio LM. High expression of bfl-1 contributes to the apoptosis resistant phenotype in B-cell chronic lymphocytic leukemia. Int J Cancer. 2005;113(5):730-737.
21. Minkov M, Grois N, Braier J, et al. Immunosuppressive treatment for chemotherapy-resistant multisystem Langerhans cell histiocytosis. Med Pediatr Oncol. 2003;40(4):253-256.
22. Chang SH, Dong C. Signaling of interleukin-17 family cytokines in immunity and inflammation. Cell Signal. 2011;23(7):1069-1075.
23. Ulleras E, Karlberg M, Moller Westerberg C, et al. NFAT but not NF-kappaB is critical for transcriptional induction of the prosurvival gene A1 after IgE receptor activation in mast cells. Blood. 2008;111(6):3081-3089.
24. Yao Z, Fanslow WC, Seldin MF, et al. Herpesvirus Saimiri encodes a new cytokine, IL-17, which binds to a novel cytokine receptor. Immunity. 1995;3(6):811-821.
25. Badalian-Very G, Vergilio JA, Degar BA, et al. Recurrent BRAF mutations in Langerhans cell histiocytosis. Blood. 2010;116(11):1919-1923.
26. Baccarini M, Sabatini DM, App H, Rapp UR, Stanley ER. Colony stimulating factor-1 (CSF-1) stimulates temperature dependent phosphorylation and activation of the RAF-1 proto-oncogene product. EMBO J. 1990;9(11):3649-3657.
27. Carroll MP, Clark-Lewis I, Rapp UR, May WS. Interleukin-3 and granulocyte-macrophage colony-stimulating factor mediate rapid phosphorylation and activation of cytosolic c-raf. J Biol Chem. 1990;265(32):19812-19817.

28. Liu B, Tan W, Barsoum A, et al. IL-17 is a potent synergistic factor with GM-CSF in mice in stimulating myelopoiesis, dendritic cell expansion, proliferation, and functional enhancement. Exp Hematol. 2010;38(10):877-884 e871.
29. Minkov M, Steiner M, Potschger U, et al. Reactivations in multisystem Langerhans cell histiocytosis: data of the international LCH registry. J Pediatr. 2008;153(5):700-705, 705 e701-702.
30. Yang H, Ganguly A, Cabral F. Inhibition of cell migration and cell division correlate with distinct effects of microtubule inhibiting drugs. J Biol Chem. 2010.
31. Wertz IE, Kusam S, Lam C, et al. Sensitivity to antitubulin chemotherapeutics is regulated by MCL1 and FBW7. Nature. 2011;471(7336):110-114.
32. Kavallaris M. Microtubules and resistance to tubulin-binding agents. Nat Rev Cancer. 2010;10(3):194-204.

TABLE 1. Main features of the patients with Langerhans cell histiocytosis.

Case	Sex / Age at diagnosis	Organs involved during disease course	LCH chemo-immunotherapy Received	Age at study	Disease activity at evaluation	Disease activity class¤	Ongoing LCH chemo-immunotherapy at samplings	Sequelae
1 (a→b)	M / 6 yr	Bone*, ears*, pituitary*, skin, nd	Local (extirpation) + VBL + CST + 6-MP + MTX → 2CdA → 6-MP + MTX + CST	18 → 20 yr	AD, chronic	2 → 1	6-MP + MTX + CST → 6-MP + MTX	Panhypopituitarism CNS-ND
2 (a→b)	M / 4 yr	Bone*, pituitary*, nd	Local (steroids)	13 → 15 yr	NAD, sequelae	0	None	DI, GHD
3	M/ 14 mo	Bone*, skin*, spleen*	VBL+CST → 2CdA +ARAC	24 mo	NAD	0	None	None
4	F / 2 mo	Skin*, spleen	Local (steroids) → VBL + CST + 6-MP + MTX	6 yr	AD, chronic	1	6-MP + MTX	None
5	F / 5 mo	Bone*, skin, spleen, liver, bone marrow, thym, pituitary, nd	CST → VBL + MTX + 6-MP → Etanercept + 2CdA + IVIG → VBL + 6-MP + MTX + CST → 6-MP + CST → VBL	11 yr	AD, Chronic	2	None	DI, GHD, CNS-ND
6	M / 2.4 yr	Bone*, mm, lungs, pituitary	VBL + CST	2.6 yr	AD, better	1	VBL + CST	DI
7	M / 19 yr	Bone *	untreated	19 yr	Active	2	None	Walking impairment
8	F / 4 yr	Bone*	None	5 yr	NAD	0	None	None
9	M / 8 m	Skin*, lymph node*, liver*, ears*, spleen, bone marrow, intestines, bone	VBL+CST, MTX, VP-16 → 2CdA +ARAC → VBL+MTX+6-MP+CST → MTX+6-MP	5 yr	AD, better	2	6-MP + MTX	None
10	M / 2.8yr	Skin*	untreated	2.8yr	Active, diagnosis	2	None	
11	M / 3 yr	Bone*	VBL + CST	3.6yr	AD, better	1	VBL + CST	
12	F / 7.6yr	Bone*	untreated	7.6yr	Active, diagnosis	2	None	
13	M / 2 yr	Bone*	VBL + CST	3 yr	AD, better	2	VBL + CST	None

2CdA, Cladribine; 6-MP, 6-mercaptopurine; AD, active disease (persistence of signs and symptoms; no new lesions); ARAC, cytarabine; Chronic, Chronic disease; CNS-ND, symptomatic CNS neurodegeneration; CST, corticosteroids; DI, Diabetes insipidus; GHD, Growth hormone deficiency; IVIG, intravenous immunoglobulin; local, local corticosteroid injection; Mm, mucous membranes; MTX, methotrexate; NAD, no active disease, resolution of all clinical signs and symptoms; nd, CNS involvement with neurodegeneration evidenced by MRI; Progression, progressive disease (progression of signs and symptoms and/or appearance of new lesions).; VBL, vinblastine; VP-16, etoposide; → second (or further) line treatment. Disease activity classes: →, sampled two or three times, a, b and c; 0, resolution (no signs of active disease); 1, mild (regression of active disease or mild chronic disease; no hypoalbuminemia or ESR elevation); 2, moderate (moderately active disease; mild thrombocytosis, hypoalbuminemia, or ESR elevation); * indicates organ involved at diagnosis.

Figure Legends

Figure 1. Study of the *Bcl-2* family gene expression and immunocytology of p65 / RelA in monocyte-derived DC from healthy donors

(**A**) *Bcl-2* family mRNA relative expression in DC at day 0 (None) and after 12 days of culture with IL-17A or IL-17A and IFN-γ, transcriptome data representative of n = 3 donors. Left horizontal bar separates pro-apoptotic members (top) from pro-survival members (down). (**B**) Nuclear translocation of p65/RelA before and after 1h of IL-17A treatment on monocyte-derived DC from healthy donors. Right panel is a zoomed view of the left panel, representative of n = 3 donors. Scale bars, 10µm. (**C**) Dose response studies of IL-17A treatment (eight points from 2 to 0.016 ng/ml) on DC from three healthy donors. Mean fluorescence intensity (MFI) of MCL1 (all cells express MCL1) and percentages of BFL1 intracellular expressions in DC, quantified by flow cytometry.

Figure 2. Study of survival in parallel to MCL1 and BFL1 expressions in IL-17A and IFN-γ-treated DC from healthy donors

(**A**) Kinetic study of DC survival with indicated cytokines, percentages of viable DC were quantified by TRAP/ Hoechst staining. Mean and SD of n > 5. (**B, C**) Dose response studies of IL-17A treatment (eight points from 2 to 0.016 ng/ml) on DC from three healthy donors. (**B**) Percentages of $DiOC_6^+PI^-$ viable DC at day 7 relative to day 0, quantified by flow cytometry. (**C**) Two parameter polynomial statistical analysis of the three couples of data measured for each value of IL-17A concentration (Figure 1C and 2B) : percentages of $BFL1^+$ DC and viable DC (left) or MCL1 intensity and viable DC (center) or MCL1 intensity and percentages of $BFL1^+$ DC (right) were plotted as x and y, respectively. The equations of the statistical curves of tendency (left) are: donor A, $y= -0.0023x^2+0.7211x+0.3834$; donor B, $y= -0.0041x^2+0.8444x+1.0192$; donor C, $y= -0.0024x^2+0.4677x+0.9366$ with a correlation factor of 0.9975, 0.9937 and 0.9789, respectively.

Figure 3. Study of the *Bcl-2* family gene expression, survival, MCL1 and BFL1 expressions in monocyte-derived and lesional DC from patients with LCH

(**A**) *Bcl-2* family mRNA relative expression in monocyte-derived DC at day 0 from three LCH patients (p1a, p2a, p3) and one healthy donor representative of n = 4. Left horizontal bar separates pro-apoptotic members (top) from pro-survival members (down). (**B**) DC survival ($DiOC_6^+$ PI^- viable DC at day 7 relative to day 0), percentages of BFL1 intracellular expression and MFI of MCL1 expression in DC from 11 LCH patients (p1b, p2b, p4-p13), quantified by flow cytometry. (**C, D**) Representative confocal microscopy images of

immunofluorescence staining of bone lesions from patients (**C**) p8 and (**D**) p7 with LCH. CD1a (DC, green) and BFL1 (red) are stained. * indicates MGC. Scale bars, 50µm (5 x 10µm), n = 3.

Figure 4. Chemoresistance of IL-17A and IFN-γ-treated DC from healthy donors in the presence of 17 chemotherapy agents

(**A-H**) $DiOC_6^-$ PI^+ dead cells were quantified by flow cytometry. Percentages of dead DC relative to day 0 were calculated at 4 h, 24 h or 72 h. (**A**) In gray, untreated monocyte-derived DC cultured 72 h in medium alone. In black, IL-17A and IFN-γ-stimulated DC cultured with or without chemotherapy agents. Results of the screening are presented at optimal killing effect (see the "Design and method" section for full names of toxic compounds and optimal dose) then (**B to H**) detailed results are shown for the six toxic compounds that killed cytokine-stimulated DC. (**B**) Kinetic study at optimal concentration according to C to H. Mean of a triplicate experiment representative of n = 3, SD were below 10%. (**C to H**) Dose response study at optimal time, 24 or 72 h after addition of toxic compounds, according to B. Toxic compounds were added in DC cultures either concomitantly (black) or 24 h later (gray, preincubation) stimulation with IL-17A and IFN-γ. Mean and SD of a triplicate experiment representative of (**A**) *n* = 5, (**C to H**) n = 3. p-values : #, not significant: *, significant $P < 0.05$; **, very significant $P < 0.01$; ***, highly significant $P < 0.001$.

Figure 5. Study of BFL1 and MCL1 expressions and survival of monocyte-derived DC cultured with toxic compounds and neutralizing anti-IL-17A antibodies

(**A-D**) "High" doses were 0.6, 40 and 3 µM of VBL, AraC and 2CdA, respectively. "Low" doses were ten time less. DC survival ($DiOC_6^+$ PI^- viable DC at day 7 relative to day 0), MFI of MCL1 and percentages of BFL1 intracellular expressions were quantified by flow cytometry in (**A**) IL-17A and IFN-γ -stimulated DC from healthy donors and in (**B-D**) DC from LCH patients. Intracellular stainings of MCL1 and BFL1 were measured 12h after toxic compound treatment, prior $DiOC_6$ PI staining which was performed at optimum death: 24h and 48h for VBL and AraC+2CdA, respectively. One symbol per patient; monocyte-derived DC from 11 LCH patients (p1b, p2b, p4-p13) were analyzed. (**C, D**) neutralizing anti-IL-17A or isotype control was added 24h before toxic compounds. (**D**) Specific anti-IL-17A-dependent cytotoxicity was calculated with [survival without anti-IL-17A – survival with anti-IL-17A] / survival without anti-IL17A x 100 for each 11 patients from the data shown in (C). Bars represent the mean for all 11 patients. Statistical significance was determined by the Mann-Whitney test. *, significant $P < 0.05$; **, very significant $P < 0.01$.

Supplementary methods

Affymetrix Genechip study, microarray analysis:

Target labelling: Microarray analysis was performed using a high-density oligonucleotide array (Genechip human genome U133 Plus 2.0, Affymetrix, Santa Clara, CA, USA). Labeled target for microarray hybridization was prepared using the Genechip expression 3' Amplification One-cycle target labeling (Affymetrix). Briefly, total RNA (2 microg) was converted into double stranded cDNA with a modified oligo(dT)24-T7 promoter primer. After purification, cDNA was converted into cRNA and biotinylated using the IVT labeling kit (Affymetrix). Reaction was carried out for 16 hours at 37°C then at the end of incubation biotin-labeled cRNA was purified by the Genechip sample clean up module (Affymetrix). cRNA quantification was performed with a nanodrop and quality checked with the bioanalyzer 2100 (Agilent technologies, Inc, Palto Alto, CA, USA).

Arrays hybridization and scanning: Hybridization was performed following Affymetrix protocol (http://www.affymetrix.com). Briefly, 20 microg of labeled cRNA was fragmented, mixed in hybridization buffer (50 pM control oligo B2, 1X eukaryotic hybridization controls, 0,1mg/ml Herring sperm DNA, 0.5 mg/ml BSA and 1x hybridization buffer, 10% DMSO for a total volume of 300 ul), denaturated during 5 minutes at 95°C and hybridized on chip during 16 hours at 45°C with constant mixing by rotation at 60 rpm in an Genechip hybridization oven 640 (Affymetrix). After hybridization, arrays were washed and stained with streptavidin-phycoerythrin (Invitrogen Corporation, CA, USA) in a fluidic 450 (Affymetrix) according to the manufacturer's instruction. The arrays were read with a confocal laser (Genechip scanner 3000, Affymetrix) and analyzed with GCOS software. Absolute expression transcript levels were normalized for each chip by globally scaling all probe sets to a target signal intensity of 500. The detection metric (presence, absence or marginal) for a particular gene was determined by means of default parameters in the GCOS v 1.4 software (Affymetrix). Quality of RNA amplification and labeling were checked by using B.subtilis poly adenylated RNA spikes-in controls (Lys, phe, thr, dap) mixed to RNA sample before performing reverse transcription. Hybridization quality was checked by using E.coli biotinylated target (Bio B, BioC, BioD and CRE). Filtering of results was performed using Genespring ver 7.0 software (Agilent).

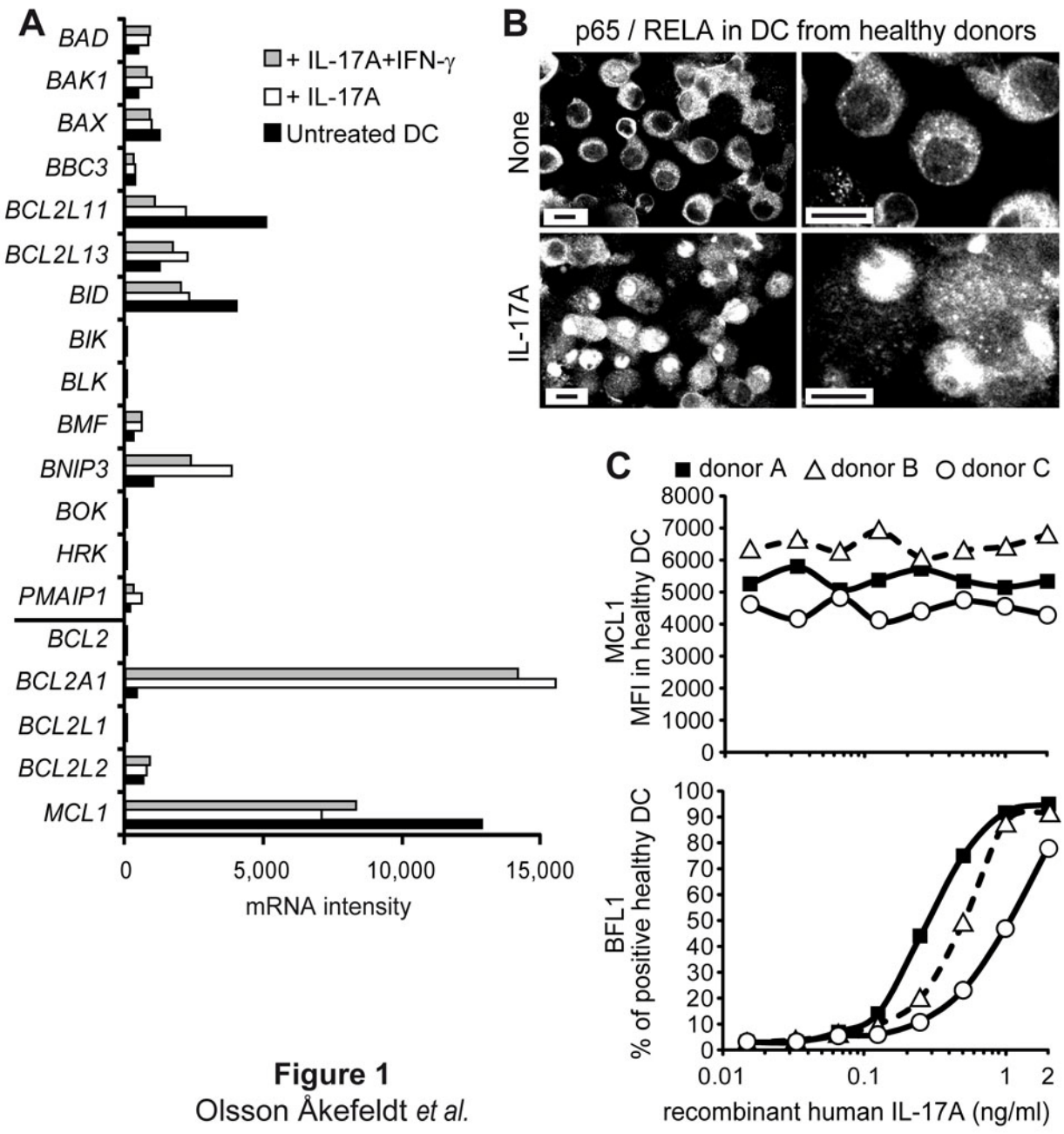

Figure 1
Olsson Åkefeldt *et al.*

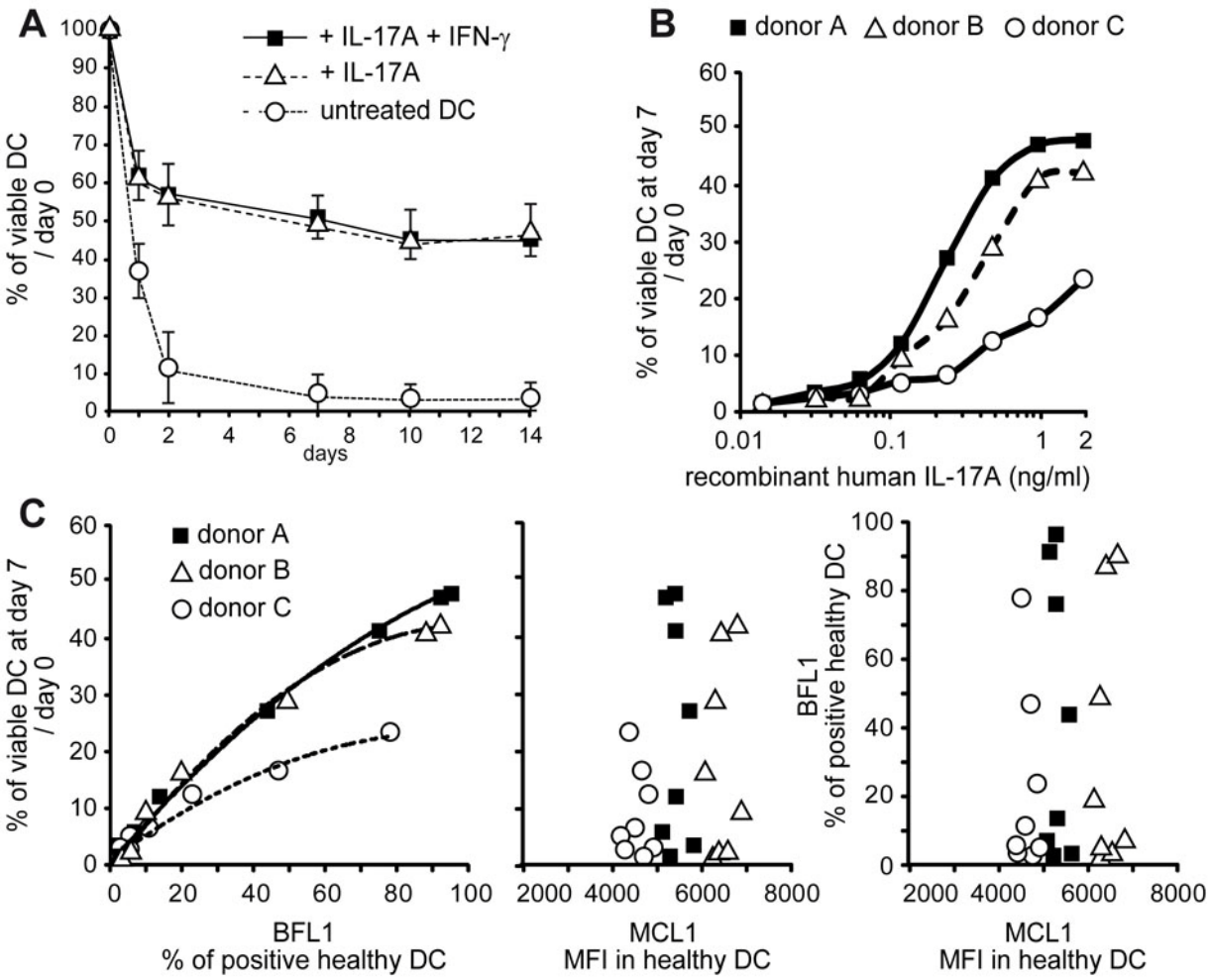

Figure 2
Olsson Åkefeldt *et al.*

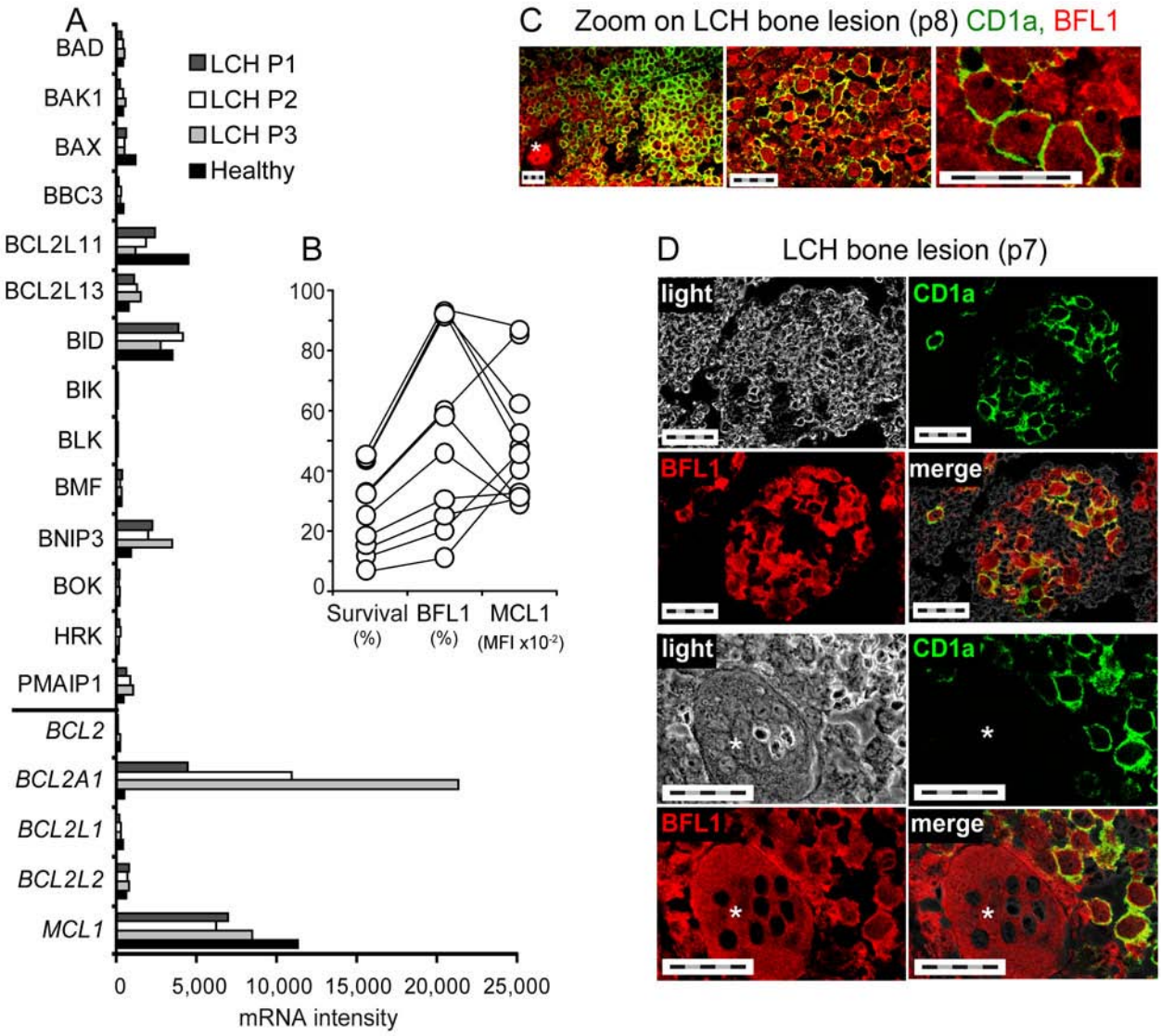

Figure 3
Olsson Åkefeldt et al.

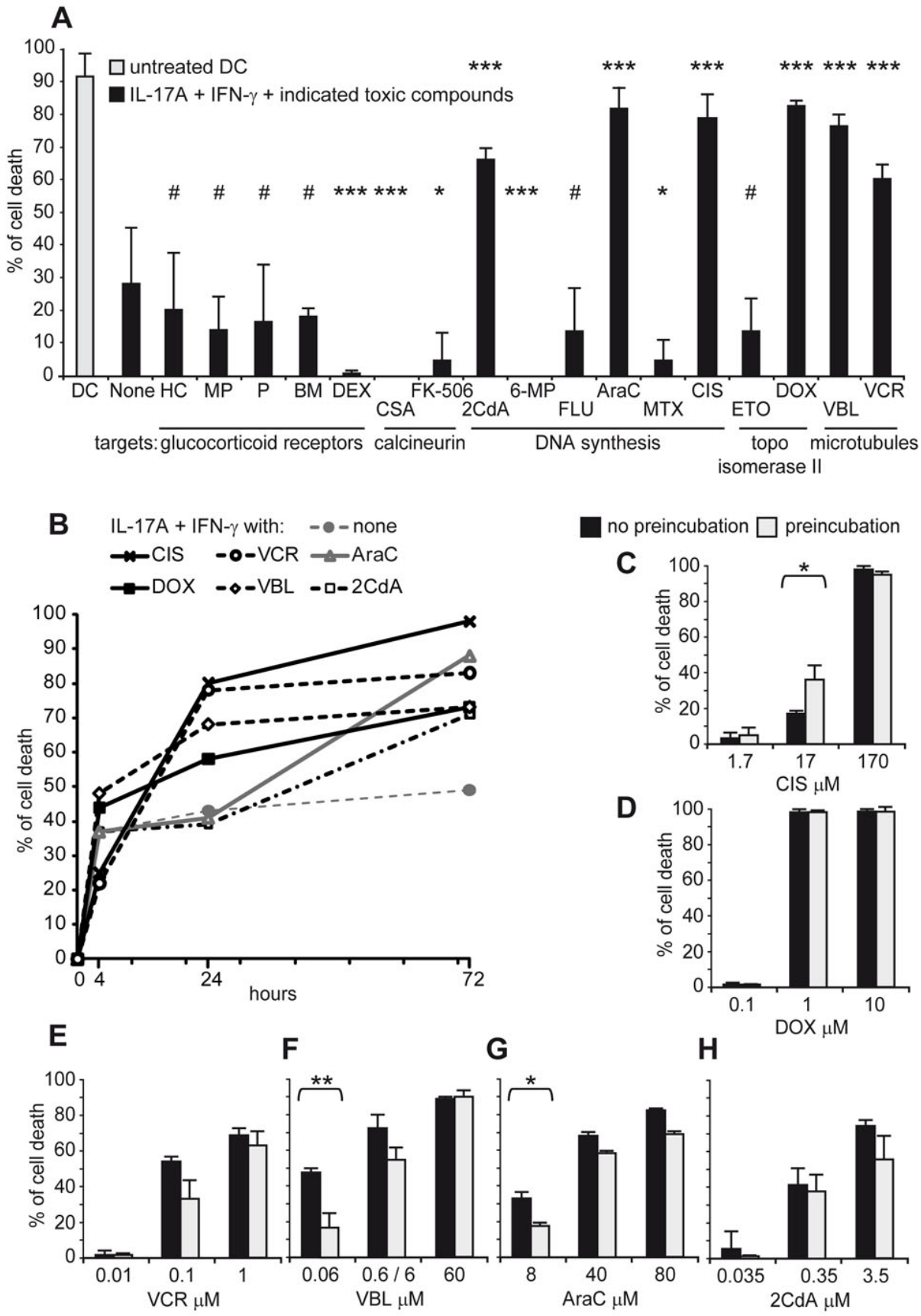

Figure 4
Olsson Åkefeldt *et al.*

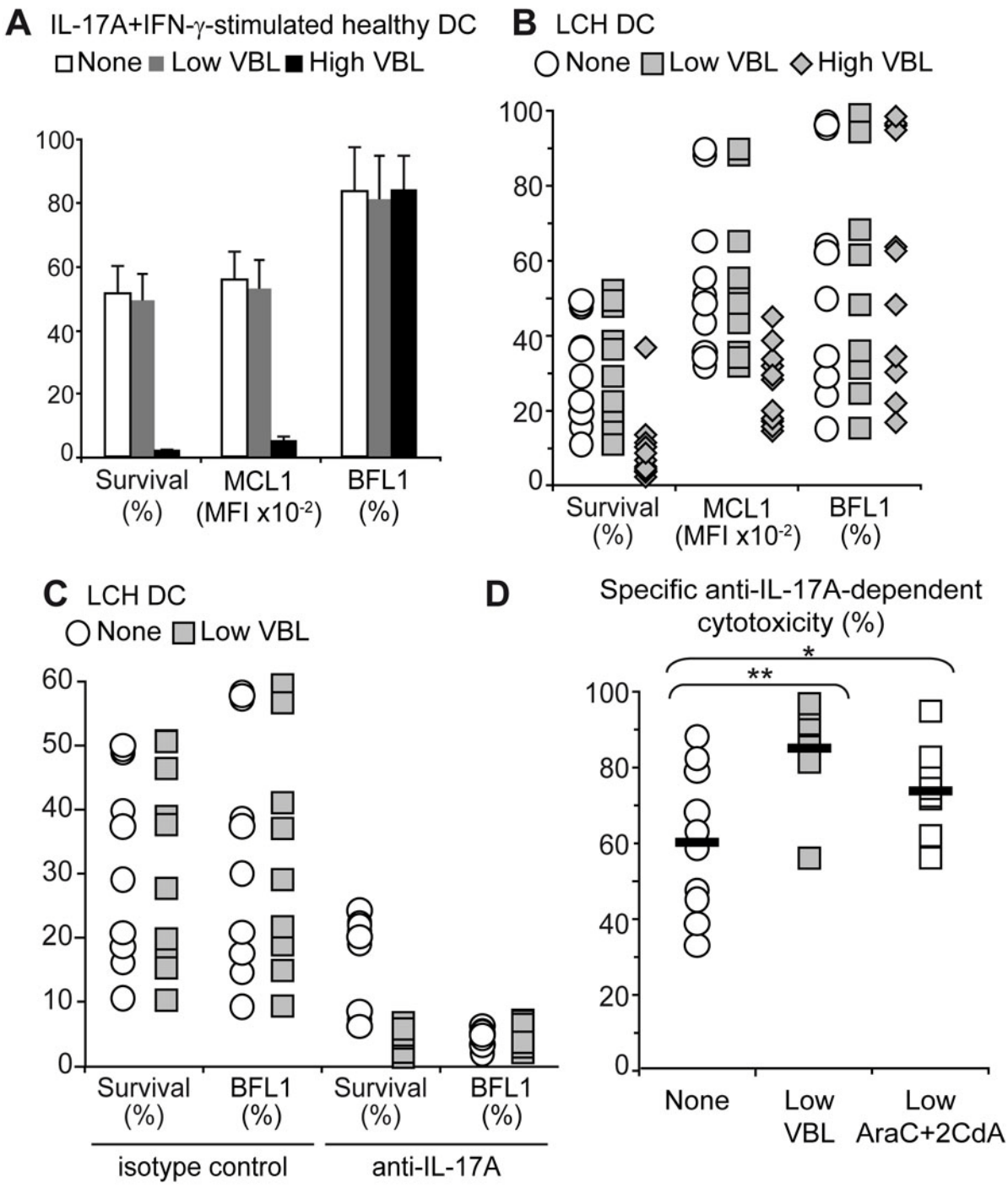

Figure 5
Olsson Åkefeldt *et al.*

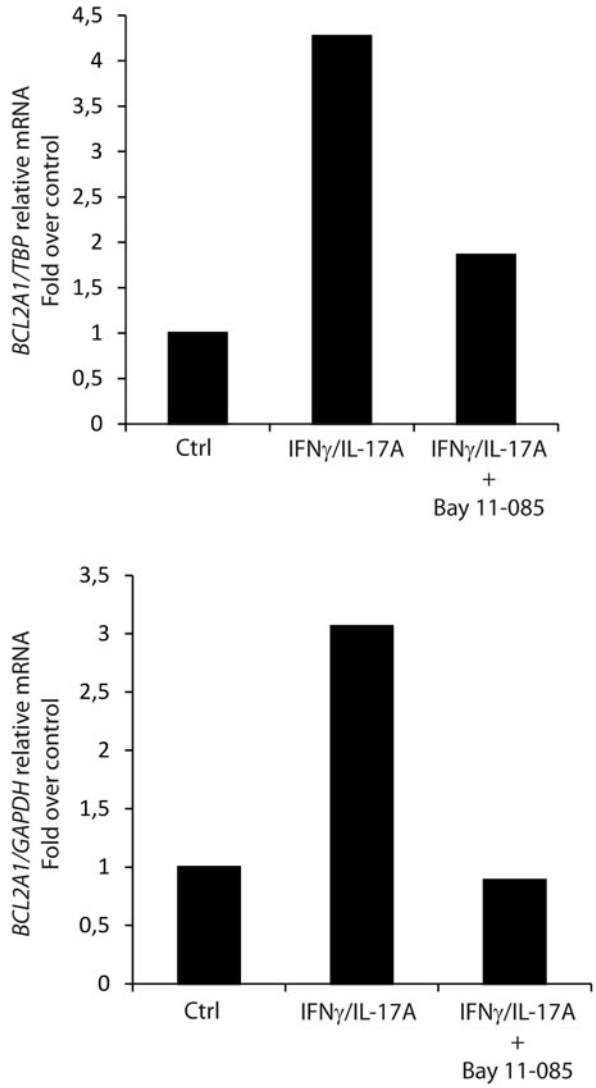

Study of BFL1 expression by RTqPCR in IL-17A+IFN-γ stimulated DC in the presence of NF-κB inhibitors

$2x10^6$ monocyte-derived dendritic cells were cultured with IL-17A and IFNγ (2ng/mL each) and eventually Bay-11-7085 (2µM, Calbiochem, Merck, Germany) in 12-well plates for 24h. After this time, cells were harvested and quantitative PCR was done as previously described. Primer sequences were as follow: *TBP*, QuantiTect® primers specific Hs_TBP_1_SG; *GAPDH*, QuantiTect® primers specific Hs_GAPDH_2_SG; *Bfl1*, QuantiTect® primers specific Hs_BCL2A1_1_SG (Qiagen).

NF-κB is required for IL-17A-dependent BFL1 induction

Peripheral blood monocytes from healthy donors were cultured in the presence of GM-CSF and IL-4 to generate DC, *in vitro*. Then DC were stimulated with IL-17A and IFN-γ in the presence or not of NF-κB inhibitor. Relative quantification of BFL1 mRNA by quantitative PCR demonstrated that inhibition of NF-κB induced inhibition of BFL1 mRNA expression, independently of the housekeeping gene chosen. Therefore NF-κB is required for IL-17A-dependent BFL1 induction.

Role of VBL on cytoskeleton of IL-17A and IFN-□-treated DC from healthy donors

Representative confocal microscopy images of triple immunofluorescence staining of IL-17A and IFN-γ-stimulated DC fixed at day 12. Hoechst blue staining localizes nuclei while green phalloidin reveals actin cytoskelon. The third color stained in red either (A and C top) tubulin or (B and C down) vinculin. (A) On merge pictures, arrow-head indicates double tubulin-actin staining in yellow. (B) Enlarged inset picture shows a ten-time magnification inside the podosome region. (C) Merge pictures of IL-17A and IFN-γ-stimulated DC two hours after addition of VBL. Arrow indicates keel-like structures of variable size. Arrow-head indicates bright blue fragment of DNA inside nuclei of apoptotic cells. * indicates MGC. Scale bars, 50μm (5 x 10μm), n = 3.

Vinblastine disorganizes microtubules and actin-containing podosomes of IL-17A and IFN-γ-treated DC

VBL was added after DC fusion to determine whether it is active on cytoskeletons of both DC and MGC. We first stained microtubules, actin and nuclei to discover that cytokines induced a giant microtubule network in MGC **(A)**. Podosomes, identified as spot-like actin-rich structures surrounded by a ring of vinculin, formed at the ventral surface of MGC **(B, inset)**. Numerous microtubules end in the cell periphery where actin spots are located, and in some cases, yellow color indicates that they directly contact each other (arrow-head). These observations are in agreement with the numerous interactions between actin and the microtubule cytoskeleton documented in the literature[1] showing direct contact of the plus ends of the microtubules with podosomes[2]. Exposure of cytokine-stimulated DC to VBL abolished the microtubule network **(C)**. In addition, subsequent lack of podosomes illustrates the requirement of an intact microtubule system for podosome assembly. Numerous keel-like unpolymerized tubulin and vinculin-rich structures of variable size (arrow), sometimes including nuclei, were budding from the cytoplasm. We identified the first apoptotic nuclei by condensed spots of DNA (arrow-head) two hours after VBL addition. We conclude that the efficacy of VBL to kill IL-17A and IFN-γ-stimulated DC is subsequent to depolymerization of the hypertrophied microtubule network which also disorganizes unexpected large areas of podosomes.

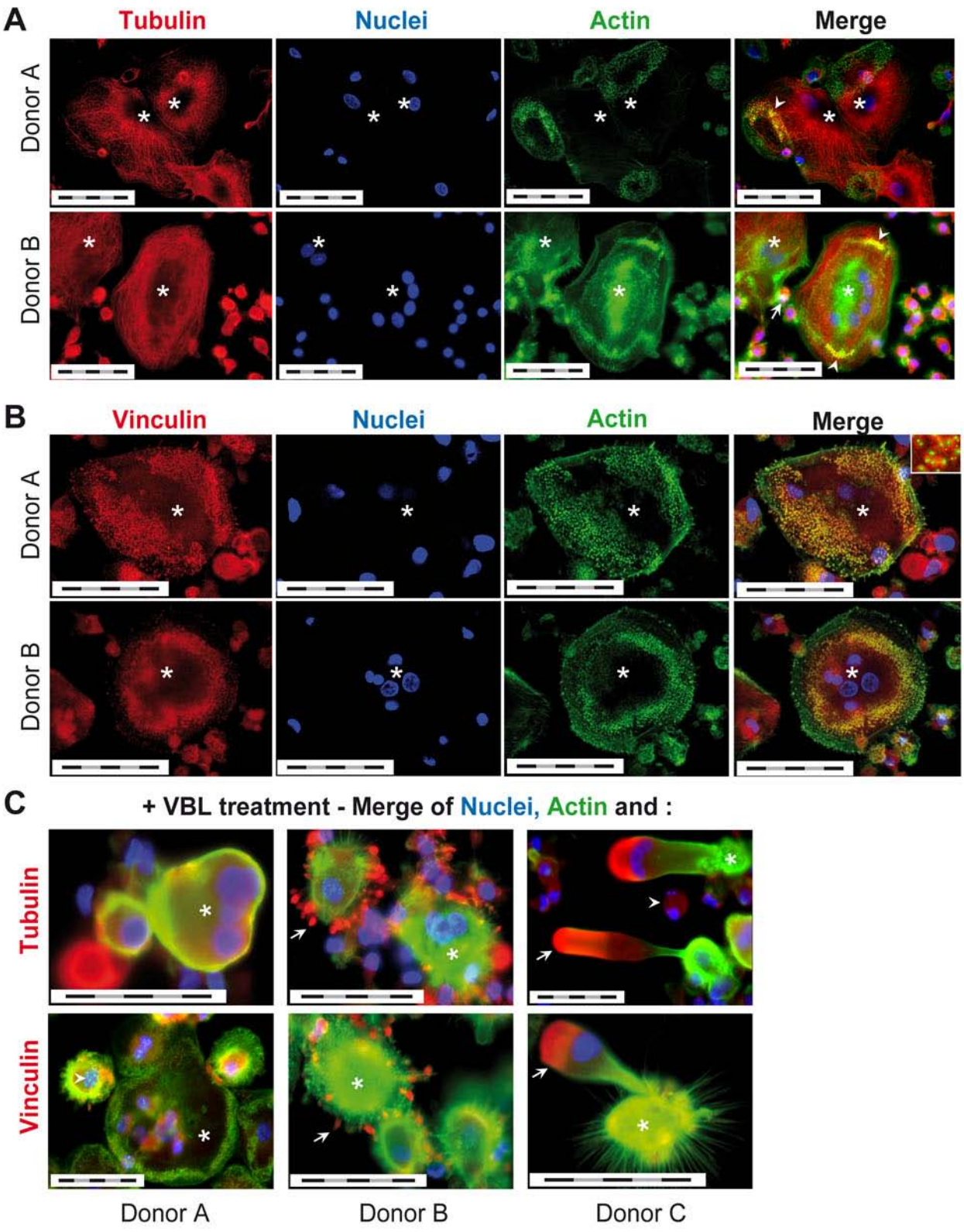
A
Tubulin
Nuclei
Actin
Merge
Donor A
Donor B
B
Vinculin
Nuclei
Actin
Merge
Donor A
Donor B
C
+ VBL treatment - Merge of Nuclei, Actin and :
Tubulin
Vinculin
Donor A
Donor B
Donor C

SUPPLEMENTARY METHODS

Immunocytofluorescence labeling

Cytoskeleton staining: All fixation and labeling procedures were conducted at room temperature. Cells treated or not with VBL were fixed 15 minutes in Busson fixation solution at pH 6.9 (4% paraformaldehyde, 60 mM PIPES, 25 mM HEPES, 20 mM EGTA, 2 mM magnesium acetate, 0.05% glutaraldehyde w/v).[3] They were then permeabilized with 0.2% (v/v) TritonX-100 in PBS for 7min. After preincubation 20 minutes in 10% normal human serum in PBS, cells were incubated for 1 hour, with either anti-vinculin (clone hVIN-1 mouse mAb, purified IgG, Sigma) or anti-tubulin (clone TUB.2.1 mouse mAb, Sigma) both diluted 1:100 in 1% BSA 3% normal human serum in PBS. Mouse IgG were used as control. Cells were then labeled with cyanin-5-conjugated goat anti-mouse secondary antibody (Jackson ImmunoResearch Laboratories), diluted 1:200 in the same buffer. At the same time F-actin distribution was revealed after incubation of the cells with Alexa 488-conjugated phalloidin (Invitrogen) according to the manufacturer's procedure. Finally, DNA nuclei were stained by incubating the cells with 10 mg/ml Hoechst 33342 (Sigma). Cells were extensively washed in PBS and coverslips were mounted in Prolong mounting medium containing anti bleaching agent (Invitrogen). Cells were observed either under a Leica TCS-SP5 laser scanning confocal microscope (Leica, Wetzlar, Germany) using a HCX PL APO 63x 1.4-0.6 oil DIC wd 0.1 mm objective or under an AxioImager Z1 (Zeiss, Jena, Germany) using a 40x-0.75 DIC wd 0.5 mm Plan Neofluar objective. Image acquisition has been done using MetaMorph 7.0 Software (Molecular Devices). To prevent cross-contamination between fluorochromes, each channel was imaged sequentially using the multi-track recording module before merging. Confocal section analyzed do not necessarily include all nuclei thus MGC are defined either by observation of strictly more than two nuclei observed on the section, or by the diameter of the cells above 25µm.

p65 / RelA nuclear translocation staining: $4x10^5$ monocyte-derived dendritic cells were cultured in 8-well Lab-Tek™ Chamber Slide™ System (Nunc, Thermo Scientific), eventually with IL-17A (2ng/mL). At the indicated times, the chamber slides were gently centrifugated and cells were fixed with PBS containing 4% paraformaldehyde for 30 min at 4°C. Cells were permeabilized with PBS containing 0.2% Triton X-100 for 20 minutes at room temperature. After saturation (30 minutes at room temperature in PBS 1% BSA, 3% human serum), cells were incubated 2h with 4µg/mL p65 / Anti-RelA in PBS 1% BSA (C-20, Santa Cruz Biotechnology, California, USA). After 3 washes in PBS 1% BSA, cells were incubated 30 minutes at room temperature in the dark with Alexa Fluor 647 Goat anti-rabbit IgG (10µg/mL, Molecular Probes, Invitrogen, Carlsbad, California USA). After 3 washes, cells were mounted in Dako Fluorescent Mounting medium (Dako, Denmark), and immunostaining images were analyzed using a Carl Zeiss inverted laser scanning confocal microscope LSM 510.

LCH bone lesions staining: 4-µm paraffin-embedded bone biopsies were deparaffinized and rehydrated. Following epitope retrieval, tissue sections were incubated 30 minutes in phosphate buffered saline (PBS) -1% bovine serum albumin (BSA) with 3% human serum to block Fc receptors. They were then incubated with primary antibodies, overnight at 37°C, in a humidity chamber. Replacement of the primary antibodies by non-relevant antibodies of the same immunoglobulin isotype was used as negative control. We used the following primary antibodies: mouse anti CD1a, (Acris Antibodies, DM363, 1:20

dilution) and rabbit anti-A1 (Biovision, 3401-100, 4µg/mL) and the following isotype control antibodies: mouse IgG1 (Dako, X0931) and Rabbit IgG (R&D, AB-105-C). Slides were then washed 3 times in PBS-1% BSA and detection of the primary antibodies was performed with suitable isotype-specific secondary Alexa Fluor 488, and 647-conjugated antibodies (Invitrogen, 10µg/mL) for 30 min. Following 3 washes in PBS-1% BSA, sections were mounted using Mowiol and then analyzed by confocal microscopy using a Carl Zeiss MicroImaging Inc. LSM 510 confocal microscope.

Affymetrix Genechip study, microarray analysis:

Target labelling: Microarray analysis was performed using a high-density oligonucleotide array (Genechip human genome U133 Plus 2.0, Affymetrix, Santa Clara, CA, USA). Labeled target for microarray hybridization was prepared using the Genechip expression 3' Amplification One-cycle target labeling (Affymetrix). Briefly, totalRNA (2□g) was converted into double stranded cDNA with a modified oligo(dT)24-T7 promoter primer. After purification, cDNA was converted into cRNA and biotinylated using the IVT labeling kit (Affymetrix). Reaction was carried out for 16 hours at 37°C then at the end of incubation biotin-labeled cRNA was purified by the Genechip sample clean up module (Affymetrix). cRNA quantification was performed with a nanodrop and quality checked with the bioanalyzer 2100 (Agilent technologies, Inc, Palto Alto, CA, USA).

Arrays hybridization and scanning: Hybridization was performed following Affymetrix protocol (http://www.affymetrix.com). Briefly, 20 □g of labeled cRNA was fragmented, mixed in hybridization buffer (50 pM control oligo B2, 1X eukaryotic hybridization controls, 0,1mg/ml Herring sperm DNA, 0.5 mg/ml BSA and 1x hybridization buffer, 10% DMSO for a total volume of 300 ul), denaturated during 5 minutes at 95°C and hybridized on chip during 16 hours at 45°C with constant mixing by rotation at 60 rpm in an Genechip hybridization oven 640 (Affymetrix). After hybridization, arrays were washed and stained with streptavidin-phycoerythrin (Invitrogen Corporation, CA, USA) in a fluidic 450 (Affymetrix) according to the manufacturer's instruction. The arrays were read with a confocal laser (Genechip scanner 3000, Affymetrix) and analyzed with GCOS software. Absolute expression transcript levels were normalized for each chip by globally scaling all probe sets to a target signal intensity of 500. The detection metric (presence, absence or marginal) for a particular gene was determined by means of default parameters in the GCOS v 1.4 software (Affymetrix). Quality of RNA amplification and labeling were checked by using B.subtilis poly adenylated RNA spikes-in controls (Lys, phe, thr, dap) mixed to RNA sample before performing reverse transcription. Hybridization quality was checked by using E.coli biotinylated target (Bio B, BioC, BioD and CRE). Filtering of results was performed using Genespring ver 7.0 software (Agilent).

1. Goode, B.L., Drubin, D.G. & Barnes, G. Functional cooperation between the microtubule and actin cytoskeletons. *Curr Opin Cell Biol* **12**, 63-71 (2000).
2. Kopp, P.*, et al.* The kinesin KIF1C and microtubule plus ends regulate podosome dynamics in macrophages. *Mol Biol Cell* **17**, 2811-2823 (2006).
3. Destaing, O.*, et al.* A novel Rho-mDia2-HDAC6 pathway controls podosome patterning through microtubule acetylation in osteoclasts. *J Cell Sci* **118**, 2901-2911 (2005).

2.2 Manuscrit 2: IL-17A-dependent maintenance of human tuberculosis granuloma is mediated by BFL1, CCL20 and CCL2

by **Mohamad Bachar ISMAIL**[1-4]*, Alexandre BELOT[1-5]*, Selma OLSSON-ÅKEFELDT[1-4,6], Carine MAISSE[1-4], Giulia SALVATORE[1-4,7-8], Nathalie BISSAY[1-4], Béatrice BANCEL[9], Olga AZOCAR[10], Franck BREYSSE[9], Maurizio ARICÒ[8], Jan-Inge HENTER[6], Chantal RABOURDIN-COMBE[3-4,10]†, Monique CHOMARAT[9], Françoise BERGER[1-4,9] and Christine DELPRAT[1-4]

**Contributed equally as first authors. †Deceased*

[1] CNRS, UMR5239, Laboratoire de Biologie Moléculaire de la Cellule, Lyon, F-69007, France ;

[2] Ecole Normale Supérieure de Lyon, Lyon, F-69007, France ;

[3] Université de Lyon, Lyon, F-69003, France ;

[4] Université de Lyon 1, Villeurbanne, F-69622, France ;

[5] Hospices Civils de Lyon, Hôpital Femme Mère Enfant, Bron, F-69500, France ;

[6] Childhood Cancer Research Unit, Department of Women's and Children's Health, Karolinska Institutet, Karolinska University Hospital Solna, S-171 76 Stockholm, Sweden;

[7] Université de Florence, Florence, I-50134, Italy ;

[8] Department of Pediatric Hematology Oncology, Azienda Ospedaliero-Universitaria Meyer Children Hospital, Florence, I-50139, Italy;

[9] Hospices Civils de Lyon, Department of Pathology, Department of Microbiology, Centre Hospitalier Lyon Sud, Pierre Bénite, F-69310, France ;

[10] INSERM, U851, 21 Avenue Tony Garnier, Lyon, F-69007, France ;

Corresponding author:

Pr Christine DELPRAT

CNRS 5239-FACULTE DE MEDECINE LYON SUD

165 Chemin du Grand Revoyet : BP12

69921 OULLINS CEDEX

FRANCE
Phone : +33 426 235 980

Fax : +33 426 235 900

e-mail : **cdelprat@free.fr**

Short Title: **Granuloma maintenance by interleukine-17A**

Abbreviations used in this paper: BCG, *Mycobacterium bovis* strain Bacille de Calmette et Guérin ; BFL1, B-cell lymphoma 2-related protein A1; CCL, chemokine ligand; CCR, chemokine (C-C motif) receptor; CXCL, Chemokine (C-X-C motif) ligand; Mtb, Mycobacterium tuberculosis; RANKL, Receptor Activator for NF-κB Ligand.

Total character counts: 31,191 (text 19,316 + figures 11,875)

ABSTRACT

In tuberculosis, granulomas are constituted by a collection of myeloid cells, including giant cells, surrounded by a ring of lymphoid cells. In humans, the mechanisms of granuloma formation and maintenance are largely unknown. We characterized the molecular profile of granulomas from ten tuberculosis patients. We detected the pro-survival Bcl-2 family gene BFL1, CCL20 and CCL2 in $CCR6^{+}CD68^{+}$ myeloid cells and GM-CSF and IL-17A in lymphoid cells. *In vitro*, we generated immature dendritic cells from monocytes with GM-CSF and IL-4. IL-17A induced long-term survival, clustering and fusion of either GM-CSF-treated monocytes or dendritic cells. IFN-γ only potentiated clustering and fusion without affecting survival. BFL1 induced by IL-17A correlated with long-term survival. CCL20 and CCL2 chemokine expression, induced by IL-17A, were mandatory for clustering and fusion, without affecting survival. Blocking CCL2 resulted in epithelioid morphology, suggesting that morphological changes, controlled by CCL2, authorized clustering and fusion. We show that in addition to GM-CSF, IL-17A potentially promotes tuberculosis granuloma maintenance through myeloid cell survival driven by the BFL1 gene, and through myeloid cell recruitment and fusion mediated by CCL20 and CCL2. These findings are at the interface of innate and adaptive immunity and will open novel strategies to control granuloma formation.

INTRODUCTION

The hallmark of tuberculosis (TB) is the formation of granulomas consisting of accumulated immune cells under the control of chemokines which direct cell migration. Human TB granulomas are composed of a core made up of pauci-bacillary multi and mononucleated myeloid cells, referred to as Langhans and epithelioid cells, respectively. A coat of lymphocytes and a tight external shell of fibroblasts surround this myeloid core. Chronic granulomatous responses will arise from antigens resisting immune elimination. And, if uncontrolled, can damage host tissues. Thus, it is crucial to understand the mechanisms how they are formed, maintained and resolved.

Differences in the role granulomas play have been reported in several animal models: in the embryos of the inferior vertebrate Zebrafish, the early spreading of *Mycobacterium marinum*-infected macrophages from primary granulomas (Davis and Ramakrishnan, 2009) suggests that granulomas favor mycobacterial expansion and dissemination. Conversely, in mice, infected macrophages are retained within the granulomas (Egen et al., 2008) thus protecting the host from bacterial spreading (Flynn and Chan, 2001; Lawn et al., 2002; Ulrichs and Kaufmann, 2006). Likewise, in humans, disruption of TB granuloma by TNF-α-neutralization induces reactivation of latent tuberculosis (Gardam et al., 2003), therefore demonstrating that granulomas control Mycobacteria.

Scientists have identified that TNF-α, GM-CSF, IFN-γ and IL-17A control murine granulomas. TNF-α affects both formation and maintenance by inducing CCL5, CXCL9 and CXCL10 thus attracting T and myeloid cells (Algood et al., 2005; Bean et al., 1999; Kindler et al., 1989). GM-CSF or IFN-γ-deficient mice, infected by M*ycobacterium tuberculosis (Mtb)* cannot form granulomas and rapidly succumb (Cooper et al., 1993; Gonzalez-Juarrero et al., 2005). GM-CSF deficiency prevents induction of CCL4 and CCL5 while IFN-γ contributes to CXCL9 and 10 chemokine productions (Fenton et al., 1997; Gonzalez-Juarrero et al., 2005). IL-17A plays a critical anti-Mycobacterium role through the induction of granuloma formation and maintenance (Lockhart et al., 2006; Okamoto Yoshida et al., 2010; Umemura et al., 2007) and is known to induce production of CXCL9, CXCL10 and CXCL11, in vivo (Khader et al., 2007).

Very little is known on the functional and sequential role of the chemokines in granuloma maintenance. Notably, CCR2-deficiency markedly impairs macrophage recruitment to sites of inflammation, inducing the mouse death early after infection with 100-

fold more Mycobacteria in their lungs compared to wild-type mice (Peters et al., 2001a). However, mice lacking CCL2, a CCR2 ligand, form granulomas and control Mycobacterium infection, suggesting that additional ligands contribute to the macrophage recruitment (Kipnis et al., 2003; Vesosky et al., 2010).

In humans, predisposition to Mycobacteria infections is associated to a deficient IL-12/ IFN-γ /Th1 axis (Casanova and Abel, 2002). Circulating *Mtb*-specific memory T cells express CCR6, the only known receptor for CCL20 (Acosta-Rodriguez et al., 2007b). Twenty per cent of these *Mtb*-specific $CD4^+$ T cells produce IL-17A (Scriba et al., 2008), consistent with the identification of CCR6 as a marker for IL-17A-producing lymphocytes (Annunziato et al., 2007). However, i*n situ* detection and the role of GM-CSF, IL-17A and CCL20/CCR6 remain to be investigated in human TB chronic granuloma as well as the mechanisms ensuring myeloid cell survival.

Here, we localized cells (CD3, CD68 and CCR6), cytokines (GM-CSF, IL-17A), chemokines (CCL20, CCL2) and the pro-survival protein BFL1, from the Bcl-2 family in the granulomas of ten TB patients. We determined that IL-17A was a potent inducer of BFL1, CCL20 and CCL2 in myeloid cells. We studied consequences on their survival, clustering and fusion. Altogether, our results support that GM-CSF combined with IL-17A maintain the human myeloid core of the TB granulomas by regulating BFL1, CCL20 and CCL2 expressions of $CCR6^+CD68^+$ myeloid cells.

RESULTS AND DISCUSSION

BFL1, CCL20 and CCL2 are expressed by myeloid cells in the heart of tuberculosis granuloma

We performed immunostainings on granulomas from ten TB patients. The GM-CSF-producing lymphoid cells (red, **Fig. 1 A)** localized in the T cell-rich granuloma periphery (**Fig. 1 B, C, D** red CD3**).** A T cell sub-population expressed CCR6 and IL-17A (**Fig. 1 C-inset** white**).** In the myeloid heart of TB granuloma, mono- and multinucleated giant cells expressed the CD68 macrophage marker (**Fig. 1 A** brown**, B** green and **E** blue) and the CCR6 chemokine receptor (**Fig. 1 C, D** blue). $CD68^+$ mono- and multinucleated cells also expressed BFL1 (**Fig. 1 B** yellow**)** and CCL2 (**Fig. 1 E** light blue**).** The $CCL20^+$ myeloid cells expressed CCR6 (**Fig. 1 D** light blue**)** but also co-expressed CCL2 (**Fig. 1 F** ~70% yellow) previously demonstrated to characterize $CD68^+$ cells. Therefore, most of the myeloid cells express CD68, CCR6 and co-expressed the BFL1 survival protein, and the CCL20 and CCL2 chemokines.

First, this study revealed BFL1 expression in myeloid cells of TB granulomas. As other members of the Bcl-2 family, BFL1 regulates sensitivity to apoptosis by governing mitochondrial outer membrane permeabilization (Frenzel et al., 2009). Expression of this pro-survival molecule is common in B cell lymphoma, but unusual in primary myeloid cells which only express the pro-survival member MCL1 at steady-state (Feuerhake et al., 2005; Monti et al., 2005). However, BFL1 can be induced by BCG in human monocytes (Kremer et al., 1997) and by the virulent *Mtb* strain H37Rv in a human monocytic cell line (Dhiman et al., 2007; Pattingre et al., 2005). Therefore BFL1 induction may result from *Mtb* infection. Secondly, we found a homogeneous phenotype between most of the mononucleated and the giant myeloid cells, suggesting that myeloid cells which undergo cell fusion inside TB granuloma express CCR6, CD68, BFL1, CCL20 and CCL2.

GM-CSF combined with IL-17A licenses long-term survival and human myeloid cell fusion, *in vitro*

We have previously demonstrated that DC undergo cell fusion in the presence of IL-17A, whereas monocytes cannot (Coury et al., 2008). To further understand the role of GM-CSF, IL-17A and IFN-γ in myeloid cell survival, clustering and fusion, independently of Mycobacterium stimulation, we purified human monocytes and generated immature DC in the

presence of GM-CSF and IL-4. Monocytes or DC were cultured for 14 days in the presence of none, GM-CSF, IL-17A, IFN-γ alone or in combination. DC underwent cell fusion in the presence of IL-17A **(Fig. 2 A).** When treated with GM-CSF, 20% of monocyte survived **(Fig. 2 B)**, contrary to IFN-γ or IL-17A alone. In GM-CSF-stimulated monocytes like in immature DC, IL-17A dose-dependently induced long-term survival, cell clustering and fusion **(Fig. 2 B-D)**. IFN-γ accelerated clustering which was visible at 4h **(Fig. 2 A)**, but did not affect myeloid cell survival **(Fig. 2 B).** IFN-γ also increased the number of cell clusters **(Fig. 2 C)** and enhanced fusion efficiency **(Fig. 2 D)** without affecting the kinetics of the fusion process (data not shown).

Murine myeloid cells within chronic *Mtb* granulomas highly express CD40, MHCII, CD11c and CD11b, which are markers typically expressed on DC (Ordway et al., 2005). Pathologists call the myeloid cells of TB granuloma: epithelioid cells, because their morphology resembles epithelial cells (Adams, 1976). In terms of phenotype, epithelioid cells co-express macrophage and DC markers. The control of *Mtb* replication realized by epithelioid myeloid cells is achieved *in vitro* by either monocytes or macrophages treated with GM-CSF (Denis and Ghadirian, 1990; Vogt and Nathan, 2011) or by DC, derived from monocytes in the presence of GM-CSF and IL-4 or IL-13 (Tailleux et al., 2003b). Moreover, a recent report confirmed that M-CSF, the cytokine used for canonical macrophage differentiation, *in vitro*, failed to control virulent *Mtb* contrary to GM-CSF (Vogt and Nathan, 2011). Here we show that GM-CSF conditioned monocytes to respond to IL-17A, similarly to the DC. Overall, the biology of epithelioid myeloid cells appears closely related to DC or GM-CSF-treated monocytes regarding their ability not only to control *Mtb* growth, but also to undergo cell fusion in the presence of IL-17A and IFN-γ, two cytokines highly expressed in TB granuloma.

IL-17A induces BFL1, CCL20 and CCL2 in human DC

We studied the expression of BFL1, CCL20 and CCL2 in IL-17A-stimulated DC. Quantitative mRNA and protein detection established that IL-17A induced BFL1 in DC **(Fig. 3 A, B).** IFN-γ did not affect BFL1 expression. We measured that exposure to IL-17A increased the percentage of $BFL1^+$ DC in a dose-dependent manner **(Fig. 3 C).** We studied the statistical correlation between DC survival and BFL1 induction **(Fig. 3 D)**. We found that the ability of DC to survive was statistically linked to BFL1 expression and in agreement with good (donors A and B) or moderate (donor C) response to IL-17A**.**

IL-17A signaling activates NF-κB (reviewed in(Chang and Dong, 2011)) and NF-κB p65 / RelA subunit is a known regulator of the BFL1 gene (D'Souza et al., 2004). In *Mtb*-infected THP1 epithelioid cell line, BFL1 transcription occurs downstream of NF-κB nuclear translocation. Therefore myeloid cells in TB granuloma may receive two available signals to induce BFL1: *Mtb* detection (Dhiman et al., 2007) and IL-17A signal transduction. According to our results, induction of BFL1 may favor long-term survival of myeloid cells inside granulomas.

In IL-17A-treated DC, the quantification of CCL20 and CCL2 chemokine expressions indicated early induction of *ccl20* mRNA in the first 12 hours then decreased while *ccl2* mRNA increased (**Fig. 3 E**). Intracellular CCL20 and CCL2 proteins were detected by flow cytometry (**Fig. 3 F**) and immunocytology (**Fig. 1 G**) showing that CCL20 was induced by IL-17A stimulation contrary to our observation that CCL2 was already expressed in immature DC then up-regulated by IL-17A. This may explain the difference in chemokine secretions quantified by ELISA, showing much more CCL2 than CCL20 in supernatants of IL-17A-stimulated DC (**Fig. 3 G**). The two chemokines were stored in distinct cytoplasmic vesicles (**Fig. 1 G-inset**). Their expressions and secretion, were not affected by adding IFN-γ (**Fig. 3 E, G**). Overall, IL-17A changed the phenotype of $BFL1^{-}CCL20^{-}CCL2^{+}$ immature DC in $BFL1^{+}CCL20^{+}CCL2^{high}$ myeloid cell, comparable to the main phenotype we previously observed in TB granuloma.

The sequential induction of *ccl20* then *ccl2* mRNA may orchestrate the anti-Mycobacterium immune response. Contrary to CCL2/CCR2, little knowledge is available concerning the role of CCR6 and its ligand CCL20, in Mycobacterium infections. CCL20 production has been documented in TB patients (Lee et al., 2008). In mice, following intratracheal infection with BCG, CCL20 was induced during the early innate stage of infection (Stolberg et al., 2011), maybe in agreement with the IL-17A production by γδ T cells (Umemura et al., 2007). In sarcoidosis, another disease with structured granulomas, CCL20 is also expressed by epithelioid and multinucleated cells infiltrating the granulomas, surrounded by IL-17A-producing T cells (Facco et al., 2007; Facco et al., 2011). It would be interesting to quantify CCL20-expressing mono and multinucleated myeloid cells in Mycobacterium-infected IL-17A-deficient mice and in IL-17A-transgenic mice which spontaneously form multinucleated myeloid cells in lungs after three month of age (Park et al., 2005).

CCR6 is expressed by myeloid immature DC, mature B cells and subpopulations of memory/effector T cells (Kucharzik et al., 2002). Intratracheal infection of CCR6-deficient mice with BCG recently established that, despite its purported role in DC function, CCR6 was not required for the establishment of T cell-mediated adaptive immunity against Mycobacteria : the $CCR6^{-/-}$ mice eliminate BCG. However, in these mice, an impaired early stage mycobacterial clearance was observed and associated to a 90% decrease in the recruitment of CD1d-restricted T cells known as iNKT cells (Stolberg et al., 2011), which provided innate resistance to *Mtb* (Sada-Ovalle et al., 2008). Thus, murine data only established a role of CCL20 in the early phase of *Mtb* infection. But murine granulomas are not structured like human granulomas and the CCL20/CCR6 co-expression we observed in myeloid cells suggests an original role for this interaction in the TB granuloma cohesion.

IL-17A-dependent expression of CCL20 and CCL2 are necessary for DC clustering and fusion

To evaluate the respective role of CCL20 and CCL2 in IL-17A-dependent survival, clustering and fusion, we conducted inhibitory assays using neutralizing antibodies on DC cultured with IL-17A and IFN-γ. Isotype control antibodies had no effect on the previous documented observations. Blocking CCL20 and CCL2 did not impact on the number of viable cells (**Fig. 4 A, B**). However, CCL20 inhibition prevented clustering and giant cell formation (**Fig. 4 C, D**). In addition, CCL2 blockade not only inhibited DC fusion, but also reproducibly modified the DC morphology which became elongated (**Fig. 4 F, A, E**). However, when we treated DC with recombinant CCL20 and/or CCL2, DC clustering occurred without cell fusion (data not shown). This indicated that additional unknown molecular modifications, under the control of IL-17A are mandatory for the fusion process. Therefore both CCL20 and CCL2 are necessary but not sufficient to trigger IL-17A-dependent DC fusion.

Early innate IL-17A production (Lockhart et al., 2006) may switch on CCL20 secretion thus attracting available $CCR6^{+}$ myeloid cells such as immature lung DC and memory IL-17A-producing T cells (Acosta-Rodriguez et al., 2007b; Khader et al., 2007; Scriba et al., 2008) (**Fig. 5**). Then IL-17A-mediated CCL2 secretion may recruit peripheral blood monocytes to differentiate into *Mtb* controller phagocytes in the presence of GM-CSF, IL-17A and IFN-γ. *In vitro*, we showed that a massive CCL2 production, driven by IL-17A, regulates myeloid cell morphology, favoring clustering and fusion. Thus, intra-granuloma IL-17A-dependent CCL2 production may represent an important player in the maintenance of

human granulomatous structure as well as CCL20 which is also maintained, *in vivo*, in chronic TB granuloma. In mice, IL-17A drives mature granuloma formation (Umemura et al., 2007) while IFN-γ-producing Th1 cells limit the IL-17A-producing T cell population and the subsequent myeloid cell recruitment, granuloma size and granulomatous immunopathology (Cruz et al., 2010; Cruz et al., 2006). IFN-γ also inhibits IL-17A production by human peripheral blood mononuclear cells of TB patients (Scriba et al., 2008). Therefore, in parallel to its role in stimulation of phagocyte microbicidal activities, IFN-γ may limit granuloma size and number while potentiating cell fusion of $BFL1^{+}CD68^{+}CCR6^{+}CCL20^{+}CCL2^{+}$ long-term surviving epithelioid cells.

As previously discussed, the crucial role of CCR2, the early impact of CCR6 and the redundant role of CCL2 have been documented in murine Mycobacterium granuloma formation. However, analysis of CCR6 expression inside granuloma is lacking in mouse models. For the first time, we document expressions of CCR6/CCL20 inside human TB granulomas and the requirement of IL-17A-dependent CCL20 induction for *in vitro* myeloid cell clustering and fusion, thus opening new strategies to monitor granuloma maintenance. Another myeloid cell fusion process is under the control of M-CSF and RANKL to form the physiological giant bone-resorbing cell called osteoclasts (Gallois et al., 2010; Rivollier et al., 2004b). IL-17A up-regulates RANKL production by murine osteoblasts thus promoting bone resorption following overproduction of osteoclasts (Kotake et al., 1999). Conversely, IFN-γ completely abrogates osteoclast formation (Takayanagi et al., 2000) and GM-CSF blocks RANKL-induced CCL2 expression and osteoclast formation (Kim et al., 2005). CCL2 is a common secondary messenger for cell fusion to generate osteoclasts as well as IL-17A-dependent giant myeloid inflammatory cells. Thus CCL20 but not CCL2 blockers may represent interesting therapeutics in granulomatous diseases to decrease inflammatory granulomatosis without lowering physiological osteoclastogenesis. IFN-γ inhibition is harmful in Mycobacterium infection. We ignore if deficiency in GM-CSF or GM-CSFR could account for Mycobacterium sensitivity in humans as is the case in mice. Finally, in granulomatous diseases, blocking IL-17A appears the best strategy to limit tissue damages.

MATERIALS AND METHODS

Tuberculosis tissue samples

We selected formalin-fixed, paraffin-embedded tissue of lung (n=5), pulmonary lymph node (n=4) and pleura (n=1) from 10 Tuberculosis patients (Centre Hospitalier Lyon Sud, France). Diagnosis of *Mtb* infection was confirmed by culture and genome PCR detection. Sections were routinely stained with haematoxylin-phloxine-safran to identify granuloma area including giant cells. The local ethics committees (Research Committee for the Hospices Civils de Lyon) approved this study, informed consent were obtained from each subject for the research use of their biopsy.

Reagents. To perform flow cytometry, we purchased the following antibodies from Becton Dickinson : PE-CD1a (HI149), FITC-CD3 (UCHT1), FITC-CD14 (M5E2), PE-CD196 (CCR6) (11A9), PerCP-Cy5.5-MHC II (HLA-DR) (G46-6), from R&D Systems: PE-CCL20 (67310) and IL-17A (41802) and from Beckman Coulter : isotype controls. To perform biological assays, we used anti-human CCL20 (MAB360, R&D System) and anti-human CCL2 (500-P34, Peprotech). Recombinant human M-CSF, GM-CSF, IL-4, IL-17A, IFN-γ, CCL2 and CCL20 were purchased from PeproTech.

Immunochemistry, triple colour immunofluorescence and confocal microscopy

4-µm paraffin-embedded TB biopsies were cut, deparaffinized and subjected to heat-mediated antigen-retrieval in a microwave using citrate buffer (10mM, pH6.0). The tissue sections were incubated 30 minutes in PBS-1% BSA with 3% human serum to block Fc receptors. For immunochemistry, primary monoclonal biotinylated antibodies directed against CD68 (clone KP1, Dako) were detected with avidin-peroxidase revealed by its substrate, the diaminobenzidine (Serotec), which gives a brown color to the positive cells, counterstained with Mayer's hematoxylin. For immunofluorescence, we incubated tissue sections overnight at 37°C with primary antibodies to CD68 (KP1, 2 µg/ml) and CD3 (A0452, 12 µg/ml) from DAKO, to GM-CSF (FL-144, 4 µg/ml) from Santa Cruz, to BFL1 (3401-100, 4 µg/ml) from Biovision and to CCR6 (53103, 25 µg/ml), IL-17A (41802, 10 µg/ml), CCL20 (67310.111, 10 µg/ml), and CCL2 (23002, 25 µg/ml) from R&D Systems or to isotype controls (mouse IgG1 X0931 from DAKO, mouse IgG2b MOPC-195 from Immunotech-Beckman Coulter and rabbit IgG (AB105-C from R&D Systems). After three washes in PBS-1% BSA, detection of the primary antibodies was performed with isotype-specific secondary Alexa Fluor 488, 546

and 647-conjugated antibodies (Invitrogen) at 10µg/mL for 30min. After 3 washes in PBS-1%BSA, the sections were mounted using Mowiol and then analyzed by confocal microscopy using a Carl Zeiss MicroImaging Inc. LSM 510 confocal microscope.

Cells: cells cultured in Lab-Tek Chamber Slide™ System were first fixed for 20 minutes with 2% paraformaldehyde in PBS. Epitope retrieval was performed twice in 0,1% glycine for 10 minutes each time. Cells cultured were permeabilized with 0.1% Triton X-100 in PBS for 5 minutes then stained for CCL20 and CCL2 as described above.

Monocyte purification and dendritic cell differentiation.

Blood was obtained from healthy adult volunteer donors (Etablissement français du sang, Lyon Gerland, France). $CD14^+$ monocytes were purified (>95% $CD14^+$) from the peripheral blood by ficoll and percoll gradients, followed by negative magnetic depletion of cells expressing CD3 or CD56 or CD19. HLA-DR^{+low} $CD1a^+$ $CD83^-$ immature monocyte-derived DC (>98%) were generated, *in vitro,* after 6 days of monocyte culture seeded at $0{,}8.10^6$ cells/mL with 50 ng/ml GM-CSF and 500 U/ml IL-4 (Rivollier et al., 2004b) in RPMI 1640 (Gibco) supplemented with 10 mM Hepes (*N*-2-hydroxyethylpiperazine-*N'*-2-ethanesulfonic acid), 2 mM L-glutamine, 40 µg/mL gentamicin (Gibco), 10% heat-inactivated FCS (Boehringer Mannheim)

Cell culture, giant cell formation, time lapse study, cluster counts, TRAP assay and Hoechst DNA staining

DC were seeded at 4800 cells/mm^2 in RPMI supplemented with 10% FCS, 2 mM L-glutamine, 10 mM HEPES, 40 µg/mL gentamicin, in the presence of IL-17A (2 ng/mL) without or with IFN-γ (2 ng/ml). Cytokines were added at the beginning of the culture and then replenished every week. We added neutralizing antibodies at indicated concentrations. For time lapse study, the plate was placed at 37°C and heated in a 5% CO_2 atmosphere and cells were imaged by Metamorph software v6 with a Coolsnap HQ monochrome camera associated with a time lapse microscope (Axiovert 100 M) and a 10× (numerical aperture, 0.25) Plan-Apochromat objective (Zeiss). Meta Imaging Series 4.5 (Universal Imaging, West Chester, PA) was used to make Quick-Time movies from image stacks from metamorph software. One picture was made every 10 min for 96h, and every second of movie represents 235.4 min (3.92 h) of culture. Images extracted from stacks were processed with Adobe Photoshop 6.0 (Adobe Systems, San Jose, CA). Cell clusters (strictly bigger than 50 nm) were

counted at day 5 with Image_J freeware. At day 12 of culture, TRAP (tartrate resistant acidic phosphatase) activity was assessed using the Leukocyte acid phosphatase kit (Sigma-Aldrich). DNA of the nuclei were then stained with 10 µg/mL of Hoechst 33342 (Sigma) for 30 min at 37°C. The staining was fixed with 1% formol. Counts were made of the total number of nuclei and the number of nuclei included in giant cells (strictly more than two nuclei) to calculate the percentage of nuclei included in giant cells among total nuclei which quantifies the fusion efficiency. Culture and TRAP/hoechst pictures were analyzed using a Leica DMiRB microscope equipped with x40/0.30 NA or x40/0.55 NA objective lenses (Leica) a Leica DC300F camera and the Leica FW400 software.

Flow cytometry quantification of viable versus dead cells

$DiOC_6(3)$ (3,39-diexyloxacarbocyanine)-propidium iodide (PI) double staining was performed to detect apoptotic cells by flow cytometry until day 7 of culture. Cells were incubated 15 min at 37°C with 40nM $DiOC_6$ (Molecular Probes) in culture medium to evaluate mitochondrial transmembrane potential ($\Delta\Psi m$). Viable cells have stable $\Delta\Psi m$ whereas $\Delta\Psi m$ decreases with cell commitment to apoptosis. PI (0.5 µg/ml) was added before FACS analysis of the cells and incorporates into DNA of dead cells whose membrane is permeabilized. Living cells remain $DiOC_6^{+}PI^{-}$ whereas apoptotic cells are $DiOC_6^{-}PI^{+}$. Cells were numbered by a time-monitored flow cytometry analysis during 2 min at high speed (1 µl/s).

Real-time quantitative PCR

Total RNA from 2 millions of cells was extracted using Trizol® (Invitrogen) and RNeasy Mini Kit® (Qiagen) to reach an RNA integrity number >9 with Agilent bioanalyzer. RT-PCR reactions were performed with SuperScript® II Reverse Transcriptase (Invitrogen). One µg total RNA was reverse-transcribed using oligo$(dT)_{12\text{-}18}$ Primers (Invitrogen). For expression studies, 25ng of cDNA were amplified in Stratagene Mx3000P apparatus (Agilent Technologies), using the QuantiTect® SYBR®Green PCR Kit (QIAGEN). Primer sequences were as follows: BFL1/*Bcl2A1*, ACAGGCTGGCTCAGGACTATCT (forward), CTCTGGACGTTTTGCTTGGAC (reverse); *GAPDH*, CACCCACTCCTCCACCTTTGAC (forward), GTCCACCACCCTGTTGCTGTAG (reverse); Ccl2, QuantiTect® primers specific Hs_CCL2_1_SG QuantiTect Primer Assay (Qiagen) ; Ccl20, QuantiTect® primers specific Hs_CCL20_1_SG QuantiTect Primer Assay (Qiagen) ; *TBP*, QuantiTect® primers specific Hs_TBP_1_SG QuantiTect Primer Assay (Qiagen). All samples were normalized to

expression of GAPDH or TBP.

Western blot analysis

Three millions of cells were harvested, sonicated and lysed 1h at 4°C with RIPA buffer (50mM Tris-HCl, pH7.5, 150mM NaCl, 1% NP-40, 0.5% sodium deoxycholate, 0.1% SDS, and 1mM DTT) containing protease inhibitor cocktail (Roche). Cellular debris were pelletted by centrifugation (10,000g 15 min at 4°C) and protein extracts (100µg per lane) were loaded onto a 12% SDS-polyacrylamide gel and blotted onto PVDF sheet (Bio-Rad Laboratories). Filters were blocked with 5% BSA in PBS/0.1% Tween 20 (PBS-T) for 2 h and then incubated over-night at 4°C with anti-BFL1, 0.9 µg/mL in PBS-T (rabbit polyclonal ab75887, Abcam). After three washes with PBS-T, filters were incubated 1 h with Biotin-conjugated goat anti-rabbit IgG, 2µg/mL in PBS-T, 5% BSA (Molecular Probes/Invitrogen). After three washes with PBS-T, filters were incubated 1 h with HRP-conjugated Streptavidin (StrepTactin-HRP, Bio-Rad Laboratories) dilution 1:50000 in PBS-T, 5% BSA. Detection was performed using Immun-Star™ WesternC™ Kit chemiluminescence system (Bio-Rad Laboratories). Actin staining was realized using a rabbit polyclonal anti-βActin from Santa Cruz (sc-130656, Santa Cruz).

Flow cytometry intracytoplasmic staining

Immunostaining of cells were performed in 1% BSA and 3% human serum-PBS, then quantified on a LSRII (Becton Dickinson) and analyzed using CellQuest Pro software. We used 2 µg/ml of primary antibodies to BFL1 (3401-100, 4 µg/ml) from Biovision and to CCL20 (67310.111, 10 µg/ml) and CCL2 (23002, 25 µg/ml) from R&D Systems then secondary antibodies to rabbit IgG (PE-F(ab')$_2$ 111-116-144 from Jackson Immunoresearch) or to mouse IgG (PE-F(ab')$_2$ goat, 115-086-062, Jackson Immunoresearch). For intracytoplasmic staining, we blocked the Golgi apparatus with BD GolgiStop™, fixed and permeabilized the cells with the Cytofix/Cytoperm reagents according to procedures from the manufacturer (Becton Dickinson).

Measurements of CCL2 and CCL20 secretions by ELISA

CCL2 and CCL20 levels in cell culture supernatants were measured using commercial ELISA kits (PeproTech). Samples were run in triplicate. Results were analyzed by the Multiskan Spectrum Spectrophotometer with SkanIt Software 2.2 (Thermo Electron).

CCL2 and CCL20 blocking Experiments

In vitro blocking assays of CCL2 and CCL20 were performed in 48-well cell culture plates at 37°C with 5% CO2. Anti-human CCL2 or CCL20 or isotype controls were added at day 0 of culture. In addition to viability staining performed at day 7, cluster counts at day 5, cell fixation and TRAP/Hoechst staining at day 12 to calculate the fusion efficiency, we counted elongated cells revealed by using anti-CCL2: 100 nuclei were counted and the percentage of elongated cells was determined.

ACKNOWLEDGEMENTS

We thank UMS3444 for the PLATIM imaging platform, N. Winter and U.Hasan for her critical readings. This work was supported by grants from (F) CNRS, INSERM, Université de Lyon, Institut Universitaire de France, Fondation Innovations en Infectiologie, Fondation de France 2008002100, Agence Nationale de la Recherche 08-MIEN-001-02; (USA) Histiocytosis Association of America 2008; (I) Ministero Sanità, Progetto di Ricerca Finalizzata 2008: “Getting deeper in histiocytosis", Regione Toscana, Progetto di Ricerca Malattie Rare 2008, Associazione Italiana Ricerca Istiocitosi (AIRI); (S) the Swedish Children's Cancer Foundation, the Swedish Research Council, the Cancer and Allergy Foundation of Sweden, Karolinska Institutet (KID project) and the Stockholm County Council (ALF project).

COMPETING INTERESTS STATEMENT

The authors have declared that no competing interests exist.

REFERENCES:

Acosta-Rodriguez, E.V., L. Rivino, J. Geginat, D. Jarrossay, M. Gattorno, A. Lanzavecchia, F. Sallusto, and G. Napolitani. 2007. Surface phenotype and antigenic specificity of human interleukin 17-producing T helper memory cells. *Nat Immunol* 8:639-646.

Adams, D.O. 1976. The granulomatous inflammatory response. A review. *Am J Pathol* 84:164-192.

Algood, H.M., P.L. Lin, and J.L. Flynn. 2005. Tumor necrosis factor and chemokine interactions in the formation and maintenance of granulomas in tuberculosis. *Clin Infect Dis* 41 Suppl 3:S189-193.

Annunziato, F., L. Cosmi, V. Santarlasci, L. Maggi, F. Liotta, B. Mazzinghi, E. Parente, L. Fili, S. Ferri, F. Frosali, F. Giudici, P. Romagnani, P. Parronchi, F. Tonelli, E. Maggi, and S. Romagnani. 2007. Phenotypic and functional features of human Th17 cells. *J Exp Med* 204:1849-1861.

Bean, A.G., D.R. Roach, H. Briscoe, M.P. France, H. Korner, J.D. Sedgwick, and W.J. Britton. 1999. Structural deficiencies in granuloma formation in TNF gene-targeted mice underlie the heightened susceptibility to aerosol Mycobacterium tuberculosis infection, which is not compensated for by lymphotoxin. *J Immunol* 162:3504-3511.

Casanova, J.L., and L. Abel. 2002. Genetic dissection of immunity to mycobacteria: the human model. *Annu Rev Immunol* 20:581-620.

Chang, S.H., and C. Dong. 2011. Signaling of interleukin-17 family cytokines in immunity and inflammation. *Cell Signal* 23:1069-1075.

Clay, H., H.E. Volkman, and L. Ramakrishnan. 2008. Tumor necrosis factor signaling mediates resistance to mycobacteria by inhibiting bacterial growth and macrophage death. *Immunity* 29:283-294.

Cooper, A.M., D.K. Dalton, T.A. Stewart, J.P. Griffin, D.G. Russell, and I.M. Orme. 1993. Disseminated tuberculosis in interferon gamma gene-disrupted mice. *J Exp Med* 178:2243-2247.

Coury, F., N. Annels, A. Rivollier, S. Olsson, A. Santoro, C. Speziani, O. Azocar, M. Flacher, S. Djebali, J. Tebib, M. Brytting, R.M. Egeler, C. Rabourdin-Combe, J.I. Henter, M. Arico, and C. Delprat. 2008. Langerhans cell histiocytosis reveals a new IL-17A-dependent pathway of dendritic cell fusion. *Nat Med* 14:81-87.

Cruz, A., A.G. Fraga, J.J. Fountain, J. Rangel-Moreno, E. Torrado, M. Saraiva, D.R. Pereira, T.D. Randall, J. Pedrosa, A.M. Cooper, and A.G. Castro. 2010. Pathological role of interleukin 17 in mice subjected to repeated BCG vaccination after infection with Mycobacterium tuberculosis. *J Exp Med* 207:1609-1616.

Cruz, A., S.A. Khader, E. Torrado, A. Fraga, J.E. Pearl, J. Pedrosa, A.M. Cooper, and A.G. Castro. 2006. Cutting edge: IFN-gamma regulates the induction and expansion of IL-17-producing CD4 T cells during mycobacterial infection. *J Immunol* 177:1416-1420.

D'Souza, B.N., L.C. Edelstein, P.M. Pegman, S.M. Smith, S.T. Loughran, A. Clarke, A. Mehl, M. Rowe, C. Gelinas, and D. Walls. 2004. Nuclear factor kappa B-dependent activation of the antiapoptotic bfl-1 gene by the Epstein-Barr virus latent membrane protein 1 and activated CD40 receptor. *J Virol* 78:1800-1816.

Davis, J.M., and L. Ramakrishnan. 2009. The role of the granuloma in expansion and dissemination of early tuberculous infection. *Cell* 136:37-49.

Denis, M., and E. Ghadirian. 1990. Granulocyte-macrophage colony-stimulating factor restricts growth of tubercle bacilli in human macrophages. *Immunol Lett* 24:203-206.

Dhiman, R., M. Raje, and S. Majumdar. 2007. Differential expression of NF-kappaB in mycobacteria infected THP-1 affects apoptosis. *Biochim Biophys Acta* 1770:649-658.

Egen, J.G., A.G. Rothfuchs, C.G. Feng, N. Winter, A. Sher, and R.N. Germain. 2008. Macrophage and T cell dynamics during the development and disintegration of mycobacterial granulomas. *Immunity* 28:271-284.

Facco, M., I. Baesso, M. Miorin, M. Bortoli, A. Cabrelle, E. Boscaro, C. Gurrieri, L. Trentin, R. Zambello, F. Calabrese, M.A. Cassatella, G. Semenzato, and C. Agostini. 2007. Expression and role of CCR6/CCL20 chemokine axis in pulmonary sarcoidosis. *J Leukoc Biol* 82:946-955.

Facco, M., A. Cabrelle, A. Teramo, V. Olivieri, M. Gnoato, S. Teolato, E. Ave, C. Gattazzo, G.P. Fadini, F. Calabrese, G. Semenzato, and C. Agostini. 2011. Sarcoidosis is a Th1/Th17 multisystem disorder. *Thorax* 66:144-150.

Fenton, M.J., M.W. Vermeulen, S. Kim, M. Burdick, R.M. Strieter, and H. Kornfeld. 1997. Induction of gamma interferon production in human alveolar macrophages by Mycobacterium tuberculosis. *Infect Immun* 65:5149-5156.

Feuerhake, F., J.L. Kutok, S. Monti, W. Chen, A.S. LaCasce, G. Cattoretti, P. Kurtin, G.S. Pinkus, L. de Leval, N.L. Harris, K.J. Savage, D. Neuberg, T.M. Habermann, R. Dalla-Favera, T.R. Golub, J.C. Aster, and M.A. Shipp. 2005. NFkappaB activity, function, and target-gene signatures in primary mediastinal large B-cell lymphoma and diffuse large B-cell lymphoma subtypes. *Blood* 106:1392-1399.

Flynn, J.L., and J. Chan. 2001. Immunology of tuberculosis. *Annu Rev Immunol* 19:93-129.

Frenzel, A., F. Grespi, W. Chmelewskij, and A. Villunger. 2009. Bcl2 family proteins in carcinogenesis and the treatment of cancer. *Apoptosis* 14:584-596.

Gallois, A., J. Lachuer, G. Yvert, A. Wierinckx, F. Brunet, C. Rabourdin-Combe, C. Delprat, P. Jurdic, and M. Mazzorana. 2010. Genome-wide expression analyses establish dendritic cells as a new osteoclast precursor able to generate bone-resorbing cells more efficiently than monocytes. *J Bone Miner Res* 25:661-672.

Gardam, M.A., E.C. Keystone, R. Menzies, S. Manners, E. Skamene, R. Long, and D.C. Vinh. 2003. Anti-tumour necrosis factor agents and tuberculosis risk: mechanisms of action and clinical management. *Lancet Infect Dis* 3:148-155.

Gonzalez-Juarrero, M., J.M. Hattle, A. Izzo, A.P. Junqueira-Kipnis, T.S. Shim, B.C. Trapnell, A.M. Cooper, and I.M. Orme. 2005. Disruption of granulocyte macrophage-colony stimulating factor production in the lungs severely affects the ability of mice to control Mycobacterium tuberculosis infection. *J Leukoc Biol* 77:914-922.

Khader, S.A., G.K. Bell, J.E. Pearl, J.J. Fountain, J. Rangel-Moreno, G.E. Cilley, F. Shen, S.M. Eaton, S.L. Gaffen, S.L. Swain, R.M. Locksley, L. Haynes, T.D. Randall, and A.M. Cooper. 2007. IL-23 and IL-17 in the establishment of protective pulmonary CD4+ T cell responses after vaccination and during Mycobacterium tuberculosis challenge. *Nat Immunol* 8:369-377.

Kim, M.S., C.J. Day, and N.A. Morrison. 2005. MCP-1 is induced by receptor activator of nuclear factor-{kappa}B ligand, promotes human osteoclast fusion, and rescues granulocyte macrophage colony-stimulating factor suppression of osteoclast formation. *J Biol Chem* 280:16163-16169.

Kindler, V., A.P. Sappino, G.E. Grau, P.F. Piguet, and P. Vassalli. 1989. The inducing role of tumor necrosis factor in the development of bactericidal granulomas during BCG infection. *Cell* 56:731-740.

Kipnis, A., R.J. Basaraba, I.M. Orme, and A.M. Cooper. 2003. Role of chemokine ligand 2 in the protective response to early murine pulmonary tuberculosis. *Immunology* 109:547-551.

Kotake, S., N. Udagawa, N. Takahashi, K. Matsuzaki, K. Itoh, S. Ishiyama, S. Saito, K. Inoue, N. Kamatani, M.T. Gillespie, T.J. Martin, and T. Suda. 1999. IL-17 in synovial fluids from patients with rheumatoid arthritis is a potent stimulator of osteoclastogenesis. *J Clin Invest* 103:1345-1352.

Kozopas, K.M., T. Yang, H.L. Buchan, P. Zhou, and R.W. Craig. 1993. MCL1, a gene expressed in programmed myeloid cell differentiation, has sequence similarity to BCL2. *Proc Natl Acad Sci U S A* 90:3516-3520.

Kremer, L., J. Estaquier, E. Brandt, J.C. Ameisen, and C. Locht. 1997. Mycobacterium bovis Bacillus Calmette Guerin infection prevents apoptosis of resting human monocytes. *Eur J Immunol* 27:2450-2456.

Kucharzik, T., J.T. Hudson, 3rd, R.L. Waikel, W.D. Martin, and I.R. Williams. 2002. CCR6 expression distinguishes mouse myeloid and lymphoid dendritic cell subsets: demonstration using a CCR6 EGFP knock-in mouse. *Eur J Immunol* 32:104-112.

Lawn, S.D., S.T. Butera, and T.M. Shinnick. 2002. Tuberculosis unleashed: the impact of human immunodeficiency virus infection on the host granulomatous response to Mycobacterium tuberculosis. *Microbes Infect* 4:635-646.

Lee, J.S., J.Y. Lee, J.W. Son, J.H. Oh, D.M. Shin, J.M. Yuk, C.H. Song, T.H. Paik, and E.K. Jo. 2008. Expression and regulation of the CC-chemokine ligand 20 during human tuberculosis. *Scand J Immunol* 67:77-85.

Lockhart, E., A.M. Green, and J.L. Flynn. 2006. IL-17 production is dominated by gammadelta T cells rather than CD4 T cells during Mycobacterium tuberculosis infection. *J Immunol* 177:4662-4669.

Monti, S., K.J. Savage, J.L. Kutok, F. Feuerhake, P. Kurtin, M. Mihm, B. Wu, L. Pasqualucci, D. Neuberg, R.C. Aguiar, P. Dal Cin, C. Ladd, G.S. Pinkus, G. Salles, N.L. Harris, R. Dalla-Favera, T.M. Habermann, J.C. Aster, T.R. Golub, and M.A. Shipp. 2005. Molecular profiling of diffuse large B-cell lymphoma identifies robust subtypes including one characterized by host inflammatory response. *Blood* 105:1851-1861.

Okamoto Yoshida, Y., M. Umemura, A. Yahagi, R.L. O'Brien, K. Ikuta, K. Kishihara, H. Hara, S. Nakae, Y. Iwakura, and G. Matsuzaki. 2010. Essential role of IL-17A in the formation of a mycobacterial infection-induced granuloma in the lung. *J Immunol* 184:4414-4422.

Oltersdorf, T., S.W. Elmore, A.R. Shoemaker, R.C. Armstrong, D.J. Augeri, B.A. Belli, M. Bruncko, T.L. Deckwerth, J. Dinges, P.J. Hajduk, M.K. Joseph, S. Kitada, S.J. Korsmeyer, A.R. Kunzer, A. Letai, C. Li, M.J. Mitten, D.G. Nettesheim, S. Ng, P.M. Nimmer, J.M. O'Connor, A. Oleksijew, A.M. Petros, J.C. Reed, W. Shen, S.K. Tahir, C.B. Thompson, K.J. Tomaselli, B. Wang, M.D. Wendt, H. Zhang, S.W. Fesik, and

S.H. Rosenberg. 2005. An inhibitor of Bcl-2 family proteins induces regression of solid tumours. *Nature* 435:677-681.

Ordway, D., M. Henao-Tamayo, I.M. Orme, and M. Gonzalez-Juarrero. 2005. Foamy macrophages within lung granulomas of mice infected with Mycobacterium tuberculosis express molecules characteristic of dendritic cells and antiapoptotic markers of the TNF receptor-associated factor family. *J Immunol* 175:3873-3881.

Park, H., Z. Li, X.O. Yang, S.H. Chang, R. Nurieva, Y.H. Wang, Y. Wang, L. Hood, Z. Zhu, Q. Tian, and C. Dong. 2005. A distinct lineage of CD4 T cells regulates tissue inflammation by producing interleukin 17. *Nat Immunol* 6:1133-1141.

Pattingre, S., A. Tassa, X. Qu, R. Garuti, X.H. Liang, N. Mizushima, M. Packer, M.D. Schneider, and B. Levine. 2005. Bcl-2 antiapoptotic proteins inhibit Beclin 1-dependent autophagy. *Cell* 122:927-939.

Peters, W., H.M. Scott, H.F. Chambers, J.L. Flynn, I.F. Charo, and J.D. Ernst. 2001. Chemokine receptor 2 serves an early and essential role in resistance to Mycobacterium tuberculosis. *Proc Natl Acad Sci U S A* 98:7958-7963.

Rivollier, A., M. Mazzorana, J. Tebib, M. Piperno, T. Aitsiselmi, C. Rabourdin-Combe, P. Jurdic, and C. Servet-Delprat. 2004. Immature dendritic cell transdifferentiation into osteoclasts: a novel pathway sustained by the rheumatoid arthritis microenvironment. *Blood* 104:4029-4037.

Roach, D.R., A.G. Bean, C. Demangel, M.P. France, H. Briscoe, and W.J. Britton. 2002. TNF regulates chemokine induction essential for cell recruitment, granuloma formation, and clearance of mycobacterial infection. *J Immunol* 168:4620-4627.

Sada-Ovalle, I., A. Chiba, A. Gonzales, M.B. Brenner, and S.M. Behar. 2008. Innate invariant NKT cells recognize Mycobacterium tuberculosis-infected macrophages, produce interferon-gamma, and kill intracellular bacteria. *PLoS Pathog* 4:e1000239.

Schreiber, O., K. Steinwede, N. Ding, M. Srivastava, R. Maus, F. Langer, J. Prokein, S. Ehlers, T. Welte, M.D. Gunn, and U.A. Maus. 2008. Mice that overexpress CC chemokine ligand 2 in their lungs show increased protective immunity to infection with Mycobacterium bovis bacille Calmette-Guerin. *J Infect Dis* 198:1044-1054.

Scriba, T.J., B. Kalsdorf, D.A. Abrahams, F. Isaacs, J. Hofmeister, G. Black, H.Y. Hassan, R.J. Wilkinson, G. Walzl, S.J. Gelderbloem, H. Mahomed, G.D. Hussey, and W.A. Hanekom. 2008. Distinct, specific IL-17- and IL-22-producing CD4+ T cell subsets contribute to the human anti-mycobacterial immune response. *J Immunol* 180:1962-1970.

Stolberg, V.R., B.C. Chiu, B.E. Martin, S.A. Shah, M. Sandor, and S.W. Chensue. 2011. Cysteine-cysteinyl chemokine receptor 6 mediates invariant natural killer T cell airway recruitment and innate stage resistance during mycobacterial infection. *J Innate Immun* 3:99-108.

Tailleux, L., O. Neyrolles, S. Honore-Bouakline, E. Perret, F. Sanchez, J.P. Abastado, P.H. Lagrange, J.C. Gluckman, M. Rosenzwajg, and J.L. Herrmann. 2003. Constrained intracellular survival of Mycobacterium tuberculosis in human dendritic cells. *J Immunol* 170:1939-1948.

Takayanagi, H., K. Ogasawara, S. Hida, T. Chiba, S. Murata, K. Sato, A. Takaoka, T. Yokochi, H. Oda, K. Tanaka, K. Nakamura, and T. Taniguchi. 2000. T-cell-mediated regulation of osteoclastogenesis by signalling cross-talk between RANKL and IFN-gamma. *Nature* 408:600-605.

Ulrichs, T., and S.H. Kaufmann. 2006. New insights into the function of granulomas in human tuberculosis. *J Pathol* 208:261-269.

Umemura, M., A. Yahagi, S. Hamada, M.D. Begum, H. Watanabe, K. Kawakami, T. Suda, K. Sudo, S. Nakae, Y. Iwakura, and G. Matsuzaki. 2007. IL-17-mediated regulation of innate and acquired immune response against pulmonary Mycobacterium bovis bacille Calmette-Guerin infection. *J Immunol* 178:3786-3796.

Vesosky, B., E.K. Rottinghaus, P. Stromberg, J. Turner, and G. Beamer. 2010. CCL5 participates in early protection against Mycobacterium tuberculosis. *J Leukoc Biol* 87:1153-1165.

Vogt, G., and C. Nathan. 2011. In vitro differentiation of human macrophages with enhanced antimycobacterial activity. *J Clin Invest*

Zhu, X.W., and J.S. Friedland. 2006. Multinucleate giant cells and the control of chemokine secretion in response to Mycobacterium tuberculosis. *Clin Immunol* 120:10-20.

FIGURES

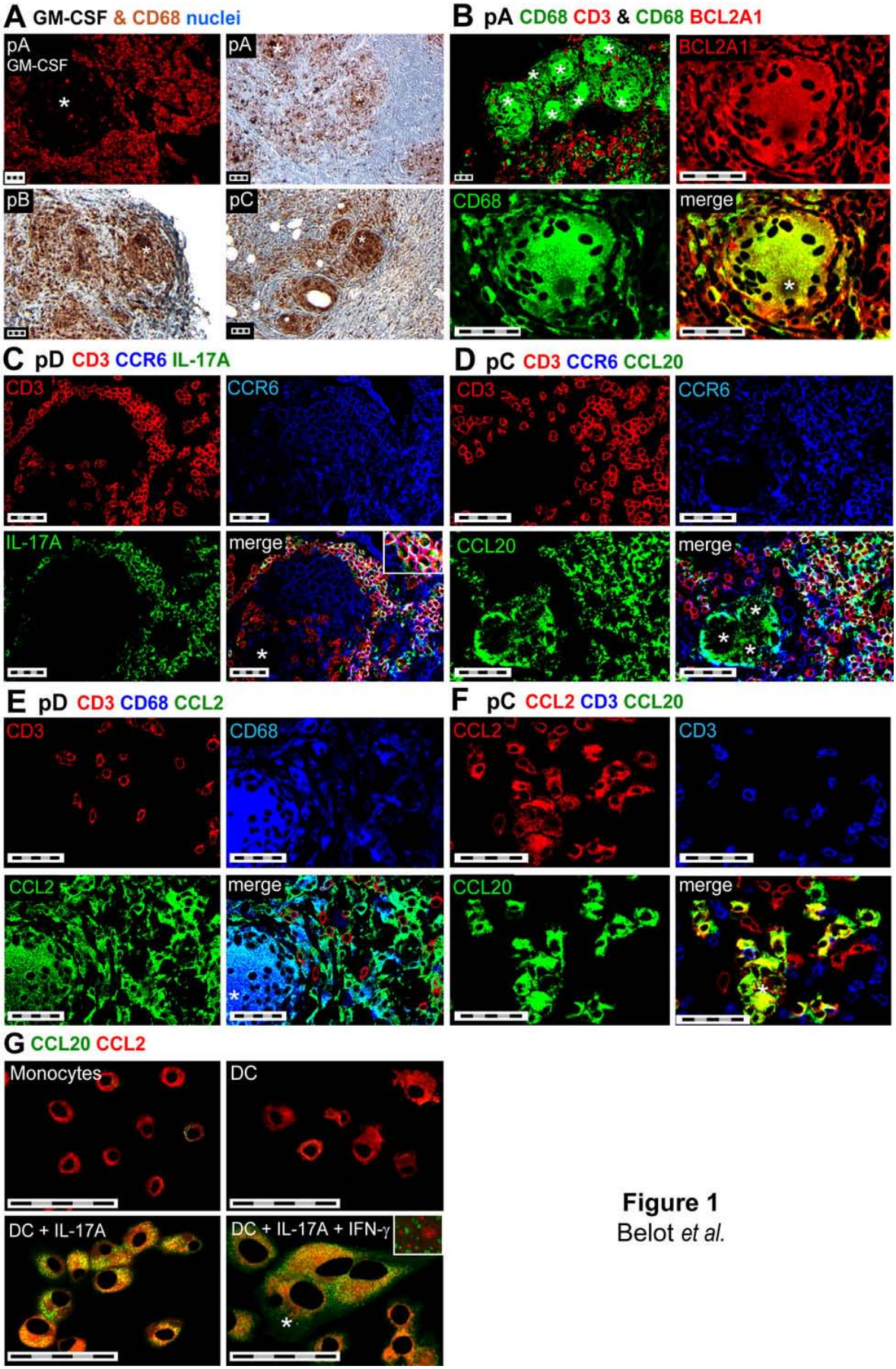

Figure 1
Belot *et al.*

Figure 1

Study of GM-CSF, CD68, CCR6, CD3, IL-17A, CCL20 and CCL2 in tuberculosis granuloma, ex vivo and CCL20 and CCL2 in human myeloid cells, in vitro

(A-F) Representative confocal microscopy images of immunofluorescence stainings of tuberculosis granuloma (n=10). **(A)** GM-CSF (up left, red) and CD68 (brown) versus nuclei (blue); **(B)** CD68 (green) versus CD3 (red) or BFL1 (red), yellow stained $CD68^{+}BFL1^{+}$ myeloid cells; **(C)** CD3 (red) versus CCR6 (blue) and IL-17A (green), three times enlarged inset shows white triple stained cells; **(D)** CD3 (red) versus CCR6 (blue) and CCL20 (green), light blue stained $CCR6^{+}CCL20^{+}$ cells; **(E)** CD3 (red) versus CD68 (blue) and CCL2 (green), light blue stained $CD68^{+}CCL2^{+}$ cells; **(F)** CCL2 (red) versus CD3 (blue) and CCL20 (green), yellow stained $CCL2^{+}CCL20^{+}$ cells. **(G)** Representative confocal microscopy images of immunofluorescence staining of human monocytes or monocyte-derived DC at day 0 or stimulated 8 days with IL-17A +/- IFN-γ (n=3), seven times enlarged inset shows the storage of CCL20 and CCL2 in distinct intracytoplasmic vesicles. On all photos, bar scale length is 50μm (5x10μm). * indicates giant cells.

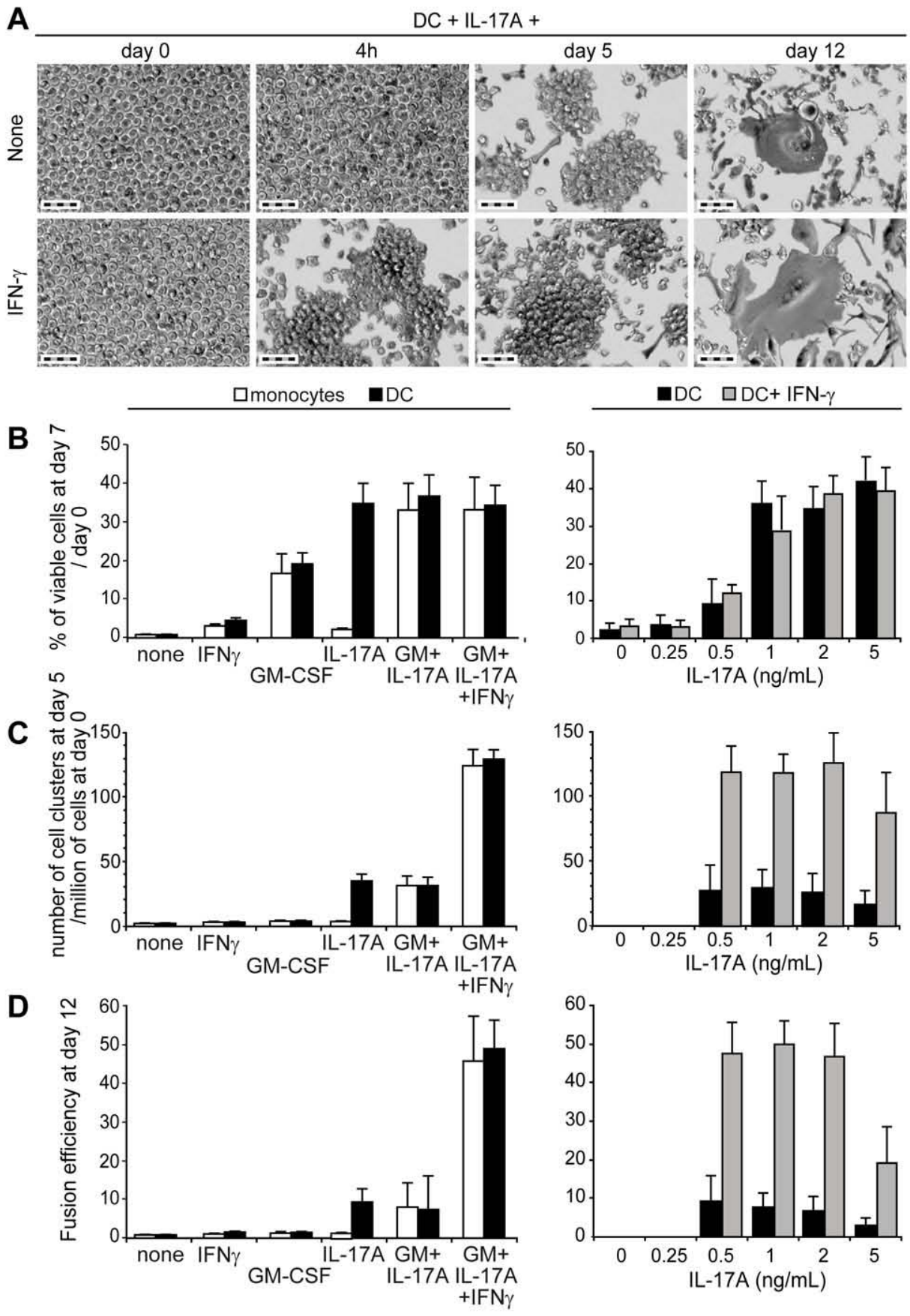

Figure 2
Belot *et al.*

Figure 2

Video-microscopy study and quantification of survival, clustering and cell fusion of human monocytes versus dendritic cells treated with IFN-γ, GM-CSF, IL-17A or their combinations

(A) Pictures extracted from a video-microscopy study at indicated time. DC were cultured in the presence of IL-17A with or without IFN-γ, bar scale length is 50μm (5x10μm), n = 4; **(B-D)** Monocytes in white, DC in black and DC with IFN-γ in gray, were cultured with indicated cytokines, n = 5. Measurements of survival, clustering and fusion: mean +/- SD of **(B)** percentages of $DiOC_6^+$ PI^- viable cells at day 7 relative to day 0, **(C)** counts of DC clusters (>50 μm diameter) at day 5, **(D)** fusion efficiency at day 12: cultures were fixed and TRAP/hoechst staining was performed to count the percentages of nuclei included in multinucleated giant cell versus the total number of nuclei.

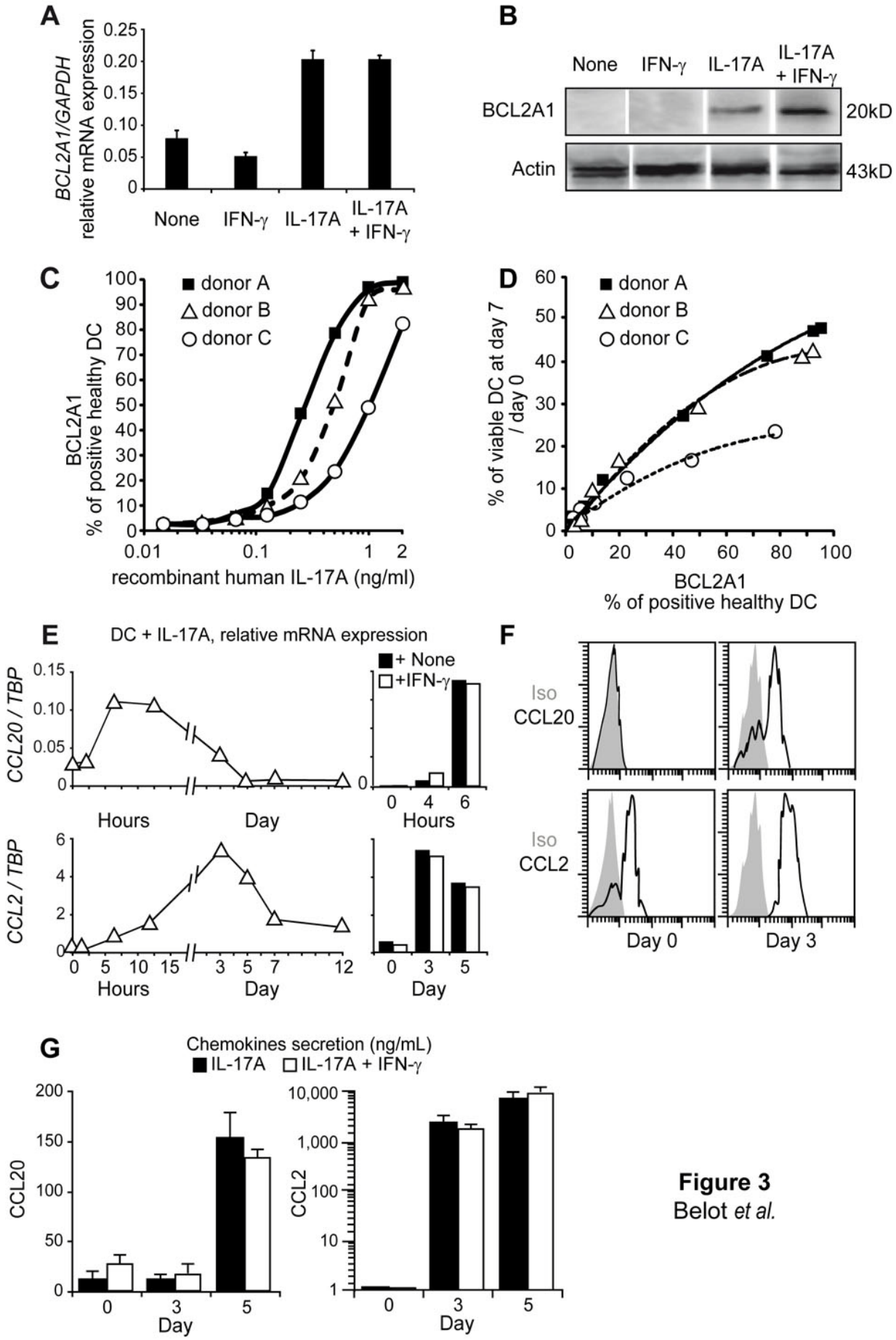

Figure 3
Belot *et al.*

Figure 3

Regulations of BFL1, CCL20 and CCL2 expressions by IL-17A in human dendritic cells

(A) mRNA levels of BFL1 gene measured by real-time PCR in DC at day 0 and day 2 after culture with IFN-γ or IL-17A or both. Mean and SD of duplicate of relative gene expression (compared with GAPDH) for one donor, representative of *n* = 3. **(B)** Western blot analysis of related BFL1 protein expression at day 5 (n = 4). **(C, D)** Dose response studies of IL-17A treatment (eight points from 2 to 0.016 ng/ml) on DC from three healthy donors. With flow cytometry (SD were below 1%), we measured **(C)** the percentages of BFL1 intracellular expressions in DC, and **(D)** the percentages of $DiOC_6^+$ PI^- viable DC at day 7 relative to day 0. A two parameter polynomial statistical analysis of BFL1 intracellular expression versus viability, measured for each value of IL-17A concentration, defined the statistical curves of tendency For donor A: $y=-0.0023x^2+0.7211x+0.3834$, donor B: $y=-0.0041x^2+0.8444x+1.019$ and donor C: $y=-0.0024x^2+0.4677x+0.9366$ with the correlation factors 0.9975, 0.9937 and 0.9789, respectively. **(E)** Kinetics study of *ccl20* and *ccl2* mRNA levels measured by real-time PCR in DC with IL-17A +/- IFN-γ. Relative gene expression compared with TBP for one donor, representative of *n* = 3. **(F)** Flow cytometry analysis of CCL20 and CCL2 intracellular expressions in IL-17A-treated DC at day 0 and 3, n = 3. **(G)** Quantification of CCL20 and CCL2 chemokine secretion by ELISA at day 0, 3 and 5 in supernatants of DC cultured with IL-17A +/- IFN-γ. Mean and SD of triplicate, representative of n = 3 donors.

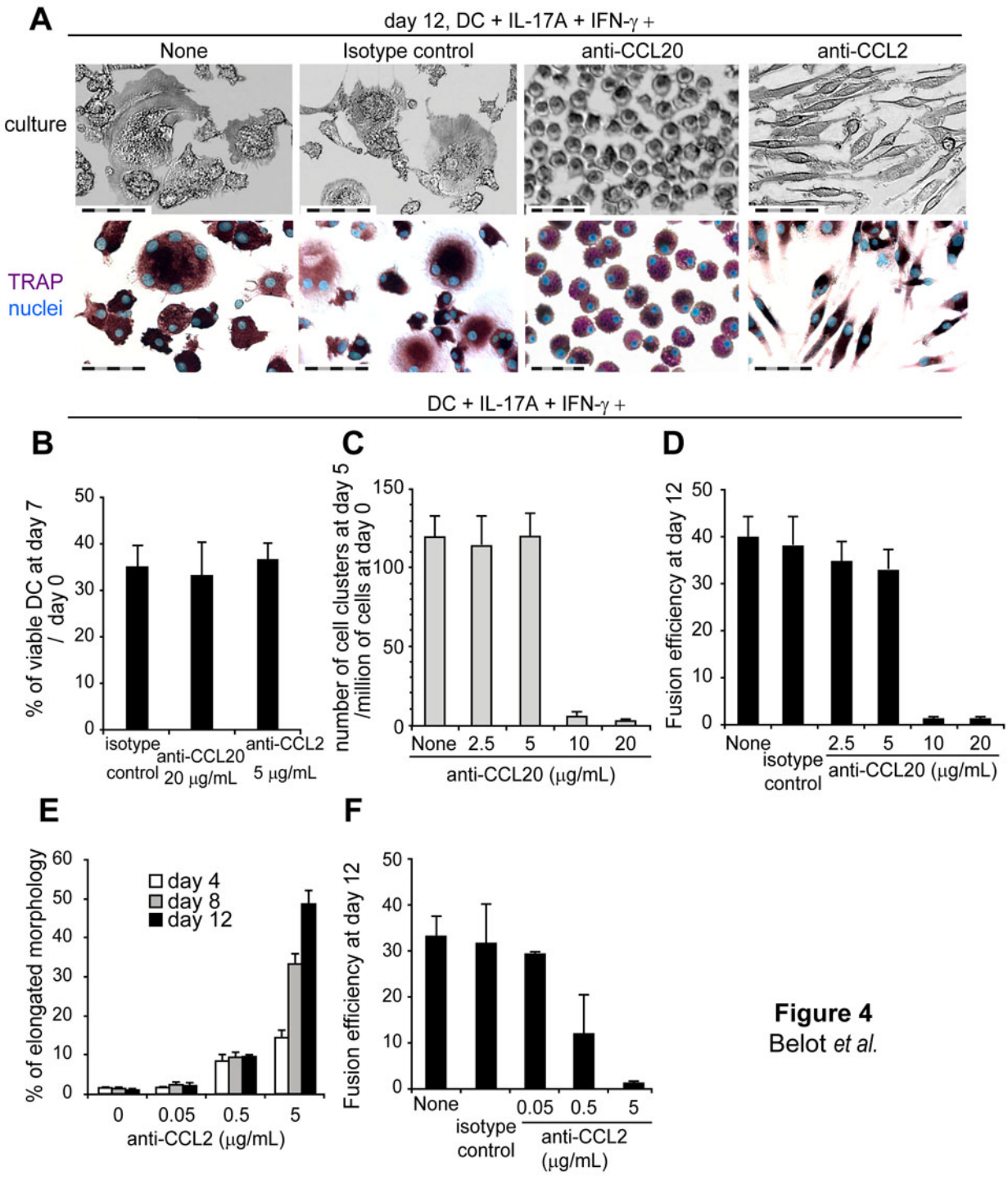

Figure 4
Belot *et al.*

Figure 4

Regulations of survival, clustering, morphology and cell fusion following CCL20 or CCL2 blockades in IL-17A and IFN-γ treated human dendritic cells

(A-F) DC treated with IL-17A and IFN-γ in the presence of none, isotype controls or antibodies directed against CCL20 or CCL2, as indicated on figures. **(A)** Photo cultures (top), cell fixation and TRAP/hoechst staining (bottom) at day 12. **(B)** Percentages of $DiOC_6^+$ PI^- viable DC at day 7 relative to day 0. **(C)** Counts of DC clusters (>50 µm diameter) at day 5. **(D, F)** Fusion efficiency at day 12. **(E)** Kinetics study of the number of elongated cells observed only in the presence of anti-CCL2.

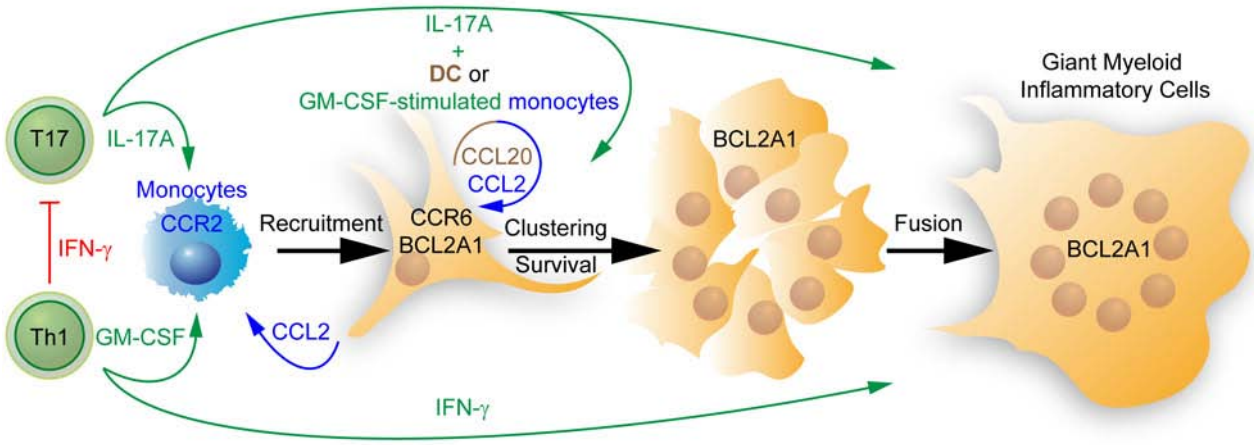

Figure 5
Belot *et al.*

Figure 5

Model for IL-17A-triggering of Giant Myeloid Inflammatory Cell formation in tuberculosis granuloma

See associated comment in discussion.

2.3 Manuscript 3: (in preparation) Giant Myeloid Inflammatory Cell: a new anti-Mycobacterium effector of the human immune system

by **Mohamad Bachar ISMAIL**[1-4]*, Fabienne COURY[2-6]*, Aymeric RIVOLLIER[7]*, Edgar BADELL[8], Marlène MAZZORANA[6], Florence CARRERAS[9], Fabienne PROAMER[10], Olga AZOCAR[11-12], Béatrice BANCEL[5], Sophia DJEBALI[12], Nathalie BISSAY[1-4], Franck BREYSSE[5], Monique CHOMARAT[5], Chantal RABOURDIN-COMBE[3-4,12]†, Pierre JURDIC[6,11], Françoise BERGER[1,5], Daniel HANAU[10], Nathalie WINTER[9] and Christine DELPRAT[1-4,13]

**Contributed equally as first authors.* †*Deceased*

Affiliations

[1] CNRS, UMR5239, Laboratoire de Biologie Moléculaire de la Cellule, Lyon, F-69007, France;

[2] Ecole Normale Supérieure de Lyon, Lyon, F-69007, France;

[3] Université de Lyon, Lyon, F-69003, France;

[4] Université de Lyon 1, Villeurbanne, F-69622, France;

[5] Hospices Civils de Lyon, Department of Rheumatology, Department of Pathology, Department of Microbiology, Centre Hospitalier Lyon Sud, Pierre-Bénite, F-69310, France;

[6] CNRS, UMR5242, Institut de Génomique Fonctionnelle de Lyon, Lyon, F-69007, France;

[7] Lund University, Department of Medicine, Lund, S-221 00, Sweden;

[8] Institut Pasteur, Unité Génétique Mycobactérienne, Paris, F-75015, France;

[9] INRA Infectiologie Animale et Santé Publique, Centre de Tours;

[10] INSERM, U725, Etablissement Francais du Sang-Alsace, Strasbourg cedex, F-67065, France ;

[11] UMS3444, Lyon, F-69007, France;

[12] INSERM, U851, Immunité Infection Vaccination, Lyon, F-69007, France;

[13] Institut Universitaire de France, Paris, F-75005, France

Contact information for correspondence

Christine DELPRAT

CNRS 5239-FACULTE DE MEDECINE LYON SUD

165 Chemin du Grand Revoyet : BP12

69921 OULLINS CEDEX
Phone : +33 426 235 980
Fax : +33 426 235 900
e-mail : **cdelprat@free.fr**

Abbreviations used in this paper:

BCG, attenuated Mycobacterium bovis strain Calmette-Guérin; DC, dendritic cells; GMIC, Giant Myeloid Inflammatory Cell; MGC, multinucleated giant cells; Mtb, Mycobacterium tuberculosis; OC, osteoclasts; TB, tuberculosis; TRAP, tartrate-resistant acidic phosphatase;

INTRODUCTION

The myeloid lineage is plastic as demonstrated by the ability of monocytes or macrophages to differentiate into dendritic cells (DC), and to monocytes or DC to differentiate into osteoclasts [1], the bone-resorbing myeloid multinucleated giant cells (MGC). We then documented that, despite significant differences between monocytes and DC, their derived OC are very similar [2]. We have previously described two pathways of DC fusion: the M-CSF and RANKL pathway that gives rise to OC formation [1] and the IL-17A-dependent pathway, characterized in the rare disease Langerhans Cell Histiocytosis [3]. However, we ignore to which extend the IL-17A-dependent MGC are genetically different from previously characterized mono or multinucleated myeloid cells such as OC or Mycobacterium-induced MGC, as observed in tuberculosis (TB) granuloma or after myeloid cell infection by Mycobacterium tuberculosis (Mtb) or bovis strain Calmette-Guérin (BCG).

DC are immune sentinels of the immune system that can detect danger signals which induce a mature phenotype including high expression of MHC-II molecules, CD80/86 co-signal molecules and CD40. Immature DC exert innate immune functions, shared with monocytes or macrophages, such as phagocytosis and TRAIL-mediated innate cytotoxicity [4]. DC are characterized by their unique ability to activate naïve T cell proliferation. A function which can be evaluated by mixing alloreactive T cells with myeloid cells: they only proliferate in the presence of DC. When stimulated by a danger signal, immature DC residing in the periphery undergo a maturation program leading to their migration to the draining lymph nodes where they interact with naïve T cells. During this DC-T cell crosstalk, the maturation program is achieved when DC receive CD40L signal from activated T cells. As part of a mycobacterial infection, the CD40L membrane antigen and IFN-γ soluble cytokine, delivered by activated T cells, are essential for granuloma formation that effectively controls Mycobacterium infection.

We previously demonstrated that IL-17A and IFN-γ are expressed in TB granuloma (manuscript 2). We also documented that IL-17A controls survival, clustering and fusion of GM-CSF-stimulated myeloid cells. Long-term survival is under the control of IL-17A-induced BCL2A1/BFL1, a pro-survival member of the Bcl-2 family molecules (manuscript 1). DC fusion is conditioned by the recruitement of DC under the control of IL-17A-induced CCL20 and CCL2 chemokines (manuscript 2). However, the ability of IL-17A-dependent giant cells to control Mycobacterium growth is unknown. In this study, we compared the phenotype and functions of giant myeloid cell induced by IL-17A to the other mono and multinucleated myeloid cells and investigated their ability to control Mycobacterium avium or

BCG growth. These cells are original newly described effectors of the immune system that we call Giant Myeloid Inflammatory Cells. Moreover, we demonstrate that BCG but not Mycobacterium avium have adapted to replicate into GMIC, depending on the activatory signal they receive.

RESULTS

The Giant Myeloid Inflammatory Cell (GMIC): a new multinucleated effector coming from IL-17A-dependent dendritic cell fusion

We purified peripheral blood monocytes of healthy donors and differentiated them into DC, in the presence of GM-CSF and IL-4. DC were cultured with either M-CSF and RANKL to generate OC or IL-17A-treatment with or without IFN-γ. We studied the intra- and extra-cellular tartrate-resistant acidic phosphatase (TRAP) activity as well as bone resorption function thank to functional test performed on bone slices. The MGC formed in response to IL-17A, with or without IFN-γ, had a very strong TRAP activity proportional to the pink/purple color of the enzymatic product accumulated after the TRAP activity assay **(Figure 1a)**. Both intra-and extra-cellular TRAP activity were very high. Unexpectedly, these giant cells were unable to resorb bone **(Figure 1b)**.

We performed a transcriptomic analysis to compare the gene expression profiles of the IL-17A-treated DC to the following myeloid cells: monocytes, DC, OC derived from either monocytes or DC and BGC-induced giant cells. OC were formed at day 14 while BGC-induced and IL-17A-dependent MGC number were stabilized at day 12. We calculated the correlation coefficients between transcriptomes, two by two. Transcriptome results are presented as scatter plots of mRNA intensities **(Figure 1c)** and a table of the respective values of correlation coefficients **(Figure 1d)**. IL-17A activates an additional genetic program (of #2000 genes) to the transcriptome (#9000 gene transcribed) of untreated DC. This gene expression profile resulting from IL-17A treatment is barely affected by the addition of IFN-γ and is responsible for the formation of a new multinucleated effector, in the immune system, different from the OC as well as from monocytes or DC. Unexpectedly, the genetic program initiated by IL-17A in DC is almost identical (R = 0.99) to the one induced by BCG infection in DC.

We finally searched in the transcriptome, differential molecular markers to identify the different myeloid cell types and we checked, at the protein level by immunocytofluorescence, the key differential molecules. IL-17A-dependent MGC were equipped with an original and rich enzyme profile, as demonstrated by the study of the cathepsin (CTS) and matrix

metalloprotease (MMP) families. IL-17A induced in DC a wide mRNA pannel of CTS and MMP, different from that of OC **(Table 1)**. Confocal microscopy analyses identified that IL-17A-dependent MGC produced increased MMP-12 and CTSD, compared with OC **(Figure 1e)**. By contrast, they synthesized MMP-9, CTSH, CTSS, CTSL and CTSK similarly as OC.

These results demonstrate that IL-17A induces the formation of an original giant cell that we propose to call GMIC for Giant Myeloid Inflammatory Cells. GMIC genetic program is different from the ones of monocytes, DC, OC. GMIC differs from OC for their function but also expression of three key enzymes. OC are $TRAP^{+}$ $MMP\text{-}12^{-/low}$ $CTSD^{-}$ bone resorbing giant cells while GMIC are $TRAP^{high}$ $MMP\text{-}12^{high}$ $CTSD^{+}$ and do not resorb bone.

IL-17A-producing T cells and CTSD-expressing myeloid cells in tuberculosis granuloma

We then performed immunohistofluorescence study by confocal microscopy in ten epithelioid granulomas from surgical lung, lymph node and pleural tuberculosis biopsy whose origin has been confirmed by culture and PCR identification of the tuberculosis complex. We looked for IL-17A, active MMP-12 and CTSD expression in TB granuloma. We used CD3 as T cell marker and Langerin/CD207 as DC marker. CD207 is expressed by Langerhans cell, a sub-population of DC which is enriched in the lung. CD207 expression was unknown in TB granuloma. We found that TB granuloma is rich in IL-17A-expressing T cells, as demonstrated by the predominace of the yellow color in the periphery of the myeloid cells **(Figure 2a)**. We detected very few cells expressing Langerin. In the heart of the granuloma, myeloid cells were all expressing CTSD while active MMP-12 was absent, contrary to what was found for GMIC **(Figure 2b)**. CTSD is the first specific marker establishing a molecular link between mononuclear myeloid cells and giant cells **(Figure 2c)** inside granuloma, thus reinforcing that giant cell may be formed from the recruited mononuclear myeloid cells, by a fusion process. We conclude that, in TB granuloma, the main source of IL-17A is T cells and the myeloid mononucleated and giant cells highly express CTSD but not active MMP-12.

IL-17A induces a mixed DC-macrophage phenotype and preserves DC functions

To functionally characterize the GMIC, we studied whether IL-17A stimulation impairs DC functions. We investigated their phenotype, phagocytic function, TRAIL-mediated cytotoxicity as well as their ability to activate alloreactive T cells. After 48h of culture, IL-17A induced a mixed phenotype combining markers of monocytes (CD14), macrophages (CD68) to DC markers (CD1a) **(Figure 3a)**. IL-17A-treated DC dysplay a semi-mature phenotype, including $CD1a^{+}$ $CCR6^{+}$ $CD83^{-}$ $HLA\text{-}DR^{low}$ and $CD40^{high}$ as expressed by

immature and mature DC, respectively. Addition of IFN-γ did not change this phenotype. BCG infection, as expected, induced a complete DC maturation characterized by $CD1a^{-}$ $CCR6^{-}$ $CD83^{+}$ $HLA\text{-}DR^{high}$ and $CD40^{high}$. The transcriptome study realized at day 12 showed that CD1a mRNA disappeared and revealed that, as observed with BCG, IL-17A induced M-CSF expression in DC, the cytokine that usually drives macrophage differentiation (**Figure 3b**). IL-17A-treated DC retained phagocytic functions as demonstrated by engulfment of inert particles in the presence of zymosan, a TLR2-stimulating protein-carbohydrate complex from yeast, as well as with the two Mycobacterium species tested: avium and BCG (**Figure 3c**). Recombinant GFP-BCG let us visualize phagocytosis of the Mycobacteria by GMIC (**Figure 3d**). TRAIL-mediated cytotoxicity was evaluated by stimulating DC with either double-stranded RNA stimulation (poly I:C) or infection with Measles virus **(Figure 3e)**. TRAIL synthesis was induced in both cases and could kill a TRAIL-sensitive cell line independently of IL-17A treatment **(Figure 3f)**. Therefore TRAIL-mediated cytotoxic innate function was preserved in IL-17A-treated DC. A unique property of DC is to activate naïve T cell proliferation of co-cultured allogeneic T cells. We used the fluorescent dye CFSE to stain allogeneic T cells and then quantify T cell divisions by the twice decreased of its fluorescence **(Figure 3g)**. Alloreactive function of DC is increased when they are stimulated by their CD40 antigen to activate their maturation, as demonstrated by the increased proportion of T cell (>50%) having completed over three divisions. After 12 days of culture with IL-17A, DC-derived giant cells still exhibited alloreactive functions while DC-derived OC, in the presence of M-CSF and RANKL did not.

In conclusion, IL-17A induces a mixed monocyte-macrophage-DC semi-mature phenotype while preserving the classical functions of DC in the GMIC: phagocytosis, TRAIL-mediated-cytotoxicity and alloreactivity.

CD40-stimulation and IFN-γ potentiate GMIC formation

CD40L signal and IFN-γ synthesis by activated T cells are essential for granuloma formation that controls Mycobacterium infection. We studied their role in GMIC versus OC formation. Quantifying the number of MGC and number of nuclei per MGC enables us to calculate the percentage of nuclei included in the MGC which reflects the fusion efficiency. IFN-γ only increased GMIC formation while it completely abolished OC formation **(Figure 4a)** and bone resorption activity (data not shown). CD40L activation potentiated both pathways of DC fusion **(Figure 4b)**. IL-17A did not induce GMIC formation from monocytes **(Figure 4c)** whereas we previously published that GM-CSF-treated monocytes could

differentiate into GMIC. Neither IFN-γ nor CD40 activation induced GMIC formation from monocytes.

Therefore when both CD40L and IFN-γ signals are provided in the microenvironment, GMIC but not OC formation is sustained from DC or GM-CSF-treated monocytes.

BCG but not Mycobacterium avium divide into GMIC when it is activated by CD40L

We studied the GMIC molecular equipement to understand how GMIC may interact with Mycobacteria. In particular for the molecules involved in adhesion of Mycobacteria to phagocytes and the different phase of the phagocytosis such as oxidative stress and vacuole acidification **(Table 2)**. The profile of receptors used by Mycobacteria is modified by IL-17A stimulation at the surface of DC. After 12 days of culture, GMIC express more TLR2 and CD14 mRNA, but less DC-SIGN (CD209), Dectin-1 and mannose receptor (MR) mRNA than untreated DC. Thus, DC exhibit the following phenotype: $CD14^{-}$ MR^{high} $CD209^{high}$ $Dectin^{high}$ while GMIC are CD14+ MR+ $CD209^{low}$ $Dectin^{low}$. Among the molecules involved in oxidative stress, the GMIC are characterized by an increased expression of CYBB/$gp91^{phox}$, while the interaction with BCG increases the expression of NCF1/$p47^{phox}$ and SOD2. Among the molecules involved in vacuolar acidification, IL-17A increases gene expression of ATP6V1H and retains a profile similar to DC for other molecules of this functional profile.

We studied the microbicidal functions of GMIC through the measure of the NADPH oxidase activity and nitric oxide production. The presence of NADPH oxidase was confirmed at the functional level by NBT test. Treatment by IL-17A is very effective to increase NADPH oxidase activity of DC, transformed in GMIC **(Figure 5a)**. The lack of expression of NOS2 was confirmed by the negativity of the Griess test (data not shown). We studied the microbicidal activity by the quantification of Mycobacteria that survive in GMIC compared to what happens with DC. DC were pre-treated with either CD40L activation or IL-17A and IFN-γ or the combination for 24 hours and then infected with either M. avium or BCG. The quantification of Mycobacteria was realized by the technique of CFU (colony forming unit for) within two weeks after infection. Growth of M. avium was controlled by three donors of five by immature DC **(Figure 5b)**. When DC were previously stimulated by CD40L activation or IL-17A and IFN-γ or both, M. avium growth was controlled by all donors. By contrast, BCG survived in DC without replicating as long as no CD40L is provided. Electronic microscopy study demonstrated that DC treated with CD40L, IL-17A and IFN-γ and then infected by BCG accumulated lipid droplets and license BCG replication **(Figure 5c)**. Quantification of BCG growth by CFU revealed that CD40L activation alone induced

replication of BCG whereas IL-17A and IFN-γ did not. Strikingly, combination of CD40L, with IL-17A and IFN-γ was very potent to sustain survival and intracellular division of BCG.

In conclusion, GMIC are molecularly equipped to deal with Mycobacteria with especially high NADPH oxidase activity. They are highly microbicidal against M. avium when activated by CD40L, IL-17A and IFN-γ, whereas under the same conditions, BCG not only resists to their microbicidal activity but also replicate in GMIC.

DISCUSSION

see PhD manuscript discussion

MATERIALS AND METHODS

Tissue samples

We selected formalin-fixed, paraffin-embedded tissue of lung (n=5), pulmonary lymph node (n=4) and pleura (n=1) from 10 patients (Centre de Ressources Biologiques des Hospices Civils de Lyon, France). Diagnosis of Mycobacterium tuberculosis infection was confirmed by culture and PCR. Sections were routinely stained with haematoxylin-phloxine-safran. Multinucleated giant cells were seen in 7 biopsies out of 10.

Reagents and Mycobacteria

We used the following antibodies for cytofluorimetry: PE-CD1a (HI149), FITC-CD14 (M5E2), PerCP-Cy5.5-MHC II (HLA-DR) (G46-6) from Becton Dickinson (Le Pont de Claix, France), isotype controls and PE-CD80 (MAB104), FITC-CD83 (HB15a), PE-CD86 (HA5.2B7) from Beckman Coulter (Villepinte, France), CD68 (EBM11) from DAKO (Glostrup, Denmark). Recombinant human macrophage colony-stimulating factor (M-CSF), granulocyte/macrophage colony-stimulating factor (GM-CSF), interferon-γ (IFN-γ), IL-17A and receptor activator of NF-κB ligand (RANKL) were purchased from PeproTech (Rocky Hill, NJ) and LPS (L-2387, *salmonella typhosa*) from Sigma. dsRNA was poly(I:C) obtained from Amersham Pharmacia Biotech (Piscataway, NJ). We used *Mycobacterium avium* and BCG strain from Pasteur Institute.

Monocyte and T cell purification, dendritic cell differentiation

Monocytes and T cells were purified from the blood of healthy adult volunteers (Etablissement français du sang, Lyon Gerland, France) after ficoll and percoll gradients and then negative magnetic depletion. Monocyte-derived DC were generated *in vitro*, as

previously described. Briefly, monocytes were seeded at $0.8x10^6$ cells/mL and maintained in RPMI 1640 (Gibco, Paisley, Scotland) supplemented with 10 mM Hepes (*N*-2-hydroxyethylpiperazine-*N'*-2-ethanesulfonic acid), 2 mM L-glutamine, 40 µg/mL gentamicin (Gibco), 10% heat-inactivated Fetal Calf Serum (Boehringer Mannheim, Meylan, France), 50 ng/mL hrGM-CSF and 500 U/mL hrIL-4. After 6 days of culture, more than 95% of the cells were immature DC as assessed by $CD1a^+$ $CD83^-$ labeling.

Bone resorption assays

To assess resorption activity, cells were cultured on bone slices (Nordic Bioscience Diagnostics, Herlev, Denmark), for 21 days in a 5% CO_2 incubator. Following complete cell removal by immersion in water, bone slices were stained with toluidine blue in order to detect resorption pits under a light microscope. Bone resorption tracks, cell culture observations as well as TRAP/Hoechst pictures were performed using a Leica DMiRB microscope equipped with x40/0.30 NA or x 40/0.55 NA objective lenses (Leica, Wetzlar, germany), a Leica DC300F camera and the Leica FW400 software. Bone resorptions were quantified by the release of C-terminal type I collagen fragments (CTX), consecutive to resorption of bone slices, in the culture supernatants, using the CrossLaps ELISA kit (Nordic Bioscience Diagnostics, Herlev, Denmark).

MGC and osteoclast formation, TRAP assay and Hoechst DNA staining

MGC and osteoclast-derived DC were generated in vitro, as previously described[3]. Briefly, DC were seeded from 1600 to 3200 cells/mm2 in RPMI supplemented with 10% fetal calf serum, 2 mM L-glutamine, 10 mM HEPES, 40µg/mL gentamicin, in the presence of IL-17A (2 ng/mL) and IFNγ (2ng/mL) or M-CSF (25 ng/mL) and RANKL (100 ng/mL). Cytokines were added at the beginning of the culture and then replenished every three days (M-CSF, RANKL) or every week (IL-17A, IFN-γ). Counts were made of the total number of nuclei, the number of MGC-included nuclei and the number of MGC (strictly more than two nuclei) at the same time in each condition. These three counts allowed the calculation of the number of mononucleated cells, the mean number of nuclei per MGC and the percentage of MGC-included nuclei in comparison to the total number of nuclei (fusion efficiency). TRAP activity was assessed using the Leukocyte acid phosphatase kit (Sigma-Aldrich, Saint Quentin Fallavier, France). DNA of the nuclei were then stained with 10 µg/mL of Hoechst 33342 (Sigma) for 30 min at 37°C. The staining was fixed with 1% formol.

Affymetrix genechip study.

We purified RNA after cell lysis, extraction in Trizol (Invitrogen) and purification on a MEGAclear column (Ambion) to reach an RNA integrity number >9 with Agilent bioanalyser. As previously described[3], the whole RNA human profile is analyzed on HG-133_plus2 affymetrix chips for either unstimulated cells, monocytes or DC, or cells cultured : monocytes or DC with M-CSF and RANKL, DC or BCG-infected DC with IL-17A and with or without IFN-γ. ProfileXpert (www.profilexpert.fr) carried out the chip analysis as follow:

Target labelling: Microarray analysis was performed using a high-density oligonucleotide array (Genechip human genome U133 Plus 2.0, Affymetrix, Santa Clara, CA, USA). Labeled target for microarray hybridization was prepared using the Genechip expression 3' Amplification One-cycle target labeling (Affymetrix). Briefly, totalRNA (2□g) was converted into double stranded cDNA with a modified oligo(dT)24-T7 promoter primer. After purification, cDNA was converted into cRNA and biotinylated using the IVT labeling kit (Affymetrix). Reaction was carried out for 16 hours at 37°C then at the end of incubation biotin-labeled cRNA was purified by the Genechip sample clean up module (Affymetrix). cRNA quantification was performed with a nanodrop and quality checked with the bioanalyzer 2100 (Agilent technologies, Inc, Palto Alto, CA, USA).

Arrays hybridization and scanning: Hybridization was performed following Affymetrix protocol (http://www.affymetrix.com). Briefly, 20 □g of labeled cRNA was fragmented, mixed in hybridization buffer (50 pM control oligo B2, 1X eukaryotic hybridization controls, 0,1mg/ml Herring sperm DNA, 0.5 mg/ml BSA and 1x hybridization buffer, 10% DMSO for a total volume of 300 ul), denaturated during 5 minutes at 95°C and hybridized on chip during 16 hours at 45°C with constant mixing by rotation at 60 rpm in an Genechip hybridization oven 640 (Affymetrix). After hybridization, arrays were washed and stained with streptavidin-phycoerythrin (Invitrogen Corporation, CA, USA) in a fluidic 450 (Affymetrix) according to the manufacturer's instruction. The arrays were read with a confocal laser (Genechip scanner 3000, Affymetrix) and analyzed with GCOS software. Absolute expression transcript levels were normalized for each chip by globally scaling all probe sets to a target signal intensity of 500. The detection metric (presence, absence or marginal) for a particular gene was determined by means of default parameters in the GCOS v 1.4 software (Affymetrix). Quality of RNA amplification and labeling were checked by using B.subtilis poly adenylated RNA spikes-in controls (Lys, phe, thr, dap) mixed to RNA sample before performing reverse transcription. Hybridization quality was checked by using E.coli biotinylated target (Bio B,

BioC, BioD and CRE). Filtering of results was performed using Genespring ver 7.0 software (Agilent).

Immunofluorescence and confocal microscopy

DC cultured on glass coverslips were first fixed for 20 minutes with 2% paraformaldehyde in PBS and after epitote retrieval performed in 0,1% glycine for 10 minutes, cells cultured were permeabilized with 0.1% Triton X-100 in PBS for 5 minutes. 4-mm paraffin-embedded biopsies were cut, deparaffinized and rehydrated. Epitope retrieval was performed in citrate buffer (10mM, pH6.0) using a water bath. Cells or tissue sections were incubated with primary antibodies, overnight at 37°C, in a humidity chamber. Replacement of the primary antibodies by non-relevant antibodies of the same immunoglobulin isotype was used as negative control. Table provides a summary of the antibodies used. Following 3 washes in PBS-1%BSA, slides were treated for 15 min in PBS-1% BSA with 10% normal goat serum or rabbit goat serum, the species in which the secondary antibodies were developed, to block non-specific staining. Detection of the primary antibodies was then performed with goat anti-mouse, goat anti-rabbit or rabbit antigoat isotype-specific secondary Alexa Fluor 488, 546 and 647-conjugated antibodies (Invitrogen, Breda, NL) for 30 min. Following 3 washes in PBS-1%BSA, the coverslips or the sections were mounted using Mowiol and then analyzed by confocal microscopy using a Carl Zeiss MicroImaging Inc. LSM 510 confocal microscope. Specimens of normal human gut and Crohn disease gut were used, respectively, as negative and positive controls for IL-17A staining.

Table. Characteristics of antibodies used in immunohistochemical studies

Antibody	Clone	Species/isotype	source
IL-17A	41802	mouse IgG1	R&D Systems
CD3		rabbit IgG	DAKOCytomation
Langerin	12D6	mouse IgG2b	Novocastra
CCR6	53103.111	mouse IgG2b	R&D Systems
CCL20	67310.111	mouse IgG1	R&D Systems
cathepsin D	E-7	mouse IgG1	Santa Cruz Biotechnology
cathepsin H		rabbit IgG	Proteintech
cathepsin K		goat IgG	Santa Cruz Biotechnology
cathepsin L	S-20	goat IgG	Santa Cruz Biotechnology
cathepsin S		goat IgG	R&D Systems
MMP-9	4A3	mouse IgG1	Santa Cruz Biotechnology
MMP-12	82902	mouse IgG2b	R&D Systems

Flow cytometry

Immunostaining were performed in 1% BSA and 3% human serum-PBS then quantified on a FACSCalibur (Becton Dickinson) and analyzed using CellQuest software. Direct immunostainings were performed using 2 mg/ml of conjugated Abs. Indirect immunostainings were performed using 2 mg/ml of the first mouse mAb and detected with 2 mg/ml of the PEconjugated, F(ab')2 goat anti-mouse IgG antibodies (115-086-062) (Jackson Immunoresearch, West Grove, PA). To perform cytoplasmic TRAIL immunostaining, 30-min permeabilization with 0.33% saponin was required. Cells were labeled by using a biotinconjugated anti-TRAIL polyclonal Ab (2.5 µg/ml; R&D Systems, Minneapolis, MN) revealed by using PE-conjugated streptavidin (Caltag Laboratories, Burlingame,CA).

Quantification of phagocytic, priming and cytotoxic activities

For **phagocytic activity evaluation**, DC cultured on glass coverslips with or without IL-17A for 2 days were washed twice and then put in medium without antibiotic, in contact with green fluorescent (FITC or GFP) *Mycobacterium avium* or BCG or bovine serum

albumincoated latex beads and zymosan (50 particles/cell) for 2 hours and washed twice with fresh medium to remove unbound particles. Phagocytosis of bacteria was determined as described previously335. Briefly, cells were fixed with 3.7% paraformaldehyde in PBS containing 15 mM sucrose, pH 7.4 for 20 min at room temperature. After neutralization with 50 mM NH4Cl, extracellular mycobacteria were labeled with rabbit polyclonal antibodies directed against Mycobacteria (Camelia antibody, 1:100), revealed by a red fluorescent (TRITC) secondary antibody. MGC containing at least one green Mycobacterium were counted out of 100 cells in duplicate samples.

For **cytotoxic activity evaluation,** TRAIL-sensitive MDA231 cells were labeled with 100 μCi of Cr for 1 h at 37°C, washed three times, and resuspended in complete medium. Then Crlabeled MDA231 cells (10^4/well) were incubated with varying numbers of DC stimulated with IL-17A for 8 h. TNR-R1:Fc (10 μg/ml;R&D Systems), TRAIL-R2;Fc (10 μg/ml) were added to some assays.

For **alloreactivity evaluation**, T $CD4^+$ cells were suspended at 10^7 cells/mL in alpha-MEM medium containing 2% FCS. After 13 min of incubation in the presence of 10 μM of carboxyfluorescein diacetate succinimidyl ester (CFSE), the CFSE incorporation was blocked by the addition of a large excess of alpha-MEM medium, containing 2% FCS. T cells were then washed twice by centrifugation at 1500 rpm for 10 min at 4 °C in alpha-MEM medium containing 2% FCS and seeded in alpha-MEM medium containing 10% FCS with DC or MGC. Cells were then harvested after 5 days of culture and expression of CFSE was measured with a FACSCalibur.

Nitric oxide and Nitroblue tetrazolium (NBT) assay

For iNOS activity evaluation, we assessed nitric oxide production using Griess reagent kit, according to the manufacturers' specifications (Molecular Probes). Samples were incubated with Griess reagent for 30 min at room temperature and absorbance was measured at 540nm.

For NADPH oxydase activity evaluation, NBT (0.1%) was prepared in PBS by adding 10 mg of NBT powder (Sigma Chemical Co, St. Louis, USA) to 100 mL of PBS (pH 7.2) and stirred at room temperature for 1 hour. NBT solution was filtered with a 0.2 μm filter. Equal volumes of 0.1% of NBT solution were added in each well and incubated for 30 minutes at 37°C.

Microbicidal activity

cDC were seeded at 3000 cells/mm2 in 12-well plates in DMEM (Gibco) supplemented with 10% FCS, 2 mM L-glutamine, 10 mM HEPES, without antibiotic, in the presence of M-CSF (25 ng/mL) and RANKL (100 ng/mL) or GM-CSF(200ng/ml), IL-17A (1 ng/mL) and IFN-g (1ng/mL) and cultured together with or without $0{,}2.10^6$/well human irradiated CD40L fibroblasts. Cytokines were added at the beginning of the culture and then replenished every three days (M-CSF, RANKL) or every week (IL-17A, IFN-g). After 24h of incubation with cytokines, cells are infected either with BCG or *Mycobacterium avium* (MOI=5). At different time points (2h, 7 days, 14 days), lysis with 0,1% Triton X-100 was performed and followed by centrifugation at 4000 rpm. Lysats were cultured in Middlebrook 7H9 medium for 21 days and then colony forming unit (CFU) contained in the supernatant were quantified.

Immunoelectron Microscopy

Cells were fixed at 37°C [5], and ultrathin sections were examined under a Philips CM 120 BioTwin electron microscope (120 kV) (Philips, Eindhove, The Netherlands).

REFERENCES:

1. Rivollier, A, *et al.* (2004). Immature dendritic cell transdifferentiation into osteoclasts: a novel pathway sustained by the rheumatoid arthritis microenvironment. *Blood* 104: 4029-4037.

2. Gallois, A, *et al.* (2010). Genome-wide expression analyses establish dendritic cells as a new osteoclast precursor able to generate bone-resorbing cells more efficiently than monocytes. *J Bone Miner Res* 25: 661-672.

3. Coury, F, *et al.* (2008). Langerhans cell histiocytosis reveals a new IL-17A-dependent pathway of dendritic cell fusion. *Nat Med* 14: 81-87.

4. Servet-Delprat, C, Vidalain, PO, Valentin, H, and Rabourdin-Combe, C (2003). Measles virus and dendritic cell functions: how specific response cohabits with immunosuppression. *Curr Top Microbiol Immunol* 276: 103-123.

5. Mc Dermott, R, *et al.* (2002). Birbeck granules are subdomains of endosomal recycling compartment in human epidermal Langerhans cells, which form where Langerin accumulates. *Mol Biol Cell* 13: 317-335.

FIGURE LEGENDS

Figure 1

Giant Myeloid Inflammatory Cells: a new IL-17A-dependent multinucleated DC-derived myeloid effector different from OC

(**a**) TRAP activity detection (standard activation/pink to over-activation/purple cytoplasm colour) and Hoechst DNA staining (blue nuclei). Values quantify soluble acidic phosphatase activity in cell culture supernatant of DC, IL-17A-treated DC with or without IFN-γ and DC-derived OC after 20 days of culture. (**b**) Microscopic pictures of bone slices show resorptive capacities and quantification of CTX (collagen fragment) release in culture supernatants of DC cultured in the same conditions. (**c**) Scatter plots comparing gene expression between both differenciation pathways into MGC-derived DC in the presence of M-CSF and RANKL or IL-17A and IFN-γ, between IL-17A-stimulated DC and DC unstimulated, between monocytes and DC, between both differenciation pathways into OC from DC and monocytes in the presence of M-CSF and RANKL, between IL-17A-stimulated DC and DC stimulated with IL-17A and IFN-γ and between BCG-infected DC and IL-17A-treated DC. (**d**) Correlation coefficient table comparing monocytes or monocyte-derived DC at day 0, monocytes or DC after 12 days of culture with M-CSF and RANKL, which give rise to OC, DC treated with IL-17A with or without IFN-γ after 12 days and BCG-infected DC with or without IL-17A and IFN-γ. (**e**) MMP-12 and CTSD staining on permeabilized OC versus GMIC. Scale bars, 50µm (5x10µm).

Figure 2

Presence of IL-17A and CTSD inside human tuberculosis granuloma

(a-c) Representative confocal microscopy images of immuno-fluorescence staining of tuberculosis granuloma. **(a)** Langerin (Langerhans cells, dark blue), CD3 (T cells, red) and IL-17A (green) were stained. Yellow cells are $CD3^+$ $IL\text{-}17A^+$ T cells that secrete IL-17A. **(b-c)** CTSD (green) and active MMP-12 (red) were stained. The green staining delineates **(b)** the myeloid heart of granuloma which includes mono and **(c)** multinucleated myeloid cells. Scale bars, 50µm (5x10µm).

Figure 3

IL-17A treatment induces a mixed DC-monocyte-macrophage phenotype, but preserves DC functions

(**a**) Maturation phenotype of monocyte-derived DC cultured for two days alone or after activation with LPS or with IL-17A or infected with BCG. Bars delineate positive regions. (**b**) mRNA expression of phenotype and maturation markers shown for DC at day 0 and for DC after 12 days of culture with M-CSF and RANKL or IL-17A and IFN-γ and after infection or not with BCG. Results are means for n = 4 (none day 0), n = 2 (M-CSF+RANKL), n = 3 (IL-17A+ IFN-γ), n = 2 (BCG-infected+IL-17A+ IFN-γ) experiments. (**c**) Phagocytosis assay of zymosan, *M. avium* and BCG by DC stimulated with or without IL-17A. (**d**) Vizualisation of the phagocytosis of recombinant GFP-BCG in GMIC. Immunocytofluorescent confocal analysis was performed after MHC-II staining in red and Hoechst staining of the nuclei in blue. **(e)** TRAIL expression in DC and IL-17A-stimulated DC by flow cytometry analysis. IL-17A-stimulated DC were either stimulated with dsRNA poly (I:C) (0.2 μg/ml) or infected with MV at 0.1 PFU/cell, then placed in culture for 24 h. DC were permeabilized and then stained with an isotypic control or an anti-TRAIL antibody. **(f)** Cytotoxic activity of IL-17A-stimulated DC. IL-17A stimulated DC were infected with MV and then placed in culture for 12h. Harvested DC were then cultured with 51Cr-labeled MDA-231 target cells at the indicated effector-to-target cell (E/T) ratios. TRAIL-R2:Fc or TNF-R1:Fc chimeras were added or not added to the assay to inhibit TRAIL or TNF-α-induced cell death, respectively. 51Cr release was measured 8 h later. (**g**) Allostimulatory properties of DC cultured for 5 days in the presence of T cells purified from allogeneic donors (n = 2). Immature DC versus CD40-stimulated DC were tested.The decrease of CFSE fluorescence attested when T cell proliferate.

Figure 4

Differential role of IFN-γ and CD40L on OC and GMIC formation

(**a**) Photo culture of DC fusion induced by M-CSf and RANKL or IL-17A with (right) or without (left) IFN-γ. Cells were fixed at day 15 and we performed a May-Grünwald-Giemsa coloration to visualize cytoplasm and nucleus morphology. **(b-c)** We quantified at day 12 the MGC counts (top), average number of nuclei per MGC (middle) and fusion efficiency *via* the percentage of nuclei included in MGC in comparison to the total number of nuclei (bottom).

Mean and SD of triplicate experiments. **(b)** Role of CD40 activation was addressed when DC is cultured in the presence of M-CSF and RANKL or IL-17A with or without IFN-γ. **(c)** Monocytes were compared to DC for their ability to undergo cell fusion in the two pathways of cell fusion.

Figure 5

BCG but not M. avium subverts CD40L-activated GMIC functions

(**a**) NADHPoxidase activity in cell culture of DC pretreated with (bottom) or without (top) IL-17A and IFN-γ : DC were then either left unstimulated or stimulated with LPS or BCG-infected and we performed a May-Grünwald-Giemsa coloration to visualize cytoplasm and nucleus morphology. **(b-d)** Monocyte-derived DC from healthy donors were infected at MOI = 5 with Mycobacteria. Colony forming Units were quantified at 2h and 336h (14 days) after infection in cell culture lyzates. DC were either untreated or received CD40L signal and/or IL-17A and IFN-γ, as indicated. **(b)** To compare the five different donors, we plotted the *M.avium* growth at 336h as a percentage of 100 *M. avium* counted at 2h. **(c)** Electronic microscopy photos of DC infected with BCG and activated with CD40L signal, IL-17A and IFN-γ. Black arrows indicate lipid droplets (LD) and BCG. Red arrow indicates division of BCG. Scale bars, 5μm (5x1μm) **(d)** BCG count for one donor, representative of n = 3.

Table 1

mRNA expression of CTS and MMP is shown for DC at day 0 (mononucleated cells, n = 4), for DC after 12 days of culture with IL-17A and IFN-γ (GMIC, n = 3) or with M-CSF and RANKL (OC, n = 2).

Table 2

mRNA expression of innate receptors involved in mycobacterial interaction, in oxidative stress and in vacuole acidification is shown for DC at day 0 (n = 3) or cultured with IL-17A and IFN-γ (GMIC, n = 3), or BCG-infected and cultured with IL-17A and IFN-γ (GMIC, n = 2).

Table 1

Common name	none day 0	IL-17A + IFN-γ day 12	M-CSF+RANKL day 12
Cathepsins (CTS)			
CTSB	37,312	45,861	59,259
CTSC	47,267	23,719	13,184
CTSD	1,105	14,363	6,259
CTSH	10,390	21,600	10,929
CTSK	-	12,290	77,147
CTSL	3,648	22,004	11,643
CTSS	16,392	38,467	20,591
CTSZ	7,763	24,091	5,070
Matrix Metalloproteases (MMP)			
MMP2	-	1,768	-
MMP7	-	3,466	1,646
MMP9	3,208	51,876	86,692
MMP12	38,309	22,239	6,448
MMP14	-	-	2,641
MMP19	-	2,718	5,376

Table 2

Common name	none day 0	IL-17A + IFN-γ day 12	BCG-infected + IL-17A + IFN-γ day 12
innate receptors			
TLR1	1,370	2,905	2,919
TLR2	2,092	4,113	4,390
TLR4	1,966	3,159	2,676
TLR6	226	268	266
TLR9	88	51	58
CD14	2,754	16,799	15,799
MR	38,223	15,643	9,876
CD209/DC-SIGN	17,866	5,226	2,016
CLECSF12/Dectin-1	26,078	6,584	7,595
CARD15/NOD2	775	500	367
oxidative stress			
RAC1	21,190	15,561	16,581
RAC2	16,153	22,641	23,337
NCF1/p47^{pnox}	1,759	2,516	8,967
NCF2/p67^{pnox}	23,241	12,841	18,549
NCF4/p40^{pnox}	2,179	6,131	4,159
CYBA/p22	8,935	13,354	12,700
CYBB/gp91^{pnox}	1,400	13,014	17,529
SOD2	1,268	4,432	18,012
CAT	19,618	12,831	11,050
GPX1	22,623	30,699	30,753
GPX3	10,992	12,045	10,472
GPX4	13,177	13,571	18,535
NOS2A	61	38	43
vacuole acidification			
ATP6AP2	21,972	30,804	28,565
ATP6V0A1	1,318	2,955	2,618
ATP6V0B	9,144	12,881	13,359
ATP6V1A	11,028	16,189	17,077
ATP6V1B2	12,337	19,781	19,109
ATP6V1E1	5,784	9,269	8,722
ATP6V1F	13,058	14,029	17,896
ATP6V1H	3,182	10,367	10,325
C7orf32/ATP6V0E2L	459	1,039	979

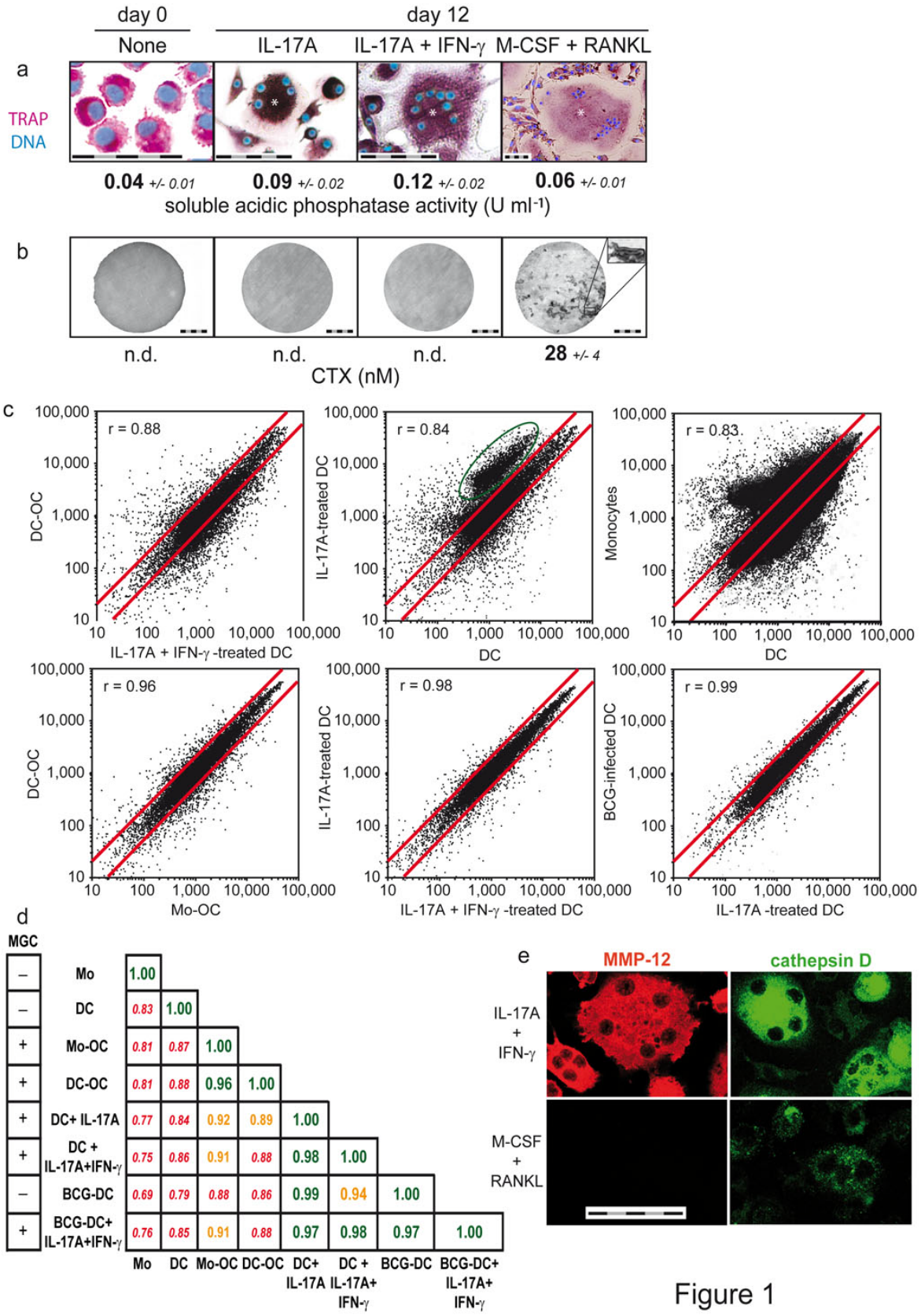

MGC		Mo	DC	Mo-OC	DC-OC	DC+ IL-17A	DC + IL-17A+ IFN-γ	BCG-DC	BCG-DC+ IL-17A+ IFN-γ
–	Mo	1.00							
–	DC	0.83	1.00						
+	Mo-OC	0.81	0.87	1.00					
+	DC-OC	0.81	0.88	0.96	1.00				
+	DC+ IL-17A	0.77	0.84	0.92	0.89	1.00			
+	DC + IL-17A+IFN-γ	0.75	0.86	0.91	0.88	0.98	1.00		
–	BCG-DC	0.69	0.79	0.88	0.86	0.99	0.94	1.00	
+	BCG-DC+ IL-17A+IFN-γ	0.76	0.85	0.91	0.88	0.97	0.98	0.97	1.00

Figure 1

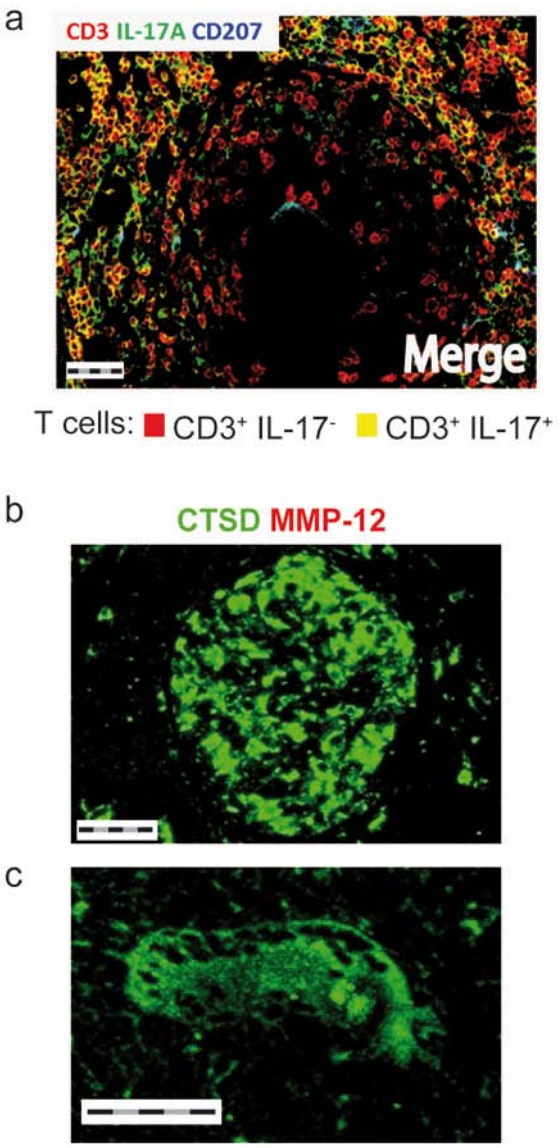
a
CD3 IL-17A CD207
Merge
T cells: CD3+ IL-17- CD3+ IL-17+
b
CTSD MMP-12
c

Figure 2

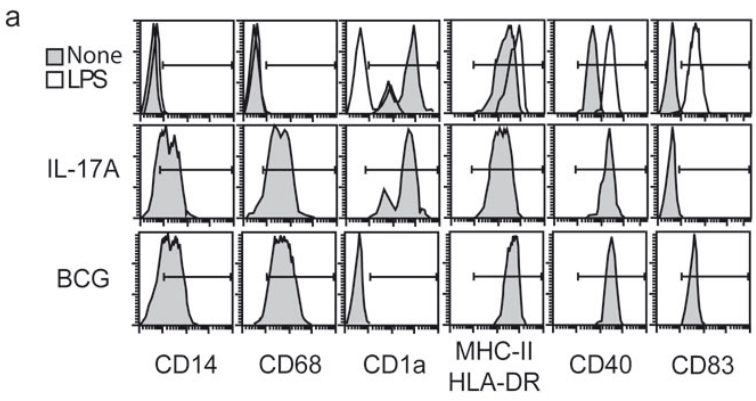

b

Common name	none day 0	M-CSF + RANKL day 12	IL-17A (+/- IFN-γ) day 12	BCG-infected (+/- IL-17A + IFN-γ) day 12
CD14	2,754	20,717	16,799	15,799
CD68	1,046	2,167	3,424	3,089
CD1a	29,462	223	123	128
CSF1/M-CSF	527	2,494	2,825	5,330
HLA-DR	67,595	45,680	53,495	49,262
CD40	2,388	753	1,333	2,098
CD83	3,416	4,002	4,726	8,107

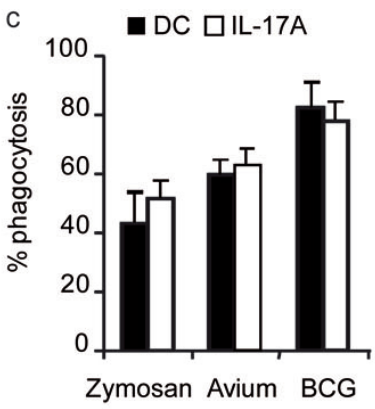

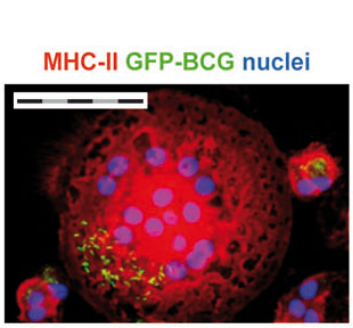

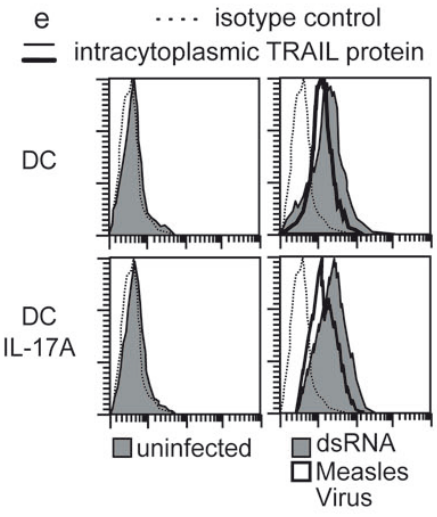

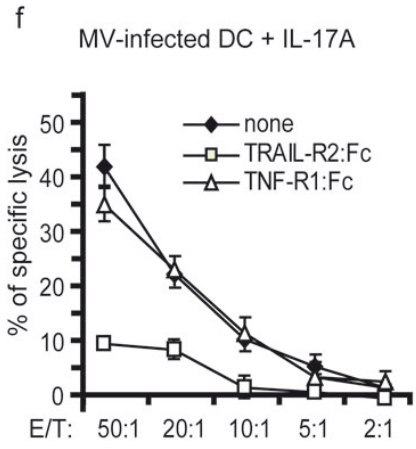

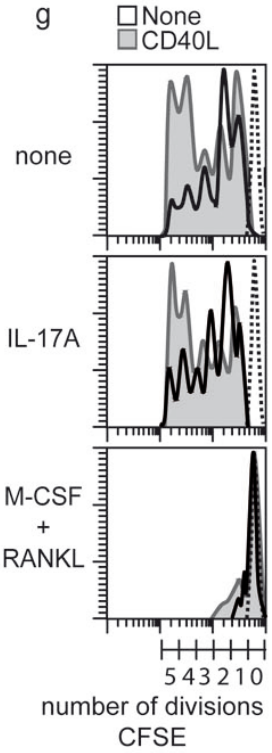

Figure 3

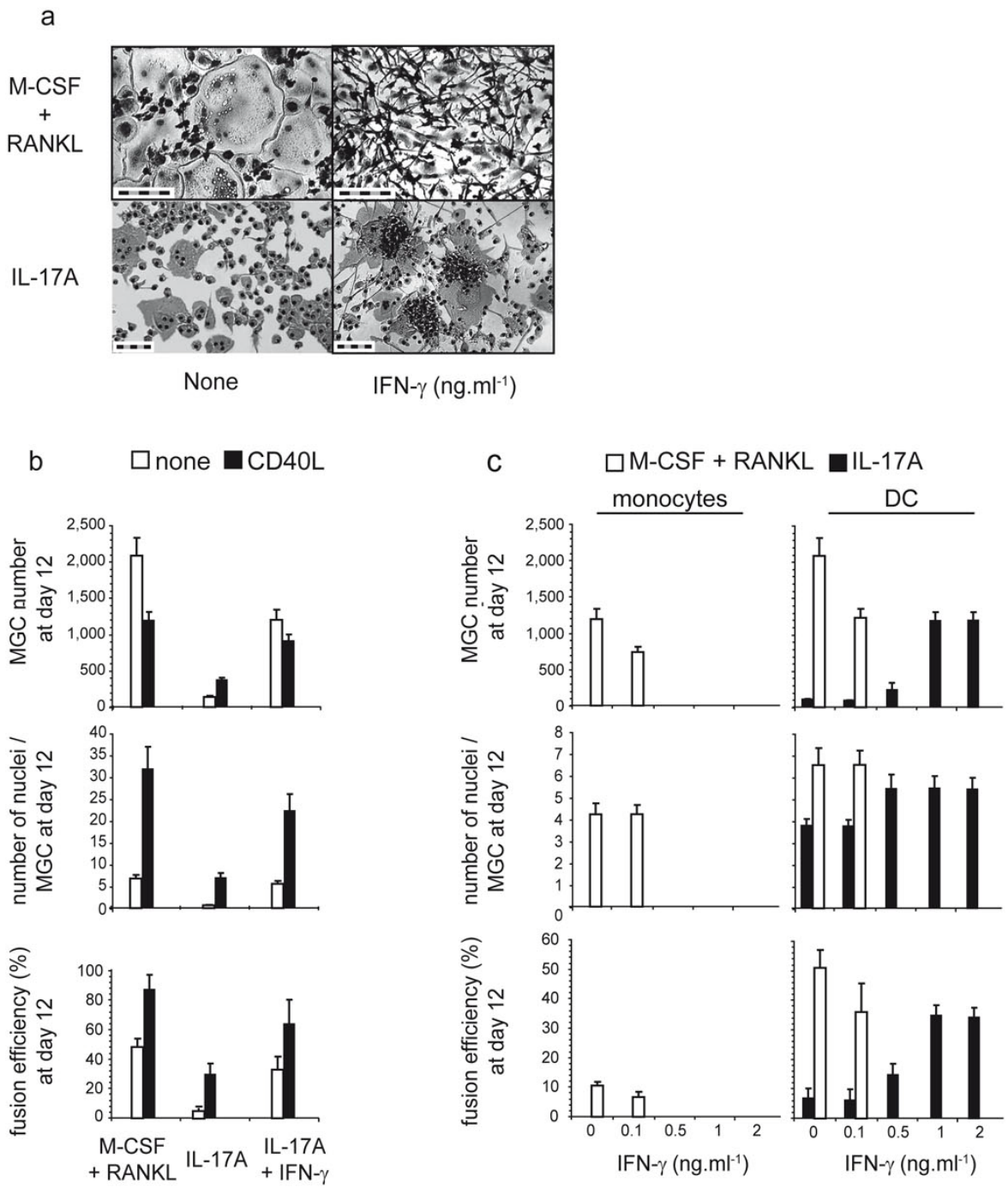
a
M-CSF + RANKL
IL-17A
None
IFN-γ (ng.ml-1)
b
none
CD40L
MGC number at day 12
number of nuclei / MGC at day 12
fusion efficiency (%) at day 12
M-CSF + RANKL
IL-17A
IL-17A + IFN-γ
c
M-CSF + RANKL
IL-17A
monocytes
DC
MGC number at day 12
number of nuclei / MGC at day 12
fusion efficiency (%) at day 12
IFN-γ (ng.ml-1)
IFN-γ (ng.ml-1)

Figure 4

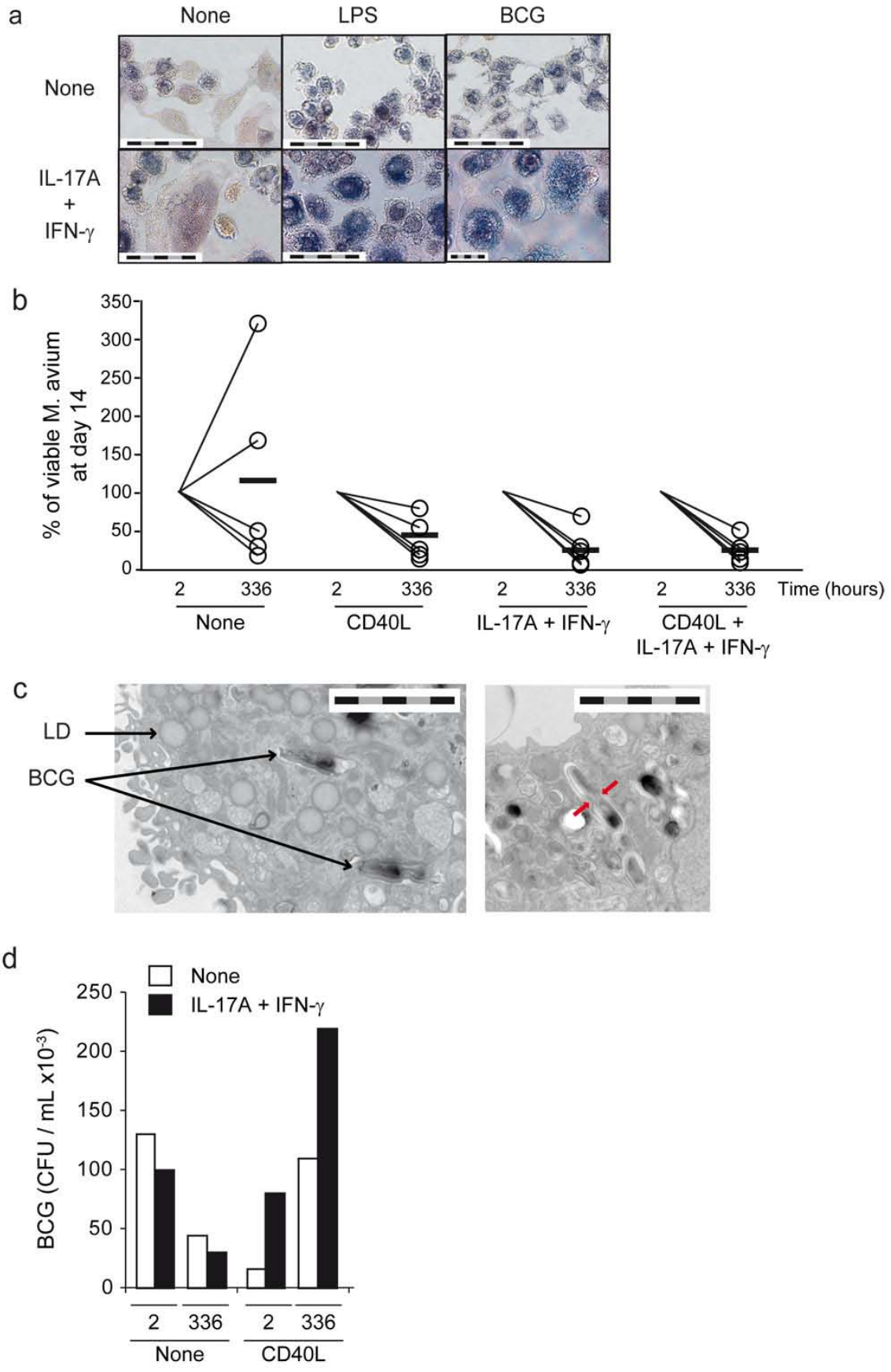
a
None
LPS
BCG
None
IL-17A
+
IFN-γ
b
% of viable M. avium
at day 14
350
300
250
200
150
100
50
0
2
336
Time (hours)
None
CD40L
IL-17A + IFN-γ
CD40L +
IL-17A + IFN-γ
c
LD
BCG
d
None
IL-17A + IFN-γ
BCG (CFU / mL x10-3)
250
200
150
100
50
0
2
336
None
CD40L

Figure 5

2.4 Manuscrit 4: (in preparation) IL-17A+MMP-12+CSTD+ DC accumulation leads to bronchoepithelium destruction: relevance in pulmonary LCH

by **Mohamad Bachar ISMAIL**[1-4]*, Alexandre BELOT[1-5]*, Nathalie BISSAY[1-4], Béatrice BANCEL[6], Jan-Inge HENTER[7], Maurizio ARICÒ[8], Françoise BERGER[1-4,6], Abdellatif TAZI[9] and Christine DELPRAT[1-4,10]

**Contributed equally as first authors.*

[1] CNRS, UMR5239, Laboratoire de Biologie Moléculaire de la Cellule, Lyon, F-69007, France ;

[2] Ecole Normale Supérieure de Lyon, Lyon, F-69007, France ;

[3] Université de Lyon, Lyon, F-69003, France ;

[4] Université de Lyon 1, Villeurbanne, F-69622, France ;

[5] Hospices Civils de Lyon, Hôpital Femme Mère Enfant, Bron, F-69500, France ;

[6] Hospices Civils de Lyon, Department of Pathology, Department of Microbiology, Centre Hospitalier Lyon Sud, Pierre Bénite, F-69310, France ;

[7] Childhood Cancer Research Unit, Department of Women's and Children's Health, Karolinska Institutet, Karolinska University Hospital Solna, S-171 76 Stockholm, Sweden;

[8] Department of Pediatric Hematology Oncology, Azienda Ospedaliero-Universitaria Meyer Children Hospital, Florence, I-50139, Italy;

[9] Centre National de Référence de l'Histiocytose Langerhansienne; Univ Paris Diderot, Sorbonne Cité; Assistance Publique Hôpitaux de Paris; Service de Pneumologie, Hôpital Saint Louis, Paris, F-75475, France.

[10] Institut Universitaire de France, 103 bd St Michel, Paris, F-75005, France

ABSTRACT

Langerhans cell histiocytosis (LCH) is a rare granulomatous disease characterized by an abnormal accumulation of IL-17A-expressing DCs in involved tissues. LCH predominately affects children but an isolated rare form of this disease, called pulmonary LCH (pLCH), occurs in adults destroying their lungs. As in childhood LCH, we identified, for the first time, that pathological DCs in pLCH express IL-17A. Moreover, we also found IL-17A-expressing multinucleated giant cells (MGC) in lung granulomas. Surprisingly, most of pathological IL-17A-expressing DCs express CD1a but not CD207. Serum studies demonstrated that IL-17A is systemically distributed in patients developing either active childhood or adult pulmonary

forms of LCH. Pathological DCs express CCL20 and CCL2 chemokines in pLCH lesions as revealed by immunofluorescent staining and high levels of CCL2 are detected in serum from patients affected with this disease. Using immunofluorescence, we also found that matrix metalloproteinase 12 (MMP-12) and cathepsin D (CTSD) proteases are expressed by pathological DCs in pLCH lesions. Importantly, using an *in vitro* co-culture system, we revealed that IL-17A-treated DCs exhibit potent aggressive functions as they were able to destroy bronchial epithelial cells. Our data supports that IL-17A-expressing DCs is responsible for the bronchiole destruction observed in pLCH patients, possibly through their aggressive proteases. Since DC granulomas constitute the hallmark of pLCH, targeting these cells and their aggressive functions may provide new avenues in pLCH treatment.

Figure 1 legend: A/ Triple CD207/blue, CD3/red and IL-17A/green staining on section "n", with CD1a/purple staining on side-section "n-1" and CD207/blue, CD3/red and IgG1 isotype/green control staining on side-section "n+1" of adult pulmonary LCH biopsy (case pulm 8). The enlarged inset picture shows the presence of IL-17A$^+$ giant cells (as previously detected in childhood LCH). Scale bars, 50 μm (5 x 10 μm). C/ Percentages of CD1a, CD3, CD207, IL-17A expressing cells in adult pulmonary Langerhans cell histiocytosis. B and D/ IL-17A measurement in childhood, adult LCH and control sera and in monocyte or monocyte-derived DC compared to control. E/ GM-CSF staining in pLCH patient in granuloma (gr) and bronchio-alveolar cells (br). Scale bars, 50 μm (5 x 10 μm)

Figure 1 results: Most of IL-17A expressing CD1a+DC are CD207-negative

In adult pulmonary LCH lesions, we consistently found more CD1a+ DC than CD207+ LC, thus numerous CD1a$^+$ CD207$^-$ DC were detected. We demonstrate that most, but not all, IL-17A-secreting DC are CD1a$^+$ CD207$^-$ non-LC DC, ranging from 2 to 52% of the CD1a+ DC (fig 1A, C). Few or no T cells express IL-17A in LCH lesions. IL-17A is increased in sera of pLCH patients as well as in monocyte-derived DC but not in monocytes (Fig 1 B, D). GM-CSF is strongly expressed in bronchial alveolar cells and slightly increased in granuloma. GM-CSF and IFN-γ are not expressed in LCH patient sera (data not shown).

Figure 1: Cytokine environment in biopsy & serum in pulmonary LCH patients

A/

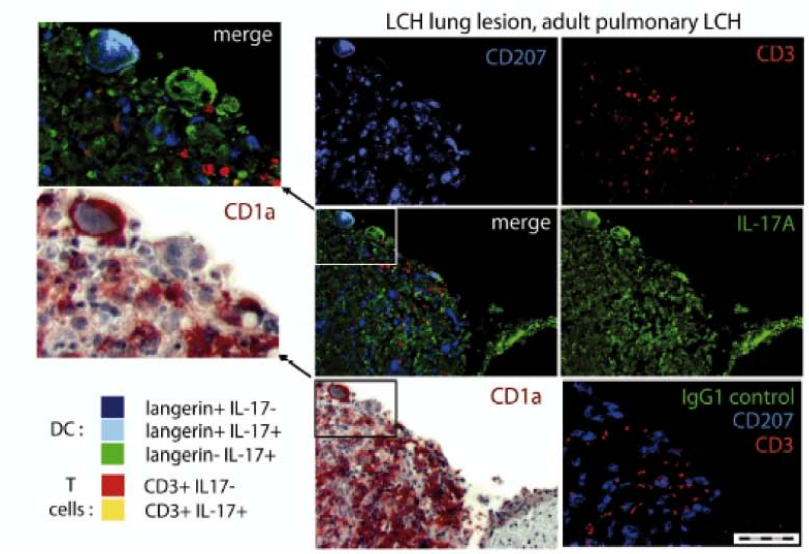

B/

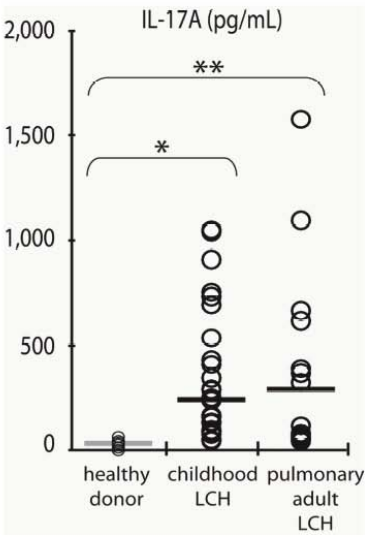

C/

Case	% in TOTAL CELLS			% in CD3+ T cells	% in CD1a+ DC		
	CD3	CD1a+	CD207+	IL-17A+	CD207+	IL-17A+ CD207+	IL-17A+ CD207-
Pulm1	13	59	27	2	45	0	6
Pulm2	33	22	2	3	7	0	13
Pulm3	27	52	30	3	57	0.5	4
Pulm4	16	43	18	0	41	1	19
Pulm5	14	66	33	0	49	0.2	2
Pulm6	9	52	32	0	61	2	9
Pulm7	10	44	19	0	43	1	52
Pulm8	21	57	27	1	48	1	10
Pulm9	17	33	19	0	58	1	17
MEAN (±SD)	16 (±8)	48 (±14)	23 (±10)	1 (±1)	45 (±16)	0.7 (±1)	15 (±15)
RANGE	9-33	22-66	2-33	0-3	7-61	0-2	2-52

D/

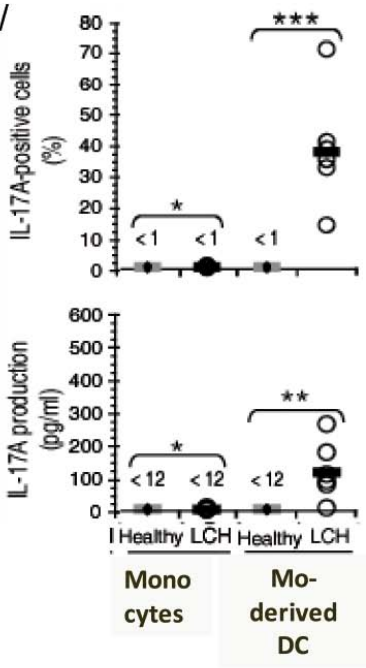

E/

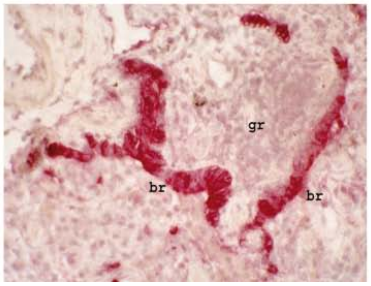

Figure 2: Chemokine CCL20 and CCL2 in PLCH lesions and serums.

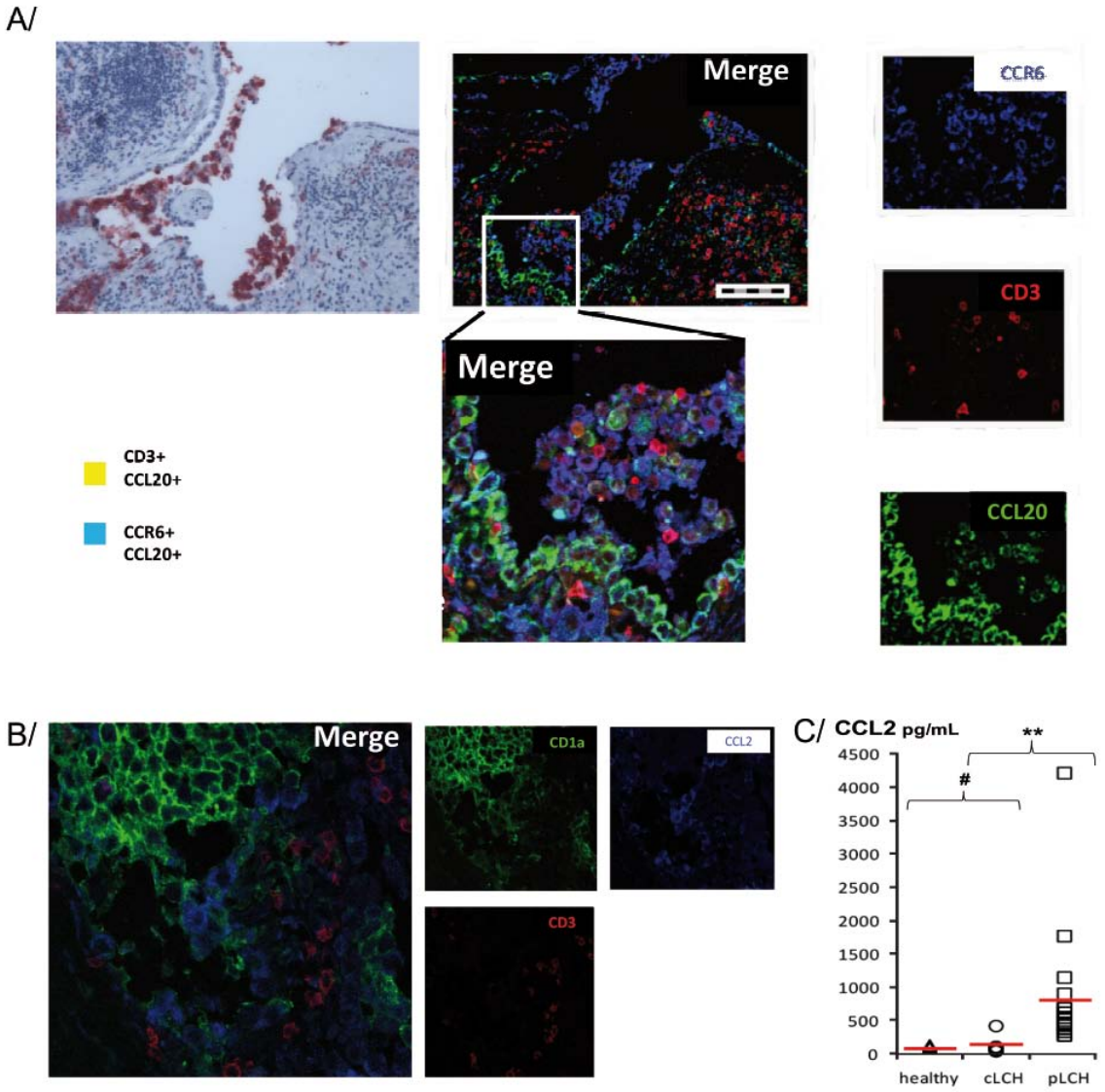

Figure 2 legend : (A) Triple CCR6/blue, CD3/red and CCL20/green staining on section "n", with CD1a/purple staining on side-section "n-1" and CD207/blue, CD3/red and IgG1 isotype/green control staining on side-section "n+1" of adult pulmonary LCH biopsy (case pulm X). The enlarged inset picture shows the presence of epithelial cells CCL20+ close to the granuloma. Specificity of immunostainings was demonstrated using isotype controls (not shown). Scale bars, 50 µm (5 x 10 µm). (B) Triple CD3/blue, CCL2/red and CD1a/green staining of adult pulmonary LCH biopsy. (C) Patient's sera measurement of CCL2.

Figure 2 results: CCL20 and CCL2 drive DC accumulation in pLCH. CCL20 and CCL2 were expressed in situ by LCH-DC (Fig2A and B). Here we show that CCL20 was also expressed by broncho-epithelial cells, in contact with DC granuloma. CCL2 was detected in patient serums contrary to CCL20 (data not shown), suggesting a distinct endocrine versus paracrine role in cell recruitment (Fig2C).

Figure 3: Detection of CTSD and MMP families in IL-17A-rich microenvironment

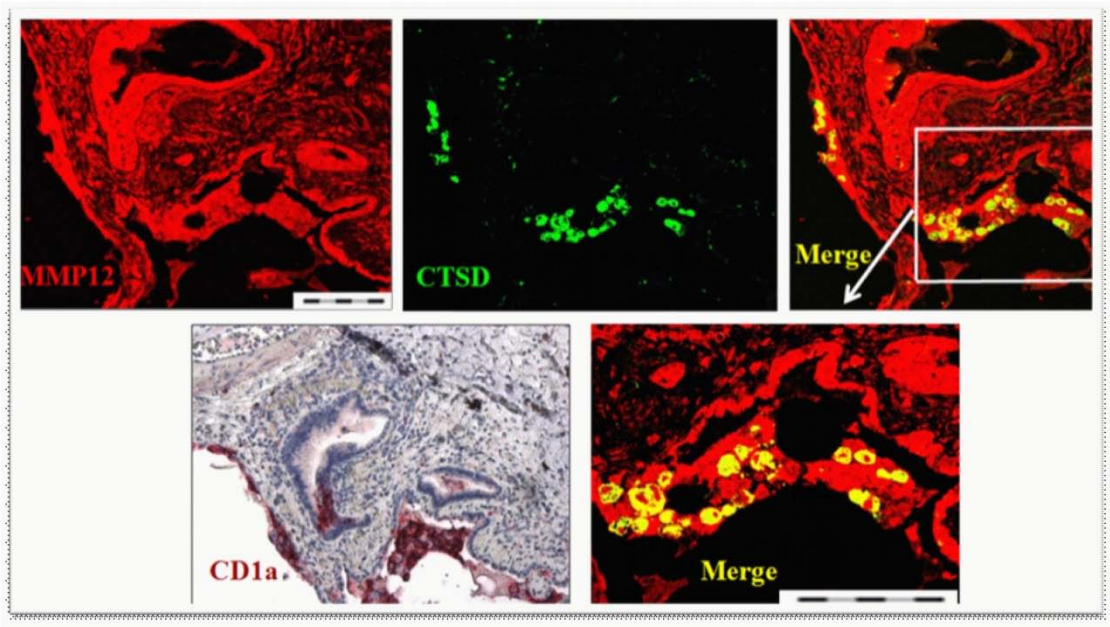

Figure 3 legend: CTSD and MMP12 expression within pLCH lesions**.** Double CTSD/green, MMP-12/red staining on section "n", with CD1a/purple staining on side-section "n-1" of adult pLCH lesions (case pulm 6). Yellow color revealed that pLCH-DC and DC-derived MGC coexpress MMP-12 and CTSD. Staining is representative of nine studied patients. MMP12 is also expressed by the bronchial epithelial cells. Specificity of immunostainings was demonstrated using isotype controls (not shown). Bar scale length is 50µm (5x10µm).

Figure 3 results: Active MMP-12 & CTSD were expressed in pulmonary LCH.. In pLCH lesion, MMP-12 was expressed by broncho-epithelial cells and LCH-DC. CTSD was expressed by large or multinucleated DC inside granuloma (Fig 3C).

Figure 4: BEAS2B destruction assessment of IL-17A treated DC

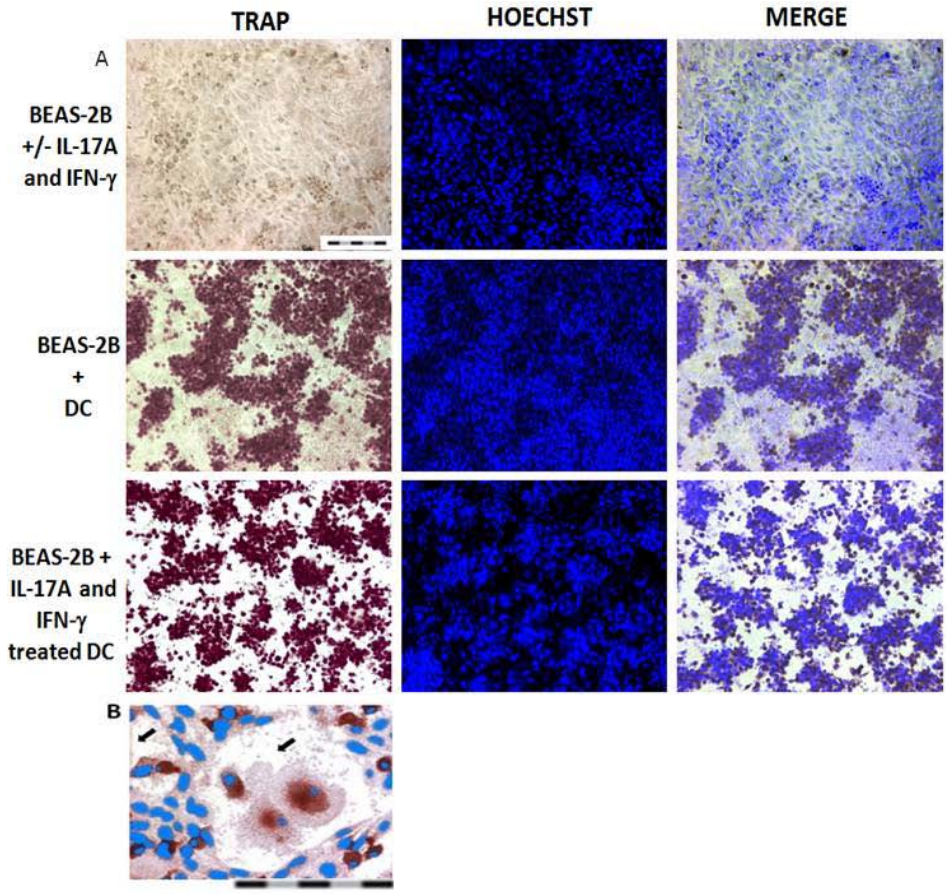

Figure 4 legend: (A) Double TRAP (purple) /Hoechst (blue) staining of BEAS-2B cells incubated with or without IL-17A and IFN-γ cytokines (top panels), with DC alone (middle panels), or with IL-17A and IFN-γ-treated DC (down panels). DC are double stained whereas BEAS-2B are only Hoechst positive. (B) High magnification picture of BEAS-2B cells incubated with IL-17A and IFN-γ-treated DC. Holes in BEAS-2B layer are observed (black arrows) around $TRAP^+$ cells. Data are representative of two experiments. Bar scale length is 50µm (5x10µm).

Figure 4 results: IL-17A-treated DC induced tissue destruction.To investigate whether IL-17A-treated DC can damage bronchial epithelial cells, we have set up an *in vitro* co-culture system involving immortalized bronchial epithelial cells (BEAS-2B) and primary monocyte-derived DC. We cultured immature DC either alone or with IL-17A and IFN-γ. In parallel, we cultured a confluent monolayer of human bronchial epithelial cells from the cell line "BEAS-2B" which has been immortalized with Sv40/Ad12 virus hybrid contruct. We then added treated DC on bronchial epithelial cells for 12h, before performing a TRAP/Hoechst staining to discriminate the two cell types. Hoechst staining localized the nuclei of all viable cells while TRAP identified DC because BEAS-2B are TRAP-negative. BEAS-2B alone displayed a nice confluent layer of blue nuclei stained by Hoechst (Fig. 4A top). Addition of IL-17A and/or IFN-γ did not affect BEAS-2B viability (Fig. 4A top).

Untreated DC were unable to induce the destruction of BEAS-2B cells (Fig. 4A middle) since Hoechst staining indicated that BEAS-2B were still alive. As previously published, IL-17A treatment increased TRAP expression in DC (Coury et al., 2008) thus explaining the higher color intensity of the DC in the bottom panel. These treated DC destroyed the BEAS-2B layer (Fig. 4A down) leading to the formation of several holes as shown at higher magnification (Fig. 4B). Treated DC were required to kill the BEAS-2B cells since neither DC nor cytokine, alone, could destroy the BEAS-2B cell layer. These data demonstrate that IL-17A and IFN-γ-treated DC exhibit a specific potent ability to destroy human bronchial epithelial cells, *in vitro*.

Figure 5: Model of bronchiole destruction by pathological infiltrating DC in pLCH lesions

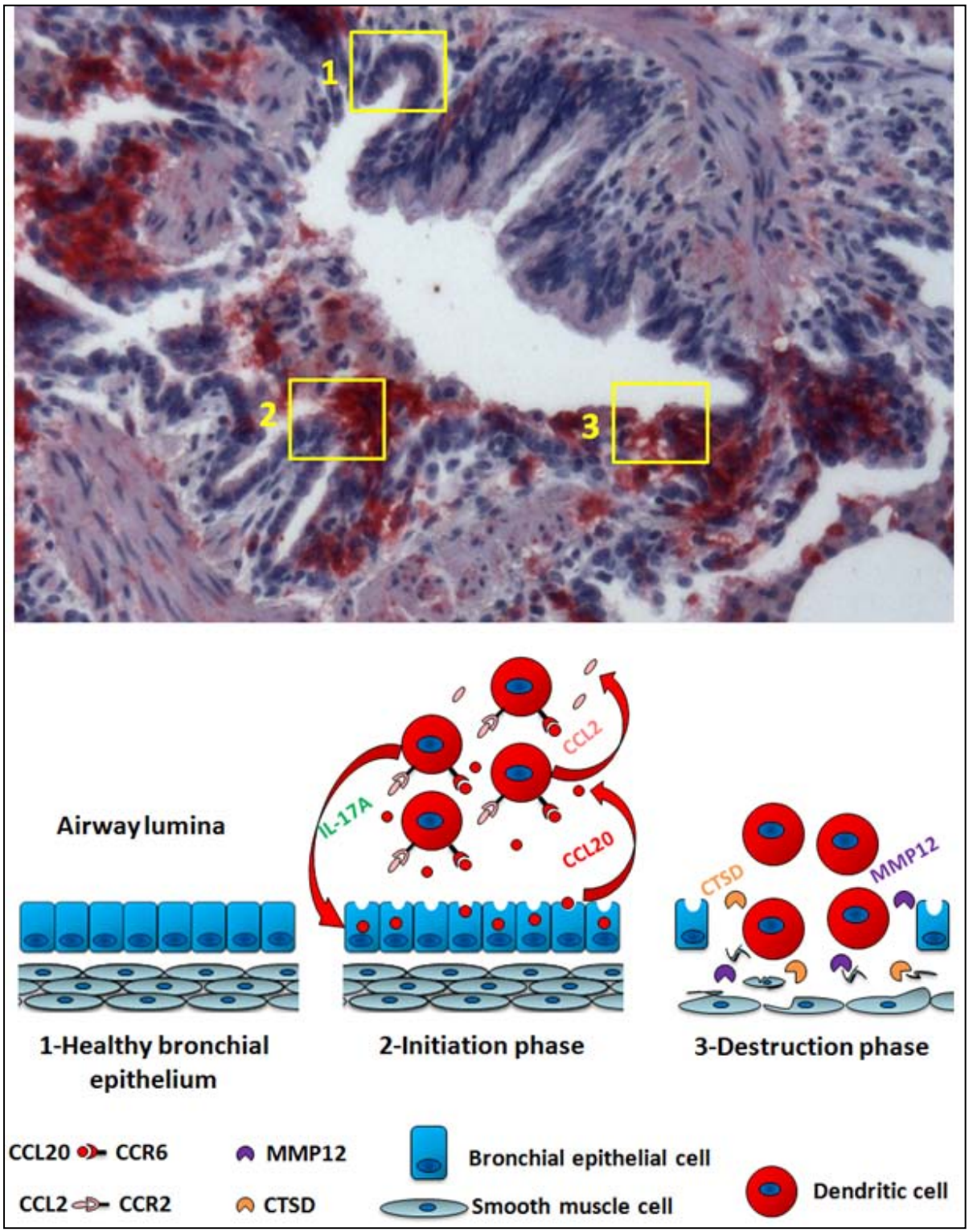

Figure 5 shows a model of bronchiole destruction in pLCH lesions visualized owing to a CD1a red staining of DC with a counter coloration of nuclei performed with hematoxylin (blue). Aligned narrow blue nuclei localize healthy bronchial epithelium (square1). In square 2, red pathological DC are localized near the bronchial epithelial cells. We propose that IL-17A induces CCL20 mainly by bronchial epithelial cells, thus attracting CCR6+ cells such as DC. CCL2 production by pathological

DC may further increase monocyte and DC recruitment. Finally, bronchial epithelium destruction (square 3) indicates that bronchial epithelial cells have been killed and digested. We propose that MMP-12 and CTSD may play an essential role in this destructive process. IL-17A, CCL20 and CCL2 as well as proteolytic enzymes like CTSD and MMP-12 may constitute several essential therapeutic targets in LCH treatment.

Material & methods:

Reagents

We used the following antibodies for DC phenotype analysis by cytofluorimetry: FITC-CD1a (21270013S), FITC-CD3 (21270033S), FITC-CD14 (21270143S), PE-HLA-DR (21278994S) all from Immunotools and FITC-CD83 (HB15a) from Beckman Coulter. We used recombinant human IL-17A and IFN-γ from PeproTech.

Patients

Biopsy section samples from 9 patients, all current or ex-smokers (7 women and 2 men, aged 40.3 ± 17 years), referred to (Centre de référence de l'Histiocytose Langerhansienne, France) and diagnosed as having pLCH, were examined in this study. For each patient, we obtained 5 Serial section slides with one previously stained for CD1a expression as well as with hematoxylin to revealed nuclei. Clinical data and manifestations of the 9 patients are shown in table 1. Serum samples from 22 pLCH patients were also obtained from the same source. Serum from 38 childhood LCH patients were collected from blood samples obtained from Sweden and Italy.

Table 1: Clinical data of patients included in the pLCH study

Case	Sex / Age at sampling	Smoking status	Extrathoracic involvement	Treatment at sampling
Pulm1	F / 47 years	Current smoker	none	none
Pulm2	M / 37 years	Ex-smoker	skin, bone, anterior pituitary insufficiency with diabetes insipidus	desmopressin and hormonal substitution
Pulm3	F / 23 years	Current smoker	diabetes insipidus	desmopressin
Pulm4	F / 53 years	Current smoker	none	none
Pulm5	F / 48 years	Ex-smoker	none	none
Pulm6	F / 36 years	Current smoker	none	none
Pulm7	F / 45 years	Ex-smoker	none	none
Pulm8	M / 24 years	Current smoker	diabetes insipidus	desmopressin
Pulm9	F / 50 years	Current smoker	none	none

Immunohistofluorescence and confocal microscopy

IL-17A and IFN-γ-treated DC cultured on glass coverslips were first fixed for 20 minutes with 2% paraformaldehyde in PBS. Cells cultured were permeabilized with 0.1% Triton X-100 in PBS for 5 minutes.

4-μm paraffin-embedded lung biopsies were deparaffinized and rehydrated. Epitope retrieval was performed in citrate buffer (10mM, pH6.0) using a water bath for one hour at 99°C.

Cells or tissue sections were incubated 30 minutes in phosphate buffered saline (PBS) -1% bovine serum albumin (BSA) with 3% human serum to block Fc receptors. They were then incubated with primary antibodies, overnight at 37°C, in a humidity chamber. Replacement of the primary antibodies by non-relevant antibodies of the same immunoglobulin isotype was used as negative control. Table 2 provides a summary of the primary antibodies used. Following 3 washes in PBS-1%BSA, slides were treated for 15 min in PBS-1% BSA. Detection of the primary antibodies was then performed with suitable isotype-specific secondary Alexa Fluor 488, 546 and 647-conjugated antibodies (Invitrogen, 1:200 dilution) for 30min. Following 3 washes in PBS-1%BSA, the sections were mounted using Mowiol and then analyzed by confocal microscopy using a Carl Zeiss MicroImaging Inc. LSM 510 confocal microscope. Immunostainings for CD1a and GM-CSF were performed by immunochemistry. Incubation with appropriate dilutions of anti-CD1a antibody (O10; Immunotech, Marseille, France) or a sheep anti-human GM-CSF polyclonal antiserum (National Institute for Biological Standards and Control, Hertfordshire, UK) conjugated to alkalin phosphate, were realized. Positive cells were revealed using the Vectastain ABC-alkaline phosphatase kit system obtained from Vector Laboratories (Burlingame, CA). We quantified percentage of positive and negative cells with ImageJ freeware of National Center for Biotechnology Information.

Table 2: Characteristics of primary antibodies used for immunohistofluorescent stainings

Antibody	Clone	Species/isotype	source	concentration μg/ml
IL-17A	MAB3171	Mouse/IgG1	R&D Systems	10
CD207/langerin	ab49730-100	Mouse/IgG2b	Abcam	20
CD3	A0452	Rabbit/IgG	DakoCytomation	12
MMP-12	82902	Mouse/IgG2b	R&D Systems	25
CTS D	E-7: sc-13148	Mouse/IgG1	santa cruz biotechnology	4
CCR6	53103	Mouse/IgG2b	R&D Systems	25
CCL20	67310	Mouse/IgG1	R&D Systems	10
CCL2	MAB2791	Mouse/ IgG2b	R&D Systems	25
CD1a	DM363	Mouse IgG1	Acris antibodies	40

IL-17A, MMP, CCL20 and CCL2 detection

Serum amounts of IL-17A and CCL2 were measured in the serum of patients diluted at 1:2 using human ELISA development kit or Luminex to detect IL-17A (Peprotech, 900-K84), CCL2 (Peprotech, 900-K31), CCL20 (R&D) and MMP . Samples were run in duplicate to ensure

reproducibility. Results were analyzed by the Multiskan Spectrum Spectrophotometer with SkanIt Software 2.2 (Thermo Electron).

Cell purification, differentiation and culture:

Blood was obtained from healthy adult volunteer donors (Etablissement français du sang, Lyon Gerland, France). Monocytes isolation and purification was performed as previously described (Fugier-Vivier et al., 1997). Briefly, monocytes were obtained after Ficoll (Lymphocyte separation medium, Eurobio, CMSMSL01-01) and percoll (GE Healthcare, 17-0891-01) density-gradient centrifugation, respectively. They are then seeded at 10^6 cells/mL and maintained in RPMI 1640 (Life Technologies, Paisley, United Kingdom) supplemented with 10 mM HEPES (N-2-hydroxyethylpiperazine-N'-2-ethanesulfonic acid), 2 mM L-glutamine, 40 µg/mL gentamicin (Life Technologies), 10% heat-inactivated fetal calf serum (FCS; Boehringer Mannheim, Meylan, France), 50 ng/mL human recombinant GM-CSF (hrGMCSF), and 500 U/mL hrIL-4. After 6 days of culture, cells developed into typical immature DC being $CD14^-$, $CD1a^+$, human leukocyte antigen (HLA)-DR^+, and $CD83^-$ (not shown).

Affymetrix gene chip study

mRNA were extracted from either unstimulated DC or DC cultured with IL-17A with or without IFN-γ, after cell lysis, extraction in Trizol (Invitrogen) and purification on a MEGAclear column (Ambion) to reach an RNA integrity number >9 with Agilent bioanalyser. ProfileXpert (www.profilexpert.fr) carried out the chip analysis study.

Culture of BEAS-2B cells and coculture with IL-17A and IFN-γ- treated DC

The BEAS-2B cell line, which is an immortalized line of normal human bronchial epithelium derived by transfection of primary cells with an adenovirus12-SV40 hybrid virus, was obtained from ATCC. Cells were cultured and maintained at 37°C with 5% CO2 in 75 cm^2-cell culture flasks precoated with a mixture of fibronectin (1:50 dilution; Sigma F0895) and Bovin I collagen (1:100 dilution; Invitrogen A1064401) both dissolved in LHC-9 serum-free medium (Invitrogen, 12680-013) . Cells were passaged every three days. For coculture assays of BEAS-2B and IL-17A and IFN-γ-treated DC; 10 000 BEAS-2B cells were plated onto 24-well cell culture plates at 37°C with 5% CO2 until confluence to cell monolayer. DC were cultured separately in LHC-9 medium with human recombinant IL-17A (2ng/ml) and IFN-γ (1ng/ml) for 6 days and then added (10^6cells/ml/well) over the BEAS-2B layer. 24 hours after, monolayers were examined, photographed, then cells were fixed and a double TRAP/Hoechst staining was performed. Experiments were repeated twice.

TRAP/Hoechst staining

TRAP activity was assessed using the Leukocyte Acid Phosphatase kit (Sigma-Aldrich). Nuclear DNA was stained with a 10 µg/ml solution of Hoechst 33342 (Invitrogen H3570) for 30 min at room temperature. Cells are then washed and fixed with 1% formol. Culture and TRAP/hoechst pictures were analyzed using a Leica DMiRB microscope equipped with x40/0.30 NA or x40/0.55 NA objective lenses (Leica, Wetzlar, Germany) a Leica DC300F camera and the Leica FW400 software

3 Part III: DISCUSSION

3.1 Differential physiopathological roles of granulomas among species & diseases

3.1.1 Evolution of the granuloma role in vertebrates

Although granulomas were discovered and extensively studied since 200 years, their definitive functions in TB remain enigmatic [367]. Classically, they were considered as host-protective structures and their formation was regarded as a host beneficial strategy. In this context, granulomas are thought to contain the infection in a limited area of the body where immune response is activated against intracellular Mycobacteria, thus impairing their replication and avoiding their spread.

Molecular signals of the immune system regulate the organization of the granulomatous response. Working with human biopsies of TB patients, we documented an *in situ* expression of several cytokines (IL-17A, GM-CSF) and chemokines (CCL20, CCL2) as well as pro-survival proteins (BFL1). *In vitro*, we found that IL-17A induced the expression of CCL20, CCL2 and BFL1 human myeloid DCs. *In vitro*, IL-17A promotes DC survival dependently on BFL1, and fusion under the control of CCL20 and CCL2 dependent recruitment. Cell cultures containing IL-17A dependent MGCs were more potent in the killing of certain mycobacterial species. Altogether, our results provide new insights on the molecular mediators and mechanisms which may regulate the maintenance of human TB granulomas.

More recently, the classical protective function of granulomas was challenged by studies conducted in the model of zebrafish embryos infected with *M. marinum*. Findings in this model showed that granulomas may help to promote infection, rather than to control it [368] [369] [370]. An important advantage of zebrafish as a TB model is its optical transparency in early life allowing the visualization of living bacteria by real-time intravital imaging [370]. Using this model, the group of L. Ramakrishnan showed that during early stages of infection, granuloma serves to expand bacterial numbers and enhances their replication by recruitment and infection of new phagocytic cells [368]. Functionally, *M. marinum*-infected MPs of the nascent lesion promote the attraction of additional MPs recruited through rapid and continuous migration. Infected cells then die, and are phagocytosed by the newly arriving MPs which become infected. Newly infected MPs thus provide a new growth niche for bacilli, sustaining their continued proliferation. Early granuloma can therefore constitute a site for bacterial expansion [368]. In a subsequent study, the same group showed that ESAT-6 is released from *M. marinum*-infected MPs and induces

the secretion of MMP9 in neighboring epithelial cells [369] **(Fig. 17)**. MMP9 secretion facilitates the migration of uninfected MPs into the nascent granuloma, promoting their infection and leading to bacterial expansion [369]. MMP9 activity may result from its ability to degrade extracellular matrix components as well as to activate chemokines [188].

Figure 17: ESAT-6-mediated MMP9 induction in epithelial cells promotes phagocyte recruitment and infection in *M. marinum*-infected zebrafish embryos. This promotes mycobacterial dissemination and expansion. From ref [370].

In contrast to the zebrafish model, granulomas in humans are commonly regarded as protective structures. This concept is supported by several observations. First, in persons who did not die from TB, calcified granulomas were found : most of them being sterile while few others contains live Mycobacteria [371] indicating that these structures are efficiently involved in mycobacterial killing. Second, the blockade of TNF-α which leads to the reactivation of latent TB, results in granuloma breakdown and disintegration, along with mycobacterial dissemination [372]. These observations suggest that granulomas in humans are host-protective structures which counteract mycobacterial growth and limit the dissemination of the infection.

Therefore, the role of the granuloma is differentially understood in various hosts. However, can findings in *M. marinum*-infected zebrafish be extrapolated to human TB

disease? And are they relevant for the understanding of the role of human mycobacterium-induced granuloma? Actually, there are several differences between *M. marinum* infection in zebrafish embryos and TB in humans [373]: first, *M. marinum* is not *Mtb* and zebrafish have no lungs. Second, experimental infection in zebrafish model is by injection and not aerosol inhalation like in TB disease. Third, the immune system is probably immature in the embryos of zebrafish and the role of granuloma may change with the immune system development. Finally, granulomas in zebrafish larvae are formed exclusively by innate immune cells and are not under the control of adaptive activated T lymphocytes. The role of granulomas may be different in various groups of vertebrates: it appears negative in lower vertebrate (fish embryos) and positive in higher vertebrate (mammal adults). Does it result from the evolution of the vertebrate immune system facing to Mycobacteria between fish and mammals? Or does it come from the differential development of the immune system between embryo and adult?

The analysis of the evolution of the vertebrate adaptive immune system may allow a better understanding of these discrepancies in the future.

3.1.2 Contributions and limitations of the murine models to understand granulomatogenesis

We studied two granulomatous diseases: TB and pLCH. pLCH has no currently any experimental model and a major difficulty in the field of TB is the lack of a suitable animal model. Our studies on TB patient biopsies and human myeloid cells showed that CCL20 and CCL2 chemokines are expressed by both myeloid mono and multinucleated giant cells of the human TB granuloma. We demonstrated that these chemokines are involved in human myeloid cell clustering and fusion *in vitro*. Taken together, these data suggest an important role of CCL20 and CCL2 in myeloid cell recruitment and fusion within human TB granulomas.

The mouse was widely used as a TB model and has provided considerable contribution in our knowledge in TB granulomatogenesis. Indeed, most of cytokine, chemokine and cellular requirements for granuloma formation and maturation were provided by the murine model. However, there are several significant differences in the granulomatous response to *Mtb* in the lung between human and mice [172].

Human TB granulomas are highly organized suggesting a potential role of chemokines, which control cell migration and clustering, in the regulation of these structures. They contain a core of epithelioid MPs and MGCs and are surrounded by T cells. Human granulomas

progressively become devoid of blood vessels and hypoxic [172] and are characterized by necrosis and caseation during TB pathology.

In mouse, the architecture of the granuloma is less organized with diffuse cellular infiltration described as a loose collection of activated cells. Studies showed that chemokines have redundant roles in the granulomatous response in this animal **(Table VI)**. In addition to epithelioid MPs and lymphocytic clusters, elevated numbers of PMNs are present while MGCs are absent in murine granulomas. Necrosis and caseation are also rarely observed within these granulomas and these structures are relatively aerobic [172].

Studies conducted in *Mtb*-infected mice deficient for CCL2 and the CCL20 receptor, CCR6, showed that these deficiencies don't affect the adaptive granulomatous response to this pathogen and revealed that deficient mice clear Mycobacteria [266] [265]. Nevertheless, based on the fact that murine granulomas are loosely organized and don't contain MGC while those of humans are well-structured and contain such giant cells, CCL2 and CCL20 roles may be different in murine and human granulomas.

In conclusion, the mouse model does not reflect the full spectrum of human granuloma formation upon infection, thus presenting certain limitations in the understanding of the human granulomatogenesis in TB [374]. The murine model was certainly fruitful to understand the role of adaptive cytokines required for granulomatogenesis (e.g. IL-12, IFN-γ, GM-CSF…). However, the role of this animal model is questionable regarding the chemokine requirements of granuloma maintenance as well as concerning the mechanisms of MGC formation and functions.

3.1.3 Emergence of the role of granulomas in the chronic control of cancer cells

Actually, it becomes well admitted that the immune system forms an important barrier facing to tumor growth and progression. Interplay between immunity and tumors may result in the elimination of cancer cells, their escape or a continuous equilibrium between them and the immune system. Importantly, the anti-mycobacterial immune response is clinically used as a tumor treatment in some instance. Indeed, since the 70's, BCG-immunotherapy constitutes the optimal choice and the most potent treatment against invasive bladder cancer. This immunotherapy is based on several intravesical instillation of BCG (inside the bladder), and results in 70% response rate. However, dramatic consequences are observed in 30% of patients related to a hypo or hyper immune responses. Moreover, the exact molecular mechanisms of this therapy are largely unknown.

It is unknown if IL-17A and IFN-γ are involved in the activation of myeloid cells to become able to control and/or destroy cancer cells. However, it is possible that such stimulated myeloid cells become able to kill cancer cells or to suppress their proliferation. *In vitro*, we set up a co-culture system between DCs and BEAS-2B, a human a transformed human cell line immortalized by an Adenovirus12-SV40 hybrid virus. Using this system, we showed that IL-17A and IFN-γ-treated DCs with BEAS-2B induces the destruction of immortalized BEAS-2B cells, while untreated DCs were unable to mediate this effect. The anti-tumoral activity was effective in close contact with the effector cytotoxic DCs and therefore probably not mediated by a soluble death ligand, although the mechanism is not characterized.

In 2007, an elegant study by Koebel *et al.* demonstrated, for the first time, that cancer cells can be chronically controlled by granulomas including giant cells, thus underling an anti-tumoral granulomatous immune response [375]. After chemical carcinogen injection in mice, authors found both tumor-developing and tumor-free animals. Importantly, tumor-free mice were not really free but had latent dormant cancer cells contained by granulomatous structures of 2-8 mm size, including giant cells [375]. Tumor control in this model was a result of both increased apoptosis and decreased proliferation of cancer cells. However, when treated with an antibody cocktail depleting $CD4^+$ and $CD8^+$ cells and neutralizing IFN-γ, these mice develop sarcomas, thus demonstrating that adaptive immune system is required for this anti-tumoral granulomatous response. Several similarities exist between the anti-tumoral response in this mouse model and the anti-Mycobacterium granulomatous responses. Both contained latent (dormant) cells which can be controlled for decades in giant cell-associated granulomas but can be re-activated after immune suppression [376]. Moreover, the adaptive immunity is required for both response types. However, the role of IL-17A was not evaluated in this study. Neutralization of IL-17A in mouse models with such induced tumors is an important issue that should be investigated in the future.

In human patients with breast cancer, occult cancer cells can be maintained in a dormant state [377] and a recent study described that long-term dormancy of breast cancer cells is maintained by small “growth-restricted micrometastasis” [378]. However, it is not clear if a granulomatous response is involved in the control of cancer cells in such patients. In the future, it would be intriguing to characterize the anti-tumoral granulomatous response in humans. *in situ* investigation of an IL-17A-dependent anti-tumoral granulomatous response in human biopsies will clarify if IL-17A is involved in such response.

3.2 IL-17A-induced genetic program promotes granulomatogenesis

3.2.1 Is IL-17A a constitutive molecular player in granulomatogenesis?

Granuloma formation is driven by several cytokines which can positively or negatively regulate this process **(Table V)**. We documented an *in situ* expression of IL-17A within both human TB and pLCH granuloma. In TB, we found that IL-17A is mostly expressed by $CD3^+$ T cells which surround the epithelioid core. In contrast, IL-17A expression was restricted to $CD1a^+$ DC and MGCs in pLCH granulomas. Our results suggest that IL-17A may induce granuloma maintenance by promoting myeloid cell survival, clustering and fusion.

IL-17A expression in granulomas was documented in several human granulomatous diseases including crohn's disease [379], childhood LCH [306] and very recently sarcoidosis [380] [381] and Blau syndrome [382]. IL-17A was initially considered as a T cell cytokine produced by Th17 lymphocytes. However, recent studies showed that this cytokine is also expressed by a wide range of myeloid cells including DCs, MPs and PMNs [306] [321]. In the context of granulomatous diseases, IL-17A expression was documented in both lymphoid and myeloid cells. IL-17A was expressed by Th17 cells as well as by myeloid epithelioid cells and MGCs in the granulomas of crohn's disease [379] sarcoidosis [380] [381] and Blau syndrome [382] patients, while it was exclusively expressed by myeloid DCs and MGCs in childhood LCH granulomas [306]

Our results suggesting a role of IL-17A in promoting granuloma maintenance are in line with those recently reported in the murine model of mycobacterial infection. In this model, IL-17A positively regulates mature granuloma formation and maintenance [144] [259]. In the absence of this cytokine, mice infected with BCG were able to form nascent but not mature granulomas characterized by an impaired cellular accumulation and organization [259].More recent findings underline also a positive correlation between IL-17A and the formation of large granulomatous lesions in a bovine TB model [383].

A growing body of evidences suggests that IL-17A plays also an essential role in granuloma formation and maintenance in other granulomatous disorders. In murine schistosomiasis, IL-17A is directly associated with the severity of the granulomatous inflammation. Indeed, the development of severe and large schistosoma -induced granulomas correlated with high levels of IL-17A and mice injected with this cytokine showed enhanced granulomatous inflammation [384] [385]. In contrast, reduced size of granulomas was associated with the production of lower amounts of IL-17A [386]. Moreover, antibody-mediated IL-17A neutralization led to a significant reduction of the granuloma size [384]

[385]. IL-17A deficiency alters the establishment of granuloma in mice infected with *listeria monocytogenes* as demonstrated by the disorganized granulomatous structures with dispersed cell organization compared with WT animals [387]. In the same way, inhibition of Th17 cell development reduced the granulomatous response in a murine model of *Propionibacterium acnes*-induced granuloma in the liver while enhanced Th17 cell differentiation exacerbated such response [388]. IL-17A plays also a role in granuloma formation in non infectious granulomatous diseases. For example, IL-17A was proposed as a central player in granuloma formation in the murine model of anti-neutrophil cytoplasmic antibodies (ANCA)-induced systemic vasculitis [389].

Overall, these data showed that IL-17A is now documented in a variety of granulomatous disorders in both human and animals, thus supporting the evidence that this cytokine participates in the regulation of granuloma formation and maintenance. An important remaining issue in our work is to determine the nature of the T cell subpopulation that produces IL-17A in human TB granulomas: are they Th17 cells or other IL-17A producing cells such as γδ T cells as described in murine Mycobacterium-induced granulomas [259]? Further *in situ* immunohistofluorescence investigations will clarify this question in the future. Another important matter is to go on investigating IL-17A expression in additional granulomatous diseases. For example, the literature reports the presence of granulomas during infections with the filamentous, but not the yeast, form of fungi, and recent studies showed that the filamentous form triggers the polarization of Th17 cells *in vitro* while the yeast form does not [339]. It would be therefore interesting to investigate the expression and the role of IL-17A in filamentous fungal granulomas. Finally it is important to characterize all the molecular events which explain why IL-17A is a constitutive factor in granulomatogenesis.

3.2.2 The role of IL-17A-induced CCL20 and CCL2 in granulomatogenesis

The recruitment of a variety of immune cell types during granuloma formation is essentially orchestrated by an intense local production of chemokines involved in the regulation of cell trafficking and migration. We focused on the role of two chemokines: CCL20 and CCL2. CCL20 is the only identified chemokine which binds the chemokine receptor CCR6 while CCL2 is one of the several ligands of CCR2. CCL20 induces chemoattraction of immature $CCR6^+$ DCs and subpopulations of effector/memory lymphocytes including IL-17A-producing lymphocytes. CCL2 regulates migration and infiltration of several immune cells, especially $CCR2^+$ monocytes/MPs and T cells.

Our results demonstrate the rapid induction of CCL20 and CCL2 chemokines by human DCs after treatment with IL-17A. While CCL2 was continually produced in large quantities until the 12th day of treatment, CCL20 was transiently produced in the initial phase with lower amounts. This demonstration may explain the correlations that we observed in two kinds of granuloma. Indeed, IL-17A expressing granulomas in TB and pLCH showed a simultaneous expression of both CCL20 and CCL2 chemokines by their myeloid cells. We also detected large amounts of circulating CCL2 in the serum of patients with LCH whereas CCL20 was undetectable. CCL20 and CCL2 chemokines may play important roles in the recruitment of myeloid cells to the granuloma, thereby promoting its formation and maintaining its integrity.
Few reports demonstrate a direct effect of IL-17A on the production of CCL2 and CCL20. Previously, it was shown that this cytokine up-regulates the expression of CCL20 and CCL2 in human renal and airway epithelial cells, respectively [390] [391]. More recently, a study reports that IL-17A treatment of human MPs induces the production of CCL2 and CCL20 by these cells *in vitro* [392].

Several studies underline a correlation between IL-17A, CCL20 and/or CCL2 and granuloma formation, maturation and/or size. A recent report in mouse showed that following intratracheal infection with BCG, CCL20 was induced during the early innate stage of infection [265] maybe in agreement with the IL-17A production by γδ T cells [259]. In humans, CCL20 expression was detected by the myeloid mono and multinucleated giant cells of both childhood LCH [393] and sarcoid [394] granulomas in which IL-17A expression was also documented in separated studies [306] [380]. In LCH, CCL20 may cause the recruitment and retention of additional lesional CCR6^{+} DCs [393] while in sarcoidosis, it may essentially drive the recruitment of CCR6^{+} Th17 cells from the blood toward the granuloma [380].

In animals, increase in granuloma size during murine schistosomiasis was associated with increased CCL2 expression in granuloma MPs and higher levels of IL-17A in granuloma cells compared to those of control animals [395]. Upon mycobacterial infection, CCL2 levels were found reduced in IL-17A-deficient mice showing impaired granuloma formation and maturation [259]. In humans, a recent study suggests a role for CCL2 in both establishment of latency and maintenance of the integrity of granulomas in asymptomatic individuals with latent TB [396]. In addition, a recent study suggests that CCL2 forms an important mediator in recruiting inflammatory CCR2^{+} cells during pulmonary sarcoidosis [397].

IL-17A-induced CCL20 and CCL2 may be involved in two essential phases of granuloma formation: initiation and maintenance. In mycobacterium-infected mice, the early IL-17A secretion [259] may rapidly induce CCL20 secretion by lung resident DCs, thereby

recruiting nearby $CCR6^+$ lung DCs to initiate early granuloma formation. The IL-17A-mediated expression of CCL2 becomes then rapidly massive and ensures the recruitment of peripheral blood monocytes. These cells differentiate *in situ* in MPs or DCs according to the local cytokine environment to promote bacterial containment. BCG-infected mice which over-express CCL2 by type-II alveolar epithelial cells showed higher bacterial clearance, a constitutively increased mononuclear phagocyte subset accumulation in their lungs and a rapid and accelerated induction and resolution of lung granuloma, compared to WT animals [398].

Overall, through CCL20 and CCL2 chemokines, the host is able to immediately attract local available tissue myeloid cells around a pathogen, such as *Mtb*, via CCL20 and then induces massive recruitment of peripheral blood cells via CCL2. These effects could promote granuloma initiation and maintenance.

3.2.3 The role of IL-17A-induced CCL20 and CCL2 in cell-cell fusion

Chemotaxis and cytoskeleton rearrangement direct cell clustering and fusion [276]. Our *in vitro* experiments showed that neutralizing antibodies against CCL20 or CCL2 efficiently abrogated the fusion of IL-17A-treated DCs. While anti-CCL20 antibodies block DC clustering and fusion without affecting their rounded shape, CCL2 neutralization also induces a morphological change in these cells. Indeed, anti-CCL2 antibodies convert the rounded DCs into elongated fusiform cells. The morphological change observed with anti-CCL2 revealed that this chemokine is involved in the regulation of the cell cytoskeleton to achieve fusion and MGC formation. These results underline the mandatory role of CCL20 and CCL2 in the chemotaxis for DC-derived MGC formation and revealed an additional role of CCL2 in the regulation of DC cytoskeleton.

CCL2 is already known to be pivotal in chemotaxis required for myeloid cell fusion. It is involved in both FBGC [399] and OC [287] formation. Indeed, Kiryakides *et al.* demonstrated that after subcutaneous foreign body (biomaterial) implantation, mice lacking CCL2 show a marked impairment in FBGC formation due to compromised MP fusion compared to their wild-type counterparts [399]. *In vitro*, authors showed that a CCL2 inhibitory peptide or an anti-CCL2 antibody reduces FBGC formation from peripheral human blood monocytes. In osteoclastogenesis, although CCL2 alone is unable to induce OC formation, this chemokine is required for the fusion of human [287] [288] [289] mouse [290] and rat [400] myeloid cells into giant OCs. In human myeloid cells, RANKL/RANK signaling activates the transcription factor NFATc1 (nuclear factor of activated T-cells, cytoplasmic 1)

resulting in CCL2 expression [287]. Human monocyte fusion into OCs was inhibited by cyclosporin A, which blocks NFATc1, and addition of CCL2 after this pharmacological blockade restored the formation of multinucleated cells although they were unable to resorb bone [287]. Human monocytes treated with M-CSF and CCL2 fused and form giant cells which express several OC markers [288]. OC formation was significantly inhibited in cells derived from CCL2-deficient mice and this inhibition was restored by addition of recombinant CCL2 [290].

The role of CCL20 in cell-cell fusion is less documented. However, *in vitro*, recombinant human CCL20 significantly increased the number of multinucleated OCs, and blocking anti-CCL20 antibodies inhibits this pro-osteoclastogenic effect [401].

CCL2 is already known to be involved in cytoskeleton rearrangement even in the absence of cell fusion. Antibody-mediated CCL2 neutralization induces remarkable changes in the morphology and size of human monocyte-derived MPs infected with HIV, reflecting important changes in their cytoskeleton organization [402]. However, this morphological change is different to what we see in DCs as it results in an increase in cell size. This suggests that morphological change under the control of CCL2 may depend on the cell type. CCL2-mediated effects on cytoskeleton are also required to cell-cell fusion. Indeed, the defective fusion of CCL2-null MPs in FBGCs was associated with their inability to undergo cytoskeletal remodeling, indicating a role of this chemokine in the regulation of this process [403] [404].

Overall, CCL2 and CCL20 regulate essential features of cell-cell fusion to form giant cells. However, we found that DCs cultured with both CCL20 and CCL2 in the absence of IL-17A did not undergo cell fusion (data not shown). This indicates that these chemokines are necessary but not sufficient for the IL-17A-dependent fusion process. Consequently, IL-17A induces additional unknown fusogenic molecules required to achieve cell fusion and MGC formation. According to our transcriptomic data, a potential candidate is DC-STAMP. The mRNA of this molecule, known to regulate both OC and FBGC formation [291], is highly expressed in IL-17A-treated DC while absent from untreated cells. DC-STAMP may thus forms a common molecule necessary for multinucleation induced by different exogenous stimuli. However, validation of this hypothesis requires additional functional analysis and blocking assays. DC-STAMP is a cell surface seven-transmembrane protein, thereby resembling chemokine receptor structures. Although the ligand for DC-STAMP is unknown, it was proposed that CCL2 may serve as a DC-STAMP ligand [405]. In this hypothesis, IL-

17A may simultaneously induce both DC-STAMP and its potential ligand CCL2 in DCs, thereby potentiating their fusion into MGCs.

3.2.4 The role of IL-17A-induced BFL1 in myeloid cell maintenance

In latent TB, granulomas persist for several decades reflecting the long-term maintenance of these structures. We were precisely interested in the maintenance of myeloid granuloma cells: are their maintenance is a result of a local proliferation and/or a long term survival?

We found that IL-17A-treated DCs did not proliferate *in vitro*. However, while unstimulated DCs did not survive more than few days, the number of IL-17A-treated DCs was stabilized at day 12, thus demonstrating that IL-17A activates long-term survival pathways in these cells. Our *in vitro* results showed that IL-17A induced a rapid NF-κB activation (revealed by the nuclear translocation of the p65/RelA subunit) which in turn stimulates the expression of the pro-survival protein BFL1. This IL-17A-dependent BFL1 induction in DCs was blocked by an NF-κB inhibitor. Finally, statistical analysis showed that BFL1 expression positively correlates with the survival of IL-17A-treated DCs.

IL-17A signaling is known to induce NF-κB activation [309]. Importantly, the promoter of the gene encoding BFL1 possesses a p65 / RelA responsive element which positively regulates BFL1 expression [406]. Therefore, in our model of human myeloid DCs, IL-17A-mediated nuclear translocation of NF-κB provides the basis for BFL1 up-regulation.

Several reports showed that the capacity of cell proliferation within granulomas is very limited. For example, in LCH granulomas, the proliferation marker Ki-67 was found in less than 3% of lesional DCs [407]. *In situ* [^{3}H]-thymidine labeling of sarcoid granuloma revealed that proliferation and cell division is rare in granuloma myeloid/epithelioid cells and absent in their derived-MGCs [277]. In the same way, during mycobacterial infections, BrdU incorporation assay showed no differences in MP proliferation between BCG-infected and uninfected mice during the first 2 weeks of granuloma development [174].

Regarding this reduced ability of cell proliferation and clonal expansion, inhibition of apoptosis of granuloma cells may form an important factor which prevents granuloma disruption and maintains the integrity of these structures. In this context, it was shown that granuloma cells express several and pro-survival proteins. For example, myeloid cells of the *Mtb*-induced granuloma express several pro-survival proteins of the TNF receptor-associated factor family [182], increased expression of the pro-survival protein BCL-2 and reduced expression of the anti-survival protein BAX [187]. Similarly, the pro-survival protein AIM

(apoptosis inhibitor expressed by macrophages) was found expressed in the murine MPs at the peripheral area of BCG-induced liver granulomas [408]. Apoptotic events are also reduced within sarcoid granulomas, and myeloid cells within these structures specifically express the cyclin-dependent kinase inhibitor $p21^{Waf1}$ [409]. Foreign body (silica) chronic granulomas were also highly resistant to apoptosis and showed a dramatic up-regulation in BCL-2 expression within granulomas myeloid MPs [410].

Overall, the long lifespan of myeloid granuloma cells is probably due to the activation of survival pathways. IL-17A may be involved in myeloid cell maintenance by inducing the BFL1, a well known pro-survival protein belonging to the BCL-2 family.

3.2.5 Multiple stimuli for NF-κB -dependent activation of BFL1 in granuloma, *in vivo*

In addition to IL-17A, a large number of diverse stimuli lead to the activation of the NF-κB transcription factor, and may subsequently result in an NF-κB -dependent activation of BFL1. *In situ*, we found that BFL1 is strongly expressed by the myeloid mono and multinucleated giant cells of both LCH and TB granuloma in which IL-17A is also detected. This provides a correlation between IL-17A and BFL1 expressions in these structures. However, *in vitro*, we showed that infection of human DCs with BCG or *M. avium* induced BFL1 expression by these cells (data not shown). DC infection by these Mycobacteria did not result in IL-17A production (data not shown), indicating that they induce BFL1 independently of this cytokine.

As cited in the introduction, Mycobacteria are potent inducers of BCL2 family members including BFL1 in myeloid cells **(see 1.4.2.2)**. In THP-1 cells infected with *Mtb* H37Rv, *BCL2A1* gene encoding BFL1 was also activated in a NF-κB dependent manner [411]. In addition, some cytokines involved in the regulation of the TB granuloma, such as TNF-α, are potent physiological inducers of NF-κB [412]. TNF-α-mediated NF-κB activation led to the induction of BFL1 in several human cell lines [413] [414] and NF-κB inhibition results in reduced BFL1 expression and impaired survival in human MPs [415].

Therefore in addition to IL-17A, Mycobacteria and other granuloma cytokines can induce NF-κB -dependent activation of BFL1. Consequently, myeloid cells in TB granuloma may have several available molecular signals to induce this pro-survival protein which may favor long-term survival.

3.3 The IL-17A-induced Giant Myeloid Inflammatory Cell (GMIC)

3.3.1 GMIC: a novel multinucleated cell type of the immune system characterized by MMP12 & CTSD co-expression

OC is the most well-characterized myeloid giant cell type. Recent studies used transcriptomic analysis to compare the genetic profile of these cells to monocytes and DCs [416]. In the same way, we compare IL-17A-dependent MGCs to monocytes, DCs and OCs by transcriptional profiling using microarrays. In addition to a common core shared by these myeloid cells, we identified transcriptional signatures that are specific to each cell type **(Fig. 18)**. Monocytes dramatically differ from all other cell types. IL-17A treatment of DCs, which leads to MGC formation, results in the induction of about 1000 new genes. This indicates that IL-17A induces a novel genetic program in DCs and underlines that IL-17A-dependent MGCs are different from DCs. Importantly, the genetic profile of IL-17A-induced MGCs shows similarities with that of DC-derived OCs, and MGCs express mRNAs of characteristic OC markers such as TRAP, CTSK and MMP9. However, further investigations at the protein level showed that IL-17A-induced MGCs co-express two proteolytic enzymes, MMP12 and CTSD, which were respectively absent and slightly expressed in DC-derived OCs. Moreover, *in vitro*, OCs and IL-17A-induced MGCs showed differential mechanisms of initial cell clustering mandatory for their fusion. Indeed, video microscopy (time lapse) experiments showed that OC formation occurs through a cell by cell fusion process which progressively increases the giant cell size. In contrast, the IL-17A-induced MGC formation requires an initial clustering of cells which subsequently undergo a simultaneous cell fusion process. Finally, while OCs are defined as bone-resorbing giant cells, IL-17A-induced MGCs were functionally unable to mediate bone resorption activities.

Comparative transcriptomic studies revealed a closer molecular profile between DCs and OCs than between monocytes and OCs, showing that OC formation can be more efficiently induced from DCs than monocytes [416] **(Fig. 18)** . In the IL-17A-dependent pathway of cell fusion, both DCs and monocytes can fuse into MGCs, but monocyte fusion requires additional signal provided by GM-CSF [306] **(Fig. 19)**. As DC differentiation also requires GM-CSF, it can be assumed that the genetic program induced by this cytokine is mandatory for the myeloid cell fusion in response to IL-17A. However, the exact role of GM-CSF in this process is currently unclear and requires future analysis of the genetic profile of GM-CSF +/- IL-17A-treated monocytes.

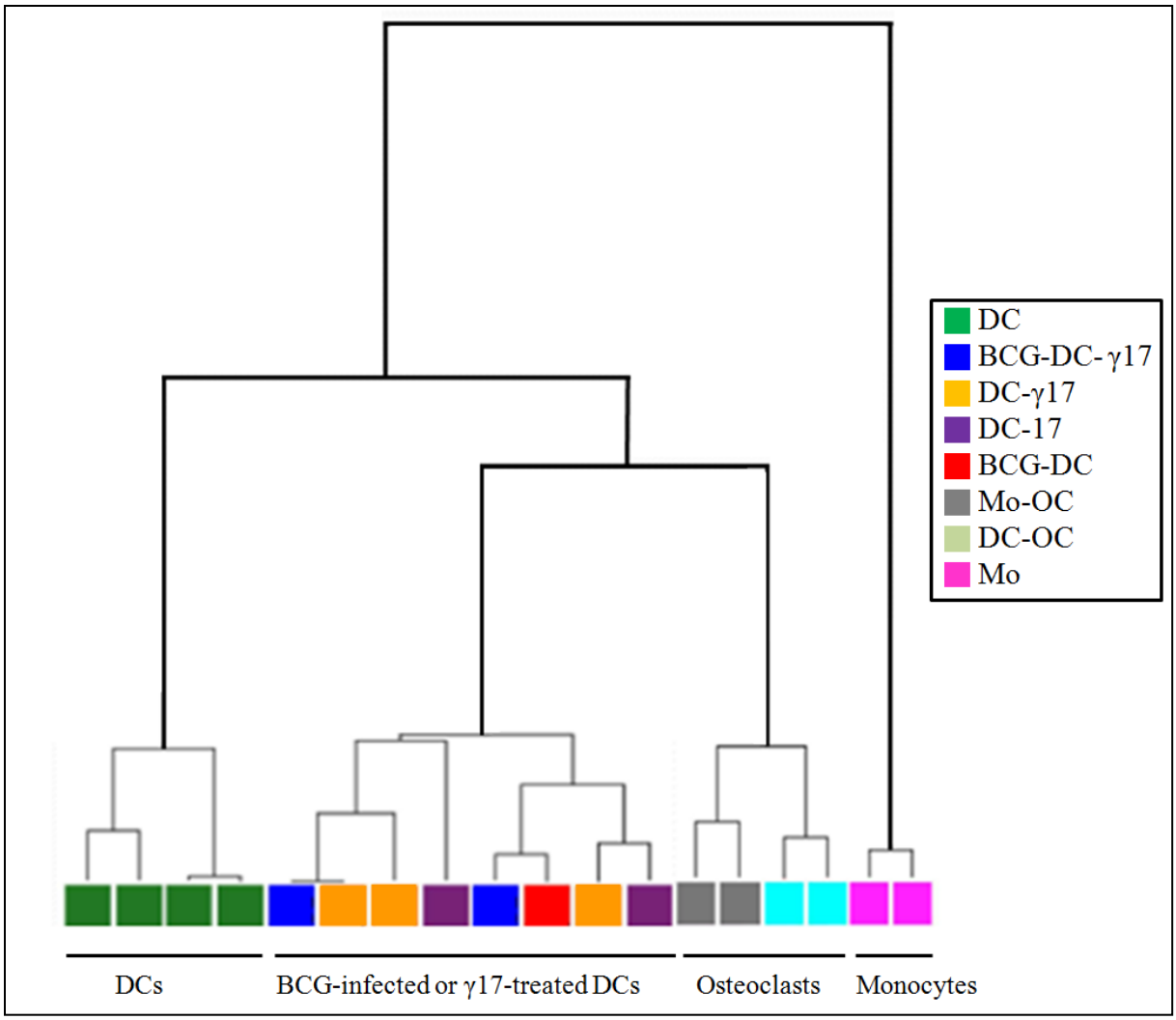

Figure 18: Dendrogram (Pearson correlation) representing the hierarchical clustering of the transcriptional distance between monocytes, DCs, OCs, BCG-infected DCs and IL-17A+/- IFN-γ-treated DCs.

Mo: monocyte; Mo-OC: Mo-derived OC; DC-OC: DC-derived OC; DC-17: IL-17A-treated DC; DC-γ17: IL-17A+IFN-γ-treated DC, BCG-DC: BCG-infected DCs.

Although both OCs and IL-17A-induced MGCs could originate from the same myeloid cells (DCs and monocytes), these giant cells are different. While they have several similarities, we showed that they differentially express the MMP12 and CTSD proteolytic enzymes and develop differential functional activities. These results establish IL-17A-dependent MGCs as a novel type of multinucleated cells of the immune system that we called Giant Myeloid Inflammatory Cells (GMICs). The newly characterized GMICs further increase the already known high degree of plasticity in the world of the mono and multinucleated giant myeloid cells **(Fig. 19)**.

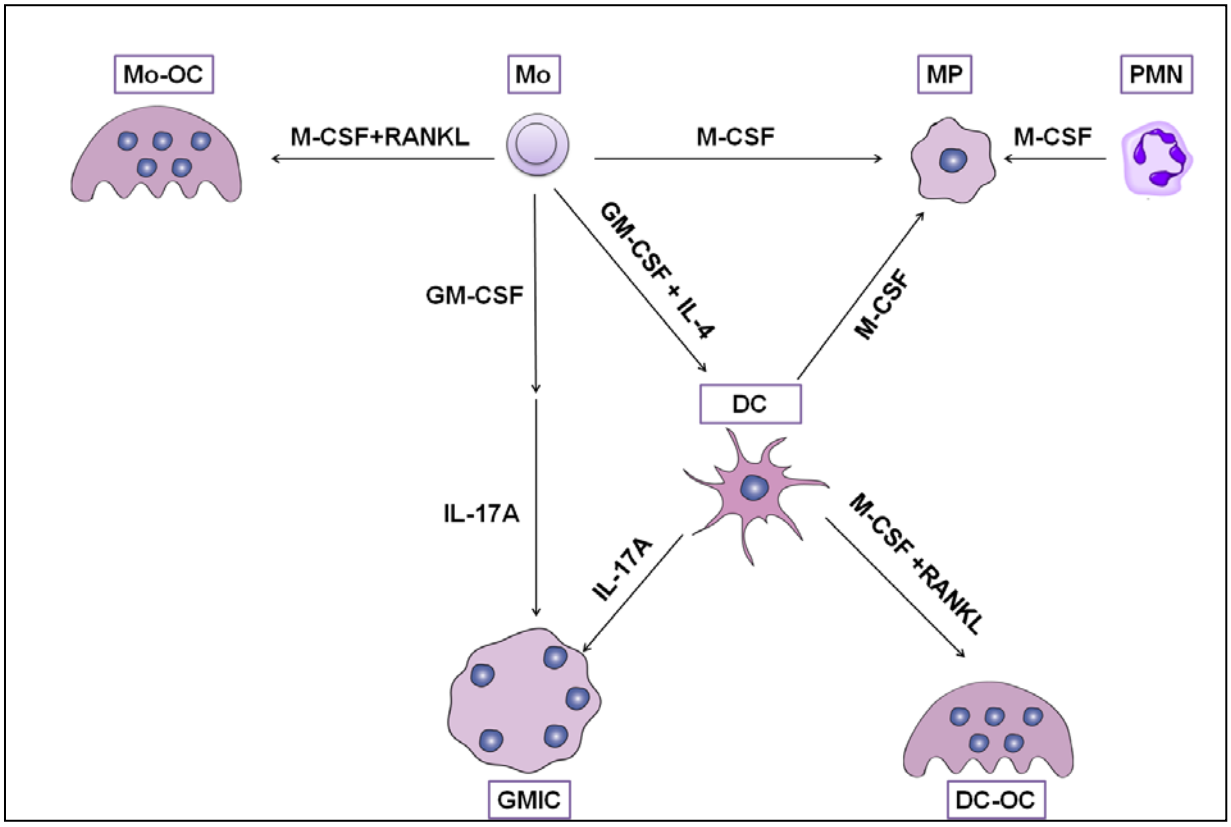

Figure 19: Myeloid cell plasticity. Details in the text – **(see 3.3.1)**

3.3.2 Comparison of GMICs with the giant cells of LCH and TB granulomas

The exact origin and role of giant cells within granulomas are poorly understood. Therefore an important issue is the *in vivo* relevance of GMIC phenotype and functions. Our results showed that IL-17A treatment of DCs induces a mixed phenotype which associates markers of both MP (CD68) and DC (CD1a) in these cells until day 8. At day 12, when the number of IL-17A-dependent GMIC is stabilized, CD1a marker has been down-regulated, while CD68 remained expressed. Importantly, we also found that BCG or *M. avium* infection induces the fusion of human DCs into giant cells *in vitro*. Strikingly, BCG-induced giant cells were very similar to GMICs at the transcriptomic level and express the mRNA of MMP12 and CTSD proteases. *In situ*, we found that both enzymes were co-expressed by the myeloid mono and multinucleated giant cells in pLCH while only CTSD was expressed by these cells in TB granuloma.

Previous studies described the giant cells in LCH granulomas as OC-like cells as they express characteristic OC markers [417]. However, the fact that these cells co-express also CTSD and MMP12 in pLCH granulomas is in favor of their similarities with GMICs. CTSD expression by these cells was not reported previously. Nevertheless, MMP12 was already

documented in childhood LCH inside the myeloid cells and its expression was associated with a bad prognosis, suggesting that this protease plays a detrimental role in this disease [418].

In TB, both epithelioid cells and MGCs were historically considered as MP derivatives [170]. This is contradictory with the fact that GMICs originate from monocytes or DCs. However, this traditional suggestion was never been formally demonstrated *in vivo*. In addition, within murine chronic *Mtb* granulomas, myeloid cells highly express characteristic DC markers such as CD11b, CD11c, and DEC205 [182]. In terms of phenotype, epithelioid cells are different from the canonical monocytes, MPs or DCs, because they showed a mixed MP-DC phenotype. Interestingly, *in vitro* control of *Mtb* replication is achieved by monocytes or MPs provided they were treated with GM-CSF [419] [228] as well as with DC, generated from monocytes in the presence of GM-CSF and IL-4 [116]. Recent report confirmed that M-CSF, the cytokine mostly used for canonical MP differentiation, *in vitro*, was highly counterproductive to control virulent *Mtb* contrary to GM-CSF. As cited above, GM-CSF conditioned the monocytes to survive and to respond to IL-17A, similarly as DCs. However, M-CSF could not replace GM-CSF for these effects [306]. We therefore suggest that the biology of epithelioid myeloid cells in TB granuloma, seems closer related to DCs or GM-CSF-treated monocytes than to monocytes or canonical MPs. This is supported by the *in vitro* ability of these cells to control *Mtb* growth and to undergo cell fusion in the presence of IL-17A expressed in TB granuloma. It can be therefore suggested that giant cells of TB granuloma may result from the fusion of DCs or GM-CSF-treated monocytes as observed for IL-17A-dependent GMICs, *in vitro*. The fact that TB granulomas highly express IFN-γ and GM-CSF [225], which positively impact GMIC formation, strengthens this hypothesis. As previously cited, both IFN-γ and GM-CSF inhibits osteoclastogenesis **(Table VII)**, thus weakening the possibility of a link between TB giant cells and RANKL-induced cell fusion.

CTSD expression was previously reported in the granuloma myeloid cells of *Mtb*-infected mice [195]. We documented the expression of this protease in the giant cells of human TB granuloma, adding an argument on their similarity with GMICs. However, we failed to detect MMP12 in these giant cells. This suggests two hypotheses: first, giant cells of the TB granulomas share strong similarities with GMICs but are different from them; second, as MMP12 mRNA was expressed upon BCG infection in human DCs *in vitro*, pathogenic *Mtb* may specifically inhibit the expression of this protease. This second hypothesis is attractive because MMP12 is a bactericidal molecule [420] **(see 3.3.3)**. It would be interesting to study MMP12 expression and regulation upon *Mtb* infection in GMICs.

In conclusion, giant cells in LCH granuloma possess several GMIC characteristics while this is questionable in the case of TB giant cells due to their lack of MMP12 expression. In the future, it would be interesting to compare the genetic profile of the giant cells of LCH and TB granulomas with that of IL-17A-dependent GMICs. This can be done through comparative transcriptomic analysis after giant cell isolation from granulomas by laser micro-dissection, a technique used to isolate individual cells from tissue sections

3.3.3 Microbicidal role of GMIC against Mycobacteria, *in vitro*

In humans, TB granulomas with giant cells are thought to control mycobacterial growth, thereby playing a protective role. In human DC, transcriptomic data showed that IL-17A modulates the expression of molecules implicated in intracellular vesicle trafficking and vacuole acidification. It also regulates the expression of oxidative stress molecules and exacerbates NADPH oxidase activity. *In vitro* studies showed that IL-17A-treated DCs kept classical DC functions such as phagocytosis, TRAIL-mediated cytotoxicity and allostimulatory properties. IFN-γ, which potentiates the IL-17A-dependent fusion of DCs, does not change the transcriptome induced by IL-17A, and would therefore act as a post-transcriptional modulator. Regarding these features, we asked if IL-17A and IFN-γ-treated DCs and their derived GMICs may play a bactericidal role facing to two different mycobacterium strains, *M. avium* and BCG. We found that bacilli of both strains were more efficiently controlled by IL-17A and IFN-γ-treated DCs than by untreated DCs. Stimulation with CD40L result in a most potent killing of *M. avium* in both untreated and IL-17A and IFN-γ-treated DCs. In contrast BCG bacilli grow in CD40L-stimulated cultures of DCs and this effect was potentiated by IL-17A and IFN-γ cytokines. Electronic microscopy confirms this finding by showing that BCG bacilli divide and replicate within CD40L-stimulated cells while this was not observed in other conditions.

Bacterial killing occurs through several microbicidal mechanisms, including protease activities. An elegant study showed that MMP12 is able to kill bacteria within murine MPs, thereby directly contributing to their antimicrobial properties [420]. Authors demonstrated that mice lacking MMP12 exhibit impaired bacterial clearance and increased mortality when challenged with bacteria. Functionally, after bacterial ingestion, MMP12 is mobilized to MP phagolysosomes where it adheres to bacterial cell walls and disrupts cellular membranes resulting in bacterial death. In this way, IL-17A-mediated up-regulation of MMP12 may play protective roles. However, the bactericidal activity of MMP12 was demonstrated facing to both $Gram^+$ and $Gram^-$ bacteria, while it is unknown if it may exert a similar effect against

Mycobacteria, characterized by their unique resistant cell wall. However, if this is the case, it can be assumed that MMP12 is an important player against BCG and *M. avium*, and efficiently contribute in their killing within IL-17A and IFN-γ -treated DCs and their derived GMICs. This can be verified through the use of selective MMP12 inhibitors in these infected cells, followed by colony-forming unit (CFU) studies to evaluate their killing abilities in the absence of this protease. It would be also interesting to evaluate MMP12 expression in CD40L-stimulated cultures in which we found that BCG, instead of being killed, showed a striking strong replication. As discussed above, *Mtb* may potentially inhibit MMP12 expression to avoid its destructive effects, and this must be verified by investigating if this protease is expressed or not by *Mtb*-infected myeloid cells treated with IL-17A and IFN-γ

CTSD may be also involved in the microbicidal activities of GMICs. CTSD is a lysosomal aspartyl protease which is essentially involved in the proteolytic activity within acidic compartments. Inhibition of CTSD in human monocyte-derived MPs led to enhanced replication of virulent *Mtb* in these cells, underlying the important role of this protease in restricting intracellular *Mtb* growth [421]. In mycobacterium-infected murine MPs, CTSD plays a major role in the processing and presentation of a mycobacterial antigen 85B epitope [422]. Inhibition of CTSD synthesis using RNA interference resulted in a marked decrease in the presentation of this process, indicating that CTSD take part in microbial degradation within phagolysosomes.

In addition to MMP12 and CTSD, IL-17A up-regulates the mRNA levels of other destructive enzymes including NADPH oxidase and TRAP. *In vitro*, IL-17A and IFN-γ-treatment potentiates NADPH oxidase activity and TRAP expression. As previously noted, NADPH oxidase may play a protective role against *Mtb* infection [212]. The knockdown of $gp91^{phox}$/NOX2 subunit of this enzyme inhibited the antimicrobial activity against viable *Mtb* in human MPs through the modulation of the expression of the antimicrobial peptide cathelicidin [423]. TRAP is expressed in human OCs, activated MPs [424], and DCs [425]. It has two distinct enzymatic functions: a phosphatase activity required for bone resorption and a catalyzing activity required for the production of oxygen radicals at neutral pH. Indeed, this enzyme possesses two isoforms: TRAP-5a, expressed in MPs and DCs, which is involved in bacterial killing, and TRAP-5b, expressed in the OC, which contributes to the fragmentation of bone matrix components [426] [427].Transgenic mice that overexpress TRAP exhibit osteoporosis and MPs from these mice produce more oxygen radicals (ROI) and showed increased bactericidal capacity [428]. The tests we used did not distinguish the two isoforms of TRAP-5, but it is likely that the significant increase in expression of TRAP activity, we

have highlighted in GMICs, is more related to TRAP-5a. It would be interesting to complement these results by a specific study of these isoforms of TRAP [427] and then, depending on the results, check if this enzyme is involved in the microbicidal activities of GMICs through blocking assays.

IL-17A and IFN-γ-treatment as well as BCG or *M. avium* infection of human DCs induces the formation of giant cells. However, Mycobacterium-infected DCs acquire the ability to efficiently kill the bacilli when treated by IL-17A and IFN-γ. This suggests that cytokine treatment rather than the presence of giant cells is important to kill Mycobacteria. Nevertheless, a previous report showed that multinucleation is important for the restriction of mycobacterial growth through a physical sequestration which may limit their cell to cell spread [429]. To investigate if multinucleation is required for mycobacterial killing, mycobacterium-infected DCs can be treated with IL-17A and IFN-γ along with fusion inhibitor molecules such as anti-CCL20 or CCL2 antibodies. The comparison of the mycobacterial growth in such GMIC-free cultures with that of GMIC-containing cultures will answer this question.

Finally, as we found that CD40L signaling promotes BCG growth within GMICs, it would be interesting to repeat this experiment using virulent *Mtb* to evaluate if, as BCG, CD40L activation stimulates *Mtb* replication in GMICs. This may identify a new critical point in the interaction between pathogenic Mycobacteria and the human immune system effectors. In TB, the specific structure of the granuloma regionalizes the expression of the CD40L signal in the periphery on activated T lymphocytes far from the *Mtb*-enriched core of myeloid cells. In the hypothesis that CD40L signaling promotes *Mtb* replication, such specific granuloma structure may result from an adaptation of the human immune system to prevent *Mtb* growth as long as bacteria are captured in the myeloid cells. This may also explain why it is crucial to maintain granuloma structure to prevent the development of active TB

3.3.4 The destructive role of GMIC against human broncho-epithelial cells

Although granulomas may play a protective role by containing infectious agents (e.g. *Mtb*), these structure also destroy the host tissues were they are embedded (e.g. lungs). Moreover, in granulomatous diseases such as pLCH in which no infectious agents were identified, granulomas play only destructive roles without any apparent benefice for the host. In this way, granulomas may form an immunopathological factor which promotes severe tissue destruction. We found that IL-17A and IFN-γ-treated DCs and their derived GMICs play aggressive roles as reflected by their ability to destroy a human bronchial epithelial cell

line (BEAS-2B). GMIC proteases such as MMP12 and CTSD may be potentially involved in such destructive activities

MMP12 can play important pathological roles in the destruction of the pulmonary tissue. The main substrate of MMP12 is elastin [430], a major component which ensures the elasticity of the pulmonary tissue. MMP12 is also involved in the degradation of other extracellular matrix proteins including type IV collagen and gelatin as well as non-matrix proteins such as myelin basic protein [431]. This protease was found markedly increased in sputum of patients chronic obstructive pulmonary disease (COPD) [432] and mice deficient for MMP12 were resistant to emphysema, a form of COPD [433]. Although we did not detect MMP12 expression in TB granuloma, this protease was expressed in pLCH myeloid cells. Others also reported a high MMP12 expression in the myeloid cells of LCH [418] and sarcoid [434] granulomas and underlined its correlation with the severity of these lung diseases. Previously, our group showed that MMP12 is tightly regulated at both transcriptional and post-transcriptional levels in DCs. IL-17A induces the accumulation of inactive MMP12 in DCs while cleavage of this inactive form in active MMP12 requires the addition of IFN-γ. Moreover, MMP12 extracellular secretion requires the presence of a danger signal such as the TLR4 agonist, LPS [306]. IL-17A and IFN-γ are expressed in both sarcoid and LCH granulomas [380] [435] [306] [436]. However, the presence of a pathogen which delivers danger signals to facilitate MMP12 release by myeloid cells is not documented in these diseases. Further work is needed to clarify LCH and sarcoidosis myeloid cells secrete MMP12 and how this process is regulated.

In addition to its role in antigen presentation CTSD plays also a role in several biological functions such as apoptosis and autophagy [437]. Moreover, this protease was found released extracellularly as reported from human MPs and keratinocytes [437] [438] [439]. CTSD expression and activity was detected in extracellular matrix, and components of this latter have been found among CTSD substrates [437]. This protease was also described as a tissue marker associated with bad prognosis and metastasis in several cancers such as breast cancer and malignant gliomas [437]. *In vitro*, breast cancer cells secreted an extracellular pro CTSD which was auto-activated at acidic pH and digested extracellular matrix components, suggesting a role of this protease in facilitating tumor invasion [440]. Moreover, efficient drug (Tamoxifen) was shown to decrease secretion of CTSD in breast cancer, *in vivo* [441]. These data showed that CTSD, especially through its extracellular form, is playing destructive functions and promotes extracellular matrix degradation and tumor cell invasion. In a model of cavitary TB in rabbits, high levels of CTSD were present in the live and dead MPs that

surround caseous and liquefied pulmonary lesions, suggesting that this enzyme is a major protease in the liquefaction process of pulmonary caseous foci [442]. We showed that granuloma myeloid cells in TB and pLCH express CTSD. It would be interesting to know if they secrete this protease extracellulary, thus promoting a possible mechanism of host tissue damage. *In vitro* models of human mycobacterial granulomas were previously developed using either BCG or beads coated with *Mtb* antigens [443]. Both systems are able to trigger a cellular aggregation reminiscent of natural mycobacterial granulomas, in terms of morphology and cell differentiation. Extracellular CTSD expression could be investigated in the medium of these structures and its destructive role may be then evaluated.

Overall, IL-17A and IFN-γ-treated DCs and their derived GMICs can play destructive roles which potentially depend on their aggressive CTSD and MMP12 proteases. The blockade of IL-17A or its induced-MMP12 and/or CTSD may thus represent a possible therapeutic strategy in diseases in which the IL-17A-dependent granulomas efficiently damage host tissues, as in pLCH or sarcoidosis.

3.3.5 Regulation of IL-17A-mediated responses

To avoid aggressive tissue destruction, granulomas must be tightly regulated and limited in size and number, and controlled in term of effector destructive functions. As discussed above, IL-17A promotes myeloid cell recruitment through chemokines, survival via pro-survival proteins and aggressive activities through destructive enzymes. If not regulated, such IL-17A-mediated effects exacerbate granuloma formation and promote its aggressive functions, thereby enhancing host immunopathological responses and tissue destruction. In this context, a recent paper showed that repeated BCG vaccination of *Mtb*-infected mice led to increased IL-17A production which results in pathological consequences [444]. This was reflected by enhanced lung neutrophila and high mortality of infected mice. These pathological effects were completely dependent on IL-17A as they were abrogated in animals treated with IL-17A-blocking antibodies. Enhanced pathology in these mice was characterized, macroscopically, by a larger number of detectable lesions and, microscopically, by lesions of increased size compared with control mice [444]. Exaggerated IL-17A production in murine schistosomiasis induces also enhanced pathology characterized by more severe and larger granulomatous lesions [384] [385]. These data reflects clear deleterious and pathological roles of excessive IL-17A production in granulomatous inflammation, indicating that this process must be finely regulated to avoid pathological consequences.

Several reports revealed an immunomodulatory role of IFN-γ which restrains and antagonizes exacerbated IL-17A-dependent effects to avoid immunopathology. Th1 cell-produced IFN-γ inhibits the differentiation of Th17 cells during BCG or *Mtb* infection in mice, thus reducing pathogenic IL-17A-mediated PMN accumulation and preventing severe granulomatous responses [445] [446]. *In vitro*, IFN-γ up-regulates IL-12 (which promotes Th1 responses) and down-regulates IL-23 (which promotes Th17 responses) in BCG-infected murine DCs [445]. Chimeric mice in which non-hematopoietic lung epithelial and endothelial cells were unable to respond to IFN-γ showed overexpressed IL-17A with massive pathological neutrophilic inflammation [447]. Rutitzky *et al.* reported that IFN-γ also regulates the IL-17A-dependent deleterious granulomatous response in mice with induced severe schistosomiasis. In this model, animals deficient in T-bet (lacking Th1 responses and IFN-γ production) or in IFN-γ, showed a greater enhancement of hepatic immunopathology which correlate with a marked increase in IL-17A production by Th17 cells. This correlated with a concomitant influx of PMNs to granulomas resulting in larger and poorly circumscribed lesions compared to WT animals [448] [449].

In humans, Mycobacterium-infected individuals with a partial deficiency in the IFN-γ receptor (partial IFN-γR1 deficiency) developed a response which clinically and histologically mimicked LCH, thus reflecting a severe non controlled granulomatous response [450]. The role of IL-17A was not evaluated in such patients, but it can be assumed that the impairment of the immunomodulatory function of IFN-γ leads to excessive and non-regulated IL-17A responses which results in such severe response.

A fine balance between IFN-γ and IL-17A responses is therefore essential in regulating granulomatous responses, and disruption of this balance may lead to important immunopathological consequences. In this equilibrium state, IFN-γ regulates IL-17A production and counteracts its detrimental effects. This occurs most likely by inhibiting the generation of Th17 cells and limiting their dependent response, thus blocking an essential source of IL-17A. However, Th17 cells are not the exclusive source of IL-17A. Consequently, the role of IFN-γ in limiting deleterious IL-17A effects may be ineffective in cases where IL-17A is essentially produced by other cells than Th17 lymphocytes. This might be the case in LCH in which IL-17A and IFN-γ are both secreted by the same lesional myeloid DCs **(Fig. 20)**. In such conditions, IFN-γ cannot limit IL-17A effects, but in contrast it potentiates their impact on myeloid cell recruitment, clustering and fusion in destructive MGCs within granulomas. This may explain the potent aggressive granuloma functions in the highly destructive LCH disease.

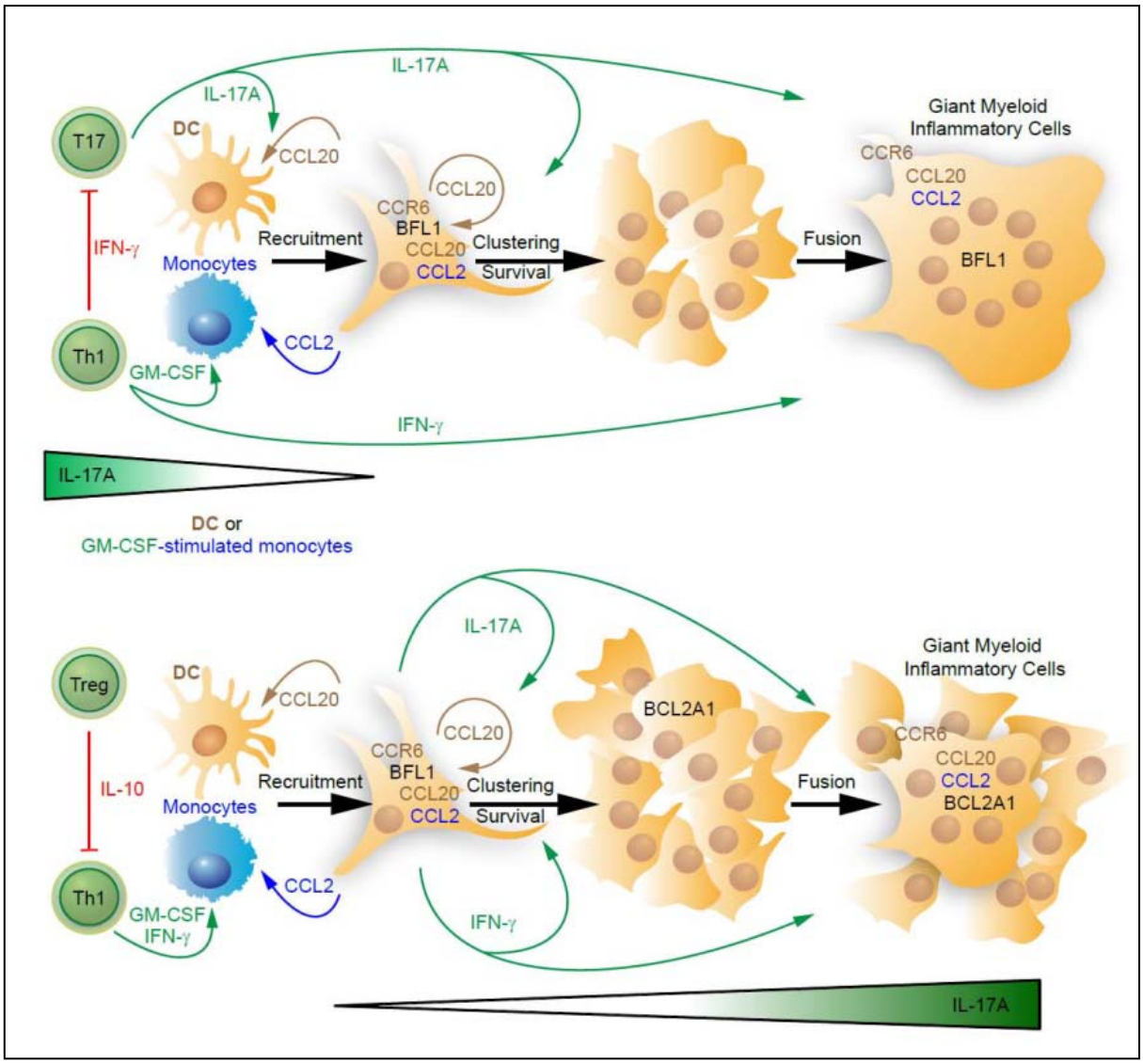

Figure 20: IFN-γ differentially regulates IL-17A-mediated effects in TB and LCH.

Top: In TB, IFN-γ limits the expansion of IL-17A-producing T cells and may thus regulate IL-17A effects on myeloid cells and attenuate its destructive and pathological-dependent consequences.

Bottom: in pLCH, the initial production of IFN-γ by Th1 is limited by Tregs [407]. IFN-γ produced by the same IL-17A-expressing myeloid cells is unable to inhibit IL-17A production but, in contrast, enhances IL-17A functions leading to a positive amplification loop which promotes the accumulation of pathological DCs and their destructive abilities.

4 Part IV: CONCLUSIONS & PERSPECTIVES

In 2008, our group demonstrated that IL-17A induces the fusion of human DCs into MGCs [306]. In this work we characterized this IL-17A-dependent fusion pathway and demonstrated that *in vitro*, IL-17A positively regulates survival, clustering and fusion of DCs. We investigated the molecular mechanisms by which IL-17A regulates these three features. We found that IL-17A treatment of DCs induces the production of BFL1, a pro survival protein of the BCL2 family. IL-17A-mediated BFL1 production was correlated with DC survival, indicating the role of BFL1 in promoting the prolonged lifespan of these cells. We also found that IL-17A induces CCL2 and CCL20 in DCs, and demonstrated that these chemokines are critical mediators in regulating DC clustering and fusion in MGCs. However, CCL20 and CCL2alone were not sufficient to mediate DC fusion, indicating that IL-17A induces additional molecules required for the fusion process. It would be interesting to determine IL-17A-induced fusogenic molecules in our transcriptomic data, and then validate their involvement in this fusion pathway using *in vitro* blocking assays. As several fusion mediators were identified in other pathways of giant cell formation (OCs, FBGCs); such experiments would clarify if the IL-17A-dependent fusion pathway relies on the same or on different fusogenic molecules.

MGCs are the hallmark of granulomas in several granulomatous disorders including TB. In human TB granuloma, we found that IL-17A was expressed by T lymphocytes while BFL1, CCL2 and CCL20 were expressed by mono- and multinucleated myeloid giant cells within these structures. We also found that IL-17A, BFL1, CCL2 and CCL20 were expressed by the myeloid granuloma cells in pLCH, another pulmonary granulomatous disorder. Along with our *in vitro* findings, these results suggest that IL-17A may participate in the maintenance of human granulomas by promoting myeloid cell survival through BFL1 as well as clustering and fusion trough CCL2 and CCL20. In diseases in which granulomas play destructive roles such as pLCH, IL-17A and/or its induced BFL1, CCL2 and CCL20 may form potential therapeutic targets.

Several types of giant cells were previously described including bone-resorbing OCs. Our transcriptomic data showed that IL-17A-induced MGCs are different from OCs, and *in vitro* experiments revealed that they were unable to resorb bone. Moreover, MGCs were characterized by the co-expression of MMP12 and CTSD and such co-expression may form marker of these cells. Investigating the nature and the origin of giant cells in granulomatous diseases may open new avenues for the understanding, classification and treatments of these disorders. Regarding the origin and characteristics of the IL-17A-induced MGCs we called them GMICs (giant myeloid inflammatory cells) and we suggest that they form a novel myeloid effector of the immune system. Methodological skills depicted in a recent paper which characterize follicular helper

$CD4^+$ T cell dynamics during Simian immunodeficiency virus infection [451] can be used to better characterize GMICs. Indeed in this paper, authors elegantly characterized follicular helper T cells in rhesus macaques at the phenotypic, molecular, functional and tissue localization level. The techniques depicted in this publication will indeed allow investigating the relationship between cellular subsets, which means that any divergent functions of cells such as giant cells could be spatially resolved within an environment tractable to in depth characterization.

IL-17A-treated DCs and their derived GMICs, have a mixed DC-MP phenotype, kept DC immune functions, express destructive enzymes and possess potent microbicidal functions. They were more potent in Mycobacterium (*M. avium* and BCG) killing than untreated DCs. Strikingly, when stimulated by CD40L, they showed differential bactericidal abilities: they better control *M. avium* while become unable to control BCG growth and replication. *Mtb* ability to grow within unstimulated or CD40L stimulated GMIC is an important issue which must be investigated to clarify the behavior of this pathogen in these giant cells.

Importantly, in addition to their bactericidal roles, we found that IL-17A-treated DCs and their derived GMICs are potent destructive cells. *In vitro*, they were able to destroy a layer of bronchial epithelial cells, while untreated DCs did not. Further investigations are needed to identify the exact molecular mediators involved in this destructive process. Based on recent findings which associate IL-17A-induced MMP12 to pulmonary tissue damage in lung inflammatory diseases such as emphysema [452], this enzyme may represent a potential candidate. CTSD may also represent another candidate as this protease was found released extracellulary where it promotes tissue damage. Neutralization of IL-17A-induced destructive enzymes such as MMP12 may be thus beneficial to avoid tissue damage destruction by aggressive granulomas.

Although granulomas can be detected *in vivo* (e.g. using radiology or computed tomography), the monitoring of the temporal evolution of a granulomatous response is difficult. We showed that CTSD is highly and specifically expressed by the myeloid cells of IL-17A-dependent granulomas in pLCH and TB. The use of a CTSD substrate (commercially available) may be therefore used as a screening tool to localize and follow IL-17A-dependent granulomas through medical imaging techniques. For example, a CSTD substrate can be coupled to a radioactive medicine to create a “radiotracer”. The substrate targets the radiotracer to the CTSD rich myeloid cells of the granuloma and a nuclear imaging technique

such as positron emission tomography (PET) scan can be used to localize and follow these $CTSD^+$ structures. This technique can be used as a diagnostic tool which may provide useful information on granuloma presence, localization, number and size and allows a precise monitoring of the stability of these features. This may help the treatment as it may become easier to decide when treating, with which drugs and for how many time.

Finally, granulomatous structures may be found in the vicinity of the tumors, and granulomatous reaction may be associated with a better prognosis as reported in some cancers [453]. Recent data from animal models suggest that tumoral cells, similar to *Mtb*, may be packaged and chronically controlled within giant cell-associated granulomas [375]. The anti mycobacterial response induced by BCG is used to treat invasive bladder cancer through intravesical instillation of live BCG. However, mechanisms of this treatment remain poorly understood. Based on the facts that i) BCG induces a granulomatous response ii) granulomas may control tumoral cells and iii) IL-17A promotes BCG-induced granuloma formation; we propose that the unknown mechanism which control bladder cancer, following BCG therapy, is an IL-17A-dependent anti-tumoral granulomatous response induced by BCG infection. Moreover, as we showed that IL-17A induces myeloid cell fusion into destructive GMICs, it can be suggested that these cells may control and/or destroy bladder tumoral cells as we reported for the transformed BEAS-2B cells *in vitro*. Validation of this hypothesis requires an *in vitro* model of co-culture between GMIC and bladder cancer cell lines such as T24, to investigate if they are destroyed by GMICs. The set-up of this system is already initialized in the laboratory to determine optimal co-culture conditions. Moreover, it would be interesting to co-culture bladder cancer cells along with the *in vitro* granuloma models induced by BCG or mycobacterial antigens to understand if these granulomas are able to control cancer progression and to determine the role of IL-17A in this process. If IL-17A-associated to mycobacterial antigens, can lead to the same granulomatous response with GMIC formation, able to control and/or destroy cancer cells, this could improve bladder cancer treatment, avoiding side effects seen in 30% of patients due to infection with live BCG. Moreover, understanding the molecular mechanisms of BCG immunotherapy may open new avenues to control cancer cells in other tumors.

5 REFERENCES

1. Rosenblueth, M., et al., *Environmental mycobacteria: a threat to human health?* DNA Cell Biol, 2011. **30**(9): p. 633-40.
2. Driscoll, J.R., *Spoligotyping for molecular epidemiology of the Mycobacterium tuberculosis complex.* Methods Mol Biol, 2009. **551**: p. 117-28.
3. Smith, N.H., et al., *Myths and misconceptions: the origin and evolution of Mycobacterium tuberculosis.* Nat Rev Microbiol, 2009. **7**(7): p. 537-44.
4. Rodrigues, L.C. and D. Lockwood, *Leprosy now: epidemiology, progress, challenges, and research gaps.* Lancet Infect Dis, 2011. **11**(6): p. 464-70.
5. Demangel, C., T.P. Stinear, and S.T. Cole, *Buruli ulcer: reductive evolution enhances pathogenicity of Mycobacterium ulcerans.* Nat Rev Microbiol, 2009. **7**(1): p. 50-60.
6. Silva, M.T., F. Portaels, and J. Pedrosa, *Pathogenetic mechanisms of the intracellular parasite Mycobacterium ulcerans leading to Buruli ulcer.* Lancet Infect Dis, 2009. **9**(11): p. 699-710.
7. Turenne, C.Y., et al., *Sequencing of hsp65 distinguishes among subsets of the Mycobacterium avium complex.* J Clin Microbiol, 2006. **44**(2): p. 433-40.
8. Sreevatsan, S., et al., *Restricted structural gene polymorphism in the Mycobacterium tuberculosis complex indicates evolutionarily recent global dissemination.* Proc Natl Acad Sci U S A, 1997. **94**(18): p. 9869-74.
9. Musser, J.M., A. Amin, and S. Ramaswamy, *Negligible genetic diversity of mycobacterium tuberculosis host immune system protein targets: evidence of limited selective pressure.* Genetics, 2000. **155**(1): p. 7-16.
10. Gagneux, S. and P.M. Small, *Global phylogeography of Mycobacterium tuberculosis and implications for tuberculosis product development.* Lancet Infect Dis, 2007. **7**(5): p. 328-37.
11. Brosch, R., et al., *A new evolutionary scenario for the Mycobacterium tuberculosis complex.* Proc Natl Acad Sci U S A, 2002. **99**(6): p. 3684-9.
12. Eisenstadt, J. and G.S. Hall, *Microbiology and classification of mycobacteria.* Clin Dermatol, 1995. **13**(3): p. 197-206.
13. Chao, M.C. and E.J. Rubin, *Letting sleeping dos lie: does dormancy play a role in tuberculosis?* Annu Rev Microbiol, 2010. **64**: p. 293-311.
14. Gengenbacher, M. and S.H. Kaufmann, *Mycobacterium tuberculosis: success through dormancy.* FEMS Microbiol Rev, 2012.
15. Wayne, L.G. and C.D. Sohaskey, *Nonreplicating persistence of mycobacterium tuberculosis.* Annu Rev Microbiol, 2001. **55**: p. 139-63.
16. Voskuil, M.I., et al., *Inhibition of respiration by nitric oxide induces a Mycobacterium tuberculosis dormancy program.* J Exp Med, 2003. **198**(5): p. 705-13.
17. Leistikow, R.L., et al., *The Mycobacterium tuberculosis DosR regulon assists in metabolic homeostasis and enables rapid recovery from nonrespiring dormancy.* J Bacteriol, 2010. **192**(6): p. 1662-70.
18. Cole, S.T., et al., *Deciphering the biology of Mycobacterium tuberculosis from the complete genome sequence.* Nature, 1998. **393**(6685): p. 537-44.
19. McKinney, J.D., et al., *Persistence of Mycobacterium tuberculosis in macrophages and mice requires the glyoxylate shunt enzyme isocitrate lyase.* Nature, 2000. **406**(6797): p. 735-8.
20. Neyrolles, O., et al., *Is adipose tissue a place for Mycobacterium tuberculosis persistence?* PLoS One, 2006. **1**: p. e43.
21. Pandey, A.K. and C.M. Sassetti, *Mycobacterial persistence requires the utilization of host cholesterol.* Proc Natl Acad Sci U S A, 2008. **105**(11): p. 4376-80.
22. Daniel, J., et al., *Mycobacterium tuberculosis uses host triacylglycerol to accumulate lipid droplets and acquires a dormancy-like phenotype in lipid-loaded macrophages.* PLoS Pathog, 2011. **7**(6): p. e1002093.

23. D'Avila, H., et al., *Mycobacterium bovis bacillus Calmette-Guerin induces TLR2-mediated formation of lipid bodies: intracellular domains for eicosanoid synthesis in vivo.* J Immunol, 2006. **176**(5): p. 3087-97.
24. Peyron, P., et al., *Foamy macrophages from tuberculous patients' granulomas constitute a nutrient-rich reservoir for M. tuberculosis persistence.* PLoS Pathog, 2008. **4**(11): p. e1000204.
25. Kaur, D., et al., *Chapter 2: Biogenesis of the cell wall and other glycoconjugates of Mycobacterium tuberculosis.* Adv Appl Microbiol, 2009. **69**: p. 23-78.
26. Brennan, P.J. and H. Nikaido, *The envelope of mycobacteria.* Annu Rev Biochem, 1995. **64**: p. 29-63.
27. Brennan, P.J., *Structure, function, and biogenesis of the cell wall of Mycobacterium tuberculosis.* Tuberculosis (Edinb), 2003. **83**(1-3): p. 91-7.
28. Rajni, N. Rao, and L.S. Meena, *Biosynthesis and Virulent Behavior of Lipids Produced by Mycobacterium tuberculosis: LAM and Cord Factor: An Overview.* Biotechnol Res Int, 2011. **2011**: p. 274693.
29. WHO, *Global tuberculosis control 2011. Geneva, Switzerland*, 2011.
30. Lin, P.L. and J.L. Flynn, *Understanding latent tuberculosis: a moving target.* J Immunol, 2010. **185**(1): p. 15-22.
31. Gideon, H.P. and J.L. Flynn, *Latent tuberculosis: what the host "sees"?* Immunol Res, 2011. **50**(2-3): p. 202-12.
32. Lawn, S.D. and A.I. Zumla, *Tuberculosis.* Lancet, 2011. **378**(9785): p. 57-72.
33. North, R.J. and Y.J. Jung, *Immunity to tuberculosis.* Annu Rev Immunol, 2004. **22**: p. 599-623.
34. Golden, M.P. and H.R. Vikram, *Extrapulmonary tuberculosis: an overview.* Am Fam Physician, 2005. **72**(9): p. 1761-8.
35. Sonnenberg, P., et al., *How soon after infection with HIV does the risk of tuberculosis start to increase? A retrospective cohort study in South African gold miners.* J Infect Dis, 2005. **191**(2): p. 150-8.
36. Shafer, R.W., et al., *Extrapulmonary tuberculosis in patients with human immunodeficiency virus infection.* Medicine (Baltimore), 1991. **70**(6): p. 384-97.
37. Sierra-Madero, J.G., et al., *Relationship between load of virus in alveolar macrophages from human immunodeficiency virus type 1-infected persons, production of cytokines, and clinical status.* J Infect Dis, 1994. **169**(1): p. 18-27.
38. Nakata, K., et al., *Low copy number and limited variability of proviral DNA in alveolar macrophages from HIV-1-infected patients: evidence for genetic differences in HIV-1 between lung and blood macrophage populations.* Mol Med, 1995. **1**(7): p. 744-57.
39. Diedrich, C.R. and J.L. Flynn, *HIV-1/mycobacterium tuberculosis coinfection immunology: how does HIV-1 exacerbate tuberculosis?* Infect Immun, 2011. **79**(4): p. 1407-17.
40. Russell, D.G., et al., *Foamy macrophages and the progression of the human tuberculosis granuloma.* Nat Immunol, 2009. **10**(9): p. 943-8.
41. Russell, D.G., C.E. Barry, 3rd, and J.L. Flynn, *Tuberculosis: what we don't know can, and does, hurt us.* Science, 2010. **328**(5980): p. 852-6.
42. Wallis, R.S., et al., *Biomarkers and diagnostics for tuberculosis: progress, needs, and translation into practice.* Lancet, 2010. **375**(9729): p. 1920-37.
43. Parida, S.K. and S.H. Kaufmann, *The quest for biomarkers in tuberculosis.* Drug Discov Today, 2010. **15**(3-4): p. 148-57.
44. Walzl, G., et al., *Immunological biomarkers of tuberculosis.* Nat Rev Immunol, 2011. **11**(5): p. 343-54.
45. Shi, W., et al., *Pyrazinamide inhibits trans-translation in Mycobacterium tuberculosis.* Science, 2011. **333**(6049): p. 1630-2.
46. Goldberg, D.E., R.F. Siliciano, and W.R. Jacobs, Jr., *Outwitting Evolution: Fighting Drug-Resistant TB, Malaria, and HIV.* Cell, 2012. **148**(6): p. 1271-83.
47. *Controlled clinical trial of short-course (6-month) regimens of chemotherapy for treatment of pulmonary tuberculosis.* Lancet, 1972. **1**(7760): p. 1079-85.

48. Koul, A., et al., *The challenge of new drug discovery for tuberculosis.* Nature, 2011. **469**(7331): p. 483-90.
49. Zhang, M., et al., *Treatment of tuberculosis with rifamycin-containing regimens in immune-deficient mice.* Am J Respir Crit Care Med, 2011. **183**(9): p. 1254-61.
50. Udwadia, Z.F., et al., *Totally drug-resistant tuberculosis in India.* Clin Infect Dis, 2012. **54**(4): p. 579-81.
51. Gler, M.T., et al., *Delamanid for multidrug-resistant pulmonary tuberculosis.* N Engl J Med, 2012. **366**(23): p. 2151-60.
52. Behr, M.A., et al., *Comparative genomics of BCG vaccines by whole-genome DNA microarray.* Science, 1999. **284**(5419): p. 1520-3.
53. Mahairas, G.G., et al., *Molecular analysis of genetic differences between Mycobacterium bovis BCG and virulent M. bovis.* J Bacteriol, 1996. **178**(5): p. 1274-82.
54. Lewis, K.N., et al., *Deletion of RD1 from Mycobacterium tuberculosis mimics bacille Calmette-Guerin attenuation.* J Infect Dis, 2003. **187**(1): p. 117-23.
55. Andersen, P. and T.M. Doherty, *The success and failure of BCG - implications for a novel tuberculosis vaccine.* Nat Rev Microbiol, 2005. **3**(8): p. 656-62.
56. Azzopardi, P., et al., *Bacille Calmette-Guerin vaccine-related disease in HIV-infected children: a systematic review.* Int J Tuberc Lung Dis, 2009. **13**(11): p. 1331-44.
57. Mansoor, N., et al., *HIV-1 infection in infants severely impairs the immune response induced by Bacille Calmette-Guerin vaccine.* J Infect Dis, 2009. **199**(7): p. 982-90.
58. Parida, S.K. and S.H. Kaufmann, *Novel tuberculosis vaccines on the horizon.* Curr Opin Immunol, 2010. **22**(3): p. 374-84.
59. Kaufmann, S.H., G. Hussey, and P.H. Lambert, *New vaccines for tuberculosis.* Lancet, 2010. **375**(9731): p. 2110-9.
60. Kaufmann, S.H.E., *Fact and fiction in tuberculosis vaccine research: 10 years later.* The Lancet Infectious Diseases, 2011. **11**(8): p. 633-640.
61. Martin, C., et al., *The live Mycobacterium tuberculosis phoP mutant strain is more attenuated than BCG and confers protective immunity against tuberculosis in mice and guinea pigs.* Vaccine, 2006. **24**(17): p. 3408-19.
62. Sambandamurthy, V.K., et al., *Mycobacterium tuberculosis DeltaRD1 DeltapanCD: a safe and limited replicating mutant strain that protects immunocompetent and immunocompromised mice against experimental tuberculosis.* Vaccine, 2006. **24**(37-39): p. 6309-20.
63. Sweeney, K.A., et al., *A recombinant Mycobacterium smegmatis induces potent bactericidal immunity against Mycobacterium tuberculosis.* Nat Med, 2011. **17**(10): p. 1261-8.
64. Kaufmann, S.H., *Future vaccination strategies against tuberculosis: thinking outside the box.* Immunity, 2010. **33**(4): p. 567-77.
65. McShane, H. and A. Hill, *Prime-boost immunisation strategies for tuberculosis.* Microbes Infect, 2005. **7**(5-6): p. 962-7.
66. Jo, E.K., *Mycobacterial interaction with innate receptors: TLRs, C-type lectins, and NLRs.* Curr Opin Infect Dis, 2008. **21**(3): p. 279-86.
67. Huynh, K.K., S.A. Joshi, and E.J. Brown, *A delicate dance: host response to mycobacteria.* Curr Opin Immunol, 2011. **23**(4): p. 464-72.
68. Schafer, G., et al., *Non-opsonic recognition of Mycobacterium tuberculosis by phagocytes.* J Innate Immun, 2009. **1**(3): p. 231-43.
69. Tanne, A. and O. Neyrolles, *C-type lectins in immunity to Mycobacterium tuberculosis.* Front Biosci (Schol Ed), 2011. **3**: p. 1147-64.
70. Schlesinger, L.S., et al., *Phagocytosis of Mycobacterium tuberculosis is mediated by human monocyte complement receptors and complement component C3.* J Immunol, 1990. **144**(7): p. 2771-80.
71. Ernst, J.D., *Macrophage receptors for Mycobacterium tuberculosis.* Infect Immun, 1998. **66**(4): p. 1277-81.

72. Korbel, D.S., B.E. Schneider, and U.E. Schaible, *Innate immunity in tuberculosis: myths and truth.* Microbes Infect, 2008. **10**(9): p. 995-1004.
73. Tailleux, L., et al., *DC-SIGN is the major Mycobacterium tuberculosis receptor on human dendritic cells.* J Exp Med, 2003. **197**(1): p. 121-7.
74. Tailleux, L., et al., *DC-SIGN induction in alveolar macrophages defines privileged target host cells for mycobacteria in patients with tuberculosis.* PLoS Med, 2005. **2**(12): p. e381.
75. Geurtsen, J., et al., *Identification of mycobacterial alpha-glucan as a novel ligand for DC-SIGN: involvement of mycobacterial capsular polysaccharides in host immune modulation.* J Immunol, 2009. **183**(8): p. 5221-31.
76. Bafica, A., et al., *TLR9 regulates Th1 responses and cooperates with TLR2 in mediating optimal resistance to Mycobacterium tuberculosis.* J Exp Med, 2005. **202**(12): p. 1715-24.
77. Coulombe, F., et al., *Increased NOD2-mediated recognition of N-glycolyl muramyl dipeptide.* J Exp Med, 2009. **206**(8): p. 1709-16.
78. Geijtenbeek, T.B., et al., *Mycobacteria target DC-SIGN to suppress dendritic cell function.* J Exp Med, 2003. **197**(1): p. 7-17.
79. Tanne, A., et al., *A murine DC-SIGN homologue contributes to early host defense against Mycobacterium tuberculosis.* J Exp Med, 2009. **206**(10): p. 2205-20.
80. Flannagan, R.S., V. Jaumouille, and S. Grinstein, *The cell biology of phagocytosis.* Annu Rev Pathol, 2012. **7**: p. 61-98.
81. Vieira, O.V., et al., *Distinct roles of class I and class III phosphatidylinositol 3-kinases in phagosome formation and maturation.* J Cell Biol, 2001. **155**(1): p. 19-25.
82. Vergne, I., J. Chua, and V. Deretic, *Tuberculosis toxin blocking phagosome maturation inhibits a novel Ca2+/calmodulin-PI3K hVPS34 cascade.* J Exp Med, 2003. **198**(4): p. 653-9.
83. Christoforidis, S., et al., *The Rab5 effector EEA1 is a core component of endosome docking.* Nature, 1999. **397**(6720): p. 621-5.
84. Simonsen, A., et al., *EEA1 links PI(3)K function to Rab5 regulation of endosome fusion.* Nature, 1998. **394**(6692): p. 494-8.
85. Quinn, M.T., M.C. Ammons, and F.R. Deleo, *The expanding role of NADPH oxidases in health and disease: no longer just agents of death and destruction.* Clin Sci (Lond), 2006. **111**(1): p. 1-20.
86. Nathan, C. and M.U. Shiloh, *Reactive oxygen and nitrogen intermediates in the relationship between mammalian hosts and microbial pathogens.* Proc Natl Acad Sci U S A, 2000. **97**(16): p. 8841-8.
87. Li, W. and J. Xie, *Role of mycobacteria effectors in phagosome maturation blockage and new drug targets discovery.* J Cell Biochem, 2011. **112**(10): p. 2688-93.
88. Via, L.E., et al., *Arrest of mycobacterial phagosome maturation is caused by a block in vesicle fusion between stages controlled by rab5 and rab7.* J Biol Chem, 1997. **272**(20): p. 13326-31.
89. Fratti, R.A., et al., *Mycobacterium tuberculosis glycosylated phosphatidylinositol causes phagosome maturation arrest.* Proc Natl Acad Sci U S A, 2003. **100**(9): p. 5437-42.
90. Sun, J., et al., *Mycobacterial nucleoside diphosphate kinase blocks phagosome maturation in murine RAW 264.7 macrophages.* PLoS One, 2010. **5**(1): p. e8769.
91. Vergne, I., et al., *Mechanism of phagolysosome biogenesis block by viable Mycobacterium tuberculosis.* Proc Natl Acad Sci U S A, 2005. **102**(11): p. 4033-8.
92. Bach, H., et al., *Mycobacterium tuberculosis virulence is mediated by PtpA dephosphorylation of human vacuolar protein sorting 33B.* Cell Host Microbe, 2008. **3**(5): p. 316-22.
93. Wong, D., et al., *Mycobacterium tuberculosis protein tyrosine phosphatase (PtpA) excludes host vacuolar-H+-ATPase to inhibit phagosome acidification.* Proc Natl Acad Sci U S A, 2011. **108**(48): p. 19371-6.
94. Deghmane, A.E., et al., *Lipoamide dehydrogenase mediates retention of coronin-1 on BCG vacuoles, leading to arrest in phagosome maturation.* J Cell Sci, 2007. **120**(Pt 16): p. 2796-806.

95. Ferrari, G., et al., *A coat protein on phagosomes involved in the intracellular survival of mycobacteria.* Cell, 1999. **97**(4): p. 435-47.
96. Pieters, J., *Mycobacterium tuberculosis and the macrophage: maintaining a balance.* Cell Host Microbe, 2008. **3**(6): p. 399-407.
97. Schuller, S., et al., *Coronin is involved in uptake of Mycobacterium bovis BCG in human macrophages but not in phagosome maintenance.* Cell Microbiol, 2001. **3**(12): p. 785-93.
98. Walburger, A., et al., *Protein kinase G from pathogenic mycobacteria promotes survival within macrophages.* Science, 2004. **304**(5678): p. 1800-4.
99. Pethe, K., et al., *Isolation of Mycobacterium tuberculosis mutants defective in the arrest of phagosome maturation.* Proc Natl Acad Sci U S A, 2004. **101**(37): p. 13642-7.
100. Stewart, G.R., et al., *Mycobacterial mutants with defective control of phagosomal acidification.* PLoS Pathog, 2005. **1**(3): p. 269-78.
101. Brodin, P., et al., *High content phenotypic cell-based visual screen identifies Mycobacterium tuberculosis acyltrehalose-containing glycolipids involved in phagosome remodeling.* PLoS Pathog, 2010. **6**(9): p. e1001100.
102. Ehrt, S. and D. Schnappinger, *Mycobacterial survival strategies in the phagosome: defence against host stresses.* Cell Microbiol, 2009. **11**(8): p. 1170-8.
103. Chan, J., et al., *Lipoarabinomannan, a possible virulence factor involved in persistence of Mycobacterium tuberculosis within macrophages.* Infect Immun, 1991. **59**(5): p. 1755-61.
104. Ng, V.H., et al., *Role of KatG catalase-peroxidase in mycobacterial pathogenesis: countering the phagocyte oxidative burst.* Mol Microbiol, 2004. **52**(5): p. 1291-302.
105. Pathania, R., et al., *Nitric oxide scavenging and detoxification by the Mycobacterium tuberculosis haemoglobin, HbN in Escherichia coli.* Mol Microbiol, 2002. **45**(5): p. 1303-14.
106. Gandotra, S., M.B. Lebron, and S. Ehrt, *The Mycobacterium tuberculosis proteasome active site threonine is essential for persistence yet dispensable for replication and resistance to nitric oxide.* PLoS Pathog, 2010. **6**(8): p. e1001040.
107. Purwantini, E. and B. Mukhopadhyay, *Conversion of NO2 to NO by reduced coenzyme F420 protects mycobacteria from nitrosative damage.* Proc Natl Acad Sci U S A, 2009. **106**(15): p. 6333-8.
108. Fortune, S.M., et al., *Mycobacterium tuberculosis inhibits macrophage responses to IFN-gamma through myeloid differentiation factor 88-dependent and -independent mechanisms.* J Immunol, 2004. **172**(10): p. 6272-80.
109. Henderson, R.A., S.C. Watkins, and J.L. Flynn, *Activation of human dendritic cells following infection with Mycobacterium tuberculosis.* J Immunol, 1997. **159**(2): p. 635-43.
110. Thurnher, M., et al., *Bacillus Calmette-Guerin mycobacteria stimulate human blood dendritic cells.* Int J Cancer, 1997. **70**(1): p. 128-34.
111. Humphreys, I.R., et al., *A role for dendritic cells in the dissemination of mycobacterial infection.* Microbes Infect, 2006. **8**(5): p. 1339-46.
112. Wolf, A.J., et al., *Mycobacterium tuberculosis infects dendritic cells with high frequency and impairs their function in vivo.* J Immunol, 2007. **179**(4): p. 2509-19.
113. Reljic, R., et al., *Time course of mycobacterial infection of dendritic cells in the lungs of intranasally infected mice.* Tuberculosis (Edinb), 2005. **85**(1-2): p. 81-8.
114. Russell, D.G., *Mycobacterium tuberculosis: here today, and here tomorrow.* Nat Rev Mol Cell Biol, 2001. **2**(8): p. 569-77.
115. Jiao, X., et al., *Dendritic cells are host cells for mycobacteria in vivo that trigger innate and acquired immunity.* J Immunol, 2002. **168**(3): p. 1294-301.
116. Tailleux, L., et al., *Constrained intracellular survival of Mycobacterium tuberculosis in human dendritic cells.* J Immunol, 2003. **170**(4): p. 1939-48.
117. Tailleux, L., et al., *Probing host pathogen cross-talk by transcriptional profiling of both Mycobacterium tuberculosis and infected human dendritic cells and macrophages.* PLoS One, 2008. **3**(1): p. e1403.

118. van Crevel, R., T.H. Ottenhoff, and J.W. van der Meer, *Innate immunity to Mycobacterium tuberculosis.* Clin Microbiol Rev, 2002. **15**(2): p. 294-309.
119. Russell, D.G., *Who puts the tubercle in tuberculosis?* Nat Rev Microbiol, 2007. **5**(1): p. 39-47.
120. Torrado, E. and A.M. Cooper, *IL-17 and Th17 cells in tuberculosis.* Cytokine Growth Factor Rev, 2010. **21**(6): p. 455-62.
121. Roach, D.R., et al., *TNF regulates chemokine induction essential for cell recruitment, granuloma formation, and clearance of mycobacterial infection.* J Immunol, 2002. **168**(9): p. 4620-7.
122. Lockhart, E., A.M. Green, and J.L. Flynn, *IL-17 production is dominated by gammadelta T cells rather than CD4 T cells during Mycobacterium tuberculosis infection.* J Immunol, 2006. **177**(7): p. 4662-9.
123. Hickman, S.P., J. Chan, and P. Salgame, *Mycobacterium tuberculosis induces differential cytokine production from dendritic cells and macrophages with divergent effects on naive T cell polarization.* J Immunol, 2002. **168**(9): p. 4636-42.
124. Giacomini, E., et al., *Infection of human macrophages and dendritic cells with Mycobacterium tuberculosis induces a differential cytokine gene expression that modulates T cell response.* J Immunol, 2001. **166**(12): p. 7033-41.
125. Redford, P.S., P.J. Murray, and A. O'Garra, *The role of IL-10 in immune regulation during M. tuberculosis infection.* Mucosal Immunol, 2011. **4**(3): p. 261-70.
126. O'Leary, S., M.P. O'Sullivan, and J. Keane, *IL-10 Blocks Phagosome Maturation in Mycobacterium tuberculosis-infected Human Macrophages.* Am J Respir Cell Mol Biol, 2011.
127. Lowe, D.M., et al., *Neutrophils in tuberculosis: friend or foe?* Trends Immunol, 2012. **33**(1): p. 14-25.
128. Eum, S.Y., et al., *Neutrophils are the predominant infected phagocytic cells in the airways of patients with active pulmonary TB.* Chest, 2010. **137**(1): p. 122-8.
129. Khader, S.A., et al., *Interleukin 12p40 is required for dendritic cell migration and T cell priming after Mycobacterium tuberculosis infection.* J Exp Med, 2006. **203**(7): p. 1805-15.
130. Abadie, V., et al., *Neutrophils rapidly migrate via lymphatics after Mycobacterium bovis BCG intradermal vaccination and shuttle live bacilli to the draining lymph nodes.* Blood, 2005. **106**(5): p. 1843-50.
131. Morel, C., et al., *Mycobacterium bovis BCG-infected neutrophils and dendritic cells cooperate to induce specific T cell responses in humans and mice.* Eur J Immunol, 2008. **38**(2): p. 437-47.
132. Blomgran, R. and J.D. Ernst, *Lung neutrophils facilitate activation of naive antigen-specific CD4+ T cells during Mycobacterium tuberculosis infection.* J Immunol, 2011. **186**(12): p. 7110-9.
133. Schaible, U.E., et al., *Apoptosis facilitates antigen presentation to T lymphocytes through MHC-I and CD1 in tuberculosis.* Nat Med, 2003. **9**(8): p. 1039-46.
134. Perskvist, N., et al., *Mycobacterium tuberculosis promotes apoptosis in human neutrophils by activating caspase-3 and altering expression of Bax/Bcl-xL via an oxygen-dependent pathway.* J Immunol, 2002. **168**(12): p. 6358-65.
135. Persson, Y.A., et al., *Mycobacterium tuberculosis-induced apoptotic neutrophils trigger a pro-inflammatory response in macrophages through release of heat shock protein 72, acting in synergy with the bacteria.* Microbes Infect, 2008. **10**(3): p. 233-40.
136. Aleman, M., et al., *Spontaneous or Mycobacterium tuberculosis-induced apoptotic neutrophils exert opposite effects on the dendritic cell-mediated immune response.* Eur J Immunol, 2007. **37**(6): p. 1524-37.
137. Hedlund, S., et al., *Dendritic cell activation by sensing Mycobacterium tuberculosis-induced apoptotic neutrophils via DC-SIGN.* Hum Immunol, 2010. **71**(6): p. 535-40.
138. Esin, S., et al., *Direct binding of human NK cell natural cytotoxicity receptor NKp44 to the surfaces of mycobacteria and other bacteria.* Infect Immun, 2008. **76**(4): p. 1719-27.
139. Junqueira-Kipnis, A.P., et al., *NK cells respond to pulmonary infection with Mycobacterium tuberculosis, but play a minimal role in protection.* J Immunol, 2003. **171**(11): p. 6039-45.

140. Schierloh, P., et al., *Increased susceptibility to apoptosis of CD56dimCD16+ NK cells induces the enrichment of IFN-gamma-producing CD56bright cells in tuberculous pleurisy.* J Immunol, 2005. **175**(10): p. 6852-60.
141. Tanaka, Y., et al., *Nonpeptide ligands for human gamma delta T cells.* Proc Natl Acad Sci U S A, 1994. **91**(17): p. 8175-9.
142. Tsukaguchi, K., B. de Lange, and W.H. Boom, *Differential regulation of IFN-gamma, TNF-alpha, and IL-10 production by CD4(+) alphabetaTCR+ T cells and vdelta2(+) gammadelta T cells in response to monocytes infected with Mycobacterium tuberculosis-H37Ra.* Cell Immunol, 1999. **194**(1): p. 12-20.
143. Dieli, F., et al., *Characterization of lung gamma delta T cells following intranasal infection with Mycobacterium bovis bacillus Calmette-Guerin.* J Immunol, 2003. **170**(1): p. 463-9.
144. Umemura, M., et al., *IL-17-mediated regulation of innate and acquired immune response against pulmonary Mycobacterium bovis bacille Calmette-Guerin infection.* J Immunol, 2007. **178**(6): p. 3786-96.
145. Peng, M.Y., et al., *Interleukin 17-producing gamma delta T cells increased in patients with active pulmonary tuberculosis.* Cell Mol Immunol, 2008. **5**(3): p. 203-8.
146. Fischer, K., et al., *Mycobacterial phosphatidylinositol mannoside is a natural antigen for CD1d-restricted T cells.* Proc Natl Acad Sci U S A, 2004. **101**(29): p. 10685-90.
147. Sada-Ovalle, I., et al., *Innate invariant NKT cells recognize Mycobacterium tuberculosis-infected macrophages, produce interferon-gamma, and kill intracellular bacteria.* PLoS Pathog, 2008. **4**(12): p. e1000239.
148. Vankayalapati, R. and P.F. Barnes, *Innate and adaptive immune responses to human Mycobacterium tuberculosis infection.* Tuberculosis (Edinb), 2009. **89 Suppl 1**: p. S77-80.
149. Brill, K.J., et al., *Human natural killer cells mediate killing of intracellular Mycobacterium tuberculosis H37Rv via granule-independent mechanisms.* Infect Immun, 2001. **69**(3): p. 1755-65.
150. Dieli, F., et al., *Vgamma9/Vdelta2 T lymphocytes reduce the viability of intracellular Mycobacterium tuberculosis.* Eur J Immunol, 2000. **30**(5): p. 1512-9.
151. Dieli, F., et al., *Granulysin-dependent killing of intracellular and extracellular Mycobacterium tuberculosis by Vgamma9/Vdelta2 T lymphocytes.* J Infect Dis, 2001. **184**(8): p. 1082-5.
152. Gansert, J.L., et al., *Human NKT cells express granulysin and exhibit antimycobacterial activity.* J Immunol, 2003. **170**(6): p. 3154-61.
153. Ladel, C.H., et al., *Protective role of gamma/delta T cells and alpha/beta T cells in tuberculosis.* Eur J Immunol, 1995. **25**(10): p. 2877-81.
154. D'Souza, C.D., et al., *An anti-inflammatory role for gamma delta T lymphocytes in acquired immunity to Mycobacterium tuberculosis.* J Immunol, 1997. **158**(3): p. 1217-21.
155. Schierloh, P., et al., *NK cell activity in tuberculosis is associated with impaired CD11a and ICAM-1 expression: a regulatory role of monocytes in NK activation.* Immunology, 2005. **116**(4): p. 541-52.
156. Laochumroonvorapong, P., et al., *Perforin, a cytotoxic molecule which mediates cell necrosis, is not required for the early control of mycobacterial infection in mice.* Infect Immun, 1997. **65**(1): p. 127-32.
157. Cooper, A.M., et al., *The course of Mycobacterium tuberculosis infection in the lungs of mice lacking expression of either perforin- or granzyme-mediated cytolytic mechanisms.* Infect Immun, 1997. **65**(4): p. 1317-20.
158. Kaufmann, S.H., *How can immunology contribute to the control of tuberculosis?* Nat Rev Immunol, 2001. **1**(1): p. 20-30.
159. Baena, A. and S.A. Porcelli, *Evasion and subversion of antigen presentation by Mycobacterium tuberculosis.* Tissue Antigens, 2009. **74**(3): p. 189-204.
160. Schaible, U.E. and S.H. Kaufmann, *CD1 and CD1-restricted T cells in infections with intracellular bacteria.* Trends Microbiol, 2000. **8**(9): p. 419-25.

161. Barral, D.C. and M.B. Brenner, *CD1 antigen presentation: how it works.* Nat Rev Immunol, 2007. **7**(12): p. 929-41.
162. Woodworth, J.S. and S.M. Behar, *Mycobacterium tuberculosis-specific CD8+ T cells and their role in immunity.* Crit Rev Immunol, 2006. **26**(4): p. 317-52.
163. Weerdenburg, E.M., P.J. Peters, and N.N. van der Wel, *How do mycobacteria activate CD8+ T cells?* Trends Microbiol, 2010. **18**(1): p. 1-10.
164. Teitelbaum, R., et al., *Mycobacterial infection of macrophages results in membrane-permeable phagosomes.* Proc Natl Acad Sci U S A, 1999. **96**(26): p. 15190-5.
165. Lewinsohn, D.M., et al., *Secreted proteins from Mycobacterium tuberculosis gain access to the cytosolic MHC class-I antigen-processing pathway.* J Immunol, 2006. **177**(1): p. 437-42.
166. Mishra, B.B., et al., *Mycobacterium tuberculosis protein ESAT-6 is a potent activator of the NLRP3/ASC inflammasome.* Cell Microbiol, 2010. **12**(8): p. 1046-63.
167. Winau, F., et al., *Apoptotic vesicles crossprime CD8 T cells and protect against tuberculosis.* Immunity, 2006. **24**(1): p. 105-17.
168. Chen, M., et al., *Lipid mediators in innate immunity against tuberculosis: opposing roles of PGE2 and LXA4 in the induction of macrophage death.* J Exp Med, 2008. **205**(12): p. 2791-801.
169. Divangahi, M., et al., *Eicosanoid pathways regulate adaptive immunity to Mycobacterium tuberculosis.* Nat Immunol, 2010. **11**(8): p. 751-8.
170. Adams, D.O., *The granulomatous inflammatory response. A review.* Am J Pathol, 1976. **84**(1): p. 164-92.
171. Philips, J.A. and J.D. Ernst, *Tuberculosis pathogenesis and immunity.* Annu Rev Pathol, 2012. **7**: p. 353-84.
172. Tsai, M.C., et al., *Characterization of the tuberculous granuloma in murine and human lungs: cellular composition and relative tissue oxygen tension.* Cell Microbiol, 2006. **8**(2): p. 218-32.
173. Via, L.E., et al., *Tuberculous granulomas are hypoxic in guinea pigs, rabbits, and nonhuman primates.* Infect Immun, 2008. **76**(6): p. 2333-40.
174. Egen, J.G., et al., *Macrophage and T cell dynamics during the development and disintegration of mycobacterial granulomas.* Immunity, 2008. **28**(2): p. 271-84.
175. Kataoka, T., *The caspase-8 modulator c-FLIP.* Crit Rev Immunol, 2005. **25**(1): p. 31-58.
176. Dempsey, P.W., et al., *The signaling adaptors and pathways activated by TNF superfamily.* Cytokine Growth Factor Rev, 2003. **14**(3-4): p. 193-209.
177. Youle, R.J. and A. Strasser, *The BCL-2 protein family: opposing activities that mediate cell death.* Nat Rev Mol Cell Biol, 2008. **9**(1): p. 47-59.
178. Fratazzi, C., et al., *Macrophage apoptosis in mycobacterial infections.* J Leukoc Biol, 1999. **66**(5): p. 763-4.
179. Oddo, M., et al., *Fas ligand-induced apoptosis of infected human macrophages reduces the viability of intracellular Mycobacterium tuberculosis.* J Immunol, 1998. **160**(11): p. 5448-54.
180. Zhang, J., et al., *Survival of virulent Mycobacterium tuberculosis involves preventing apoptosis induced by Bcl-2 upregulation and release resulting from necrosis in J774 macrophages.* Microbiol Immunol, 2005. **49**(9): p. 845-52.
181. Loeuillet, C., et al., *Mycobacterium tuberculosis subverts innate immunity to evade specific effectors.* J Immunol, 2006. **177**(9): p. 6245-55.
182. Ordway, D., et al., *Foamy macrophages within lung granulomas of mice infected with Mycobacterium tuberculosis express molecules characteristic of dendritic cells and antiapoptotic markers of the TNF receptor-associated factor family.* J Immunol, 2005. **175**(6): p. 3873-81.
183. Kremer, L., et al., *Mycobacterium bovis Bacillus Calmette Guerin infection prevents apoptosis of resting human monocytes.* Eur J Immunol, 1997. **27**(9): p. 2450-6.
184. Kausalya, S., et al., *Requirement of A1-a for bacillus Calmette-Guerin-mediated protection of macrophages against nitric oxide-induced apoptosis.* J Immunol, 2001. **166**(7): p. 4721-7.

185. Sly, L.M., et al., *Survival of Mycobacterium tuberculosis in host macrophages involves resistance to apoptosis dependent upon induction of antiapoptotic Bcl-2 family member Mcl-1.* J Immunol, 2003. **170**(1): p. 430-7.
186. Hasan, Z., et al., *M. leprae inhibits apoptosis in THP-1 cells by downregulation of Bad and Bak and upregulation of Mcl-1 gene expression.* BMC Microbiol, 2006. **6**: p. 78.
187. Mogga, S.J., et al., *Increased Bcl-2 and reduced Bax expression in infected macrophages in slowly progressive primary murine Mycobacterium tuberculosis infection.* Scand J Immunol, 2002. **56**(4): p. 383-91.
188. Parks, W.C., C.L. Wilson, and Y.S. Lopez-Boado, *Matrix metalloproteinases as modulators of inflammation and innate immunity.* Nat Rev Immunol, 2004. **4**(8): p. 617-29.
189. Chang, J.C., et al., *Effect of Mycobacterium tuberculosis and its components on macrophages and the release of matrix metalloproteinases.* Thorax, 1996. **51**(3): p. 306-11.
190. Price, N.M., et al., *Identification of a matrix-degrading phenotype in human tuberculosis in vitro and in vivo.* J Immunol, 2001. **166**(6): p. 4223-30.
191. Quiding-Jarbrink, M., D.A. Smith, and G.J. Bancroft, *Production of matrix metalloproteinases in response to mycobacterial infection.* Infect Immun, 2001. **69**(9): p. 5661-70.
192. Elkington, P.T., et al., *Mycobacterium tuberculosis, but not vaccine BCG, specifically upregulates matrix metalloproteinase-1.* Am J Respir Crit Care Med, 2005. **172**(12): p. 1596-604.
193. Price, N.M., et al., *Unopposed matrix metalloproteinase-9 expression in human tuberculous granuloma and the role of TNF-alpha-dependent monocyte networks.* J Immunol, 2003. **171**(10): p. 5579-86.
194. Rivera-Marrero, C.A., et al., *The down-regulation of cathepsin G in THP-1 monocytes after infection with Mycobacterium tuberculosis is associated with increased intracellular survival of bacilli.* Infect Immun, 2004. **72**(10): p. 5712-21.
195. Stewart, J.N., et al., *Increased pathology in lungs of mice after infection with an alpha-crystallin mutant of Mycobacterium tuberculosis: changes in cathepsin proteases and certain cytokines.* Microbiology, 2006. **152**(Pt 1): p. 233-44.
196. Reece, S.T., et al., *Serine protease activity contributes to control of Mycobacterium tuberculosis in hypoxic lung granulomas in mice.* J Clin Invest, 2010. **120**(9): p. 3365-76.
197. Buhling, F., et al., *Cathepsin K--a marker of macrophage differentiation?* J Pathol, 2001. **195**(3): p. 375-82.
198. Elkington, P.T., J.M. D'Armiento, and J.S. Friedland, *Tuberculosis immunopathology: the neglected role of extracellular matrix destruction.* Sci Transl Med, 2011. **3**(71): p. 71ps6.
199. Co, D.O., et al., *T cell contributions to the different phases of granuloma formation.* Immunol Lett, 2004. **92**(1-2): p. 135-42.
200. Epstein, W.L., et al., *T-cell independent transfer of organized granuloma formation.* Immunol Lett, 1986. **14**(1): p. 59-63.
201. Suya, H., et al., *Skin granuloma formation in mice immunosuppressed by cyclosporine.* J Invest Dermatol, 1988. **90**(4): p. 430-3.
202. Caruso, A.M., et al., *Mice deficient in CD4 T cells have only transiently diminished levels of IFN-gamma, yet succumb to tuberculosis.* J Immunol, 1999. **162**(9): p. 5407-16.
203. Ladel, C.H., S. Daugelat, and S.H. Kaufmann, *Immune response to Mycobacterium bovis bacille Calmette Guerin infection in major histocompatibility complex class I- and II-deficient knock-out mice: contribution of CD4 and CD8 T cells to acquired resistance.* Eur J Immunol, 1995. **25**(2): p. 377-84.
204. Saunders, B.M., et al., *CD4 is required for the development of a protective granulomatous response to pulmonary tuberculosis.* Cell Immunol, 2002. **216**(1-2): p. 65-72.
205. Fallon, P.G., et al., *Elevated type 1, diminished type 2 cytokines and impaired antibody response are associated with hepatotoxicity and mortalities during Schistosoma mansoni infection of CD4-depleted mice.* Eur J Immunol, 2000. **30**(2): p. 470-80.

206. Hernandez, H.J., et al., *Expression of class II, but not class I, major histocompatibility complex molecules is required for granuloma formation in infection with Schistosoma mansoni.* Eur J Immunol, 1997. **27**(5): p. 1170-6.
207. Barnes, P.F., et al., *Tuberculosis in patients with human immunodeficiency virus infection.* N Engl J Med, 1991. **324**(23): p. 1644-50.
208. Sandor, M., J.V. Weinstock, and T.A. Wynn, *Granulomas in schistosome and mycobacterial infections: a model of local immune responses.* Trends Immunol, 2003. **24**(1): p. 44-52.
209. Cooper, A.M., A. Solache, and S.A. Khader, *Interleukin-12 and tuberculosis: an old story revisited.* Curr Opin Immunol, 2007. **19**(4): p. 441-7.
210. MacMicking, J.D., et al., *Identification of nitric oxide synthase as a protective locus against tuberculosis.* Proc Natl Acad Sci U S A, 1997. **94**(10): p. 5243-8.
211. Cooper, A.M., et al., *Transient loss of resistance to pulmonary tuberculosis in p47(phox-/-) mice.* Infect Immun, 2000. **68**(3): p. 1231-4.
212. Lau, Y.L., et al., *The role of phagocytic respiratory burst in host defense against Mycobacterium tuberculosis.* Clin Infect Dis, 1998. **26**(1): p. 226-7.
213. Sousa, A.O., et al., *Relative contributions of distinct MHC class I-dependent cell populations in protection to tuberculosis infection in mice.* Proc Natl Acad Sci U S A, 2000. **97**(8): p. 4204-8.
214. Turner, J., et al., *CD8- and CD95/95L-dependent mechanisms of resistance in mice with chronic pulmonary tuberculosis.* Am J Respir Cell Mol Biol, 2001. **24**(2): p. 203-9.
215. Flynn, J.L., et al., *Major histocompatibility complex class I-restricted T cells are required for resistance to Mycobacterium tuberculosis infection.* Proc Natl Acad Sci U S A, 1992. **89**(24): p. 12013-7.
216. Behar, S.M., et al., *Susceptibility of mice deficient in CD1D or TAP1 to infection with Mycobacterium tuberculosis.* J Exp Med, 1999. **189**(12): p. 1973-80.
217. D'Souza, C.D., et al., *A novel nonclassic beta2-microglobulin-restricted mechanism influencing early lymphocyte accumulation and subsequent resistance to tuberculosis in the lung.* Am J Respir Cell Mol Biol, 2000. **23**(2): p. 188-93.
218. Thoma-Uszynski, S., C.H. Ladel, and S.H. Kaufmann, *Abscess formation in Listeria monocytogenes-infected gamma delta T cell deficient mouse mutants involves alpha beta T cells.* Microb Pathog, 1997. **22**(2): p. 123-8.
219. Hernandez-Pando, R., et al., *Pulmonary tuberculosis in BALB/c mice with non-functional IL-4 genes: changes in the inflammatory effects of TNF-alpha and in the regulation of fibrosis.* Eur J Immunol, 2004. **34**(1): p. 174-83.
220. Lee, C.G., et al., *Interleukin-13 induces tissue fibrosis by selectively stimulating and activating transforming growth factor beta(1).* J Exp Med, 2001. **194**(6): p. 809-21.
221. Sandler, N.G., et al., *Global gene expression profiles during acute pathogen-induced pulmonary inflammation reveal divergent roles for Th1 and Th2 responses in tissue repair.* J Immunol, 2003. **171**(7): p. 3655-67.
222. Gonzalez-Juarrero, M., et al., *Disruption of granulocyte macrophage-colony stimulating factor production in the lungs severely affects the ability of mice to control Mycobacterium tuberculosis infection.* J Leukoc Biol, 2005. **77**(6): p. 914-22.
223. Szeliga, J., et al., *Granulocyte-macrophage colony stimulating factor-mediated innate responses in tuberculosis.* Tuberculosis (Edinb), 2008. **88**(1): p. 7-20.
224. Nambiar, J.K., et al., *Modulation of pulmonary DC function by vaccine-encoded GM-CSF enhances protective immunity against Mycobacterium tuberculosis infection.* Eur J Immunol, 2010. **40**(1): p. 153-61.
225. Bergeron, A., et al., *Cytokine patterns in tuberculous and sarcoid granulomas: correlations with histopathologic features of the granulomatous response.* J Immunol, 1997. **159**(6): p. 3034-43.
226. Verreck, F.A., et al., *Human IL-23-producing type 1 macrophages promote but IL-10-producing type 2 macrophages subvert immunity to (myco)bacteria.* Proc Natl Acad Sci U S A, 2004. **101**(13): p. 4560-5.

227. Makino, M., et al., *Contribution of GM-CSF on the enhancement of the T cell-stimulating activity of macrophages.* Microbes Infect, 2007. **9**(1): p. 70-7.
228. Vogt, G. and C. Nathan, *In vitro differentiation of human macrophages with enhanced antimycobacterial activity.* J Clin Invest, 2011. **121**(10): p. 3889-901.
229. Trinchieri, G., *Interleukin-12 and the regulation of innate resistance and adaptive immunity.* Nat Rev Immunol, 2003. **3**(2): p. 133-46.
230. Parham, C., et al., *A receptor for the heterodimeric cytokine IL-23 is composed of IL-12Rbeta1 and a novel cytokine receptor subunit, IL-23R.* J Immunol, 2002. **168**(11): p. 5699-708.
231. Cooper, A.M., et al., *Interleukin 12 (IL-12) is crucial to the development of protective immunity in mice intravenously infected with mycobacterium tuberculosis.* J Exp Med, 1997. **186**(1): p. 39-45.
232. Cooper, A.M., et al., *Disseminated tuberculosis in interferon gamma gene-disrupted mice.* J Exp Med, 1993. **178**(6): p. 2243-7.
233. Flynn, J.L., et al., *An essential role for interferon gamma in resistance to Mycobacterium tuberculosis infection.* J Exp Med, 1993. **178**(6): p. 2249-54.
234. Feng, C.G., et al., *Maintenance of pulmonary Th1 effector function in chronic tuberculosis requires persistent IL-12 production.* J Immunol, 2005. **174**(7): p. 4185-92.
235. Ottenhoff, T.H., D. Kumararatne, and J.L. Casanova, *Novel human immunodeficiencies reveal the essential role of type-I cytokines in immunity to intracellular bacteria.* Immunol Today, 1998. **19**(11): p. 491-4.
236. Ozbek, N., et al., *Interleukin-12 receptor beta 1 chain deficiency in a child with disseminated tuberculosis.* Clin Infect Dis, 2005. **40**(6): p. e55-8.
237. Tabarsi, P., et al., *Lethal tuberculosis in a previously healthy adult with IL-12 receptor deficiency.* J Clin Immunol, 2011. **31**(4): p. 537-9.
238. Bustamante, J., et al., *Genetic lessons learned from X-linked Mendelian susceptibility to mycobacterial diseases.* Ann N Y Acad Sci, 2011. **1246**: p. 92-101.
239. Bogunovic, D., et al., *Mycobacterial Disease and Impaired IFN-gamma Immunity in Humans with Inherited ISG15 Deficiency.* Science, 2012.
240. Khader, S.A., et al., *IL-23 compensates for the absence of IL-12p70 and is essential for the IL-17 response during tuberculosis but is dispensable for protection and antigen-specific IFN-gamma responses if IL-12p70 is available.* J Immunol, 2005. **175**(2): p. 788-95.
241. Aujla, S.J., P.J. Dubin, and J.K. Kolls, *Th17 cells and mucosal host defense.* Semin Immunol, 2007. **19**(6): p. 377-82.
242. Khader, S.A., et al., *IL-23 and IL-17 in the establishment of protective pulmonary CD4+ T cell responses after vaccination and during Mycobacterium tuberculosis challenge.* Nat Immunol, 2007. **8**(4): p. 369-77.
243. Gerosa, F., et al., *Differential regulation of interleukin 12 and interleukin 23 production in human dendritic cells.* J Exp Med, 2008. **205**(6): p. 1447-61.
244. Scriba, T.J., et al., *Distinct, specific IL-17- and IL-22-producing CD4+ T cell subsets contribute to the human anti-mycobacterial immune response.* J Immunol, 2008. **180**(3): p. 1962-70.
245. Britton, W.J., et al., *A tumor necrosis factor mimetic peptide activates a murine macrophage cell line to inhibit mycobacterial growth in a nitric oxide-dependent fashion.* Infect Immun, 1998. **66**(5): p. 2122-7.
246. Garcia, I., et al., *High sensitivity of transgenic mice expressing soluble TNFR1 fusion protein to mycobacterial infections: synergistic action of TNF and IFN-gamma in the differentiation of protective granulomas.* Eur J Immunol, 1997. **27**(12): p. 3182-90.
247. Algood, H.M., P.L. Lin, and J.L. Flynn, *Tumor necrosis factor and chemokine interactions in the formation and maintenance of granulomas in tuberculosis.* Clin Infect Dis, 2005. **41 Suppl 3**: p. S189-93.
248. Kindler, V., et al., *The inducing role of tumor necrosis factor in the development of bactericidal granulomas during BCG infection.* Cell, 1989. **56**(5): p. 731-40.

249. Flynn, J.L., et al., *Tumor necrosis factor-alpha is required in the protective immune response against Mycobacterium tuberculosis in mice.* Immunity, 1995. **2**(6): p. 561-72.
250. Mohan, V.P., et al., *Effects of tumor necrosis factor alpha on host immune response in chronic persistent tuberculosis: possible role for limiting pathology.* Infect Immun, 2001. **69**(3): p. 1847-55.
251. Murray, P.J., et al., *T cell-derived IL-10 antagonizes macrophage function in mycobacterial infection.* J Immunol, 1997. **158**(1): p. 315-21.
252. Turner, J., et al., *In vivo IL-10 production reactivates chronic pulmonary tuberculosis in C57BL/6 mice.* J Immunol, 2002. **169**(11): p. 6343-51.
253. Redford, P.S., et al., *Enhanced protection to Mycobacterium tuberculosis infection in IL-10-deficient mice is accompanied by early and enhanced Th1 responses in the lung.* Eur J Immunol, 2010. **40**(8): p. 2200-10.
254. Jacobs, M., et al., *Increased resistance to mycobacterial infection in the absence of interleukin-10.* Immunology, 2000. **100**(4): p. 494-501.
255. Gong, J.H., et al., *Interleukin-10 downregulates Mycobacterium tuberculosis-induced Th1 responses and CTLA-4 expression.* Infect Immun, 1996. **64**(3): p. 913-8.
256. Higgins, D.M., et al., *Lack of IL-10 alters inflammatory and immune responses during pulmonary Mycobacterium tuberculosis infection.* Tuberculosis (Edinb), 2009. **89**(2): p. 149-57.
257. Mogues, T., et al., *The relative importance of T cell subsets in immunity and immunopathology of airborne Mycobacterium tuberculosis infection in mice.* J Exp Med, 2001. **193**(3): p. 271-80.
258. Bean, A.G., et al., *Structural deficiencies in granuloma formation in TNF gene-targeted mice underlie the heightened susceptibility to aerosol Mycobacterium tuberculosis infection, which is not compensated for by lymphotoxin.* J Immunol, 1999. **162**(6): p. 3504-11.
259. Okamoto Yoshida, Y., et al., *Essential role of IL-17A in the formation of a mycobacterial infection-induced granuloma in the lung.* J Immunol, 2010. **184**(8): p. 4414-22.
260. Allen, S.J., S.E. Crown, and T.M. Handel, *Chemokine: receptor structure, interactions, and antagonism.* Annu Rev Immunol, 2007. **25**: p. 787-820.
261. Saunders, B.M. and W.J. Britton, *Life and death in the granuloma: immunopathology of tuberculosis.* Immunol Cell Biol, 2007. **85**(2): p. 103-11.
262. Mendez-Samperio, P., *Expression and regulation of chemokines in mycobacterial infection.* J Infect, 2008. **57**(5): p. 374-84.
263. Rhoades, E.R., A.M. Cooper, and I.M. Orme, *Chemokine response in mice infected with Mycobacterium tuberculosis.* Infect Immun, 1995. **63**(10): p. 3871-7.
264. Lee, J.S., et al., *Expression and regulation of the CC-chemokine ligand 20 during human tuberculosis.* Scand J Immunol, 2008. **67**(1): p. 77-85.
265. Stolberg, V.R., et al., *Cysteine-cysteinyl chemokine receptor 6 mediates invariant natural killer T cell airway recruitment and innate stage resistance during mycobacterial infection.* J Innate Immun, 2011. **3**(1): p. 99-108.
266. Kipnis, A., et al., *Role of chemokine ligand 2 in the protective response to early murine pulmonary tuberculosis.* Immunology, 2003. **109**(4): p. 547-51.
267. Vesosky, B., et al., *CCL5 participates in early protection against Mycobacterium tuberculosis.* J Leukoc Biol, 2010. **87**(6): p. 1153-65.
268. Peters, W., et al., *Chemokine receptor 2 serves an early and essential role in resistance to Mycobacterium tuberculosis.* Proc Natl Acad Sci U S A, 2001. **98**(14): p. 7958-63.
269. Scott, H.M. and J.L. Flynn, *Mycobacterium tuberculosis in chemokine receptor 2-deficient mice: influence of dose on disease progression.* Infect Immun, 2002. **70**(11): p. 5946-54.
270. Stolberg, V.R., et al., *CC chemokine receptor 4 contributes to innate NK and chronic stage T helper cell recall responses during Mycobacterium bovis infection.* Am J Pathol, 2011. **178**(1): p. 233-44.

271. Algood, H.M. and J.L. Flynn, *CCR5-deficient mice control Mycobacterium tuberculosis infection despite increased pulmonary lymphocytic infiltration.* J Immunol, 2004. **173**(5): p. 3287-96.
272. Olmos, S., S. Stukes, and J.D. Ernst, *Ectopic activation of Mycobacterium tuberculosis-specific CD4+ T cells in lungs of CCR7-/- mice.* J Immunol, 2010. **184**(2): p. 895-901.
273. Goncalves, A.S. and R. Appelberg, *The involvement of the chemokine receptor CXCR2 in neutrophil recruitment in LPS-induced inflammation and in Mycobacterium avium infection.* Scand J Immunol, 2002. **55**(6): p. 585-91.
274. Seiler, P., et al., *Early granuloma formation after aerosol Mycobacterium tuberculosis infection is regulated by neutrophils via CXCR3-signaling chemokines.* Eur J Immunol, 2003. **33**(10): p. 2676-86.
275. Hall, J.D., et al., *The impact of chemokine receptor CX3CR1 deficiency during respiratory infections with Mycobacterium tuberculosis or Francisella tularensis.* Clin Exp Immunol, 2009. **156**(2): p. 278-84.
276. Helming, L. and S. Gordon, *Molecular mediators of macrophage fusion.* Trends Cell Biol, 2009. **19**(10): p. 514-22.
277. van Maarsseveen, T.C., W. Vos, and P.J. van Diest, *Giant cell formation in sarcoidosis: cell fusion or proliferation with non-division?* Clin Exp Immunol, 2009. **155**(3): p. 476-86.
278. Kurihara, N., S. Gluck, and G.D. Roodman, *Sequential expression of phenotype markers for osteoclasts during differentiation of precursors for multinucleated cells formed in long-term human marrow cultures.* Endocrinology, 1990. **127**(6): p. 3215-21.
279. Fujikawa, Y., et al., *The human osteoclast precursor circulates in the monocyte fraction.* Endocrinology, 1996. **137**(9): p. 4058-60.
280. Rivollier, A., et al., *Immature dendritic cell transdifferentiation into osteoclasts: a novel pathway sustained by the rheumatoid arthritis microenvironment.* Blood, 2004. **104**(13): p. 4029-37.
281. Arai, F., et al., *Commitment and differentiation of osteoclast precursor cells by the sequential expression of c-Fms and receptor activator of nuclear factor kappaB (RANK) receptors.* J Exp Med, 1999. **190**(12): p. 1741-54.
282. Lacey, D.L., et al., *Osteoprotegerin ligand is a cytokine that regulates osteoclast differentiation and activation.* Cell, 1998. **93**(2): p. 165-76.
283. Yasuda, H., et al., *Osteoclast differentiation factor is a ligand for osteoprotegerin/osteoclastogenesis-inhibitory factor and is identical to TRANCE/RANKL.* Proc Natl Acad Sci U S A, 1998. **95**(7): p. 3597-602.
284. Kong, Y.Y., et al., *OPGL is a key regulator of osteoclastogenesis, lymphocyte development and lymph-node organogenesis.* Nature, 1999. **397**(6717): p. 315-23.
285. Wiktor-Jedrzejczak, W., et al., *Total absence of colony-stimulating factor 1 in the macrophage-deficient osteopetrotic (op/op) mouse.* Proc Natl Acad Sci U S A, 1990. **87**(12): p. 4828-32.
286. Yoshida, H., et al., *The murine mutation osteopetrosis is in the coding region of the macrophage colony stimulating factor gene.* Nature, 1990. **345**(6274): p. 442-4.
287. Kim, M.S., C.J. Day, and N.A. Morrison, *MCP-1 is induced by receptor activator of nuclear factor-{kappa}B ligand, promotes human osteoclast fusion, and rescues granulocyte macrophage colony-stimulating factor suppression of osteoclast formation.* J Biol Chem, 2005. **280**(16): p. 16163-9.
288. Kim, M.S., et al., *MCP-1-induced human osteoclast-like cells are tartrate-resistant acid phosphatase, NFATc1, and calcitonin receptor-positive but require receptor activator of NFkappaB ligand for bone resorption.* J Biol Chem, 2006. **281**(2): p. 1274-85.
289. Hounoki, H., et al., *Activation of peroxisome proliferator-activated receptor gamma inhibits TNF-alpha-mediated osteoclast differentiation in human peripheral monocytes in part via suppression of monocyte chemoattractant protein-1 expression.* Bone, 2008. **42**(4): p. 765-74.

290. Miyamoto, K., et al., *MCP-1 expressed by osteoclasts stimulates osteoclastogenesis in an autocrine/paracrine manner.* Biochem Biophys Res Commun, 2009. **383**(3): p. 373-7.
291. Yagi, M., et al., *DC-STAMP is essential for cell-cell fusion in osteoclasts and foreign body giant cells.* J Exp Med, 2005. **202**(3): p. 345-51.
292. Saginario, C., et al., *MFR, a putative receptor mediating the fusion of macrophages.* Mol Cell Biol, 1998. **18**(11): p. 6213-23.
293. Han, X., et al., *CD47, a ligand for the macrophage fusion receptor, participates in macrophage multinucleation.* J Biol Chem, 2000. **275**(48): p. 37984-92.
294. Destaing, O., et al., *Podosomes display actin turnover and dynamic self-organization in osteoclasts expressing actin-green fluorescent protein.* Mol Biol Cell, 2003. **14**(2): p. 407-16.
295. Lakkakorpi, P., et al., *Organization of osteoclast microfilaments during the attachment to bone surface in vitro.* J Bone Miner Res, 1989. **4**(6): p. 817-25.
296. Vaananen, H.K. and M. Horton, *The osteoclast clear zone is a specialized cell-extracellular matrix adhesion structure.* J Cell Sci, 1995. **108 (Pt 8)**: p. 2729-32.
297. Roux, S., *New treatment targets in osteoporosis.* Joint Bone Spine, 2010. **77**(3): p. 222-8.
298. Takayanagi, H., *Osteoimmunology: shared mechanisms and crosstalk between the immune and bone systems.* Nat Rev Immunol, 2007. **7**(4): p. 292-304.
299. Arron, J.R. and Y. Choi, *Bone versus immune system.* Nature, 2000. **408**(6812): p. 535-6.
300. Li, H., et al., *Cross talk between the bone and immune systems: osteoclasts function as antigen-presenting cells and activate CD4+ and CD8+ T cells.* Blood, 2010. **116**(2): p. 210-7.
301. Anderson, J.M., *Multinucleated giant cells.* Curr Opin Hematol, 2000. **7**(1): p. 40-7.
302. McNally, A.K. and J.M. Anderson, *Interleukin-4 induces foreign body giant cells from human monocytes/macrophages. Differential lymphokine regulation of macrophage fusion leads to morphological variants of multinucleated giant cells.* Am J Pathol, 1995. **147**(5): p. 1487-99.
303. DeFife, K.M., et al., *Interleukin-13 induces human monocyte/macrophage fusion and macrophage mannose receptor expression.* J Immunol, 1997. **158**(7): p. 3385-90.
304. Kao, W.J., et al., *Role for interleukin-4 in foreign-body giant cell formation on a poly(etherurethane urea) in vivo.* J Biomed Mater Res, 1995. **29**(10): p. 1267-75.
305. Puissegur, M.P., et al., *Mycobacterial lipomannan induces granuloma macrophage fusion via a TLR2-dependent, ADAM9- and beta1 integrin-mediated pathway.* J Immunol, 2007. **178**(5): p. 3161-9.
306. Coury, F., et al., *Langerhans cell histiocytosis reveals a new IL-17A-dependent pathway of dendritic cell fusion.* Nat Med, 2008. **14**(1): p. 81-7.
307. Rouvier, E., et al., *CTLA-8, cloned from an activated T cell, bearing AU-rich messenger RNA instability sequences, and homologous to a herpesvirus saimiri gene.* J Immunol, 1993. **150**(12): p. 5445-56.
308. Yao, Z., et al., *Human IL-17: a novel cytokine derived from T cells.* J Immunol, 1995. **155**(12): p. 5483-6.
309. Iwakura, Y., et al., *Functional specialization of interleukin-17 family members.* Immunity, 2011. **34**(2): p. 149-62.
310. Wright, J.F., et al., *Identification of an interleukin 17F/17A heterodimer in activated human CD4+ T cells.* J Biol Chem, 2007. **282**(18): p. 13447-55.
311. Gaffen, S.L., *Structure and signalling in the IL-17 receptor family.* Nat Rev Immunol, 2009. **9**(8): p. 556-67.
312. Novatchkova, M., et al., *The STIR-domain superfamily in signal transduction, development and immunity.* Trends Biochem Sci, 2003. **28**(5): p. 226-9.
313. Qian, Y., et al., *The adaptor Act1 is required for interleukin 17-dependent signaling associated with autoimmune and inflammatory disease.* Nat Immunol, 2007. **8**(3): p. 247-56.
314. Bulek, K., et al., *The inducible kinase IKKi is required for IL-17-dependent signaling associated with neutrophilia and pulmonary inflammation.* Nat Immunol, 2011. **12**(9): p. 844-52.

315. Sun, D., et al., *Treatment with IL-17 prolongs the half-life of chemokine CXCL1 mRNA via the adaptor TRAF5 and the splicing-regulatory factor SF2 (ASF).* Nat Immunol, 2011. **12**(9): p. 853-60.
316. Mosmann, T.R., et al., *Two types of murine helper T cell clone. I. Definition according to profiles of lymphokine activities and secreted proteins.* J Immunol, 1986. **136**(7): p. 2348-57.
317. Mosmann, T.R. and R.L. Coffman, *TH1 and TH2 cells: different patterns of lymphokine secretion lead to different functional properties.* Annu Rev Immunol, 1989. **7**: p. 145-73.
318. Harrington, L.E., et al., *Interleukin 17-producing CD4+ effector T cells develop via a lineage distinct from the T helper type 1 and 2 lineages.* Nat Immunol, 2005. **6**(11): p. 1123-32.
319. Langrish, C.L., et al., *IL-23 drives a pathogenic T cell population that induces autoimmune inflammation.* J Exp Med, 2005. **201**(2): p. 233-40.
320. Park, H., et al., *A distinct lineage of CD4 T cells regulates tissue inflammation by producing interleukin 17.* Nat Immunol, 2005. **6**(11): p. 1133-41.
321. Cua, D.J. and C.M. Tato, *Innate IL-17-producing cells: the sentinels of the immune system.* Nat Rev Immunol, 2010. **10**(7): p. 479-89.
322. Veldhoen, M., et al., *TGFbeta in the context of an inflammatory cytokine milieu supports de novo differentiation of IL-17-producing T cells.* Immunity, 2006. **24**(2): p. 179-89.
323. Ghoreschi, K., et al., *Generation of pathogenic T(H)17 cells in the absence of TGF-beta signalling.* Nature, 2010. **467**(7318): p. 967-71.
324. Hu, W., et al., *Priming Microenvironments Dictate Cytokine Requirements for T Helper 17 Cell Lineage Commitment.* Immunity, 2011.
325. Manel, N., D. Unutmaz, and D.R. Littman, *The differentiation of human T(H)-17 cells requires transforming growth factor-beta and induction of the nuclear receptor RORgammat.* Nat Immunol, 2008. **9**(6): p. 641-9.
326. McGeachy, M.J. and D.J. Cua, *Th17 cell differentiation: the long and winding road.* Immunity, 2008. **28**(4): p. 445-53.
327. Annunziato, F., et al., *Phenotypic and functional features of human Th17 cells.* J Exp Med, 2007. **204**(8): p. 1849-61.
328. Hirota, K., et al., *Preferential recruitment of CCR6-expressing Th17 cells to inflamed joints via CCL20 in rheumatoid arthritis and its animal model.* J Exp Med, 2007. **204**(12): p. 2803-12.
329. Curtis, M.M. and S.S. Way, *Interleukin-17 in host defence against bacterial, mycobacterial and fungal pathogens.* Immunology, 2009. **126**(2): p. 177-85.
330. Ouyang, W., J.K. Kolls, and Y. Zheng, *The biological functions of T helper 17 cell effector cytokines in inflammation.* Immunity, 2008. **28**(4): p. 454-67.
331. Hu, Y., et al., *The IL-17 pathway as a major therapeutic target in autoimmune diseases.* Ann N Y Acad Sci, 2011. **1217**: p. 60-76.
332. Gaffen, S.L., *An overview of IL-17 function and signaling.* Cytokine, 2008. **43**(3): p. 402-7.
333. Iwakura, Y., et al., *The roles of IL-17A in inflammatory immune responses and host defense against pathogens.* Immunol Rev, 2008. **226**: p. 57-79.
334. Fossiez, F., et al., *T cell interleukin-17 induces stromal cells to produce proinflammatory and hematopoietic cytokines.* J Exp Med, 1996. **183**(6): p. 2593-603.
335. Schwarzenberger, P., et al., *IL-17 stimulates granulopoiesis in mice: use of an alternate, novel gene therapy-derived method for in vivo evaluation of cytokines.* J Immunol, 1998. **161**(11): p. 6383-9.
336. Forlow, S.B., et al., *Increased granulopoiesis through interleukin-17 and granulocyte colony-stimulating factor in leukocyte adhesion molecule-deficient mice.* Blood, 2001. **98**(12): p. 3309-14.
337. Laan, M., et al., *Neutrophil recruitment by human IL-17 via C-X-C chemokine release in the airways.* J Immunol, 1999. **162**(4): p. 2347-52.
338. Witowski, J., et al., *IL-17 stimulates intraperitoneal neutrophil infiltration through the release of GRO alpha chemokine from mesothelial cells.* J Immunol, 2000. **165**(10): p. 5814-21.

339. Acosta-Rodriguez, E.V., et al., *Surface phenotype and antigenic specificity of human interleukin 17-producing T helper memory cells.* Nat Immunol, 2007. **8**(6): p. 639-46.
340. Pene, J., et al., *Chronically inflamed human tissues are infiltrated by highly differentiated Th17 lymphocytes.* J Immunol, 2008. **180**(11): p. 7423-30.
341. Shibata, K., et al., *Resident Vdelta1+ gammadelta T cells control early infiltration of neutrophils after Escherichia coli infection via IL-17 production.* J Immunol, 2007. **178**(7): p. 4466-72.
342. Liu, J., et al., *Early production of IL-17 protects against acute pulmonary Pseudomonas aeruginosa infection in mice.* FEMS Immunol Med Microbiol, 2010.
343. Ye, P., et al., *Interleukin-17 and lung host defense against Klebsiella pneumoniae infection.* Am J Respir Cell Mol Biol, 2001. **25**(3): p. 335-40.
344. Huang, W., et al., *Requirement of interleukin-17A for systemic anti-Candida albicans host defense in mice.* J Infect Dis, 2004. **190**(3): p. 624-31.
345. Kelly, M.N., et al., *Interleukin-17/interleukin-17 receptor-mediated signaling is important for generation of an optimal polymorphonuclear response against Toxoplasma gondii infection.* Infect Immun, 2005. **73**(1): p. 617-21.
346. Lin, Y., et al., *Interleukin-17 is required for T helper 1 cell immunity and host resistance to the intracellular pathogen Francisella tularensis.* Immunity, 2009. **31**(5): p. 799-810.
347. Khader, S.A. and R. Gopal, *IL-17 in protective immunity to intracellular pathogens.* Virulence, 2010. **1**(5): p. 423-7.
348. Lu, Y.J., et al., *Interleukin-17A mediates acquired immunity to pneumococcal colonization.* PLoS Pathog, 2008. **4**(9): p. e1000159.
349. Higgins, S.C., et al., *TLR4 mediates vaccine-induced protective cellular immunity to Bordetella pertussis: role of IL-17-producing T cells.* J Immunol, 2006. **177**(11): p. 7980-9.
350. Yang, D., et al., *Beta-defensins: linking innate and adaptive immunity through dendritic and T cell CCR6.* Science, 1999. **286**(5439): p. 525-8.
351. Milner, J.D., et al., *Impaired T(H)17 cell differentiation in subjects with autosomal dominant hyper-IgE syndrome.* Nature, 2008. **452**(7188): p. 773-6.
352. Ferwerda, B., et al., *Human dectin-1 deficiency and mucocutaneous fungal infections.* N Engl J Med, 2009. **361**(18): p. 1760-7.
353. Glocker, E.O., et al., *A homozygous CARD9 mutation in a family with susceptibility to fungal infections.* N Engl J Med, 2009. **361**(18): p. 1727-35.
354. Kisand, K., et al., *Chronic mucocutaneous candidiasis in APECED or thymoma patients correlates with autoimmunity to Th17-associated cytokines.* J Exp Med, 2010. **207**(2): p. 299-308.
355. Puel, A., et al., *Chronic mucocutaneous candidiasis in humans with inborn errors of interleukin-17 immunity.* Science, 2011. **332**(6025): p. 65-8.
356. Pappu, R., V. Ramirez-Carrozzi, and A. Sambandam, *The interleukin-17 cytokine family: critical players in host defence and inflammatory diseases.* Immunology, 2011. **134**(1): p. 8-16.
357. Nakae, S., et al., *Suppression of immune induction of collagen-induced arthritis in IL-17-deficient mice.* J Immunol, 2003. **171**(11): p. 6173-7.
358. Lubberts, E., et al., *IL-1-independent role of IL-17 in synovial inflammation and joint destruction during collagen-induced arthritis.* J Immunol, 2001. **167**(2): p. 1004-13.
359. Duerr, R.H., et al., *A genome-wide association study identifies IL23R as an inflammatory bowel disease gene.* Science, 2006. **314**(5804): p. 1461-3.
360. Nair, R.P., et al., *Genome-wide scan reveals association of psoriasis with IL-23 and NF-kappaB pathways.* Nat Genet, 2009. **41**(2): p. 199-204.
361. Lubberts, E., *IL-17/Th17 targeting: on the road to prevent chronic destructive arthritis?* Cytokine, 2008. **41**(2): p. 84-91.
362. Egeler, R.M., et al., *Langerhans cell histiocytosis: fascinating dynamics of the dendritic cell-macrophage lineage.* Immunol Rev, 2010. **234**(1): p. 213-32.

363. Merad, M., et al., *Langerhans cells renew in the skin throughout life under steady-state conditions.* Nat Immunol, 2002. **3**(12): p. 1135-41.
364. Wang, Y., et al., *IL-34 is a tissue-restricted ligand of CSF1R required for the development of Langerhans cells and microglia.* Nat Immunol, 2012. **13**(8): p. 753-60.
365. Peters, T.L., K.L. McClain, and C.E. Allen, *Neither IL-17A mRNA nor IL-17A protein are detectable in Langerhans cell histiocytosis lesions.* Mol Ther, 2011. **19**(8): p. 1433-9.
366. Feuillet, S., B. Giroux-Leprieur, and A. Tazi, *[Pulmonary Langerhans cell histiocytosis in adults].* Presse Med, 2010. **39**(1): p. 107-15.
367. Reece, S.T. and S.H. Kaufmann, *Floating between the poles of pathology and protection: can we pin down the granuloma in tuberculosis?* Curr Opin Microbiol, 2012. **15**(1): p. 63-70.
368. Davis, J.M. and L. Ramakrishnan, *The role of the granuloma in expansion and dissemination of early tuberculous infection.* Cell, 2009. **136**(1): p. 37-49.
369. Volkman, H.E., et al., *Tuberculous granuloma induction via interaction of a bacterial secreted protein with host epithelium.* Science, 2010. **327**(5964): p. 466-9.
370. Ramakrishnan, L., *Revisiting the role of the granuloma in tuberculosis.* Nat Rev Immunol, 2012. **12**(5): p. 352-66.
371. Cosma, C.L., D.R. Sherman, and L. Ramakrishnan, *The secret lives of the pathogenic mycobacteria.* Annu Rev Microbiol, 2003. **57**: p. 641-76.
372. Ehlers, S., *Tumor necrosis factor and its blockade in granulomatous infections: differential modes of action of infliximab and etanercept?* Clin Infect Dis, 2005. **41 Suppl 3**: p. S199-203.
373. Ehlers, S., *TB or not TB? Fishing for Molecules Making Permissive granulomas.* Cell Host Microbe, 2010. **7**(1): p. 6-8.
374. Basaraba, R.J., *Experimental tuberculosis: the role of comparative pathology in the discovery of improved tuberculosis treatment strategies.* Tuberculosis (Edinb), 2008. **88 Suppl 1**: p. S35-47.
375. Koebel, C.M., et al., *Adaptive immunity maintains occult cancer in an equilibrium state.* Nature, 2007. **450**(7171): p. 903-7.
376. Melief, C.J., *Cancer: immune pact with the enemy.* Nature, 2007. **450**(7171): p. 803-4.
377. Brackstone, M., J.L. Townson, and A.F. Chambers, *Tumour dormancy in breast cancer: an update.* Breast Cancer Res, 2007. **9**(3): p. 208.
378. Willis, L., et al., *Breast cancer dormancy can be maintained by small numbers of micrometastases.* Cancer Res, 2010. **70**(11): p. 4310-7.
379. Fujino, S., et al., *Increased expression of interleukin 17 in inflammatory bowel disease.* Gut, 2003. **52**(1): p. 65-70.
380. Facco, M., et al., *Sarcoidosis is a Th1/Th17 multisystem disorder.* Thorax, 2011. **66**(2): p. 144-50.
381. Ten Berge, B., et al., *Increased IL-17A expression in granulomas and in circulating memory T cells in sarcoidosis.* Rheumatology (Oxford), 2012. **51**(1): p. 37-46.
382. Janssen, C.E., et al., *Morphologic and immunohistochemical characterization of granulomas in the nucleotide oligomerization domain 2-related disorders Blau syndrome and Crohn disease.* J Allergy Clin Immunol, 2012. **129**(4): p. 1076-84.
383. Blanco, F.C., et al., *Increased IL-17 expression is associated with pathology in a bovine model of tuberculosis.* Tuberculosis (Edinb), 2011. **91**(1): p. 57-63.
384. Rutitzky, L.I., J.R. Lopes da Rosa, and M.J. Stadecker, *Severe CD4 T cell-mediated immunopathology in murine schistosomiasis is dependent on IL-12p40 and correlates with high levels of IL-17.* J Immunol, 2005. **175**(6): p. 3920-6.
385. Wen, X., et al., *Dynamics of Th17 Cells and Their Role in Schistosoma japonicum Infection in C57BL/6 Mice.* PLoS Negl Trop Dis, 2011. **5**(11): p. e1399.
386. Smith, P.M., et al., *Genetic control of severe egg-induced immunopathology and IL-17 production in murine schistosomiasis.* J Immunol, 2009. **183**(5): p. 3317-23.

387. Hamada, S., et al., *IL-17A produced by gammadelta T cells plays a critical role in innate immunity against listeria monocytogenes infection in the liver.* J Immunol, 2008. **181**(5): p. 3456-63.
388. Tanaka, T., et al., *PDLIM2 Inhibits T Helper 17 Cell Development and Granulomatous Inflammation Through Degradation of STAT3.* Sci Signal, 2011. **4**(202): p. ra85.
389. Kallenberg, C.G., *Pathophysiology of ANCA-associated small vessel vasculitis.* Curr Rheumatol Rep, 2010. **12**(6): p. 399-405.
390. Van Kooten, C., et al., *Interleukin-17 activates human renal epithelial cells in vitro and is expressed during renal allograft rejection.* J Am Soc Nephrol, 1998. **9**(8): p. 1526-34.
391. Kao, C.Y., et al., *Up-regulation of CC chemokine ligand 20 expression in human airway epithelium by IL-17 through a JAK-independent but MEK/NF-kappaB-dependent signaling pathway.* J Immunol, 2005. **175**(10): p. 6676-85.
392. Shahrara, S., et al., *IL-17-mediated monocyte migration occurs partially through CC chemokine ligand 2/monocyte chemoattractant protein-1 induction.* J Immunol, 2010. **184**(8): p. 4479-87.
393. Annels, N.E., et al., *Aberrant chemokine receptor expression and chemokine production by Langerhans cells underlies the pathogenesis of Langerhans cell histiocytosis.* J Exp Med, 2003. **197**(10): p. 1385-90.
394. Facco, M., et al., *Expression and role of CCR6/CCL20 chemokine axis in pulmonary sarcoidosis.* J Leukoc Biol, 2007. **82**(4): p. 946-55.
395. Joshi, A.D., et al., *TLR3 modulates immunopathology during a Schistosoma mansoni egg-driven Th2 response in the lung.* Eur J Immunol, 2008. **38**(12): p. 3436-49.
396. Hussain, R., et al., *CCL2/MCP-I genotype-phenotype relationship in latent tuberculosis infection.* PLoS One, 2011. **6**(10): p. e25803.
397. Palchevskiy, V., et al., *Immune response CC chemokines CCL2 and CCL5 are associated with pulmonary sarcoidosis.* Fibrogenesis Tissue Repair, 2011. **4**: p. 10.
398. Schreiber, O., et al., *Mice that overexpress CC chemokine ligand 2 in their lungs show increased protective immunity to infection with Mycobacterium bovis bacille Calmette-Guerin.* J Infect Dis, 2008. **198**(7): p. 1044-54.
399. Kyriakides, T.R., et al., *The CC chemokine ligand, CCL2/MCP1, participates in macrophage fusion and foreign body giant cell formation.* Am J Pathol, 2004. **165**(6): p. 2157-66.
400. Li, X., et al., *Parathyroid hormone stimulates osteoblastic expression of MCP-1 to recruit and increase the fusion of pre/osteoclasts.* J Biol Chem, 2007. **282**(45): p. 33098-106.
401. Giuliani, N., et al., *CC-chemokine ligand 20/macrophage inflammatory protein-3alpha and CC-chemokine receptor 6 are overexpressed in myeloma microenvironment related to osteolytic bone lesions.* Cancer Res, 2008. **68**(16): p. 6840-50.
402. Fantuzzi, L., et al., *Endogenous CCL2 (monocyte chemotactic protein-1) modulates human immunodeficiency virus type-1 replication and affects cytoskeleton organization in human monocyte-derived macrophages.* Blood, 2003. **102**(7): p. 2334-7.
403. Jay, S.M., et al., *Foreign body giant cell formation is preceded by lamellipodia formation and can be attenuated by inhibition of Rac1 activation.* Am J Pathol, 2007. **171**(2): p. 632-40.
404. MacLauchlan, S., et al., *Macrophage fusion, giant cell formation, and the foreign body response require matrix metalloproteinase 9.* J Leukoc Biol, 2009. **85**(4): p. 617-26.
405. Vignery, A., *Macrophage fusion: the making of osteoclasts and giant cells.* J Exp Med, 2005. **202**(3): p. 337-40.
406. D'Souza, B.N., et al., *Nuclear factor kappa B-dependent activation of the antiapoptotic bfl-1 gene by the Epstein-Barr virus latent membrane protein 1 and activated CD40 receptor.* J Virol, 2004. **78**(4): p. 1800-16.
407. Senechal, B., et al., *Expansion of regulatory T cells in patients with Langerhans cell histiocytosis.* PLoS Med, 2007. **4**(8): p. e253.

408. Miyazaki, T., et al., *Increased susceptibility of thymocytes to apoptosis in mice lacking AIM, a novel murine macrophage-derived soluble factor belonging to the scavenger receptor cysteine-rich domain superfamily.* J Exp Med, 1999. **189**(2): p. 413-22.
409. Xaus, J., et al., *High expression of p21 Waf1 in sarcoid granulomas: a putative role for long-lasting inflammation.* J Leukoc Biol, 2003. **74**(2): p. 295-301.
410. Langley, R.J., et al., *Granuloma formation induced by low-dose chronic silica inhalation is associated with an anti-apoptotic response in Lewis rats.* J Toxicol Environ Health A, 2010. **73**(10): p. 669-83.
411. Dhiman, R., M. Raje, and S. Majumdar, *Differential expression of NF-kappaB in mycobacteria infected THP-1 affects apoptosis.* Biochim Biophys Acta, 2007. **1770**(4): p. 649-58.
412. Schutze, S., et al., *TNF-induced activation of NF-kappa B.* Immunobiology, 1995. **193**(2-4): p. 193-203.
413. Wang, C.Y., et al., *NF-kappaB induces expression of the Bcl-2 homologue A1/Bfl-1 to preferentially suppress chemotherapy-induced apoptosis.* Mol Cell Biol, 1999. **19**(9): p. 5923-9.
414. Takada, Y., M. Andreeff, and B.B. Aggarwal, *Indole-3-carbinol suppresses NF-kappaB and IkappaBalpha kinase activation, causing inhibition of expression of NF-kappaB-regulated antiapoptotic and metastatic gene products and enhancement of apoptosis in myeloid and leukemia cells.* Blood, 2005. **106**(2): p. 641-9.
415. Pagliari, L.J., et al., *Macrophages require constitutive NF-kappaB activation to maintain A1 expression and mitochondrial homeostasis.* Mol Cell Biol, 2000. **20**(23): p. 8855-65.
416. Gallois, A., et al., *Genome-wide expression analyses establish dendritic cells as a new osteoclast precursor able to generate bone-resorbing cells more efficiently than monocytes.* J Bone Miner Res, 2010. **25**(3): p. 661-72.
417. da Costa, C.E., et al., *Presence of osteoclast-like multinucleated giant cells in the bone and nonostotic lesions of Langerhans cell histiocytosis.* J Exp Med, 2005. **201**(5): p. 687-93.
418. Rust, R., et al., *Gene expression analysis of dendritic/Langerhans cells and Langerhans cell histiocytosis.* J Pathol, 2006. **209**(4): p. 474-83.
419. Denis, M. and E. Ghadirian, *Granulocyte-macrophage colony-stimulating factor restricts growth of tubercle bacilli in human macrophages.* Immunol Lett, 1990. **24**(3): p. 203-6.
420. Houghton, A.M., et al., *Macrophage elastase kills bacteria within murine macrophages.* Nature, 2009. **460**(7255): p. 637-41.
421. Welin, A., et al., *Importance of phagosomal functionality for growth restriction of Mycobacterium tuberculosis in primary human macrophages.* J Innate Immun, 2011. **3**(5): p. 508-18.
422. Singh, C.R., et al., *Processing and presentation of a mycobacterial antigen 85B epitope by murine macrophages is dependent on the phagosomal acquisition of vacuolar proton ATPase and in situ activation of cathepsin D.* J Immunol, 2006. **177**(5): p. 3250-9.
423. Yang, C.S., et al., *NADPH oxidase 2 interaction with TLR2 is required for efficient innate immune responses to mycobacteria via cathelicidin expression.* J Immunol, 2009. **182**(6): p. 3696-705.
424. Efstratiadis, T. and D.W. Moss, *Tartrate-resistant acid phosphatase in human alveolar macrophages.* Enzyme, 1985. **34**(3): p. 140-3.
425. Hayman, A.R., et al., *Tartrate-resistant acid phosphatase (Acp 5): identification in diverse human tissues and dendritic cells.* J Histochem Cytochem, 2001. **49**(6): p. 675-84.
426. Halleen, J.M., et al., *Intracellular fragmentation of bone resorption products by reactive oxygen species generated by osteoclastic tartrate-resistant acid phosphatase.* J Biol Chem, 1999. **274**(33): p. 22907-10.
427. Halleen, J.M., et al., *Tartrate-resistant acid phosphatase 5b (TRACP 5b) as a marker of bone resorption.* Clin Lab, 2006. **52**(9-10): p. 499-509.

428. Raisanen, S.R., et al., *Macrophages overexpressing tartrate-resistant acid phosphatase show altered profile of free radical production and enhanced capacity of bacterial killing.* Biochem Biophys Res Commun, 2005. **331**(1): p. 120-6.
429. Byrd, T.F., *Multinucleated giant cell formation induced by IFN-gamma/IL-3 is associated with restriction of virulent Mycobacterium tuberculosis cell to cell invasion in human monocyte monolayers.* Cell Immunol, 1998. **188**(2): p. 89-96.
430. Shapiro, S.D., D.K. Kobayashi, and T.J. Ley, *Cloning and characterization of a unique elastolytic metalloproteinase produced by human alveolar macrophages.* J Biol Chem, 1993. **268**(32): p. 23824-9.
431. Chakraborti, S., et al., *Regulation of matrix metalloproteinases: an overview.* Mol Cell Biochem, 2003. **253**(1-2): p. 269-85.
432. Demedts, I.K., et al., *Elevated MMP-12 protein levels in induced sputum from patients with COPD.* Thorax, 2006. **61**(3): p. 196-201.
433. Hautamaki, R.D., et al., *Requirement for macrophage elastase for cigarette smoke-induced emphysema in mice.* Science, 1997. **277**(5334): p. 2002-4.
434. Crouser, E.D., et al., *Gene expression profiling identifies MMP-12 and ADAMDEC1 as potential pathogenic mediators of pulmonary sarcoidosis.* Am J Respir Crit Care Med, 2009. **179**(10): p. 929-38.
435. Moller, D.R., *Cells and cytokines involved in the pathogenesis of sarcoidosis.* Sarcoidosis Vasc Diffuse Lung Dis, 1999. **16**(1): p. 24-31.
436. Colasante, A., et al., *Langerhans cells in Langerhans cell histiocytosis and peripheral adenocarcinomas of the lung.* Am Rev Respir Dis, 1993. **148**(3): p. 752-9.
437. Benes, P., V. Vetvicka, and M. Fusek, *Cathepsin D--many functions of one aspartic protease.* Crit Rev Oncol Hematol, 2008. **68**(1): p. 12-28.
438. Hakala, J.K., et al., *Lysosomal enzymes are released from cultured human macrophages, hydrolyze LDL in vitro, and are present extracellularly in human atherosclerotic lesions.* Arterioscler Thromb Vasc Biol, 2003. **23**(8): p. 1430-6.
439. Vashishta, A., et al., *Procathepsin D secreted by HaCaT keratinocyte cells - A novel regulator of keratinocyte growth.* Eur J Cell Biol, 2007. **86**(6): p. 303-13.
440. Briozzo, P., et al., *In vitro degradation of extracellular matrix with Mr 52,000 cathepsin D secreted by breast cancer cells.* Cancer Res, 1988. **48**(13): p. 3688-92.
441. Dabrosin, C., A.C. Johansson, and K. Ollinger, *Decreased secretion of Cathepsin D in breast cancer in vivo by tamoxifen: mediated by the mannose-6-phosphate/IGF-II receptor?* Breast Cancer Res Treat, 2004. **85**(3): p. 229-38.
442. Converse, P.J., et al., *Cavitary tuberculosis produced in rabbits by aerosolized virulent tubercle bacilli.* Infect Immun, 1996. **64**(11): p. 4776-87.
443. Puissegur, M.P., et al., *An in vitro dual model of mycobacterial granulomas to investigate the molecular interactions between mycobacteria and human host cells.* Cell Microbiol, 2004. **6**(5): p. 423-33.
444. Cruz, A., et al., *Pathological role of interleukin 17 in mice subjected to repeated BCG vaccination after infection with Mycobacterium tuberculosis.* J Exp Med, 2010. **207**(8): p. 1609-16.
445. Cruz, A., et al., *Cutting edge: IFN-gamma regulates the induction and expansion of IL-17-producing CD4 T cells during mycobacterial infection.* J Immunol, 2006. **177**(3): p. 1416-20.
446. Nandi, B. and S.M. Behar, *Regulation of neutrophils by interferon-gamma limits lung inflammation during tuberculosis infection.* J Exp Med, 2011. **208**(11): p. 2251-62.
447. Desvignes, L. and J.D. Ernst, *Interferon-gamma-responsive nonhematopoietic cells regulate the immune response to Mycobacterium tuberculosis.* Immunity, 2009. **31**(6): p. 974-85.
448. Rutitzky, L.I., P.M. Smith, and M.J. Stadecker, *T-bet protects against exacerbation of schistosome egg-induced immunopathology by regulating Th17-mediated inflammation.* Eur J Immunol, 2009. **39**(9): p. 2470-81.

449. Rutitzky, L.I. and M.J. Stadecker, *Exacerbated egg-induced immunopathology in murine Schistosoma mansoni infection is primarily mediated by IL-17 and restrained by IFN-gamma.* Eur J Immunol, 2011. **41**(9): p. 2677-87.
450. Edgar, J.D., et al., *Interferon-gamma receptor deficiency mimicking Langerhans' cell histiocytosis.* J Pediatr, 2001. **139**(4): p. 600-3.
451. Petrovas, C., et al., *CD4 T follicular helper cell dynamics during SIV infection.* J Clin Invest, 2012. **122**(9): p. 3281-94.
452. Chen, K., et al., *IL-17RA is required for CCL2 expression, macrophage recruitment, and emphysema in response to cigarette smoke.* PLoS One, 2011. **6**(5): p. e20333.
453. Pavic, M., et al., *[Sarcoidosis and sarcoid reactions in cancer].* Rev Med Interne, 2008. **29**(1): p. 39-45.

ABSTRACT

Tuberculosis **(TB)**, caused by *Mycobacterium tuberculosis* infection, is a deadly disease which mainly affects lungs. The histological hallmark of TB is the formation of small nodules called granulomas in affected tissues. These structures, crucial to restrict mycobacterial growth, are formed by a myeloid cell core, containing multinucleated giant cells **(MGCs)** and surrounded by T lymphocytes. In humans, mechanisms of granuloma and MGC formation and functions are largely unclear.

Previously, our group showed that the pro-inflammatory cytokine IL-17A induces the fusion of human dendritic cells **(DCs)** in MGCs. In this work, we identified IL-17A-dependent molecules that regulate DC survival such as the pro-survival protein BFL1, and clustering and fusion such as the chemokines CCL20 and CCL2, to form MGCs *in vitro*. Working on human TB granulomas, we showed that IL-17A was expressed by T lymphocytes while BFL1, CCL20 and CCL2 were expressed by the mono and MGCs of the myeloid core. This suggests a role of IL-17A in granuloma maintenance and giant cell formation by promoting survival, clustering and fusion of myeloid cells.

Using transcriptomic analysis and *in vitro* experiments, we then characterized the phenotype, the immune functions and the microbicidal roles of IL-17A-treated DC and their derived MGCs. They showed a mixed DC-macrophage phenotype, kept classical DC functions, co-express the destructive proteases matrix metalloproteinase 12 and cathepsin D, and have increased microbicidal activities against Mycobacteria. *In vitro*, IL-17A-induced MGCs were also able to destroy a human bronchial epithelial cell line. We called these IL-17A-dependent giant cells **GMICs** for Giant Myeloid Inflammatory Cells, and propose that they constitute a new inflammatory myeloid effector with strong bactericidal and destructive activities. We found that infection of human DCs with Mycobacteria induces the formation of giant cells independently of IL-17A. We compared giant cells of TB granuloma to myeloid giant cells either generated *in vitro* such as osteoclasts, GMICs, BCG-induced giant cells or generated *in vivo* in other granulomatous disease such as Langerhans cells histiocytosis. IL-17A-induced GMICs share striking similarities and genotypic and phenotypic characteristics with Mycobacterium-induced giant cells.

Altogether, our results show that IL-17A may maintain the integrity of the myeloid core of the human TB granuloma and promotes the formation of original myeloid giant cells with potent microbicidal and destructive functions. These results offer a better understanding of the molecular mechanisms of granuloma and giant cell formation and functions and may help the development of new TB therapeutic and vaccination strategies.